OPTIMAL ALLOCATION OF THERMODYNAMIC IRREVERSIBILITY FOR THE INTEGRATED DESIGN OF PROPULSION AND THERMAL MANAGEMENT SYSTEMS

A Thesis
Presented to
The Academic Faculty

by

Adam Charles Maser

In Partial Fulfillment
of the Requirements for the Degree
Doctor of Philosophy in the
School of Aerospace Engineering

Georgia Institute of Technology
December 2012

OPTIMAL ALLOCATION OF THERMODYNAMIC IRREVERSIBILITY FOR THE INTEGRATED DESIGN OF PROPULSION AND THERMAL MANAGEMENT SYSTEMS

Approved by:

Dr. Dimitri N. Mavris,
Advisor and Committee Chair
School of Aerospace Engineering
Georgia Institute of Technology

Dr. Elena Garcia
School of Aerospace Engineering
Georgia Institute of Technology

Dr. Brian J. German
School of Aerospace Engineering
Georgia Institute of Technology

Dr. J. Mitch Wolff
Propulsion Directorate
Air Force Research Laboratory

Dr. Jechiel I. Jagoda
School of Aerospace Engineering
Georgia Institute of Technology

Date Approved: November 12, 2012

"Why join the navy if you can be a pirate?"

-Steve Jobs

ACKNOWLEDGEMENTS

First of all, I must say that this has been an incredibly humbling experience, from the qualifying examinations, to the thesis proposal, to the writing of this document. When I first decided to come to Georgia Tech after high school in 2003, I never imagined that I would still be here writing this nine years later. Even still, in retrospect, I would not have changed anything. I would like to thank all of the people in Atlanta that have helped me over the years; particular thanks goes out to Robert Combier and Ghislain Retaureau. Your friendship during the most difficult years at the end was instrumental to the completion of this thesis. Also, the months that we spent on Cerevis and the Business Plan Competition were an incredible adventure that I will not soon forget. I also must thank Pamela Amparo. Pam, thanks for all of the wonderful memories while trying to finish everything up towards the end. You gave me the extra motivation to keep pushing and were always supportive, especially at the very end when "just a couple more weeks" seemed to continue on forever!

Of course, I am indebted to my thesis committee. Dr. Mavris, you taught me so much and are certainly the best advisor that one could have. Thank you for your patience and advice throughout the years. Our late night discussions in your office were especially important to me, and I hope that I am able to live up to your high expectations in my post-grad school life. Dr. Garcia, thanks for all of your time over the last five years. I appreciate the guidance that you provided in the completion of my research during our many meetings throughout those years. I would also like to thank you in particular for all of your feedback and revisions to this thesis. Dr. German, your technical knowledge in propulsion and thermal systems and your ability to approach them from a design perspective was a big help. I also

owe you thanks for your instruction in the propulsion systems design class during my first year of graduate school; that class was instrumental in this work. Dr. Wolff, thanks for all of your insight into the big picture and showing me how everything fits together; it was particular valuable to have you as a member of my committee since you have the unique experience as both an academic and an outsider due to your dual roles at Wright State University and the Air Force Research Laboratory. Also, it was a pleasure to have the opportunity to work with you at AFRL over the summer. Dr. Jagoda, even though you came onboard a little later than the rest of the committee, I greatly benefited from your contributions, and I thank you for that. Your mastery of thermodynamics helped beef up all of my work, and your instruction in my undergraduate and graduate coursework not only helped me in this research, but also aided me throughout my academic career.

Finally, and most importantly, I would like to thank my family. They have always been there for me throughout my life. I would like to start by thanking my parents, Sherry and Richard. Mom, thanks for always helping me to put things in perspective and for believing in me. You have helped me a lot especially when I needed it most; I would have never accomplished this without you. Your business insight and advice (and the books that you always gave to me each year) have also been influential. Dad, you taught me the importance of hard work at a very early age; I still have not met anyone that has worked as hard as you. Also, I think it is somewhat obvious that your interest in electronics, cars, and technology certainly sparked my interest in the engineering work that I do today. My sisters, Ashley and Amanda, thanks for all of your support. I am really lucky to have you both, and I also hope you know how proud I am of the two of you. Finally, my grandmother Sara, thanks for all of our conversations over the years. They have helped more than you will ever know.

-Adam

November 2012

TABLE OF CONTENTS

LIST OF TABLES

LIST OF FIGURES

SUMMARY

More electric aircraft systems, high power avionics, and a reduction in heat sink capacity have placed a larger emphasis on correctly satisfying aircraft thermal management requirements during conceptual design. Thermal management systems must be capable of dealing with these rising heat loads, while simultaneously meeting mission performance. Since all subsystem power and cooling requirements are ultimately traced back to the engine, the growing interactions between the propulsion and thermal management systems are becoming more significant. As a result, it is necessary to consider their integrated performance during the conceptual design of the aircraft gas turbine engine cycle to ensure that thermal requirements are met.

This can be accomplished by using thermodynamic subsystem modeling and simulation while conducting the necessary design trades to establish the engine cycle. However, this approach also poses technical challenges associated with the existence of elaborate aircraft subsystem interactions. This research addresses these challenges through the creation of a parsimonious, transparent thermodynamic model of propulsion and thermal management systems performance with a focus on capturing the physics that have the largest impact on propulsion design choices. This modeling environment, known as Cycle Refinement for Aircraft Thermodynamically Optimized Subsystems (CRATOS), is capable of operating in on-design (parametric) and off-design (performance) modes and includes a system-level solver to enforce design constraints. A key aspect of this approach is the incorporation of physics-based formulations involving the concurrent usage of the first and second laws of thermodynamics, which are necessary to achieve a clearer view of the component-level losses across the

propulsion and thermal management systems. This is facilitated by the direct prediction of the exergy destruction distribution throughout the system and the resulting quantification of available work losses over the time history of the mission.

The characterization of the thermodynamic irreversibility distribution helps give the propulsion systems designer an absolute and consistent view of the tradeoffs associated with the design of the entire integrated system. Consequently, this leads directly to the question of the proper allocation of irreversibility across each of the components. The process of searching for the most favorable allocation of this irreversibility is the central theme of the research and must take into account production cost and vehicle mission performance. The production cost element is accomplished by including an engine component weight and cost prediction capability within the system model. The vehicle mission performance is obtained by directly linking the propulsion and thermal management model to a vehicle performance model and flying it through a mission profile. A canonical propulsion and thermal management systems architecture is then presented to experimentally test each element of the methodology separately: first the integrated modeling and simulation, then the irreversibility, cost, and mission performance considerations, and then finally the proper technique to perform the optimal allocation.

A goal of this research is the description of the optimal allocation of system irreversibility to enable an engine cycle design with improved performance and cost at the vehicle-level. To do this, a numerical optimization was first used to minimize system-level production and operating costs by fixing the performance requirements and identifying the best settings for all of the design variables. There are two major drawbacks to this approach: It does not allow the designer to directly trade off the performance requirements and it does not allow the individual component losses to directly factor into the optimization.

An irreversibility allocation approach based on the economic concept of resource allocation is then compared to the numerical optimization. By posing the problem in economic terms, exergy destruction is treated as a true common currency to barter for improved efficiency, cost, and performance. This allows the designer to clearly see how changes in the irreversibility distribution impact the overall system. The inverse design is first performed through a filtered Monte Carlo to allow the designer to view the irreversibility design space. The designer can then directly perform the allocation using the exergy destruction, which helps to place the design choices on an even thermodynamic footing. Finally, two use cases are presented to show how the irreversibility allocation approach can assist the designer. The first describes a situation where the designer can better address competing system-level requirements; the second describes a different situation where the designer can choose from a number of options to improve a system in a manner that is more robust to future requirements.

CHAPTER I

INTRODUCTION AND MOTIVATION

The importance of aircraft integrated propulsion and thermal management systems design is growing, and this is a result of the continued drive towards more electric aircraft systems, the desire to include high power avionics systems, and a reduction in heat sink capacity. This motivation is first throughly examined before moving into the more specific motivation for the central theme of this research: the optimal allocation of thermodynamic losses throughout the integrated propulsion and thermal management systems. Characterization of this irreversibility on a component basis provides the designer with an absolute and consistent metric that can be compared in conjunction with cost and mission performance. The direct allocation of the system-level irreversibility is then presented as an effective means of improving the conceptual design of propulsion systems in the context of thermal management challenges by better meeting the requirements.

1.1 Aircraft Mission Performance Demands and Challenging Thermal Requirements

The modern aircraft is a collection of complicated and heterogeneous subsystems that exist to fulfill multiple needs [134]. The aircraft, like all complex systems, becomes much easier to conceptually manage when it is decomposed into its respective subsystems [50]. All of the main subsystems on the modern aircraft, including flight control and actuation, environmental control and pressurization, electrical power generation, and cooling and thermal management, provide essential services that enable the flight and mission capability. Figure 1 illustrates the complex subsystem interactions for a typical aircraft.

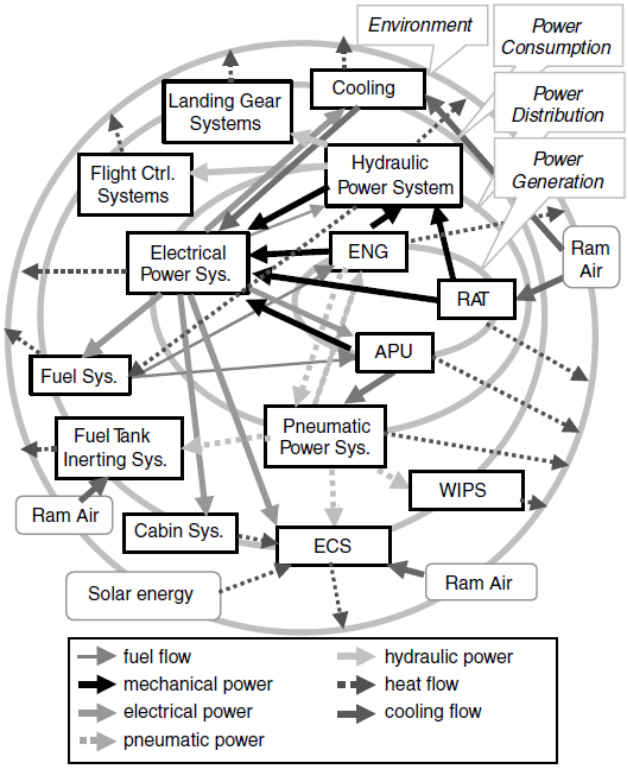

Figure 1: Typical Aircraft Subsystem Interactions [97].

Traditionally, these subsystems are powered either hydraulically, pneumatically, or electrically [113]. These three types of secondary power are transported through a multitude of complex distribution networks. In the end, all power requirements trace back to the main engines, specifically the engine shaft or compressor. This power extraction from the engine results in a reduction in engine propulsive efficiency [141, 104] and an increase in fuel consumption.

It is important to understand how each of these separate subsystems interacts and participates in the operation of the whole aircraft system. However, many of the interactions are often defaulted or ignored during the conceptual design process. One of the major drawbacks to this federated approach is the significant overdesign, duplication, and excess weight resulting from the use of three separate systems.

Aircraft subsystem interactions are rising and are now a more important aspect of conceptual design. It is no longer appropriate to consider these subsystems in isolation

during the design process. This is especially true in the case of the propulsion system. The aircraft engine provides all of the propulsion and power onboard the aircraft; as a result, every aspect of design comes back to the engine.

1.1.1 The Shift to More Electric Aircraft Subsystems

The aerospace community is currently in the midst of a transformation in the design of aircraft subsystems. This change involves the replacement of traditional aircraft subsystems with their electrical counterparts. This results in a reduction or elimination of hydraulic and pneumatic power in favor of electrical power. Collectively, this effort is often referred to as the more electric aircraft (MEA) [57]. The end goal is the achievement of the all electric aircraft in which the aircraft is comprised of only electrical subsystems, with the exception of power generation and propulsion through the traditional combustion of fuel. The more electric aircraft focuses on "the utilization of electrical power as opposed to hydraulic, pneumatic, and mechanical power for optimizing aircraft performance and life cycle cost" [181].

Performance benefits can be realized through the elimination of the hydraulic and pneumatic systems. Blanding has stated that the "MEA approach offers an increase in design flexibility, a reduction in operation and maintenance cost, and overall reduction in system weight. A more notable benefit of the MEA approach is the reduction in power conversion, where you no longer have to convert engine shaft power to electric, hydraulic and pneumatic power" [22]. An illustration of a power optimized aircraft architecture is shown in Fig. 2.

One of the most important elements of the more electric aircraft is its on-demand capability, where the various devices are turned on only when needed. This also has the potential to result in significant savings since power is not constantly required. In traditional systems, this is not always the case.

For example, in hydraulic actuation systems, the pumps are constantly running in order to maintain the required pressure even when the actuators are not being used.

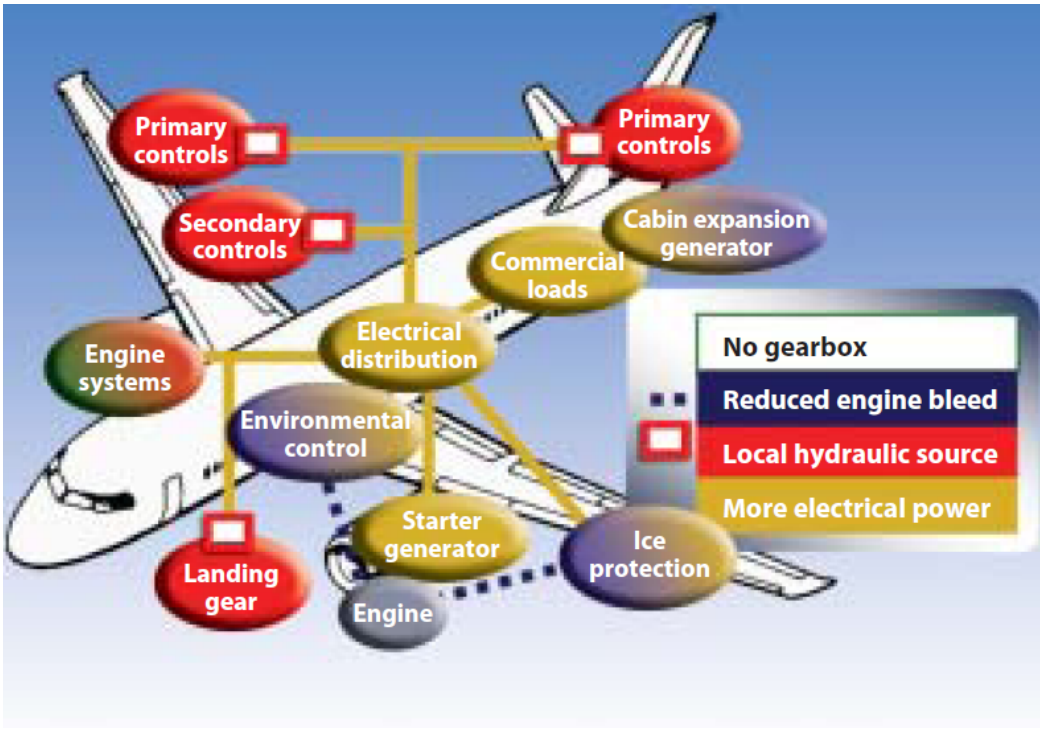

Figure 2: Power Optimized Aircraft Architecture [57].

It has been shown that the elimination of the hydraulic and pneumatic aircraft subsystems and their subsequent replacement by more electric systems can result in many improvements. However, from a performance viewpoint many of these improvements, such as a reduction in complexity and required maintenance and an increase in reliability, can only be seen at the system-level. Consequently, there exists the potential for a large engine performance increase as many of its loads are decreased or removed.

Multiple studies conducted by the U.S. Air Force support the case for the more electric aircraft and have demonstrated more electric benefits in terms of "reliability, maintainability and supportability" [181]. Most of these improvements ultimately result in a reduction in fuel usage and maintenance and an increase in reliability. This can translate into a significant monetary savings for both the military and the

commercial airlines. Reductions in fuel consumption are becoming increasingly important due to the current economic, environmental, and political climates. The United States Government Accountability Office has reported that in "2008, when global fuel prices were high, jet fuel accounted for about 30 percent of U.S. airlines' total operating expenses, compared with 23 percent during 2007" [169].

1.1.2 The Escalating Thermal Challenge

There are many important benefits of the more electric revolution as has been previously discussed. However, as with all engineering efforts, tradeoffs are involved and some drawbacks do exist. The major problem, which will be the focus of this research, is the thermal challenge. As the all electric aircraft becomes more of a reality, so do increasingly larger thermal loads.

In addition to the loads resulting from the more electric efforts, additional loads are also increasing at a rapid rate. Commercial aircraft are seeing a larger demand in passenger electrical power for entertainment and convenience. On military aircraft, avionics have continued to increase in power demand. Increasing electrical power generation for more electric subsystems and advanced avionics usage leads to increasing heat loads that must be removed from the aircraft. The most extreme military increase in thermal load potential is the load resulting from the inclusion of a directed energy weapon (DEW). Vrable and Donovan have summarized this by stating that "currently the electrical power and thermal management systems to support the concepts for airborne DEW systems do not exist. A major challenge will be thermal management, since it goes hand-in-hand with high power generation and consumption" [177]. Figure 3 shows the rise in heat loads for current and future military applications.

However, it is important to note that the current thermal challenge is not simply a consequence of rising heat loads. It is also a result of the opposite side of the

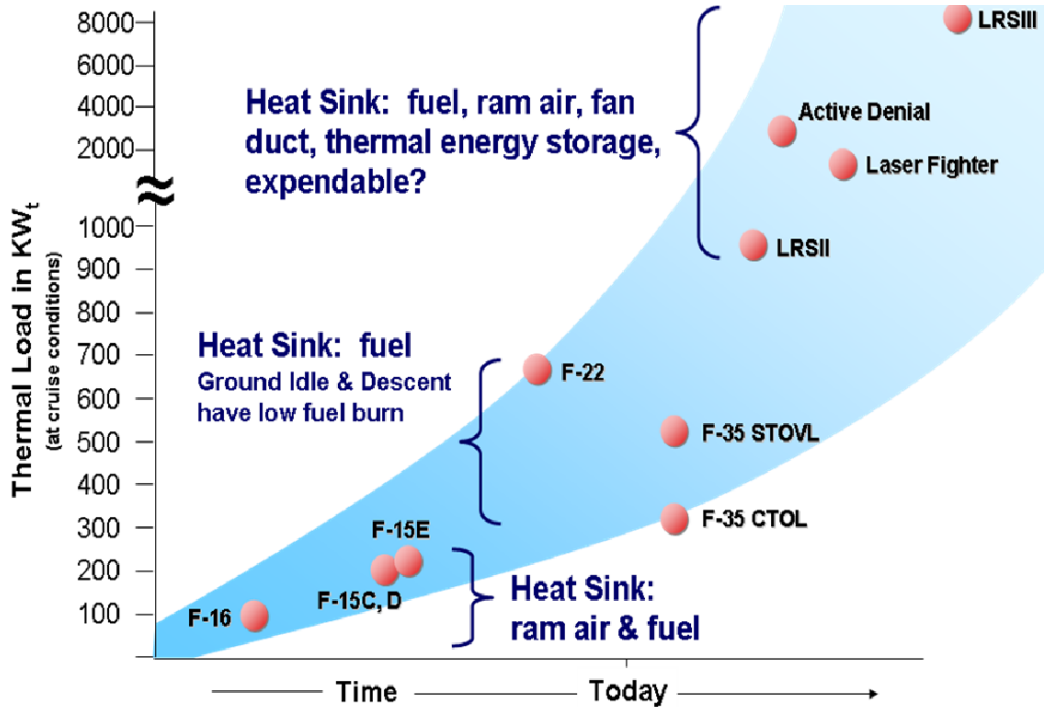

Figure 3: Thermal Load Rise for Military Aircraft Platforms [76].

same coin: a reduction in cooling capability. Like the rising heat loads, some of the reductions in cooling capability are the result of current more electric efforts, while others are not. Future and current aircraft see a reduction in cooling capability due to composite skin, reduced ram air, and the elimination of traditional hydraulic and pneumatic heat sinks. Composites reduce the ability for the aircraft to rely on convective skin cooling as was traditionally used with aluminum aircraft. Low-observability requirements result in the elimination of ram air, which leads to requirements incorporating engine bypass cooling or third-stream technology [89]. The elimination of hydraulic lines results in a cooling problem for modern electric actuators due to the removal of the traditional cooling routes. In hydraulic actuation systems, the circulating hydraulic fluid naturally removes the generated heat through convection; current electro-hydrostatic actuators (EHAs) and electro-mechanical actuators (EMAs) obviously do not have this capability. Chen summarizes this situation succinctly:

"The MEA approach of replacing inefficient centralized hydraulic and pneumatic bleed systems with power-on-demand electrical system is advantageous in terms of reliability, maintainability, and supportability (RM&S), survivability, and weight, resulting in reduction in life-cycle cost (LCC). Removing the centralized hydraulic system will, however, eliminate an effective heat transfer network, thus resulting in an aircraft with less overall heat to reject but with localized 'hot spots' such as high-power motors and motor controllers. The conventional centralized environmental control system (ECS) cooling approach may need to be augmented with local thermal control techniques and improved heat sinks to eliminate any requirements for coolant lines running all over the aircraft" [37].

1.1.3 Thermal Management is an Essential Design Requirement

All of these developments lead to the generation of large amounts of waste heat by the aircraft subsystems. This heat must be dissipated to keep the aircraft within the appropriate operating limits. Furthermore, reductions in aircraft cooling capability are occurring due to mission performance requirements. This has led to a big thermal management challenge in the design of modern aircraft. The basic premise of this research is the idea of bringing this thermal information forward in the conceptual propulsion systems design process as a means of avoiding the problem.

Many of the subsystems aboard the aircraft require a certain range of operating temperatures to function effectively. In order to ensure that this remains the case during the entire mission, a cooling system must be created and included onboard the aircraft.

Thermal management is present in nearly every aspect of engineering. From computers to automobiles to modern fighter aircraft, the heat generated must be dealt with in order to prevent failure. In the modern computer, elaborate heat sinks

and fans are used to cool high performance microprocessors to the optimal operating temperatures [116]. Similarly, a radiator, water pump, and cooling loop are used in the car to cool the engine to an acceptable level.

Although the basic cooling system on many automobiles has changed very little since the designs of the 1920's [124], the same cannot be said for aerospace applications in response to the stringent thermal requirements. The modern aircraft thermal management system is vastly different from that found on the 1903 Wright Flyer. Today, thermal management systems have become extremely complex in both commercial and military applications. Modern thermal management systems can contain intricate networks of multiple coolants as well as air and vapor cycle machinery to provide additional cooling when necessary.

An example of one such thermal management system is shown in Fig. 4. As seen in this diagram, fuel, oil, air, and water cooling are all used. In addition, an air cycle machine is used along with engine fan stream cooling.

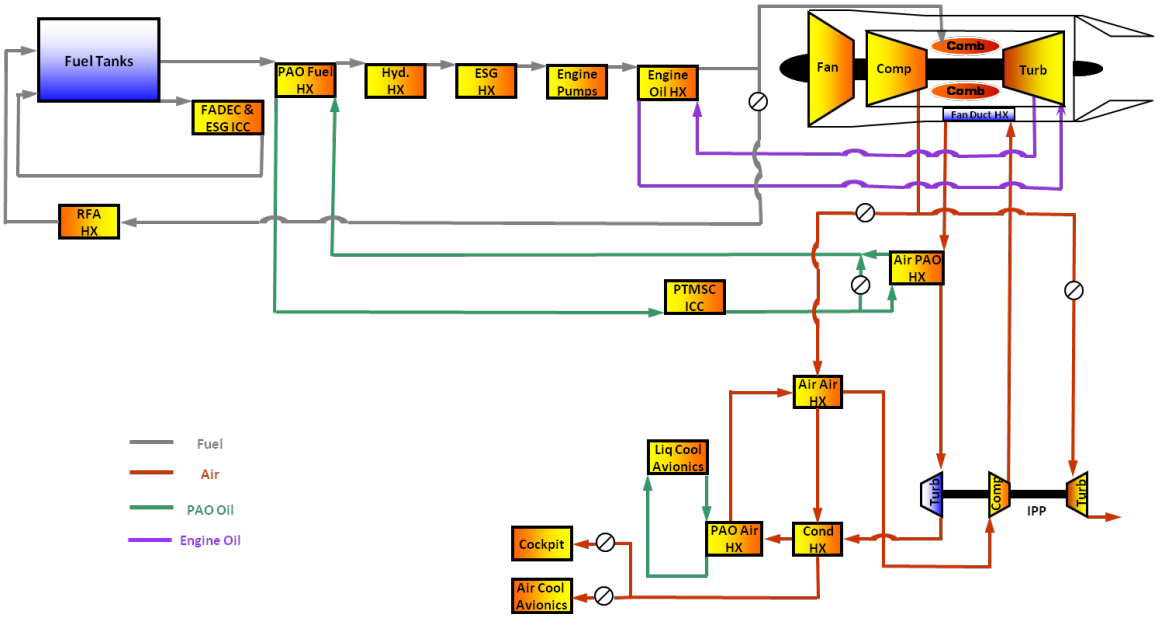

Figure 4: Modern Fighter Aircraft Thermal Management System Schematic [102].

Thermal management system design must be accounted for earlier in the design of aircraft due to the fact that electric power and resulting heat loads continue to rise in both military and commercial aircraft [177]. In fact, "High power and high heat flux cooling requirements, coupled with a limited payload capacity, is one of the primary design challenges" for military DEW systems [100]. Vrable goes on to stress that "A TMS that can couple the advantages of both a smaller and lighter weight system with the ability to maintain component temperature excursions during peak operation is of paramount importance..." [178].

A major reason that thermal management system design has become such an important focus is due to its ability to actually impact mission effectiveness in combat operations: "Many of the electronic control components have strict requirements as to the temperature at which they are cooled. Cooling above the required temperature for these components can result in degradation of performance or loss of reliability" [75]. Furthermore, thermal management has been described as a "Top Priority" for the U.S. Air Force [130] and it is a key aspect of the Air Force Research Laboratory (AFRL) Integrated Vehicle & Energy Technology (INVENT) program [179]. Thermal management was a major design challenge going from the F-16 and F-22 aircraft and resulted in many design improvements, such as the development of the integrated power package, for the F-35 [98]. Even still, the F-35 has experienced thermal management issues and may require future redesign efforts [180, 129]. These thermal problems are even discussed at length in a recent *Time* magazine article [161].

1.2 Getting the Requirements Right with Integrated Modeling and Simulation

Traditionally, the aircraft engines have been designed in relative isolation from other systems. After their design, the other "less important" ancillary subsystems are designed as necessary. In other words, the engine is designed to provide a certain amount of thrust; then, the thermal management system is designed to provide the

required cooling to the engine. One must then ask, does it not make more sense to design these systems simultaneously to reduce the heat generation to begin with?

A shift has resulted in conceptual design through the use of integrated modeling and simulation. The development of physics-based models of multiple subsystems and their concurrent simulation allows the designer to predict their future performance. The interactions between all of the subsystems are continuing to increase with the addition of more electric and more integrated subsystems. For example, the differences in subsystem interactions between the fourth generation (F-16) and fifth generation (F-22/F-35) fighter aircraft are substantial; the interactions are becoming larger in number and thus more complex [88]. As a result, it is not possible to examine the aircraft thermal management subsystem in isolation; instead it must be viewed in the context of all of the interactions between the subsystems that occurs onboard the aircraft. Therefore, the aircraft thermal management challenge is actually a *vehicle-level problem* [77].

These issues need to be understood and dealt with earlier in the design process in order to minimize costly future redesigns later. Moir actually goes as far as to to say that the "success or failure in the Aerospace and Defense sector is determined by the approach taken in the development of systems and how well or otherwise the systems or their interactions are modelled, understood and optimised" [113]. This is particularly important in approaching the current thermal challenge. Optimization of the thermal management subsystem design must be conducted in conjunction with the other subsystems, especially propulsion and power [68].

Bodie, Russell, McCarthy, et al. at the Air Force Research Laboratory (AFRL) have taken this approach and developed an extensive tip-to-tail thermal model for a blended wing-body long range aircraft [25]. A schematic of this modern tip-to-tail aircraft thermal model is shown in Fig. 5.

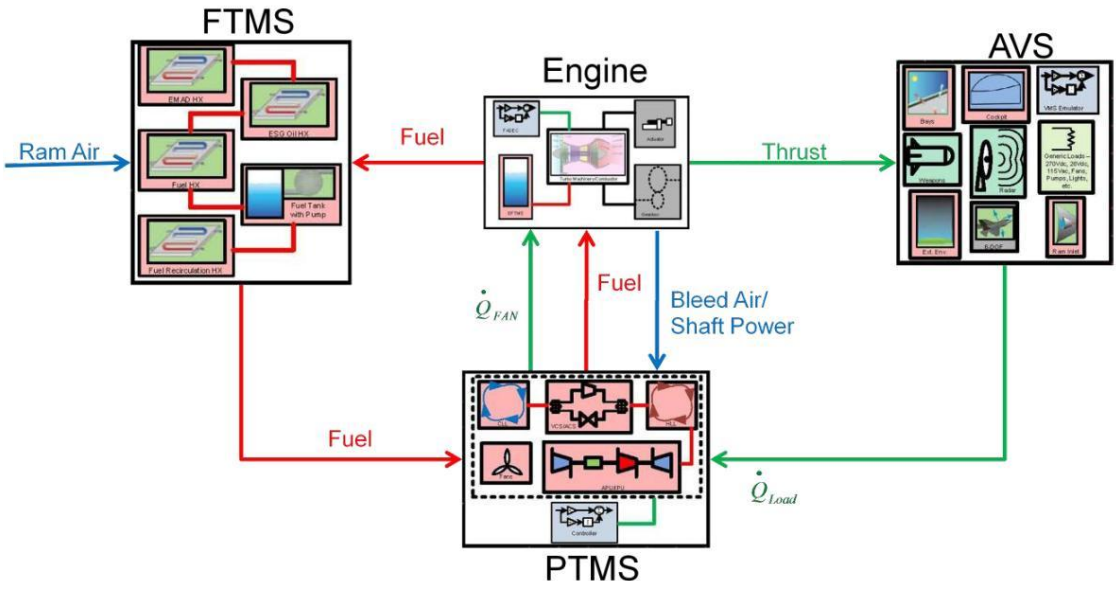

Figure 5: Integrated Tip-to-Tail Aircraft Simulation Developed at AFRL [25].

As shown in the figure, models of the power thermal management system (PTMS), fuel thermal management system (FTMS), and engine are all integrated together and linked to an air vehicle model. This integrated modeling environment then enables the investigation of the vehicle-level implications of thermal management system design modifications.

1.2.1 Accounting for Thermal Management Requirements during Conceptual Design

It is very important to realize that the other aircraft subsystems are accounted for in conceptual propulsion systems design to some degree already: They are implicitly accounted for as requirements. The greater emphasis on thermal management systems design should be seen as a means of getting the requirements right.

As an example, consider the following analogy. It is a requirement for humans to consume a certain amount of food per day. However, everything that one consumes is normally not directly accounted for every day because of the simple fact that it is unnecessary. It is important to note that the food requirement is not being neglected though; it is just that it is not a major focus. Instead, this requirement is implicitly

accounted for in the background throughout the day. However, this certainly changes if the person is training for a big race where every tenth of a second of improvement matters. In this case, more emphasis is placed on the food requirement because any possible increase in performance improvement is extremely important.

This is exactly the same as the present situation of propulsion and thermal management systems design. Here, the thermal management requirements have always been implicitly accounted for in conceptual engine design. These are normally represented as constant thermal loads and power extraction values that are defined through the system-level requirements. These are historically based and may or may not actually be correct. Now that the propulsion and thermal management systems are being pushed to their maximum capability and are experiencing challenges in performing their mission, a greater explicit emphasis must be placed on meeting these requirements.

1.2.2 Integrated Propulsion and Thermal Management Systems Design

As previously explained, all subsystem power and cooling requirements are ultimately traced back to the propulsion system. As with all of the other subsystems, the propulsion subsystem is becoming much more integrated with the aircraft. This is especially true with modern military aircraft, such as the F-35 [21]. Therefore, it is necessary to consider subsystem effects in an enhanced manner during the conceptual design of the aircraft engine cycle due to their impact on engine performance.

Power is extracted from the engine either mechanically through the engine shaft or pneumatically by bleeding air from the compressors. Additionally, the engine can serve as a heat exchanger through the fuel or fan stream and requires a heat sink for its oil system. Subsystem weight and volume requirements also ultimately impact the engine by requiring the engine to deliver a greater amount of thrust in order for the aircraft to perform its mission. Finally, cost and mission performance requirements

are also important factors. Figure 6 shows the main interactions between the aircraft gas turbine engine and the other aircraft subsystems.

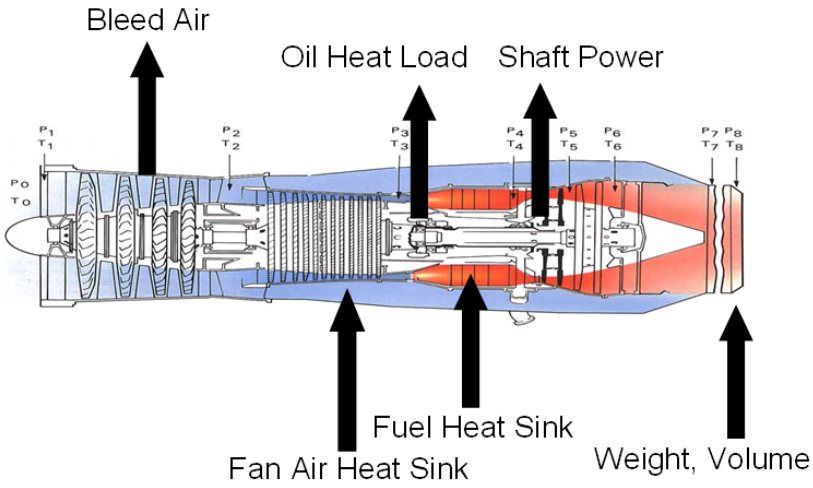

Figure 6: Engine and Subsystem Interactions. Adapted from [141].

The integrated performance of propulsion and thermal management systems must be investigated during the conceptual design of the engine cycle. This involves the investigation of engine bleed, power extraction, and cooling capabilities in the presence of thermal management requirements. The consideration of the associated thermal aspects early in the design of the engine and the resulting cycle design modifications may preempt some issues that would have otherwise been discovered later. However, this integrated design effort requires the subsystem analyses that are most important in influencing the engine design to be determined and appropriately modeled.

Research Observation: It is necessary to more explicitly consider thermal management subsystem requirements during the conceptual design of the aircraft engine cycle due to their impact on mission performance.

1.3 Propulsion Systems Design in the Context of Thermal Management Challenges

Challenging thermal requirements have placed a new and essential emphasis on aircraft thermal management requirements during the early stages of conceptual design [107, 179]. The central focus of this research is on the improved design of the aircraft propulsion system in the context of the new thermal management challenges. Integrated modeling and simulation is utilized as a way to predict the performance of the system. Previous integrated systems research provides a solid foundation for the current study, but does not directly cast the problem in terms of conceptual propulsion systems design. Current thermal challenges must be addressed during the conceptual phase of the aircraft engine design process. To do this effectively, they must be dealt with in a systematic fashion, while focusing on the design of the integrated propulsion and thermal management systems.

A challenge that was identified during this research was the inconsistent characterization of the interactions and losses between the subsystem models. The various propulsion and thermal management losses all have different impacts on the system performance; therefore, it is necessary to transform all of the subsystem losses into a common metric so that the system-level tradeoffs can be effectively performed.

Research Observation: In order to appropriately consider thermal requirements during the integrated design of the propulsion and thermal management subsystems, a consistent characterization of the interactions and losses between these subsystems is needed.

1.3.1 Thermodynamic Irreversibility for Integrated Propulsion Systems Design

The preceding discussion leads to the following question: How can the propulsion systems designer effectively take thermal management systems performance into account during the conceptual design process? A modern approach to deal with the lack of a consistent and absolute metric of comparison for integrated thermodynamic systems is to frame the analysis in terms of thermodynamic irreversibility or loss of work potential. Such an approach is accomplished using the thermodynamic concept of exergy, which is essentially a measure of the ideal work potential. Then, the loss of work potential of each component is measured as the exergy destruction. This is commonly used in the design of ground-based power systems and has increasingly been proposed for aerospace applications. The idea of using thermodynamic irreversibility in aircraft design decision making has also been widely discussed [114, 128].

Past research in the area of integrated propulsion and thermal management systems design has focused on the development of transient, thermodynamic subsystem models [102, 139, 67]. These allow for the investigation of thermal effects while conducting the necessary design trades to establish the engine cycle. However, much of this work has primarily examined the flow of energy between the subsystems with no direct thermodynamic characterization of the system losses, while the rest generally treats the irreversibility losses as an output of the engineering analysis.

This work seeks to build on these previous studies by directly considering the exergy destruction throughout the integrated system. In turn, this irreversibility information can be utilized as the primary driver of the system design. This should prove to be a powerful and insightful tool because it enables the designer to view the entire system on a consistent and absolute basis. This could then lead to rapid design tradeoffs that enable better allocation of the unavoidable thermodynamic losses and result in improved system performance.

Research Observation: The direct characterization of the thermodynamic irreversibility using second-law-based techniques is often used in other industries to provide an absolute and consistent metric in the design of thermodynamic systems.

1.3.2 Designing for Optimal Irreversibility Allocation

If it is shown that there is a need to conduct the integrated propulsion and thermal management system design and that the irreversibility characterization is an important tool in this process, then the next question is, is there a way to optimally allocate this irreversibility? This question essentially becomes the major emphasis for the remainder of the present research study. There are additional questions as to how the traditional design process is modified to take this irreversibility characterization into account. For example, is it necessary to directly address other disciplines, and if so, how can they be accounted for concurrently with the irreversibility?

The investigation of the optimal irreversibility allocation requires the application of multidisciplinary design, analysis, and optimization (MDAO) techniques at the system-level. The irreversibility allocation should enable the designer to rapidly trade off various designs using a consistent, absolute metric. The search for this optimal allocation can lead to integrated system designs that result in improved mission performance [171, 18].

The key idea here is for the designer to allow the irreversibility allocation to drive the conceptual design process. This is done by setting a total irreversibility (exergy destruction) budget and allowing it to flow down to the individual components. Figure 7 illustrates this concept.

1.3.3 Irreversibility Allocation Analogy

The beauty of the exergy-based approach is that it enables the designer to obtain a quick view of all of the losses across the system on a consistent and absolute basis. The approach will ultimately result in the same solution as a traditional approach,

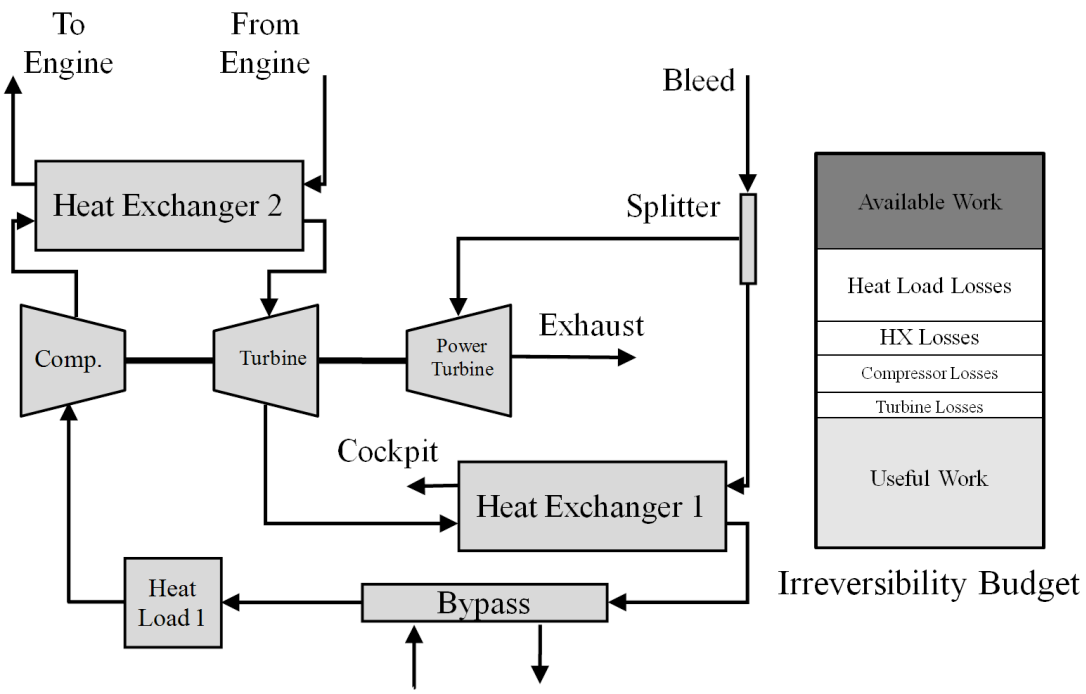

Figure 7: Formulation of Design Process in Terms of Irreversibility Budget Allocation.

but it is much more insightful to the designer. Consider the following analogy of a family purchasing a new home. Suppose that when they receive their first electricity bill, they find that it is twice as much as the previous owner's. The obvious solution to this is to reduce their electricity usage by half. However, the information provided in their bill is not very useful in and of itself in going about this electricity usage reduction. It would be much more useful if the family obtained a breakdown of all of their electricity usage throughout their household. For example, maybe they find that 25% was a result of their air conditioning system and that this could be significantly reduced if they raised the temperature setting by a few degrees. This is essentially what the exergy analysis provides. Furthermore, it is even more helpful since the absolute losses in a thermodynamic system are not as intuitively obvious as an electrical system because a specific inefficiency occurring at a higher temperature or pressure is worse than the same inefficiency at a lower one.

Now that the family has a breakdown of their usage across their household, they can start to make some choices. They are still not going to go about blindly reducing their usage; instead, they will likely take a couple of additional factors into account. After all, they are consuming electricity for a reason. Two of the main reasons are the cost to make a change and the family's preference for particular performance from their household electrical devices. As an example of cost, consider their washing machine. Perhaps they determine that they can reduce their electricity consumption fairly significantly by purchasing a newer model. However, this purchase should only be made if it is also determined that the cost of the purchase justifies this decision. As another example to illustrate performance, consider their dishwasher. Maybe the family finds that they are using a lot of electricity to use their dishwasher. They could eliminate this by simply washing the dishes by hand. On the other hand, they might determine that this is something that is very important to them because they have a large family and the time savings is very beneficial.

Families often arrive implicitly at these same decisions through trial and error. By making small changes to their behavior that they can tolerate and watching their change in electricity usage from month to month, they can slowly reduce their usage. Yet it should also be fairly clear that a breakdown of their consumption throughout their household combined with the rapid estimation of the cost and performance repercussions of their choices would help them do their job better, faster, and easier.

The previous discussion can be directly applied to aircraft propulsion and thermal management design challenge and is fundamentally the same as the irreversibility allocation approach taken here. The irreversibility allocation allows the designer to explicitly make decisions at the system-level in regards to thermodynamic losses, cost, and performance. For novel, complex aerospace systems where the designer has little familiarity, this approach can be especially insightful.

1.4 Overview of Thesis

This first chapter has focused on the motivation for conducting integrated propulsion and thermal management systems design. Integrated modeling and simulation is used to better satisfy the aircraft thermal requirements during conceptual design. The next chapter will provide background on this topic and lay out the research questions that will guide the remainder of the effort. Particular focus is on the concept of irreversibility characterization during the conceptual design process and its subsequent system-level allocation.

In response to the major research questions that are encountered in Chapter II, Chapters III through VII each cover a specific element of the research. The first of these is concentrated on the idea of integrated modeling and simulation. Chapter IV then tackles the second-law formulation and the benefits of an explicit irreversibility characterization in conceptual propulsion and thermal management systems design. Chapters V and VI tackle the cost and performance aspects of the research. The optimal allocation of this irreversibility is brought to the forefront in Chapters VII. Each of these three chapters is similarly organized. First, the research hypotheses and experimental approach are presented. This experimental plan leads to a discussion of the specific theory used in this research and then its implementation. Lastly, the experimental results for the chapter are discussed.

Finally, Chapter VIII offers the final conclusions of the research and presents avenues for future research.

CHAPTER II

BACKGROUND LITERATURE REVIEW AND FORMULATION OF RESEARCH QUESTIONS

The discussion of the research motivation in the previous chapter presented an overview of the integrated propulsion and thermal management systems design problem, and it also allowed for a glimpse of the high-level research questions. It is now time to examine the background literature and state the research questions with more formality.

Before embarking on the discussion of the background literature, the overall objective of this research is now stated based on the observations uncovered from the motivation research. This overarching objective will then help guide the discussion in this chapter.

Research Objective: Enable the system-level designer to better satisfy integrated aircraft propulsion and thermal management subsystem performance requirements during the conceptual design of the gas turbine engine cycle by leveraging the knowledge available from thermodynamic subsystem modeling and simulation to optimally allocate irreversibility throughout the system.

2.1 Traditional Subsystem Conceptual Design

The growing relationship between the propulsion and thermal management systems onboard the modern aircraft is an important aspect of this research. Since the initial thrust of this research is on the integrated modeling and simulation of these systems, it is first necessary to take a look at the traditional approach to their design. In order to

tackle the propulsion and thermal management systems integration problem, current aircraft subsystem modeling and simulation techniques must be well understood. A little background on the design of these two systems will then help identify the opportunities for improvement. The next section contains a review of the traditional modeling techniques used in the conceptual design of the propulsion subsystem; the subsequent section then discusses the design of the thermal management system.

2.1.1 Conceptual Propulsion Systems Design

During the conceptual design stage of aircraft propulsion systems, there is a large emphasis on the thermodynamic and aerodynamic physics of the system. This cycle analysis is a well defined and well documented effort. In cycle analysis, there is first an on-design (parametric) study, where the components are sized for a specific operating point. Then, the off-design (performance) analysis occurs where the operating conditions are changed for the specific engine [105, 104]. This allows the engine cycle designer to investigate the effectiveness of various designs for specific missions and to trade off design requirements. Some recent efforts have also looked into a multiple design point approach, which combines aspects of both on-design and off-design studies [151].

Engine cycle analysis can be performed in a very simplified fashion using closed-form equations. To further increase the sophistication and complexity, there are engine cycle solver software packages. In these programs, quasi-one-dimensional, lumped element control volumes are used to model each stage of the engine. The complex three-dimensional flow physics present in the turbomachinery elements are usually represented by means of performance maps that were previously obtained using more detailed analyses.

The main objective of this conceptual engine cycle design process is the determination of the engine performance (thrust and fuel consumption) as a function of

various design parameters within the engine cycle. The calculation of engine thrust as a function of nozzle outlet pressure and velocity is stated as [104]:

$$T = (\dot{m}_0 + \dot{m}_f)\, V_e - \dot{m}_0 V_0 + (p_e - p_0)\, A_e \tag{1}$$

where $\dot{m}_0$ is the mass flow rate of the inlet air, $\dot{m}_f$ is the fuel mass flow rate, and A_e is the nozzle exit area.

These outlet properties are determined by starting at the inlet and methodically stepping through each component of the engine using thermodynamic relationships. Figure 8 illustrates the standard components and the traditional station numbering scheme for a basic turbofan engine.

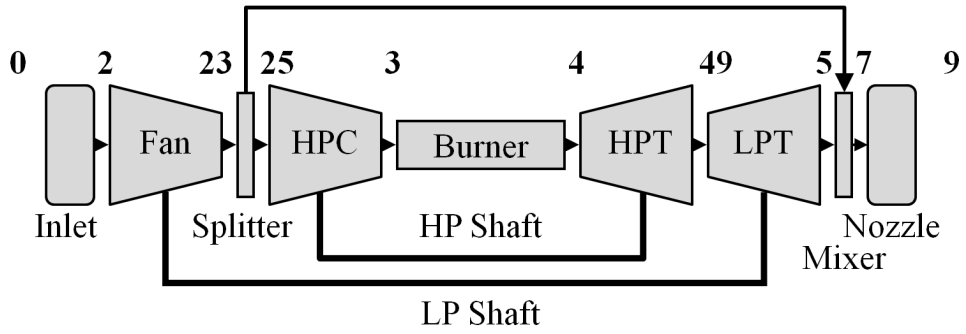

Figure 8: Standard Turbofan Engine Station Numbering Scheme.

Then, the calculation of the engine thermal and propulsive efficiencies are calculated as [104]:

$$\eta_T = \frac{\dot{W}_{out}}{\dot{Q}_{in}} \tag{2}$$

and

$$\eta_P = \frac{TV_0}{\dot{W}_{out}} \tag{3}$$

where $\dot{W}_{out}$ is the power output of the cycle and $\dot{Q}_{in}$ is the heat rate input from the combustion of the fuel.

The overall cycle efficiency is simply determined as the product of the thermal and propulsive efficiency:

$$\eta_O = \eta_P \eta_T = \frac{TV_0}{\dot{Q}_{in}} = \frac{TV_0}{\dot{m}_f h_{PR}} \tag{4}$$

Here the heat input is specified in terms of the fuel mass flow rate and the heat of combustion, h_{PR}.

Comparing Eqs. 1 and 4 clearly illustrates the main tradeoff involved with gas turbine engines: fuel consumption versus thrust. This tradeoff is graphically illustrated in the form of a traditional aircraft engine "carpet plot" in Fig. 9. This plot shows the effect of the two most important engine design parameters (overall pressure ratio and turbine inlet temperature) on thrust and fuel consumption of the engine.

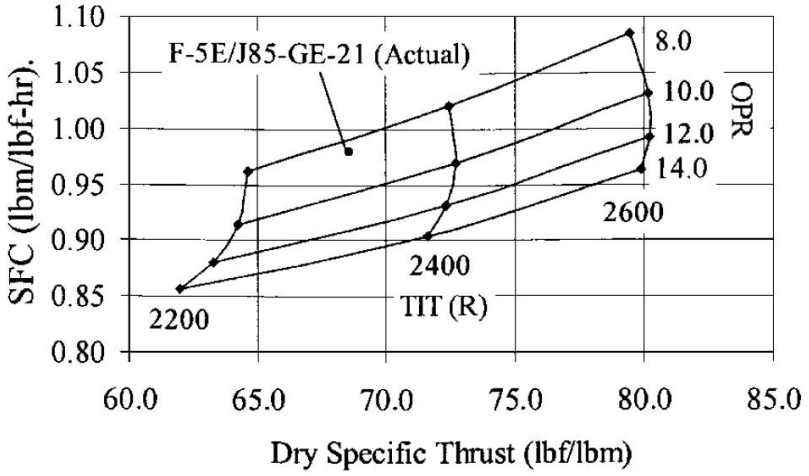

Figure 9: Example Illustration of an Aircraft Engine Carpet Plot [144].

Although various proprietary engine design programs are used by each of the engine manufacturing companies, the standard for aircraft engine design has become the Numerical Propulsion System Simulation (NPSS) [173]. This software was initially designed by a consortium of government, industry, and academic organizations and is based on the earlier NASA Engine Performance Program (NEPP). NPSS is a multidisciplinary platform [99] and has been used on numerous projects including a dynamic

fuel cell model [65], heat exchangers for space applications [8], and a dual Brayton cycle [83]. There has also been work dealing with integrated controller modeling [126] and integrated vehicle modeling [123] directly within the NPSS environment. In addition, the NPSS software can directly interface with the Weight Analysis of Turbine Engines (WATE++) engine weights estimation software to rapidly predict physical engine characteristics [166]. This software is actually used as the basis for the cost estimation in Chapter V. A recent Ph.D. dissertation also details the modeling of a third stream turbofan engine in NPSS [157].

In addition, there have been studies into the development of generic engine models in Simulink [45]. This work was initially created by Gastineau for use on his Ph.D. dissertation [112]. Further development by researchers at AFRL has led to the creation of a generic engine model with transient effects that has also been used in hardware-in-the-loop efforts [110]. The significant disadvantage to this model, however, is that it lacks an on-design (parametric) capability. This function would have to be conducted separately with the result then used to manually reconfigure the model.

Various efforts have also dealt with capturing dynamic characteristics within engine performance models. One of the first efforts was conducted by Rolls-Royce and AFRL using the proprietary Rolls-Royce Fortran software Turbine Engine Reverse Modeling Aid Program (TERMAP) [44]. This work included shaft dynamics within TERMAP for use in a hardware-in-the-loop simulation connected to a physical generator. There has also been similar work conducted in NPSS by AFRL demonstrating transient propulsion systems modeling [43].

There has been substantial research in the area of dynamic engine modeling to enable hardware-in-the-loop efforts [42], aid in controller design [87], and better predict compressor surge effects [136]. The main engine dynamic effects that have been included in recent work are the dynamics of the shafts, heat soak from the hot gases

into the metal components of the engine, and the dynamics associated with the fluid flow within the gas path. As an example, the shaft inertia dynamic is physically modeled as a first order ordinary differential equation [87]:

$$\frac{dN_i}{dt} = \frac{T}{J_i} \tag{5}$$

where N represents the rotational speed of the engine spool, T the net torque, and J the rotational inertia of the spool. This is normally the slowest engine dynamic effect and the most important to include in a dynamic engine simulation. The shaft rotational speed is then treated as the state variable and calculated at each time step using a numerical integration scheme.

For this study, system dynamics are neglected due to their complexity and implementation difficulty. Instead, steady-state formulations are used to demonstrate the irreversibility allocation approach. Another further complication of dynamic models is that they necessitate the development of a controller for the simulation. For the case of a simple feedback controller, the controller tracks specific metrics within the model (e.g. shaft rotational speed) and compares it to a specific set point. Then, the error between these two values is used to adjust an independent model variable (e.g. fuel flow). More sophisticated model predictive controllers have also been developed and demonstrated on a dynamic engine model by Kestner [87].

2.1.2 Conceptual Thermal Management Systems Design

Thermal management design has customarily been a secondary concern during conceptual aircraft design. The detailed interactions are usually investigated later in the design process after many of the engine cycle decisions are already made. Often trade studies are conducted using simple spreadsheet steady-state calculations to determine thermal management system feasibility [155]. An important aspect of thermal management system modeling is the heat exchanger model. The classic text by Kays and

London has been traditionally used for conceptual heat exchanger design [86].

There has been significant research into the simulation of aircraft thermal systems. Most of this work has involved the development of object-oriented environments in MATLAB/Simulink. McKinley and Allyne developed such an environment that they then leveraged in the evaluation of land vehicle cooling systems [109]. A similar, open source thermal toolset was created by McCarthy to enable object-oriented modeling of aircraft thermal management systems in the MATLAB/Simulink environment [107]. This toolset features one-dimensional dynamic effects for many components as well as detailed fuel tank models.

There has been some success in developing thermal management system models directly in the NPSS environment. Butzin, Johnson, and Creekmore demonstrated that a steady-state aircraft thermal model could be created in NPSS [31]. Similarly, Clough investigated the integrated propulsion and power modeling in NPSS for rocket applications [41]. Maser, Garcia, and Mavris successfully leveraged these concepts to develop a transient vapor-cycle thermal model coupled with basic electrical and propulsion models that "takes into account the component physics, solver constraints, and fluid properties of the entire system. The TMS model determines the required coolant pressures, temperatures, and flow rates throughout the duration of the system's operation" [101].

A wealth of literature has started to sprout up in the field of automotive thermal management. This renewed interest is due to the reduction in fuel consumption that is expected through a more intelligent and better controlled thermal management system [85]. This has even been identified as the "last frontier" for fuel savings [124]. As a result of this, there have been several studies using dynamic modeling and simulation to predict the thermal behavior in ground vehicles [10]. Advanced engine thermal management dynamic modeling [153] along with the modeling of its associated controller [154] has been conducted by Setlur.

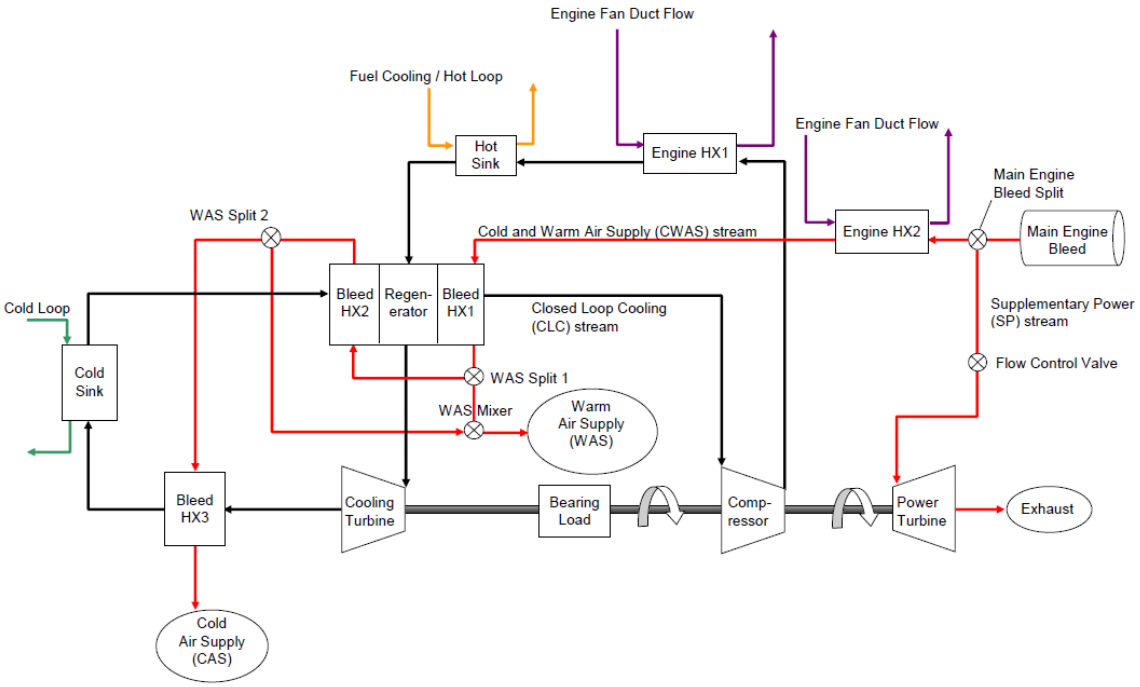

Figure 10: Thermal Management System Developed by Butzin, Johnson, and Creekmore in NPSS [31].

Various modeling platforms have been used for thermal management system modeling during preliminary design. In the past, these have included Modelogics Thermal Systems Analysis Tools (TSAT) and its commercialized counterpart ModelEngineer [69, 74]. These software developments resulted from the earlier Integrated Thermal Energy Management (I-TEM) [30] and Vehicle Integrated Thermal Management Analysis Code (VITMAC) [70] modeling softwares. The design of a fuel thermal management system using the ModelEngineer software has been documented in [63]. The advantages to these programs are that they are object-oriented and contain increasing levels of fidelity. However, one drawback of most of these proprietary softwares is that they are difficult to modify and are therefore not as suitable for research efforts.

The industry standard for subsystem modeling has essentially become MATLAB/Simulink. The Thermal Toolset developed by PCKA for Simulink has been widely adopted [107]. Besides Simulink, AMESim is another popular commercial multi-domain modeling software with thermo-fluid and aerospace functionality. This

software has been successfully applied to the design of an automotive thermal management system [53]. This software is quite similar to Simulink and can model one-dimensional dynamic systems. Other relevant commercial software packages include Easy5, Flowmaster, GT-COOL, and Dymola [109].

There has also been much research into the creation of detailed individual component-level models to use with these types of dynamic thermal management systems simulations. Models capturing the dynamic heat generation from an EMA system [184] and dynamic heat exchanger effects [72] are currently in development. In addition, a reduced order radiation model using the PCKA Thermal Toolset components has been created in Simulink [108].

Dynamic thermal management simulations have been conducted in other fields outside of aerospace. Research on the all-electric ship demonstrated a dynamic modeling capability [58]. Li and Weston also developed simulations for the Integrated Reconfigurable Intelligent Systems (IRIS) program that featured cooling networks with the potential to reroute themselves in the event of ship damage [95, 182].

As in the previous discussion within the propulsion systems design section, controller design has become an important topic in the thermal management arena. Many researchers have investigated the use of active thermal control as a means of improving performance and decreasing fuel consumption [119]. Trzebinski specifically compares the results for an uncontrolled versus controlled cycle and notes the possible improvements [167]. An optimal controller for heat dissipation in electronic devices has been designed by Jang [82].

2.2 Integrated Propulsion Systems Modeling and Simulation

The integrated modeling and simulation approach to systems design is leveraged in this propulsion and thermal management systems research. Since an important objective of this research involves this integrated design of the propulsion and thermal

management systems, it is appropriate to examine the past work in this area. One of the first researchers to directly address integrated engine thermal management was Ahern [1]. This reference also discusses an exergy-based second-law analysis and suggests its usefulness for integrated propulsion and thermal management analysis.

An important study of the fuel savings associated with more electric aircraft systems was conducted using a simple steady-state thermodynamic model by Ramalingam, Mahefkey, and Donovan [131]. This study showed that pneumatic bleed had a more significant impact on engine performance than shaft power extraction. Additionally, this study examined the thermal implications of the inclusion of an airborne solid-state laser system.

Some of the earliest work on integrated thermal modeling was conducted by AFRL and used VITMAC thermal modeling and NNEP turbine modeling software linkages [79, 80]. This work was one of the first to directly interface an engine cycle model with a thermal model. In this instance, both software packages only examined steady-state characteristics. An illustration of the combined VITMAC and turbojet model is shown in Fig. 11.

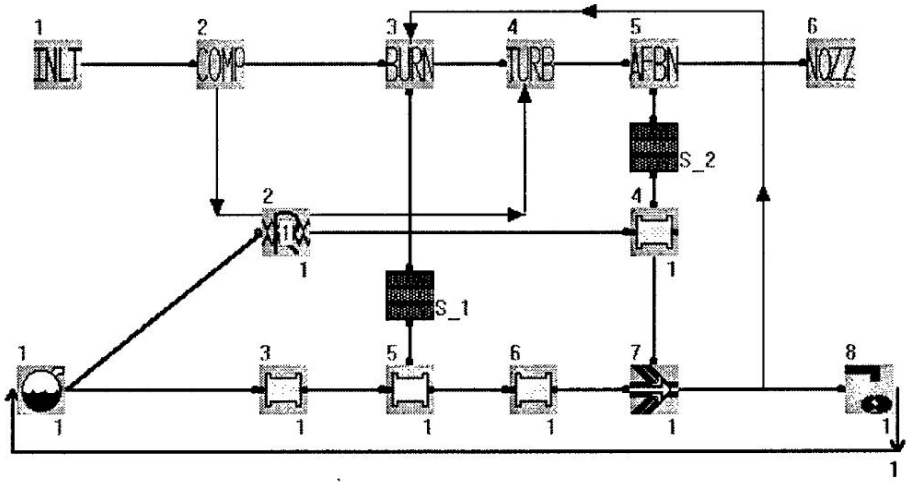

Figure 11: Example of Early Turbojet Engine Cooling Network Modeling Work [80].

Cipollone and Villante have used this approach to develop a fully transient engine and thermal management simulation to predict the warm-up behavior of ground vehicles [38, 39]. Similarly, Roberts has done significant work in the development of an integrated solid oxide fuel cell (SOFC) and turbine engine dynamic simulation in Simulink [140].

Tradeoffs have been conducted on a hybrid power thermal management system that relies on both on engine bleed and electrical power and have demonstrated some of the benefits of this hybrid approach [121]. Similarly, Bodie investigated a power thermal management system architecture in order to achieve optimum performance [24].

2.3 Improved Design through Integrated Modeling and Simulation

The current trend in conceptual design at the vehicle-level is to integrate together higher-fidelity simulations. This allows the designer to directly see the vehicle-level impact of complex subsystem interactions. Liscouët-Hanke published a very important article emphasizing the benefits of system-level power system architecting [97]. This work examined the development of an integrated framework that was comprised of multiple subsystem models in order to arrive at an "energy-balanced design." She continually stressed the need for integrated modeling and simulation and parametric architecture tradeoffs.

Researchers at AFRL have created an integrated electrical subsystem Simulink model used on the INVENT program. This work includes an electrical accumulator, generator, and distribution system integrated into a system-level simulation [188]. Additional work in industry has looked at integrated aircraft energy modeling [93] with a recent effort examining integrated electrical and thermal subsystem optimization using Simulink [23]. In the context of thermal management, Moorhouse has emphasized that "a system-level thermal management analysis capability, centered

on modeling and simulation (M&S), is the single most important technology that requires development" [115].

A substantial amount of research on aircraft subsystem design and optimization has been conducted by von Spakovsky and Rancruel [3]. The most relevant to this research is the creation of a multidisciplinary fighter aircraft model [132], which is illustrated in Fig. 12.

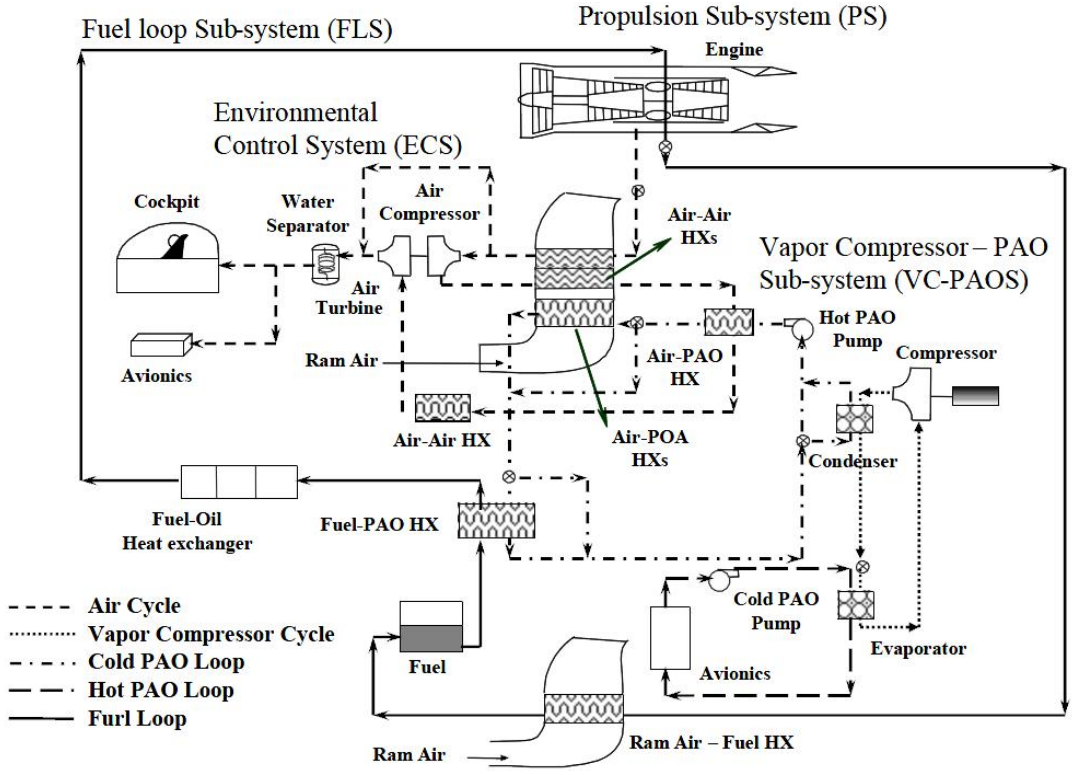

Figure 12: Integrated Aircraft and Subsystems Simulation with Exergy Formulation [132].

This was a significant advancement in the field of integrated aircraft modeling and simulation, and the subsystems also consisted of transparent, physics-based models. These researchers examined the use of multi-level optimization to attempt to optimize the total system with respect to a global exergy metric. This will be discussed further in later sections of this chapter.

Recent work, such as the tip-to-tail modeling work by Bodie, Russell, McCarthy,

et al. at AFRL, has embraced this approach. However, a significant drawback to this work was that some of the included models were proprietary and their contents inaccessible to the designer [25]. This prevented the user from modifying their contents or viewing their underlying physics. A similar approach was taken by Maser, Garcia, and Mavris in the development of an integrated propulsion and thermal management modeling environment without proprietary restrictions [102]. For that effort, the propulsion system was modeled in NPSS and the thermal management system was modeled in Simulink. This work was further improved and transitioned to a generic, system-level tip-to-tail modeling environment by Roberts, Eastbourn, and Maser [139]. That effort was conducted entirely in Simulink. These two simulations served as a foundation for the work in this study. As a result, the tactical fighter simulation is discussed in detail in Appendix A, and the generic tip-to-tail is detailed in Appendix B.

The preceding discussion of integrated modeling and simulation and its benefits suggests that this approach could be a useful tool to the propulsion systems designer in dealing with the thermal management challenges outlined in Chapter I. The integrated simulation of the propulsion and thermal management would also seem to provide the designer with the necessary information concerning their interactions and performance. This leads to the development of the first major research question and its formal statement:

Research Question #1a: Does the integrated simulation of the propulsion and thermal management systems during the conceptual engine design process significantly improve the designer's ability to explicitly consider and fulfill thermal requirements than simply designing the engine in isolation?

Chapter III is devoted to this research question. A hypothesis is first posed there, followed by the requisite experimental approach, theory, implementation, and results.

2.4 Thermodynamic Work Potential and Irreversibility Losses

The previous integrated propulsion and thermal management systems design work by Maser, Garcia, and Mavris [102] and Roberts, Eastbourn, and Maser [139] focused on the energy exchanges between the subsystems, i.e. a first law energy balance. However, Szargut notes that:

> *"The majority of causes of thermodynamic imperfection of thermal and chemical processes cannot be detected by means of an energy balance. For example, irreversible heat loss, throttling, and adiabatic combustion are not associated with an energy loss, but they lead to a decrease of the energy quality, reduce its ability to be transformed into other kinds of energy, and, therefore, increase the operational costs or the first costs of installation"* [164].

Since energy is actually a conserved quantity, what is really required is a way to quantify the energy that is available to do useful work. This leads to the concept of exergy, which Bejan defines as "a measure of quality of various kinds of energy" [15]. These exergy-based analyses are developed from a combination of the first and second laws of thermodynamics. These techniques are widely used within the ground-based power generation industry [56], but only limited work has been conducted within aircraft subsystems design.

Unlike energy, exergy is not a conserved quantity and irreversible processes result in its destruction. The main contributors to the destruction of exergy are "friction, heat transfer with finite temperature difference, diffusion, [and] combustion" [15]. Exergy destruction is directly related to the entropy production through the Gouy-Stodola Theorem: [33]

$$\dot{X}_{loss} = T_{amb}\,\dot{S}_{prod} \tag{6}$$

where $\dot{X}_{loss}$ is the exergy destruction rate, $\dot{S}_{prod}$ the entropy production rate, and T_{amb} the ambient temperature. Figure 13 illustrates the concept of exergy on the traditional Mollier diagram with respect to the Carnot loss.

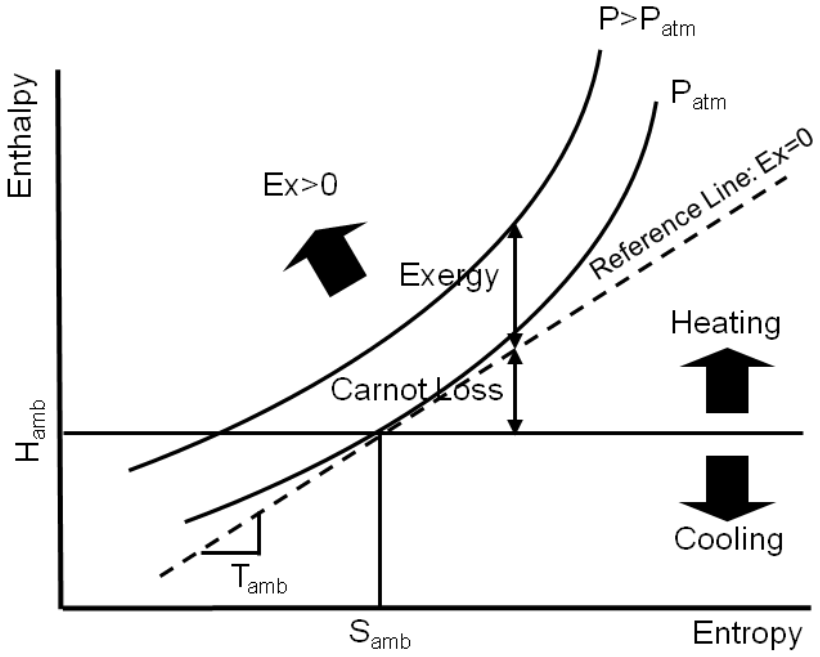

Figure 13: Illustration of Exergy Definition [147].

Exergy is also closely related to the concept of free energy with the important distinction of being defined at the ambient dead state. Gibbs free energy is a special cases for an isothermal and isobaric process, while Helmholtz free energy is for an isothermal and isochoric process. It represents the maximum flow work available to the system by coming into equilibrium with the environment [33]. Further discussion of exergy and its theoretical underpinnings is provided in Chapter IV.

2.4.1 Application to Propulsion Systems Design

Although thermodynamic work potential techniques first found widespread usage in ground-based systems, there has also been research into their application to aircraft propulsion systems design. The seminal journal article in this area by Clarke and Horlock entitled "Availability and Propulsion" serves as the basis for future work

on exergy in propulsion systems design [40]. Roth further expanded this work and demonstrated the benefits of a second-law analysis in the conceptual design of aircraft engines [147]. In this work, Roth notes that: "Propulsion system performance can be analytically quantified in terms of work potential (and loss thereof) relative to a thermodynamic ideal through the use of combined first and second law methods" [147]. Denton actually examines the origins and the mechanisms of losses within engines instead of only focusing on their prediction [49].

Roth took the work potential concept one step further and translated it into a chargeable fuel weight characterization [146], which he then used to perform propulsion technology impact evaluations [144]. Figure 14 illustrates the effect of propulsion systems design trades on the amount of work potential lost as well as the breakdown of losses in terms of a fuel weight.

An important point to note is that since exergy calculates useful work by assuming the potential for equilibrium with the environment in terms of pressure and temperature, the ideal Brayton cycle will still result in the destruction of exergy due to the heat and kinetic energy remaining in the exhaust as well as the incomplete combustion within the burner. There are other thermodynamic work potential figures of merit that can be used in place of exergy, such as available energy and thrust work potential, which relax some of these constraints. For example, available energy only enforces an equilibrium in pressure and not temperature. Roth and Mavris provide an excellent review on the subject [145].

Roth has derived formulations of these figures of merit for each of the components within the propulsion system. As an example of this, the pressure loss across an engine component can be converted into an exergy loss and then effectively compared to the other losses within the system [143]:

$$x_{loss} = T_{amb} R \left(1 - \frac{\Delta p}{p}\right) \tag{7}$$

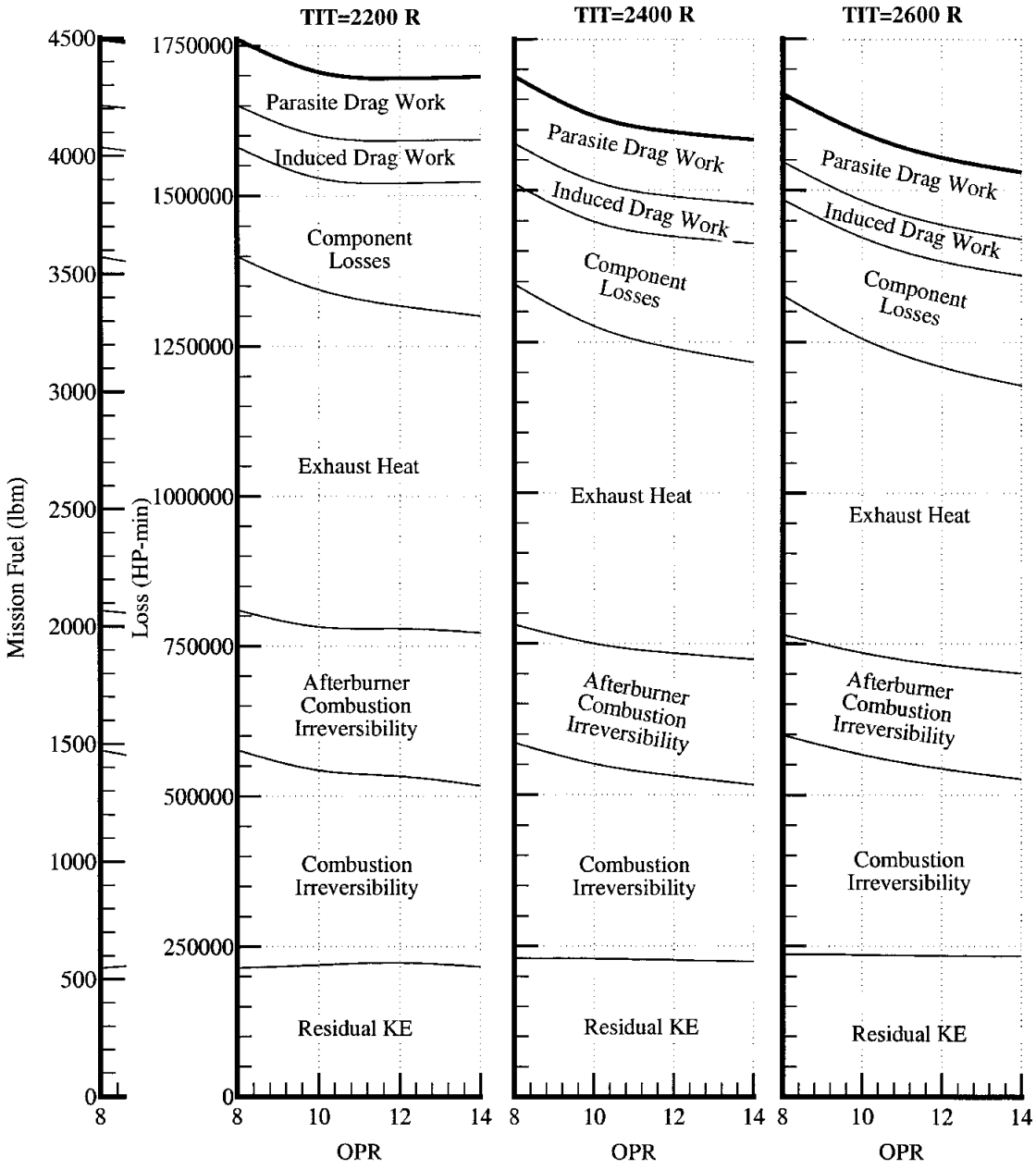

Figure 14: Impact of Engine Design Choices on Exergy Destruction and Chargeable Fuel Weight [144].

where x_{loss} is the intensive exergy destruction, T_{amb} the ambient temperature, R the gas constant, and p the pressure.

2.4.2 Irreversibility Characterization of Aircraft Subsystems

In addition to the work advanced by Roth in conceptual engine design, the concept of using exergy analysis has also been demonstrated in aircraft design decision making [114, 128]. Roth has even explicitly suggested that "total airframe thermal management...is germane to the topic of [work potential]" [147]. A significant summary of research into the application of exergy design techniques for aerospace vehicle design is presented in a recent book by Camberos and Moorhouse [33].

Thermodynamic work potential techniques have also been successfully applied to aircraft thermal subsystem design. Vargas, Bejan, and Siems first applied the concept of entropy generation minimization to the design of a simple aircraft environmental control system (ECS) [171]. The most prolific work in this area was a follow-on study conducted by Tipton and Figliola [165]. They investigated the thermal optimization of an environmental control system using a second-law analysis [62]. This work is of particular interest to the current research efforts and is illustrated in Fig. 15. These researchers conducted their second-law analysis using a normalized entropy generation equation that they used to track the losses within their model.

Rancruel and later Smith applied an exergy optimization approach to aircraft subsystem design [159]. Furthermore, Riggens has performed an analysis on the interactions between the vehicle and its wake from a second-law perspective [138], and he has also investigated the thermodynamic availability of an integrated vehicle and scramjet engine configuration.

Thermodynamic irreversibility is identified as a common metric that can be used with second-law-based design techniques to trade off and visualize integrated subsystem interactions. Models incorporating these second-law techniques can help to

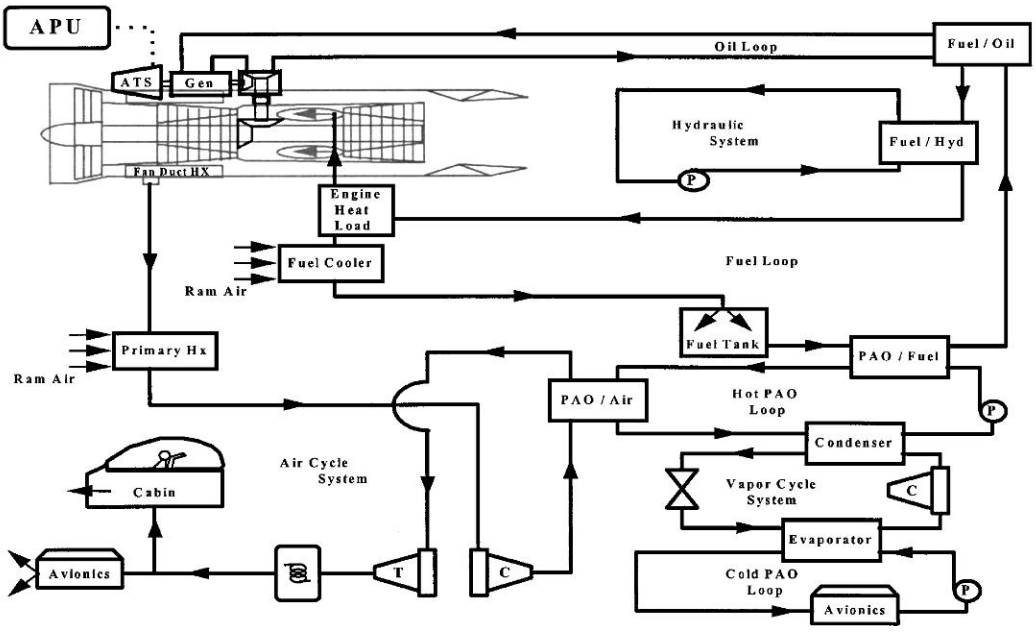

Figure 15: Entropy Generation Analysis of Combined Engine and ECS [61].

achieve a clearer view of the associated integrated propulsion and thermal management tradeoffs.

Riggens has summarized this:

> *"Because of this correspondence between current methods and the global availability, the single but critical advantage of the global availability methodology over current optimization techniques is in the uniformity of the loss metric (i.e., the 'common currency' of entropy production) and the ability to analyze in fluid and thermodynamic detail losses in component and subsystem performance in terms of that single loss metric"* [33].

One of the challenges that motivated this research effort was the inconsistent performance metrics that describe the behavior and losses of the propulsion and thermal management systems. This concept of directly invoking the second-law of thermodynamic to characterize the irreversibility environment of the system shows obvious promise in addressing this challenge. This leads to the statement of the second research question:

Research Question #1b: Is the characterization of the exergy destruction on a component basis able to provide the propulsion systems designer a more consistent and absolute metric to trade off the integrated performance of the propulsion and thermal management system?

The investigation of this research question is further explored in Chapter IV.

2.5 Second-Law-Based Design Techniques

There are three main categories of second-law-based techniques. These are generally grouped into exergy analysis, thermodynamic optimization (or entropy generation minimization), and thermoeconomics [13]. Each of these techniques have shown promise in the design of thermodynamic systems, and they are all worthy of investigation with respect to their application into integrated propulsion and thermal management systems design. The next three sections provide an overview of each of these categories.

2.5.1 Exergy Analysis

The first of these, exergy analysis, is the most general in its application. Essentially exergy analysis is the direct application of the second-law during the analysis of thermodynamic systems. It is focuses on "identifying the mechanisms and system components that are responsible for losses...[and] the sizes of these losses" [15]. This concept is now introduced in many recent introductory engineering thermodynamic texts [34, 94]. *Advanced Engineering Thermodynamics* by Bejan provides a particularly useful discussion of the concept [14]. The idea of leveraging exergy analysis for aircraft design was discussed in [15].

2.5.2 Thermodynamic Optimization

Entropy generation minimization (EGM) takes the concept of exergy analysis a step further by combining constrained optimization techniques with the idea of exergy analysis. EGM is simply stated as the "minimization of thermodynamic irreversibility in real-world applications by accounting for the finite-size constraints of actual devices and the finite-time constraints of actual processes" [16]. This concept is mathematically described as [13]:

$$\sum_{\text{components}} \sum_{\text{features}} \sum_{\text{dx dy dz}} S_{gen,min} \tag{8}$$

where $S_{gen,min}$ is the minimum entropy generation per unit volume. Here the system is designed in such a way that the entropy generation is minimized at each level from the discretization of a feature of a component up to the system. Bejan summarizes by saying that "Thermodynamic optimization is, literally, the search for the best thermodynamic performance subject to present-day constraints" [16].

Entropy generation minimization (EGM) work by Vargas, Bejan, and Siems was applied to heat exchanger sizing [171]. The system that they used consisted of an air cycle machine, a ram air heat exchanger, and engine compressor bleed air. It is illustrated in Fig. 16. Using this model, the overall entropy generation minimization was performed by minimizing the quantity:

$$\begin{aligned}\dot{S}_{gen} =& \dot{m}_e \left[\left(c_p ln\frac{T_1}{T_a} - Rln\frac{p_1}{p_a} \right) + \left(c_p ln\frac{T_2}{T_1} - Rln\frac{p_2}{p_1} \right) \right. \\ &\left. + \left(c_p ln\frac{T_3}{T_2} - Rln\frac{p_3}{p_2} \right) + \left(c_p ln\frac{T_4}{T_3} - Rln\frac{p_4}{p_3} \right) \right]_e \\ &+ \dot{m}_a \left(c_p ln\frac{T_{out}}{T_{in}} - Rln\frac{p_{out}}{p_{in}} \right)_a + \dot{m}_a c_p ln\frac{T_a}{T_{a,out}} + \frac{\dot{Q}_e}{T_a}\end{aligned} \tag{9}$$

In this equation, $\dot{S}_{gen}$ represents the extensive entropy generation rate, $\dot{m}_e$ the mass flow rate through the hot side of the heat exchanger, $\dot{m}_a$ the mass flow rate through

the cool side of the heat exchanger, and $\dot{Q}_e$ the heat transfer to ambient. R represents the gas constant and c_p the specific heat.

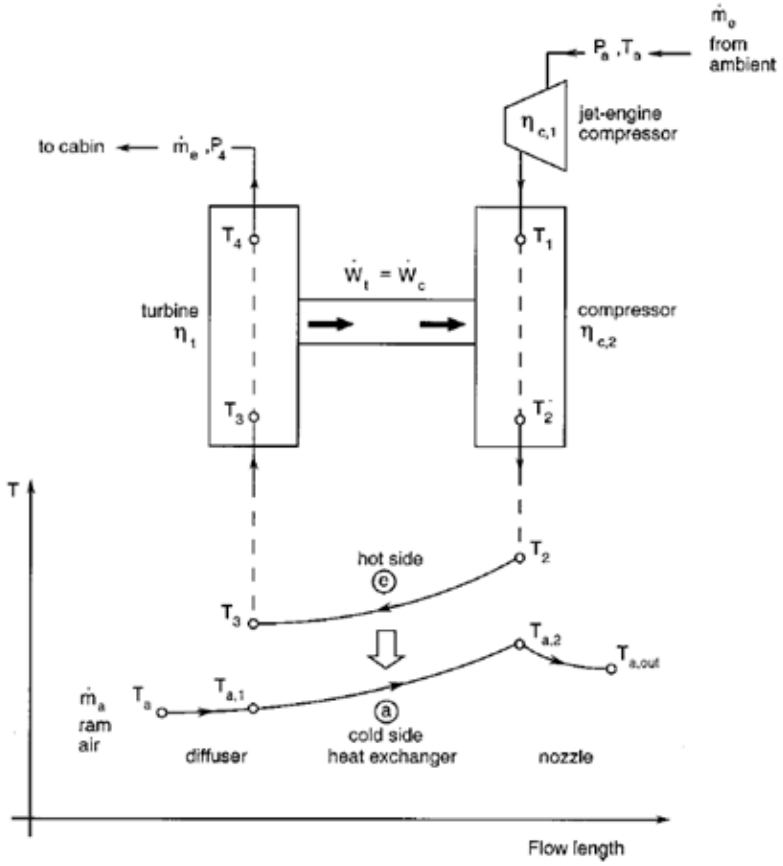

Figure 16: Vargas, Bejan, and Siems Environmental Control System Model [171].

In this case, this is accomplished by redesigning the heat exchanger in isolation. This optimization is constrained by the physical dimensions of the heat exchanger, which are related to the performance through physical relationships. One issue noted by Berry is that "The major limitation of the exergy approach is that it takes into account only those contributions to the irreversibility of the process which are due to equalization of system parameters with those of the environment" [20].

Bejan has broadened the concept of thermodynamic optimization to the evolution of natural systems by developing a concept that he has termed the constructal theory [17, 19, 12]. The basic concept of constructal theory is that natural systems are constantly searching to minimize their losses. He formally states the theory as: "For

a finite-size open system to persist in time (to survive) it must evolve in such a way that it provides easier and easier access to the currents that flow through it" [18].

2.5.3 Thermoeconomics

The concept of thermoeconomics builds on the thermodynamic optimization philosophy by directly considering exergy destruction and cost minimization simultaneously [56, 55, 176]. There is some controversy in regards to this concept since cost is not an absolute metric and is difficult to estimate. Therefore, it is viewed by some as a corruption of the absolute and consistent features of pure thermodynamics. Szargut has noted that "Exergy is a thermodynamic notion, not an economic one, and these attempted economical applications were strongly criticized" [164].

Nevertheless, cost must somehow be brought into the fold as the thermodynamic ideal is of little use the propulsion systems designer who must juggle multiple design criteria. There has also been significant success in the application of thermoeconomics to the design of large ground-based power systems [56]. Finally, it should be noted that "Exergy loss indicates always the possibility of thermodynamic improvement of the process, but the profitability of such an improvement should be checked by means of an economical analysis" [16]. There are three essential elements to thermoeconomics: calculation of exergy destruction on a component basis, calculation of cost on a component basis, and then the minimization of a combined exergy and cost metric. The minimization is written as [56]:

$$\min \sum_i \left(c_D D_i + c_z z_i\right) \tag{10}$$

Here D_i represents the component exergy destruction and z_i represents the component cost. They are then related through the constants c_D and c_z so that they can be treated as a single metric in the minimization.

A thermoeconomic formulation of the integrated propulsion and thermal management systems design problem seems to be a reasonable means of beginning to address the irreversibility allocation question described in Chapter I. It should provide guidance to the propulsion systems designer in the proper way of handling the allocation of system losses in the context of non-thermodynamic criteria. This leads to the first of three research questions dealing with the proper allocation of irreversibility:

Research Question #2a: Does the posing of the integrated thermal management systems design problem in thermoeconomic terms enable the designer to quantitatively identify more favorable system-level designs?

Chapter V is devoted to answering this research question and addresses the thermoeconomic formulation in more detail.

2.6 Extension of Exergy-Based Methods to Aircraft Conceptual Design

Dinçer has noted two major differences between aircraft and ground-based energy systems. The first is a change in the engine cycle: Jet engines rely on the open Brayton cycle. Secondly, jet engines experience a constantly changing operating environment [51].

These translate to three main differences between ground-based power production and jet engine design. The change in the engine cycle means that there is now considerable wasted exergy in the exhaust that is required for thrust production. This wasted exergy is in the form of kinetic energy and heat. The exhaust of ground-based power production systems, on the other hand, has almost reached the ambient state. This means that the exhaust must be taken into account in the system-level exergy calculations for aerospace vehicles as Riggens has previously noted [137].

The ever-changing environment also results in two additional design differences. The first is the simple fact that the ambient conditions change throughout mission.

This impacts both the inlet air properties as well as the definition of the environment for the exergy calculations. The second is that the aerospace vehicle's mission requirements become very important to the design. Ground-based power systems are usually designed to operate at a single design point for their duration. Yet in aerospace systems, the engine must continuously throttle up or down to fulfill the requirements of the vehicle as dictated by the mission. This necessitates the consideration of off-design operation during the design of the propulsion system.

The culmination of this research is intended to link the integrated propulsion and thermal management systems design to its impact at the vehicle-level. In order to achieve this, it is essential to bridge the gap between the integrated systems design and the vehicle-level impacts of these design choices. A traditional approach to examining the integrated effects of the propulsion and thermal management systems at the vehicle-level is to relate the thermal management design elements to engine performance impacts through empirical curve fits. Accounting for horsepower extraction and engine compressor bleed air is an important aspect of the propulsion modeling that is directly affected by the thermal management system. As an example, the following approximation is used to assess the fuel weight bleed air penalty [148]:

$$\Delta w_f = 0.0335 \left[\frac{T_{tb}}{2000}\right] w_b \tag{11}$$

where w_f is the fuel flow rate in lb/hr, T_{tb} is the turbine inlet temperature in °R, and w_b is the bleed air flow rate in lb/hr.

This is further expressed at the vehicle-level in terms of a fuel weight penalty by assuming a constant power extraction penalty [148]:

$$\frac{W_{fo}}{w_b} = 0.0335 \left[\frac{L/D}{(SFC)_{th}}\right] \left[\frac{T_{tb}}{2000}\right] \left[\left(e^{\frac{(SFC)_{th}\tau}{L/D}}\right) - 1\right] \tag{12}$$

where W_{fo} is the takeoff fuel weight in lb, L/D is the lift-to-drag ratio of the vehicle, τ is the mission duration in hr, and SFC is the specific fuel consumption in lb/hr-hp.

Likewise, the similar expression for shaft power extraction fuel weight penalty as a first approximation is [148]:

$$\frac{W_{fo}}{P\,(SFC)_p} = \frac{L/D}{(SFC)_{th}} \left[\left(e^{\frac{(SFC)_{th}\tau}{L/D}} \right) - 1 \right] \tag{13}$$

where P is the power consumed in hp.

Empirical models are often similarly used to model aircraft engine thrust and fuel consumption effects [152, 9]. This type of approach has been used to evaluate heat sink options for a more electric aircraft concept [11]. The author of that work includes a very relevant discussion concerning engine and thermal management system interactions. It specifically examines the associated bleed air and shaft power penalties for a vapor cycle system and their effect on engine performance by using a simple engine model.

A more sophisticated means of linking the mission performance requirements to the design of the integrated propulsion and thermal management systems is through a model of the air vehicle itself. This approach was also taken in the previous efforts of Bodie, Russell, McCarthy, et al. [25], Maser, Garcia, and Mavris [102], and Roberts, Eastbourn, and Maser [139].

The energy-based formulation of [104] that was used previously by Maser, Garcia, and Mavris [102] calculates a thrust requirement at each point as a result of the current vehicle drag, weight, and mission profile requirements:

$$[T - (D + R)]\,V = W\frac{dh}{dt} + \frac{W}{g}\frac{d}{dt}\left(\frac{V^2}{2}\right) \tag{14}$$

where T is the thrust, D the drag, R the other resistive forces, V the velocity, W the weight, h the altitude, g the acceleration due to gravity, and t time. In Eq. 14, the left-hand side represents the rate of mechanical energy input, while the right-hand side is the sum of the storage rate of potential and kinetic energy [104].

The inclusion of an off-design modeling capability and vehicle model enables the

designer to better consider mission requirements. This can lead to more accurate and less conservative results by cutting into vehicle safety margins.

Now this brings the discussion to the second irreversibility allocation research question. Due to the critical differences between the design of aerospace systems and ground-based power systems, it seems that the consideration of the design point thermodynamics and cost only may fail to capture an important aspect of the design of aerospace systems: vehicle mission performance. The fourth research questions is formally stated here:

Research Question #2b: How can the design process be modified so that the designer can explicitly take vehicle mission performance into account along with thermodynamics and cost for the integrated propulsion and thermal management problem?

More detail on the vehicle model, off-design performance, and mission requirements will be covered in Chapter VI, which is focused on addressing this research question.

2.7 System-Level Optimization Implications

Now that the importance of thermodynamics, cost, and performance has been established, it is necessary for the designer to consider how best to balance these competing metrics and design a configuration that is optimal at the system-level. Vanderplaats writes that "The purpose of numerical optimization is to aid us in rationally searching for the best design to meet our needs" [170]. Numerical optimization is widespread in all fields of engineering, especially in aerospace systems design. One challenge in aerospace systems design is that there are often competing metrics vying for improvement, such as cost and performance. The AFRL INVENT program has been very

interested in the concept of the energy optimized aircraft. Due to the program's understanding of these competing goals, it defines the energy optimized aircraft as "an aircraft that is optimized for broad capabilities while maximizing energy utilization (aircraft and ground support) with the minimum complexity system architecture" [179].

2.7.1 Multidisciplinary Design, Analysis, and Optimization

The field of multidisciplinary design optimization (MDO) is well established, and within this community there are numerous multi-level MDO methods. These methods focus on local-level subsystem optimizations, while managing subsystem contributions to the global-level (vehicle) optimization. The two most well-known multi-level MDO methods are Collaborative Optimization (CO) [27, 26], which was developed by Braun, and Bi-Level Integrated System Synthesis (BLISS) [160], which was developed by Sobieszczanski-Sobieski. The Collaborative Optimization method is shown in Fig. 17.

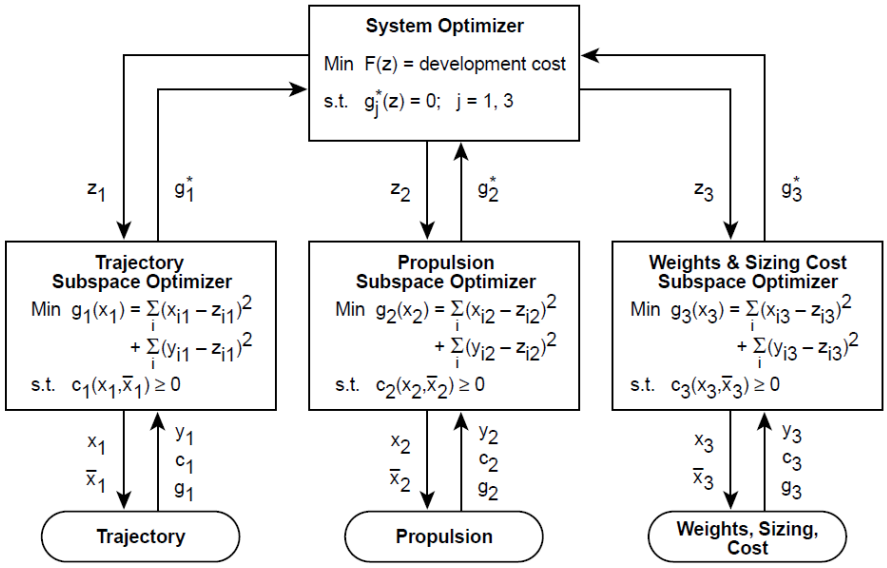

Figure 17: Illustration of Collaborative Optimization Technique [28].

The previously discussed integrated aircraft model by Munoz used a similar MDO method that they refer to as Local-Global Optimization (LGO) [117]. They have also introduced an improved version of this method known as Iterative Local-Global Optimization (ILGO) [175]. These researchers were able to use this method to produce partially optimized results; however, they stated that 'initial partial optimizations of the nine-subsystem AAF [air-to-air fighter] showed the estimated time-to-optimize at nearly 7 months" [159]. Other work has continually demonstrated this drawback to traditional system-level optimization: It has been difficult to perform meaningful optimization in this area due to numerical difficulties.

2.7.2 Benefits of Design of Experiments, Surrogate Modeling, and Stochastic Optimization

There are a few different ways to attempt to remedy these types of system-level optimization challenges. One technique that has been frequently applied successfully in the design of aerospace systems is to leverage knowledge from the the field of design of experiments (DOE) to create simpler and computationally faster surrogate models of the initial physics-based models. A DOE is an intelligent way of organizing and selecting the necessary model runs so as to obtain the most information with the minimum executions [118].

The field of surrogate modeling is already very mature and is regularly implemented in many aspects of aerospace design, such as compressor blade optimization [149], airfoil design [172], and multifidelity simulations. An excellent comparison of surrogate modeling techniques applied to design is presented in [125]. This discussion directly compares response surface equation, kriging, and artificial neural network techniques. The popular second-order response surface equation, which has found applicability in a large variety of problems is of the form [118]:

$$\eta = \beta_0 + \sum_{i=1}^{k} \beta_i x_i + \sum_{i=1}^{k} \beta_{ii} x_i^2 + \sum_{i=1}^{k-1} \sum_{j=i+1}^{k} \beta_{ij} x_i x_j \tag{15}$$

where the response η is in terms of linear constants β and the design parameters x.

Another technique for dealing with system-level optimization challenges is to use non-gradient-based optimization routines, such as genetic algorithms, simulated annealing, or particle swarm optimization [170]. The popular genetic algorithm routine represents the design variables as a single binary string. A large population of randomly generated design strings is created, and subsequent rounds perform various operations on these strings until they begin to converge on a specific design string. The random nature of this algorithm is intended to prevent the optimizer from settling on local minima, which is a recurring problem with standard gradient-based optimizers. The principle disadvantage of stochastic optimizers, like genetic algorithms, is that they do not mathematically guarantee that any optimum will actually be obtained [170].

2.7.3 Multi-Objective Optimization and Design Space Tradeoffs

A second problem with using a second-law-based optimization approach is that it views the optimization from a strictly thermodynamic viewpoint; this problem can be best summarized by Moran:

> *"A procedure with the final objective to maximize the thermodynamic efficiency in the design of a new system has no practical value and should be considered only in conjunction with other objectives such as, for example, the minimization of costs and pollutant emissions"* [16].

This issue is most easily addressed by integrating these non-thermodynamic criteria into the system-level optimization. Since a numerical scheme must work to minimize a single metric, an overall evaluation criterion (OEC) is needed to merge

these competing goals together. This is simply a weighted average of the system metrics:

$$OEC = \alpha \frac{A}{A_{ref}} + \beta \frac{B_{ref}}{B} + \gamma \frac{\Delta \mathrm{C}}{\mathrm{C}_{ref}} \tag{16}$$

Here each of these individual metrics are normalized by a constant reference parameter, likely at the design point, so that they are of the same order of magnitude. Then, the constants α, β, and γ are used as weighting factors to represent their relative importance. The formulation can also vary slightly to address the need to maximize, minimize, or target specific metrics. In this example it is desired to minimize A, maximize B, and hit a target for C.

As an example, this concept could relate the thermodynamics, cost, and performance through a weighted average of the total exergy destruction, cost, and performance:

$$OEC = \alpha \sum_{comp} \frac{\dot{X}_D}{\dot{X}_{D_{ref}}} + \beta \sum_{comp} \frac{z}{z_{ref}} + \gamma \left(\frac{\Delta \mathrm{Perf.}}{\mathrm{Perf.}_{ref}} \right) \tag{17}$$

The obvious problem with this approach is that it relies on weightings that are fairly arbitrary. An alternative approach, which has the potential of finding a more defensible solution, is to minimize the overall system cost. This is similar to the thermoeconomic approach that was discussed earlier:

$$\min\ J = \sum_i \left(c_D D_i + c_z z_i \right) \tag{18}$$

The main difference between this approach approach and the OEC approach is that by converting the metrics to a cost, the weighting factors are chosen in a more traceable manner. In this case, the first terms represents the operating cost of the system due to fuel burn, while the second term represents the production cost. The drawback to this approach is that the cost information is often much more difficult to

accurately predict than the thermodynamic. Also, since everything must be converted to a cost, performance requirements cannot be directly accounted for and must serve as constraints on the problem.

In general, the aerospace design community has shifted away from a pure numerical form of optimization at the system-level and towards more of an emphasis on design space tradeoffs [106]. This tradeoff approach to design enables the designer to meet multiple objectives and deal with the inherent non-uniqueness encountered in the design of complex systems. This leads to the concepts of Pareto optimality, filtered Monte Carlo, and other multi-objective optimization techniques.

Paulus views exergy-based approaches as "the key to the decomposition of energy systems and allows concurrent engineering of the several devices that may make up an overall system" [127]. As such, a bulk of the work in this research is focused on the improved integration of second-law-based techniques with traditional system-level aircraft design. This then leads to the concentration on an approach to search for optimal system-level irreversibility allocations.

The culmination of this background discussion has focused on the system-level optimization approaches to concurrently considering thermodynamics, cost, and performance. Specifically, automated MDO techniques were discussed and shown to have some difficulty in addressing the irreversibility allocation problem. Finally, this leads to the fifth research question, which brings everything else together. It is formally stated here:

Research Question #2c: Can the designer improve upon a strict numerical optimization of the integrated propulsion and thermal management systems by directly allocating the component irreversibility with regards to cost and vehicle performance?

Finally, Chapter VII concentrates on the experimental plan to address this question.

2.8 Overview of Research Questions

The experiments are divided into two major groups. The first set tackles the integrated design question and serves as the foundation of the research. The second group of experiments then builds on this to form the core research, which is focused on the irreversibility allocation and the search for its optimum. The five research questions are repeated here:

- Integrated Design (Foundation)
  - **Research Question #1a:** Does the integrated simulation of the propulsion and thermal management systems during the conceptual engine design process significantly improve the designer's ability to explicitly consider and fulfill thermal requirements than simply designing the engine in isolation?
  - **Research Question #1b:** Is the characterization of the exergy destruction on a component basis able to provide the propulsion systems designer a more consistent and absolute metric to trade off the integrated performance of the propulsion and thermal management system?
- Irreversibility Optimization (Allocation)
  - **Research Question #2a:** Does the posing of the integrated thermal management systems design problem in thermoeconomic terms enable the designer to quantitatively identify more favorable system-level designs?
  - **Research Question #2b:** How can the design process be modified so that the designer can explicitly take vehicle mission performance into account along with thermodynamics and cost for the integrated propulsion and thermal management problem?

- **Research Question #2c:** Can the designer improve upon a strict numerical optimization of the integrated propulsion and thermal management systems by directly allocating the component irreversibility with regards to cost and vehicle performance?

Each of these questions is examined separately in the next five chapters and a hypothesis is formed for each as previously noted. From this, an experiment is designed to test the hypothesis. These experiments are intentionally designed to build on one another to arrive at the overall research objective.

CHAPTER III

MEETING REQUIREMENTS THROUGH INTEGRATED MODELING AND SIMULATION

This chapter addresses the first of five experiments; the next four chapters similarly concentrate on the other research questions encountered in Chapter II. The first of these, which is covered here, is the integrated modeling and simulation. This is the foundation for all of the rest of the work and is therefore a very important feature that warrants a particularly detailed discussion. Later, the thermodynamic irreversibility, economic, and aircraft mission performance elements are explored. These three elements then flow into the irreversibility allocation process, which is investigated in Chapter VII.

3.1 Statement of Research Hypothesis #1a

The first research question tackles the concept of integrated propulsion and thermal management systems design. There is specifically no mention of irreversibility yet, since it is first necessary to examine the benefits of the integrated modeling and simulation approach. It is suspected that the integrated modeling and simulation of the propulsion and thermal management systems enables the designer to create a better performing system.

This chapter begins with a formal statement of the first research hypothesis. This hypothesis stems from the background research into integrated modeling and simulation from the second chapter. Next, an experiment is designed to confirm or deny this hypothesis, and the respective experimental approach is presented. An in-depth review of the necessary theory for this experiment is reviewed; this then leads to its

implementation in the form of a software simulation. The chapter concludes with a description of the experimental results and a resulting discussion. This structure is subsequently followed for the next four chapters as well for the remaining research questions.

From the previous background research in Chapter II, a hypothesis is now posed for the first research question:

Research Question #1a: Does the integrated simulation of the propulsion and thermal management systems during the conceptual engine design process significantly improve the designer's ability to explicitly consider and fulfill thermal requirements than simply designing the engine in isolation?

Research Hypothesis #1a: The additional design information available to the system designer from the simulation of the integrated propulsion and thermal management physics during the conceptual design of the engine cycle enables the designer to better meet system-level requirements than by designing the engine cycle design in isolation.

In order to test this hypothesis, it is necessary to directly compare the design of an engine in isolation to the integrated system design. To do this, a canonical propulsion and thermal management system-level modeling and simulation environment is required to be developed. This system simulation can then be compared to the propulsion subsystem simulation in isolation.

Previously, it was explained that the integrated system simulation is particularly important in future systems due to the growing heat loads from high-power electronics. These heat loads are expected to necessitate a change in the propulsion system's design. As a result, it is also helpful to examine the case of a system with a high power heat load in comparison to the more traditional case. The difference between these two cases should demonstrate the more pressing need for integrated modeling

and simulation in future more-aggressive configurations.

The two systems, isolated engine and integrated, are compared at a single design point. At this point, the better performing configuration will be demonstrated through a reduction in fuel burn.

3.2 Experimental Approach

Now an experimental plan is presented in response to the research question. All of the experiments are divided into two major groups. The first set tackles the integrated design question and serves as the foundation of the research. The second group of experiments then builds on this to form the core research, which is focused on the irreversibility allocation and the search for its optimum.

The sequence of experiments tests each individual aspect of the allocation approach in order to build up to the final objective: a technique for directly allocating irreversibility to the integrated propulsion and thermal management system in the context of cost and performance constraints.

This first experiment is represented in Table 1 graphically. For the experiment, there are four different cases. The first case, Case A, simulates only the engine subsystem in isolation. This model is used for the design containing a traditional heat load. Case B then looks at this same heat load, but with the full integrated system-level model. The comparison between Cases A and B should be able to demonstrate the benefit of the integrated modeling and simulation approach for propulsion and thermal management systems. However, it is anticipated that this benefit may be somewhat minimal due to the smaller interactions between the two. This can be viewed as one of the justifications for previously designing the subsystems in isolation.

Cases C and D are then the corresponding cases for the higher, more-aggressive heat load. Case C corresponds to the isolated engine design shown in Case A, while Case D uses the integrated system of Case B. In is expected that the differences

between these two cases will be more significant due to the higher heat load and greater subsystem interactions.

Table 1: Experiment #1a: Integrated Propulsion Systems Design.

A Isolated engine design Traditional heat load	**B** Integrated systems design Traditional heat load
C Isolated engine design High heat load	**D** Integrated systems design High heat load

The main steps of this first experiment are summarized here:

- Include the thermal management subsystem physics in a canonical propulsion and thermal management system architecture model
- Compare this against an isolated engine simulation where simplified assumptions have been made in regards to thermal requirements
- Investigate the differences in these two simulations at a single design point
- Demonstrate a mission-level performance improvement through a reduction in fuel burn

3.3 Theory

Next, the overall theory necessary to carry out the experiment is presented. This leverages the theory of the last section and further elaborates on the experimental plan before the actual implementation is presented.

The first topic covered is the integrated modeling and simulation needed to correctly predict the engine and thermal systems interactions. This was explained earlier as a means of addressing thermal challenges during the conceptual design of the engine cycle. It is also a direct response to the first hypothesis.

Based on the previous background, it is obvious that the first major component to this research is the integrated propulsion and thermal management systems modeling and simulation. This is necessary to capture the major interactions between the configurations. Much work in this area has already been conducted, including the INVENT tip-to-tail modeling that was previously discussed [25]. Here this integrated approach to propulsion and thermal management modeling and simulation is presented. Although there can be substantial variation in the fidelity and scope of the models, this section describes the main features that must be addressed for this research.

There are a few aspects that need to be present in the subsystem models. The first is a component-level representation of the major components. Secondly, the models need to have a thermodynamic representation of the relevant physics and the capability of predicting temperatures, pressures, and other thermal performance parameters throughout the system. This requirement is especially important in the context of the irreversibility characterization highlighted in the next chapter. Finally, the integrated modeling environment should incorporate a system-level solver that can enforce physical and design constraints throughout the system. This is further discussed in [56].

Two previous research efforts by the author are reviewed extensively in the appendix. These two modeling and simulation environments, a tactical fighter [102] and generic tip-to-tail [139], provide the type of information that is required for this research. Of course, due to the emphasis on engine design here, the engine model is a critical piece of the integrated model and is discussed at length. These engine models

contain all of the necessary elements for this research as well. However, other types and fidelities of models could be used ranging from closed-form empirical equations to complex industrial codes.

There are a few problems with using the existing models in the context of conceptual design. First, the fidelity of these previous models is fairly high and the model execution can be quite lengthy. For this research, many cases are required to be run in order to examine the full design space. Even more problematic is that they were designed for a single design point solution and are not robust to changes in design parameters. Conceptual design requires that the models be extremely robust so that large sweeps of the design space can be quickly performed. Finally, since these models were designed to operate in a performance mode exclusively (i.e., fly a single design through a mission), they do not have the capability to parametrically reconfigure the system into a new design. This is a major requirement in the work performed here.

As a result of the challenges posed by the existing models, this effort uses simplified canonical models as explained in the following sections. The more complex models could be used directly instead if these challenges are solved; however, it was decided that this research should be presented as transparently as possible. An example of a research study moving towards a simpler, more canonical architecture is the fuel thermal model posed by German [67]. Nevertheless, this previous modeling and simulation work strongly influences the design decisions for the present modeling environment. This work leverages all of the lessons learned from the previous work; it adds the required on-design capabilities, while simultaneously eliminating all of the extraneous features that are unnecessary for the present studies. Although the creation of a new modeling and simulation environment required a large amount of additional work upfront, it provided significant advantages in the long term since it was tailor-made for the problem at hand.

3.3.1 Component Model Development

All of the models and components in this study are created from first principles; no ready-made components are utilized. This was done to increase the clarity of the study and prevent additional system modeling complexity. The models are intentionally more fundamental than the earlier models presented in [102] and [139]. In addition, all of the models are steady-state in nature in order to more clearly illustrate and characterize the system irreversibility. The models were developed exclusively in MATLAB with separate functions for each of the individual components. A lumped element, steady-state modeling approach similar to the approach taken in El-Sayed [56] was used. The remainder of this section highlights the major theory behind each of the component models. These component equations follow the derivations presented in Mattingly [104] and Hill and Peterson [73].

3.3.1.1 Inlet

The conditions throughout the engine are characterized in terms of stagnation properties. Stagnation temperature and pressure are calculated as a function of Mach number as

$$T_0 = T_{amb}\left(1 + \frac{\gamma - 1}{2}M^2\right) \tag{19}$$

and

$$p_0 = p_{amb}\left(1 + \frac{\gamma - 1}{2}M^2\right)^{\frac{\gamma}{\gamma-1}} \tag{20}$$

where γ is the ratio of specific heats and M the Mach number. The ratio of specific heats is defined as

$$\gamma = \frac{c_p}{c_v} = \frac{c_p}{c_p - R} \tag{21}$$

where c_p is the specific heat at constant pressure and c_v is the specific heat at constant volume. The inlet irreversibility loss is represented through an efficiency factor η that reduces the isentropic stagnation pressure as the flow proceeds through the component. This can be used to compute the output stagnation pressure as

$$p_{0_{out}} = p_{0_{amb}} \left[\eta \left(\frac{T_{0_{out}}}{T_{0_{amb}}} \right)^{\frac{\gamma}{\gamma-1}} \right] \tag{22}$$

3.3.1.2 Compressor

The pressure ratio is the main requirement for the compressor component. From this information, the output stagnation pressure and temperature are computed as

$$p_{0_{out}} = p_{0_{in}} (PR) \tag{23}$$

and

$$T_{0_{out}} = T_{0_{in}} (PR)^{\frac{\gamma-1}{\gamma \eta_{poly}}} \tag{24}$$

where η_{poly} is the polytropic efficiency of the compressor component and PR is the pressure ratio.

Alternatively, this is calculated as:

$$T_{0_{out}} = T_{0_{in}} \left[1 + \frac{1}{\eta} \left(PR^{\frac{\gamma-1}{\gamma}} - 1 \right) \right] \tag{25}$$

where η is the adiabatic efficiency.

The output mass flow rate is simply the difference of the input flow rate and the required compressor bleed:

$$\dot{m}_{out} = \dot{m}_{in} - \dot{m}_{bleed} \tag{26}$$

The required power to drive the compressor that must be delivered by the turbine is then

$$\dot{W}_{comp} = \dot{m} c_p \left(T_{0out} - T_{0in} \right) \tag{27}$$

3.3.1.3 Splitter

The splitter is a simple component used to split the flow into two separate streams. A bypass ratio is specified and the mass flow is subsequently partitioned as

$$\dot{m}_{out_{core}} = \frac{\dot{m}_{in}}{1 + BPR} \tag{28}$$

and

$$\dot{m}_{out_{bypass}} = \dot{m}_{in} \left(\frac{BPR}{1 + BPR} \right) \tag{29}$$

The stagnation temperatures and pressures remain the same as before the splitter. No irreversibility is included in this component, although a friction pressure drop could easily be included if required.

3.3.1.4 Burner

The fidelity of the combustor in the previous studies was increased to take into account the enthalpy contribution of fuel preheating. Instead of using an assumed lower heating value (LHV) as in

$$\dot{m}_{fuel} = \dot{m}_{air} \frac{c_{p_{avg}} \left(T_{out} - T_{air} \right)}{\eta LHV} \tag{30}$$

the fuel chemistry was considered directly. For the calculations, complete combustion was assumed, and chemical kinetics were neglected. The jet fuel was modeled as kerosene. The stoichiometric kerosene combustion equation is

$$2C_{12}H_{26} + 37\left(O_2 + 3.76N_2\right) \rightarrow 24CO_2 + 26H_2O + 37\left(3.76N_2\right) \tag{31}$$

This can be generalized for various amounts of fuel and air as

$$\begin{aligned} N_{fuel}\left(C_{12}H_{26}\right) + N_{air}\left(O_2 + 3.76N_2\right) \rightarrow & 12N_{fuel}\left(CO_2\right) + 13N_{fuel}\ \left(H_2O\right) + \\ & \left(N_{air} - 18.5N_{fuel}\right)\left(O_2\right) + \\ & N_{air}\left(3.76N_2\right) \end{aligned} \tag{32}$$

Using this information, an energy balance can then be used to calculate the required fuel flow rate:

$$\begin{aligned} & \sum_{i=fuel} N_i\left[h_{f_i} + c_{p_i}\left(T_{fuel} - T_{ref}\right)\right] + \\ & \sum_{i=\{O_2,N_2\}} N_i\left[h_{f_i} + c_{p_i}\left(T_{air} - T_{ref}\right)\right] = \sum_{i=prod} N_i\left[h_{f_i} + c_{p_i}\left(T_{ad} - T_{ref}\right)\right] \end{aligned} \tag{33}$$

Here h_f represents the heat of formation, N the number of moles of the substance, and T_{ad} the adiabatic flame temperature. In the model all of the temperatures and amounts of air are known and the amount of fuel is computed. The adiabatic flame temperature is the design T_4 for the engine. Tables of heats of formation and specific heats for each of the chemical constituents are also included in the burner component. Finally, there is an additional efficiency used to account for nonadiabatic and incomplete combustion effects, which serves to increase the required fuel flow rate:

$$\dot{m}_{fuel} = \frac{\dot{m}_{fuel,ideal}}{\eta} \tag{34}$$

3.3.1.5 Turbine

The output stagnation temperature of the turbine component is computed by taking into account the power that it is required to produce: the sum of the compressor

power and shaft power extraction. The resulting temperature decrease is

$$T_{0out} = T_{0in} - \frac{\dot{W}_{comp} + HPX}{\dot{m}_{in} c_p} \tag{35}$$

HPX is the shaft power extraction and $\dot{W}_{comp}$ the required compressor power. The pressure is then found by initially assuming an isentropic expansion and then applying a polytropic efficiency factor as was done with the compressor:

$$p_{0out} = p_{0in} \left(\frac{T_{0out}}{T_{0in}} \right)^{\frac{\gamma}{(\gamma-1)\eta_{poly}}} \tag{36}$$

The alternative calculation using the adiabatic efficiency is:

$$p_{0out} = p_{0in} \left[1 - \frac{1}{\eta} \left(1 - \frac{T_{0out}}{T_{0in}} \right)^{\frac{\gamma}{\gamma-1}} \right] \tag{37}$$

3.3.1.6 Mixer

The static pressures for each of the input streams are computed as

$$p_{in} = \frac{p_{0in}}{\left[1 + \left(\frac{\gamma-1}{2} \right) M_{in}^2 \right]^{\frac{\gamma}{\gamma-1}}} \tag{38}$$

and

$$T_{in} = \frac{T_{0_{in}}}{1 + \left(\frac{\gamma-1}{2} \right) M_{in}^2} \tag{39}$$

The bypass area is found using a specified Mach number as

$$A_{bypass} = \frac{\dot{m}_{bypass}}{p_{bypass} M_{bypass}} \sqrt{\frac{R T_{bypass}}{\gamma}} \tag{40}$$

The mixer is modeled to have a constant area at the inlet and outlet, and the core and bypass areas are assumed to be equal. The final exit Mach number can then be determined by

$$M_{out} = \frac{\dot{m}_{out}}{p_{out} A_{out}} \sqrt{\frac{R T_{out}}{\gamma}} \tag{41}$$

3.3.1.7 Nozzle

The nozzle exit velocity is calculated as

$$v_e = c_v \sqrt{2 \left(\frac{\gamma}{\gamma - 1} \right) R T_{0out} \left[1 - \left(\frac{p_{amb}}{p_{0out}} \right)^{\frac{\gamma - 1}{\gamma}} \right]} \tag{42}$$

where the irreversibility is modeled using the velocity coefficient, c_v, to reduce the exit velocity from the isentropic case. This exit velocity can then be used to find the exhaust temperature:

$$T_{out} = T_{0out} - \left[\frac{V_e^2 (\gamma - 1)}{2 \gamma R} \right] \tag{43}$$

3.3.1.8 Heat Exchanger

Parallel-plate heat exchanger physics were used to develop the heat exchanger model [171]. The number of transfer units (NTU) method was used to determine the heat exchanger effectiveness:

$$\epsilon = 1 - exp \left(\frac{(\dot{m} c_p)_{cold}}{(\dot{m} c_p)_{hot}} (NTU)^{0.22} \left\{ exp \left[- \frac{(\dot{m} c_p)_{hot}}{(\dot{m} c_p)_{cold}} (NTU)^{0.78} \right] - 1 \right\} \right) \tag{44}$$

where NTU is defined as:

$$NTU = \frac{1}{\dot{m}_{hot} c_{p_{hot}} \frac{t_w}{k_w A_w}} \tag{45}$$

which is in terms of the heat exchanger wall thickness t_w, the thermal conductivity k_w, and the area A_w.

This effectiveness then reduces the maximum heat exchange rate, which is determined using the heat capacities of the two streams:

$$\dot{Q} = \epsilon \left(T_{hot} - T_{cold}\right) min \left[\left(\dot{m}c_p\right)_{hot}, \left(\dot{m}c_p\right)_{cold}\right] \tag{46}$$

Once the heat rate is determined, then the output temperatures are easily computed as

$$T_{out} = T_{in} \pm \frac{\dot{Q}}{\dot{m}c_p} \tag{47}$$

where the negative sign is for the hot stream and the positive sign is for the cold stream. The heat exchanger pressure drop calculation is

$$\begin{aligned} p_{out} = & p_{in} + \frac{\dot{m}^2}{2\rho_{in}A_c^2}\left\{\left[1 - \left(\frac{A_c}{A_f}\right)^2\right] + 2\left(\frac{\rho_{in}}{\rho_{out}} - 1\right) + \right. \\ & \left. f\frac{A}{A_c}\frac{\rho_{in}}{\bar{\rho}} - \left[1 - \left(\frac{A_c}{A_f}\right)^2\right]\frac{\rho_{in}}{\rho_{out}}\right\} \end{aligned} \tag{48}$$

Here A_c represents the cross-sectional area, A_f the stream area, A the heat transfer area, and $\bar{\rho}$ the average density. Further detail regarding the heat exchanger calculations can be found in [15].

3.3.1.9 Heat Load

A pressure drop is defined for each heat load component. The output stagnation pressure then becomes

$$p_{0_{out}} = \left(1 - \frac{\Delta p}{p}\right) p_{0_{in}} \tag{49}$$

For an air stream, the stagnation temperature is first computed as an isentropic expansion and then increased due to the specified heat addition:

$$T_{0_{out}} = T_{0_{in}} \left(\frac{p_{0_{out}}}{p_{0_{in}}}\right)^{\frac{\gamma-1}{\gamma}} + \frac{\dot{Q}}{\dot{m}c_p} \tag{50}$$

This is slightly modified for the liquid fuel to

$$T_{0_{out}} = T_{0_{in}} + \frac{p_{0_{out}} - p_{0_{in}}}{c_p \rho_{in}} + \frac{\dot{Q}}{\dot{m} c_p} \tag{51}$$

3.3.1.10 Fuel Pump

The fuel pump is very similar to the compressor model; the main difference is that the working fluid is a liquid. As a result the temperature increase becomes

$$T_{0_{out}} = T_{0_{in}} + \frac{p_{0_{out}} - p_{0_{in}}}{c_p \rho_{in} \eta} \tag{52}$$

The required pressure increase is a requirement of the pump, as was the case for the previous compressor. Once again, the power requirement is

$$\dot{W}_{pump} = \dot{m} c_p \left(T_{0_{out}} - T_{0_{in}} \right) \tag{53}$$

3.3.2 Calculation of Thermodynamic Properties

The component models from the last section can be linked together to form a wide variety of propulsion and thermal management system models. To do this, however, there must also be a capability in place to track the thermodynamic properties throughout the system. For this study, thermodynamic packages were created for the air and fuel.

This approach allows the designer to instantly view the fluid properties at important stations throughout the models at any time. The thermodynamic package has the capability of calculating the mass flow rate, pressure, temperature, density, specific volume, internal energy, enthalpy, specific heats, entropy, and exergy. Most of these properties are tabulated as a function of pressure and temperature.

For the research, air was assumed to behave as a thermally perfect gas. Therefore, the specific heats are tabulated as a function of temperature

$$c_p = c_p\,(T) \tag{54}$$

and the enthalpy of the fluids is calculated as

$$h = c_p\,T \tag{55}$$

The air density is calculated using the perfect gas equation of state

$$\rho = \frac{p}{R\,T} \tag{56}$$

while the fuel is assumed to behave as an incompressible liquid. Details about the entropy and exergy calculations are presented in the next chapter.

3.3.3 System-Level Solver for Nonlinear System of Equations

Another key feature of the thermodynamic modeling capability is a system-level solver that is capable of simultaneously meeting several different design constraints. For example, it may be desired to adjust the engine inlet mass flow rate to obtain a desired design thrust. In this case, the independent variable is x and the dependent variable is the error between the actual and desired thrust values and is denoted as f. The constraint equations are then written as a vector of functions that is set equal to $\vec{0}$:

$$\vec{f} = \vec{y}_{LHS} - \vec{y}_{RHS} = \vec{0} \tag{57}$$

LHS and RHS represent the left-hand side and right-hand side of the constraint equations.

In practice, the system must solve a system of nonlinear constraint equations for each design. This is accomplished using Newton's method [120, 170], which utilizes the Taylor series expansion to linearize the system:

$$\vec{f}\left(\vec{x}+\vec{dx}\right) \approx \vec{f}\left(\vec{x}\right) + J_f\left(\vec{x}\right)\vec{dx} + \ldots \tag{58}$$

By ignoring higher order terms and setting $\vec{f}\left(\vec{x}+\vec{dx}\right) = 0$, then the update function for Newton's method is

$$\vec{x}_{k+1} - \vec{x}_k = \vec{dx} = -J^{-1}\vec{f}\left(\vec{x}_k\right) \tag{59}$$

where the Jacobian is defined as [29]

$$J = \begin{bmatrix} \dfrac{\partial f_1\left(\vec{x}\right)}{\partial x_1} & \cdots & \dfrac{\partial f_1\left(\vec{x}\right)}{\partial x_n} \\ \vdots & \ddots & \vdots \\ \dfrac{\partial f_m\left(\vec{x}\right)}{\partial x_1} & \cdots & \dfrac{\partial f_m\left(\vec{x}\right)}{\partial x_n} \end{bmatrix} \tag{60}$$

The derivatives in the Jacobian matrix are not calculated analytically. Instead, they are calculated through a finite difference

$$\frac{\partial f}{\partial x} = \frac{f\left(x+h\right) - f\left(x\right)}{h} \tag{61}$$

for a very small h.

Furthermore, a damping is added to the update function to keep the solver from overshooting the solution and causing convergence problems. The formula for the update function then simply becomes

$$\vec{x}_{k+1} - \vec{x}_k = \vec{dx} = -\alpha J^{-1}\vec{f}\left(\vec{x}_k\right) \tag{62}$$

where the damping is defined as

$$\alpha = \frac{1}{1 + \left\|\vec{dx}\right\|} \tag{63}$$

This has the effect of slowly relaxing the damping as the solver approaches the solution. Finally, it is worth noting that the Jacobian matrix should not be inverted

directly. It is much more computationally efficient to instead solve the system of equations [29]

$$J\vec{dx} = -\alpha\vec{f}(\vec{x}) = \vec{b} \tag{64}$$

by performing elementary row operations to obtain the reduced row echelon form of the augmented matrix $\left[J|\vec{b}\right]$.

The solver then terminates when the root sum of squares of the error terms is acceptably small relative to some tolerance ϵ:

$$\sqrt{\sum_i \left(y_{LHS_i} - y_{RHS_i}\right)^2} < \epsilon \tag{65}$$

3.4 Implementation

The physics formulations from the previous theory section are now used to create an integrated, system-level model of a propulsion and thermal management system in MATLAB. To do this, a canonical system architecture is first established from which all of the experiments in this study are conducted. Next, the subsystem models are explained along with details about the system-level solver and model execution.

The modeling and simulation environment detailed in this chapter is used as a baseline on which other features are then built upon in the remainder of the experiments. This tool was appropriately named Cycle Refinement for Thermodynamically Optimized Subsystems (CRATOS) after the Greek personification of power.

In Chapter IV, the second-law-based formulations are included to allow for the prediction of the component losses. Then, Chapter V details the cost prediction that is included into the environment. Chapter VI updates the environment quite substantially by adding an air vehicle model, mission profile, and off-design performance capability. This allows the designer to link the mission performance requirements directly to the propulsion and thermal management systems design. Finally, Chapter

VII looks at using the final iteration of the CRATOS environment to perform the system-level optimization and allocation.

An important feature of the CRATOS modeling and simulation environment is its ability to directly characterize the irreversibility of the integrated propulsion and thermal management system. As such, a detailed overview of the top-level user interface of CRATOS is saved for Chapter IV after the irreversibility theory is presented.

3.4.1 Subsystem Model Abstractions

For this study, it is necessary to develop canonical models of aircraft propulsion and thermal management systems. It is desired to have models that are representative of realistic subsystems, but also generic enough so as to not represent any one specific configuration. Because of this, abstractions of the propulsion and thermal management systems were created for the purpose of this research. These abstractions are intended to be as simple as possible while still capturing all of the salient characteristics. Three separate models were developed: a mixed flow turbofan (MFTF) engine, a power thermal management system (PTMS), and a fuel thermal management system (FTMS).

The MFTF engine model is illustrated in Fig. 18. The core airflow travels sequentially through the inlet, fan, splitter, high pressure compressor (HPC), burner, high pressure turbine (HPT), low pressure turbine (LPT), mixer, and nozzle. Additionally, there is a bypass stream that initially separates in the splitter, and then travels through an air-air heat exchanger before recombining in the mixer. The engine contains two spools, where the first enables the LPT to power the fan, and the second connects the HPT to the HPC. There are also additional model connection interfaces for the thermal system interactions. The MFTF model interacts with the other subsystem models through the fan-air heat exchanger and fuel, bleed, and shaft power extraction ports.

The thermal management system is subdivided into two separate subsystem abstractions for this research: the PTMS and the FTMS. The abstractions feature air and fuel loops, lumped heat loads in both the PTMS and FTMS, and an air-cycle machine. It is also desired to eliminate the need for ram air cooling; therefore, all waste heat must be rejected to either the engine fan stream or fuel. The PTMS and FTMS architecture abstractions are shown in Figs. 19 and 20.

The main feature of the PTMS is the air cycle machine, which is composed of a closed loop compressor and an additional turbine that is powered by bleed air from the engine compressor. The function of the closed loop air cycle is to first cool a portion of the engine bleed to a level suitable for the cockpit. The air loop then absorbs additional heat in series from the fuel (through a fuel-air heat exchanger) and a lumped heat load before rejecting it to the engine fan stream (through an air-air heat exchanger). This heat load is intended to represent waste heat created from components that must be air-cooled such as avionics.

The FTMS is comprised of the aircraft fuel loop and reservoir and mainly functions to pump a required fuel flow rate from the fuel tank to the MFTF engine. During this process, heat is also rejected to the fuel from a lumped heat load and the fuel-air heat exchanger. The lumped heat load is intended to represent waste heat from components such as the engine oil, generator, fuel pump, and high-power electrical loads. After fuel is delivered to the engine, the remaining fuel is pumped back to the fuel tank.

These subsystem architecture abstractions were originally presented in [103].

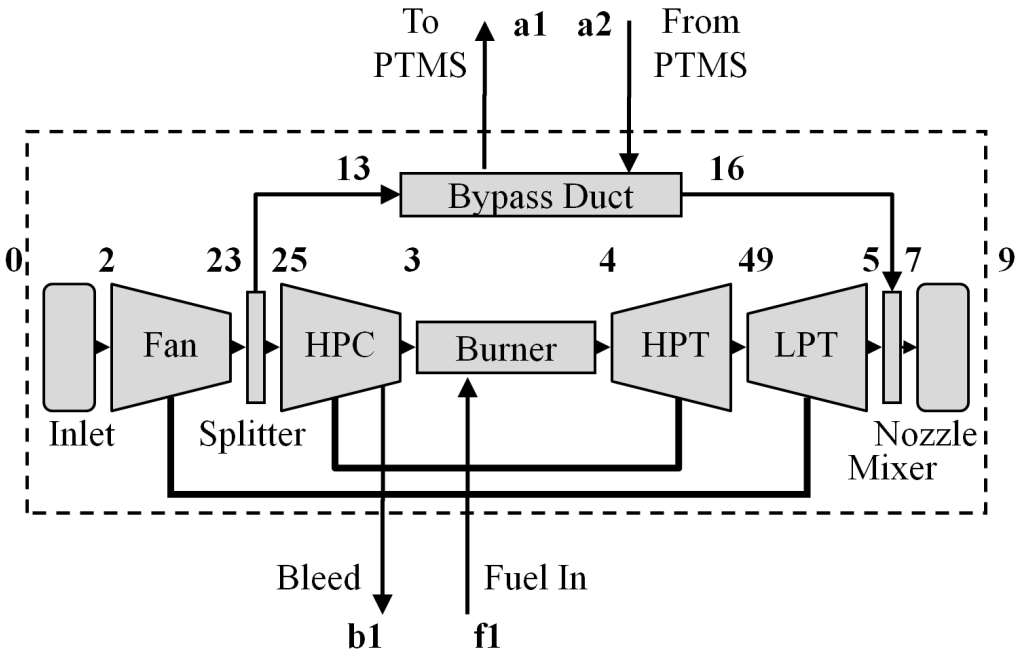

Figure 18: Canonical MFTF Engine Architecture.

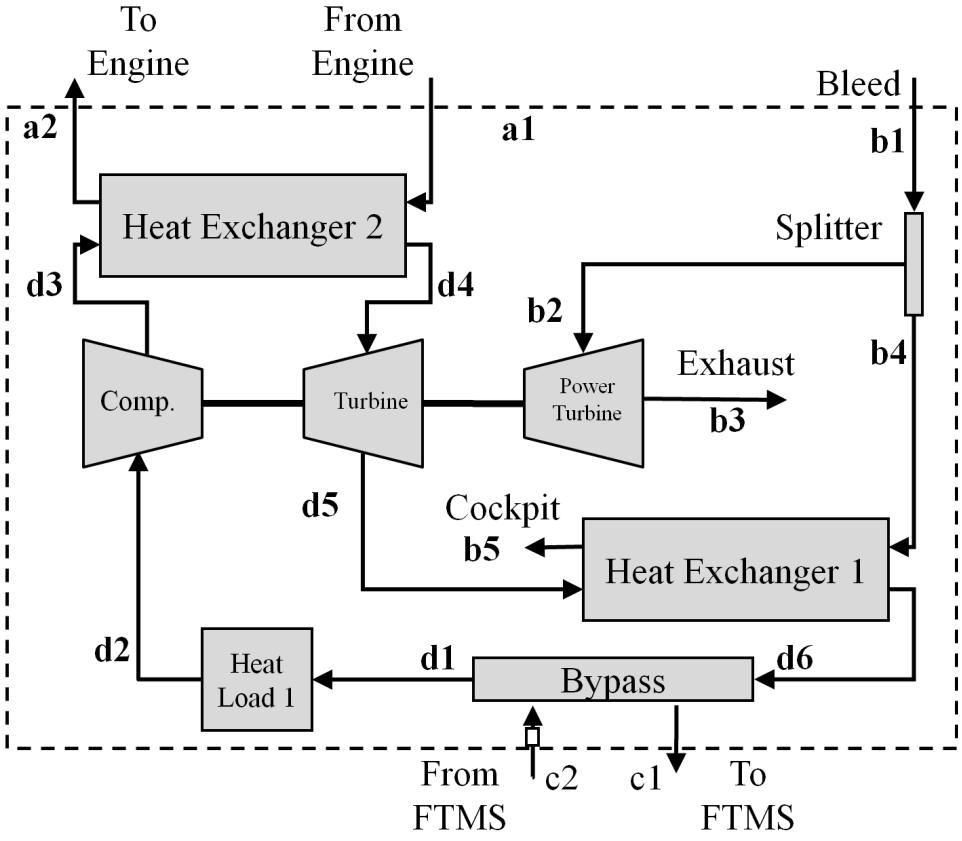

Figure 19: Canonical PTMS Architecture.

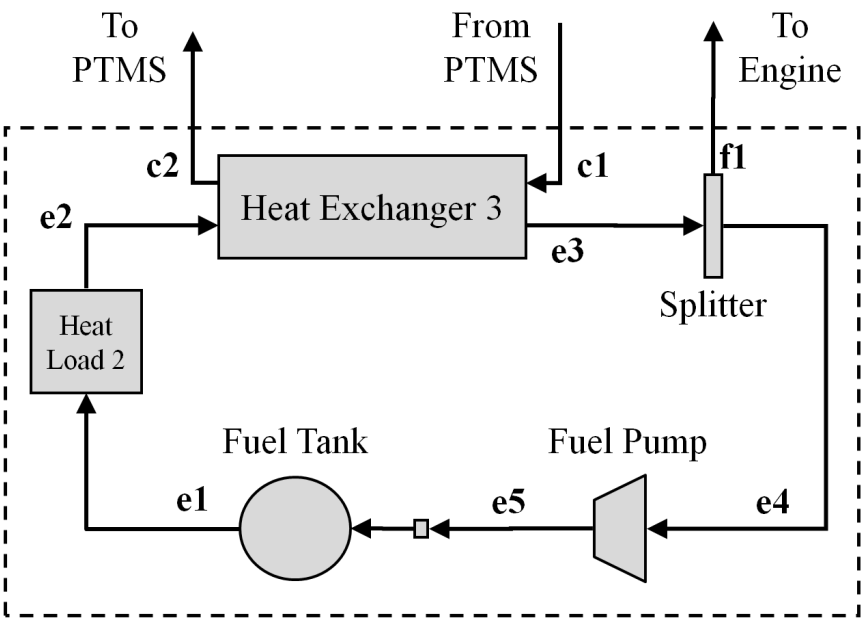

Figure 20: Canonical FTMS Architecture.

3.4.2 Subsystem Model Development

The components from the previous theory section were assembled into the engine, PTMS, and FTMS subsystems, which were subsequently integrated together. Table 2 lists the major components of each of the three subsystems used in this research. The rest of the section provides a brief overview of the major design parameters.

Table 2: Subsystem Components.

MFTF	PTMS	FTMS
Inlet	Heat Exchanger	Heat Exchanger
Compressor	Heat Load	Heat Load
Splitter	Splitter	Splitter
Burner	Compressor	Fuel Pump
Turbine	Turbine	
Mixer		
Nozzle		

A realistic baseline case was established for the integrated systems model. The inputs to the MFTF engine model are design thrust, overall pressure ratio (OPR), turbine inlet temperature (T4), and fan pressure ratio (FPR). The outputs are thrust

specific fuel consumption (TSFC), engine air mass flow, and bypass ratio (BPR). For the selected design case, the engine model chosen is based on the engine data from [104]. Table 3 shows the high-level parameters from three different military jet engines.

Table 3: Military Low-Bypass Turbofan Engine Parameters [104].

Engine	F-100-PW-229	F-101-GE-102	F-110-GE-100
Thrust [kN]	79.18	77.35	81.40
TSFC [(mg/s)/N]	20.96	15.92	41.64
Airflow [kg/s]	112.5	161.5	115.2
OPR	23.00	26.80	30.40
T4 [K]	1755	1672	-
FPR	3.800	2.310	2.980
BPR	0.4000	1.910	0.8000

Tables 4-6 list the major design parameters for each of the three subsystem models. A majority of the engine assumptions are from [104], whereas the PTMS and FTMS assumptions are from [15], [56], and [128].

Table 4: Mixed Flow Turbofan Engine Parameters.

Mach Number	0.20
Altitude	0.0
Ambient Pressure	101.3 kPa
Ambient Temperature	288.17 K
Overall Pressure Ratio	25
Fan Pressure Ratio	2.5
Turbine Inlet Temperature	1650 K
Design Thrust	90 kN
Compressor Bleed (HP)	0.70 kg/s
Compressor Bleed (LP)	0.0 kg/s
Shaft Power Extraction (HP)	37 kW
Shaft Power Extraction (LP)	0.0 kW
Inlet Efficiency	0.95
Fan Adiabatic Efficiency	0.85
HPC Adiabatic Efficiency	0.80
Burner Efficiency	0.99
HPT Adiabatic Efficiency	0.90
LPT Adiabatic Efficiency	0.90
Nozzle Velocity Coefficient	0.975

Table 5: Power Thermal Management System Parameters.

Cockpit Temperature Requirement	300 K
Cockpit Mass Flow Requirement	0.30 kg/s
Compressor Efficiency	0.70
Turbine Efficiency	0.80
Power Turbine Efficiency	0.80
Heat Exchanger (Engine/PTMS):	
Effectiveness	1.0
Normalized Pressure Drop (Hot Side)	0.20
Normalized Pressure Drop (Cold Side)	0.20
Heat Exchanger (PTMS/Bleed):	
Effectiveness	1.0
Normalized Pressure Drop (Hot Side)	0.20
Normalized Pressure Drop (Cold Side)	0.20
Closed Loop Pressure Ratio	15
Power Turbine Outlet Pressure	101.3 kPa
Heat Load:	
Heat Transfer Rate	25 kW
Normalized Pressure Drop	0.20

Table 6: Fuel Thermal Management System Parameters.

Fuel Temperature	450 K
FTMS Closed Loop Pressure	5.0 MPa
FTMS Recirculation Mass Flow	1.0 kg/s
Heat Load:	
Heat Transfer Rate	25 kW
Normalized Pressure Drop	0.20
Heat Exchanger (PTMS/FTMS):	
Effectiveness	0.50
Normalized Pressure Drop (Hot Side)	0.20
Normalized Pressure Drop (Cold Side)	0.20

3.4.3 Isolated Engine Model Execution

In order to properly conduct the experiments to compare the isolated engine and integrated system cases, two different models were created. First, the isolated engine was constructed out of the components from the theory section. The ambient conditions define the initial fluid properties entering the inlet. Then, the other components are executed linearly through the engine as shown in Table 7.

Table 7: Engine Model Component Execution Order.

Order	Component
1	Inlet
2	Fan
3	Splitter
4	HP Compressor
5	Burner
6	HP Turbine
7	LP Turbine
8	Mixer
9	Nozzle

Before the engine model is executed, it is necessary for an on-design (parametric) solver to be created. This solver uses initial guesses for various independent variables in an attempt to converge dependent constraints. For the isolated engine model, there are only two sets of independents and constraint equations. These are shown in Tables 8 and 9. Table 8 shows the independent variables, while Table 9 lists the on-design dependent constraint equations in terms of their left-hand side (LHS) and right-hand side (RHS). The first is a variation in the inlet engine mass flow rate to match a design thrust, and the second is a variation in the bypass ratio to ensure that the mixer inlet streams static pressures are equalized.

The solver iterates on the engine model until these two constraints are met, and then the necessary engine performance metrics are computed based on the final engine state properties.

Table 8: Isolated Engine Solver Independents for (Parametric) On-Design.

	Independent
1	Engine Mass Flow Rate
2	Bypass Ratio

Table 9: Isolated Engine Solver Dependents for (Parametric) On-Design.

	Dependent LHS	Dependent RHS
1	Engine Thrust	Design Thrust
2	Station 16 Static Pressure	Station 5 Static Pressure

3.4.4 Integrated System Model Execution

The integrated system model was similarly constructed using the components from the theory section and the three architecture abstractions shown earlier. Table 10 shows the model component order execution for the full integrated system model. This was specifically designed to minimize the number of solver constraints and speed up model execution time. Decreasing the number of required simultaneous constraints by trying to sequentially solve for independent variables whenever possible results in a smaller solver matrix and a much shorter model execution time.

Tables 11 and 12 list the on-design dependent constraint equations in terms of their left-hand side (LHS) and right-hand side (RHS) as well as their corresponding independent variables. The integrated system model starts with the two constraints from the isolated engine model, but also requires seven additional constraints. The first of these is a power balance on the air cycle machinery within the PTMS. The next two ensure temperature and pressure continuity in the PTMS air loop. Here the solver guesses a value at the beginning of the loop and then checks to see if this value is the same when it circles around the loop and returns to its initial location. The next equation is used to target a desired cockpit design temperature.

Constraint seven ensures temperature continuity in the FTMS fuel loop, and constraint eight sets a desired fuel recirculation flow rate. Finally, the last equation is used to target a maximum design temperature in the fuel loop.

Table 10: System Model Component Execution Order.

Order	Component	Subsystem
1	Inlet	Engine
2	Fan	Engine
3	Splitter	Engine
4	HP Compressor	Engine
5	PTMS Splitter	PTMS
6	Power Turbine	PTMS
7	Heat Load 1	PTMS
8	Closed Cycle Compressor	PTMS
9	Heat Exchanger 2	PTMS
10	Closed Cycle Turbine	PTMS
11	Heat Exchanger 1	PTMS
12	Heat Load 2	FTMS
13	Heat Exchanger 3	FTMS
14	Burner	Engine
15	FTMS Splitter	FTMS
16	Fuel Pump	FTMS
17	HP Turbine	Engine
18	LP Turbine	Engine
19	Mixer	Engine
20	Nozzle	Engine

Table 11: Integrated System Solver Independents for (Parametric) On-Design.

	Independent
1	Engine Mass Flow Rate
2	Bypass Ratio
3	Bleed Mass Flow Rate
4	Station d1 Temperature
5	Station d1 Pressure
6	Station d1 Mass Flow Rate
7	Station e1 Temperature
8	Station e1 Mass Flow Rate
9	Closed Loop Pressure Ratio

Table 12: Integrated System Solver Dependents for (Parametric) On-Design.

	Dependent LHS	Dependent RHS
1	Engine Thrust	Design Thrust
2	Station 16 Static Pressure	Station 5 Static Pressure
3	PTMS Compressor Power	PTMS Turbine Power
4	Station d1 Temperature	Station c2 Temperature
5	Station d1 Pressure	Station c2 Pressure
6	Station b5 Temperature	Cockpit Design Temperature
7	Station e1 Temperature	Station e4 Temperature
8	Station e4 Mass Flow Rate	Recirculation Design Mass Flow Rate
9	Station e2 Temperature	Fuel Loop Design Temperature

3.5 Results: Isolated Engine Versus Integrated System

Now that the foundation of the CRATOS environment is available, the first experiment can be conducted. This section will outline each of the cases and highlight their results. The graphical depiction of the first experiment is repeated in Table 13. There are four distinct cases for this experiment. These cases are intended to demonstrate the benefit of conducting an integrated propulsion and thermal management systems design as opposed to designing the engine in isolation. They also show the differences that arise from the introduction of higher thermal loads within the thermal management system.

3.5.1 Case A: Isolated Engine

For the first case, the propulsion system is examined in isolation. As previously explained, the propulsion system used in this study is a mixed-flow turbofan engine; its architecture and design parameters, at the specified design point, were also previously defined.

Table 13: Experiment #1a: Integrated Propulsion Systems Design.

A Isolated engine design Traditional heat load	**B** Integrated systems design Traditional heat load
C Isolated engine design High heat load	**D** Integrated systems design High heat load

In the modeling and simulation environment that was created for this work, there are four major interactions between the propulsion and thermal management systems. These interactions are the HP compressor bleed air, the HP shaft power extraction, the input fuel temperature, and the bypass air heat transfer rate. This high pressure air is used by the thermal management system to power the air cycle machine and cool the cockpit. The shaft power extraction is used to power the fuel pump and other ancillary equipment. The heat transfer into the fuel loop as a result of the thermal management system cooling affects the temperature of the fuel going into the engine combustor. Finally, a significant amount of heat is transfered into the engine bypass air from the PTMS heat exchanger. The compressor bleed, shaft power extraction, and bypass heat transfer were all set to zero for the isolated engine case. The input fuel temperature was set at 293 K (20°C).

The isolated engine design was then simulated using these assumptions. The major engine performance parameters obtained at the design point simulation are shown in Table 14. The engine cycle efficiencies are then shown in Table 15.

Table 14: Engine Performance Parameters.

Thrust	90.00 kN
Specific Thrust	472.95 N/(kg/s)
Air Mass Flow Rate	190.29 kg/s
Bypass Ratio	1.38
Exit Velocity	534.74 m/s
Initial Velocity	67.97 m/s
Fuel Mass Flow Rate	2.20 kg/s
Fuel-to-Air Ratio	0.0275
Thrust Specific Fuel Consumption	24.42 (mg/s)/N

Table 15: Engine Cycle Efficiencies.

Heat Input	96.77 MW
Power Output	27.08 MW
Thrust Power	6.11 MW
Thermal Efficiency	27.99%
Propulsive Efficiency	22.59%
Overall Efficiency	6.32%

As explained in the description of the on-design solver earlier, the thrust was a design variable. The other parameters were the result of the simulation. Aside from simply examining the design point, trade studies were also conducted with regards to several engine design parameters. The most important two parameters in the design of the jet engine are the overall pressure ratio (OPR) and turbine inlet temperature (T4) as previously explained in Chapter II. As a result, these were the first parameters investigated in this case. Figures 21-23 show the effect of varying the overall pressure ratio and turbine inlet temperature over a reasonable range of values on specific thrust, TSFC, and overall efficiency.

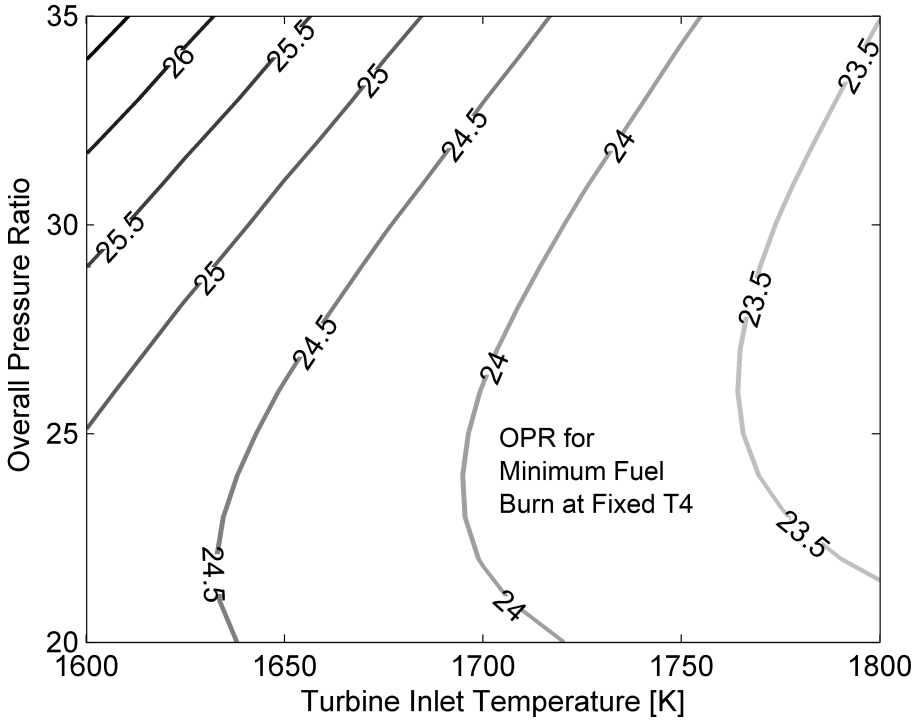

Figure 21: Isolated Engine Thrust Specific Fuel Consumption $[mg/s/N]$.

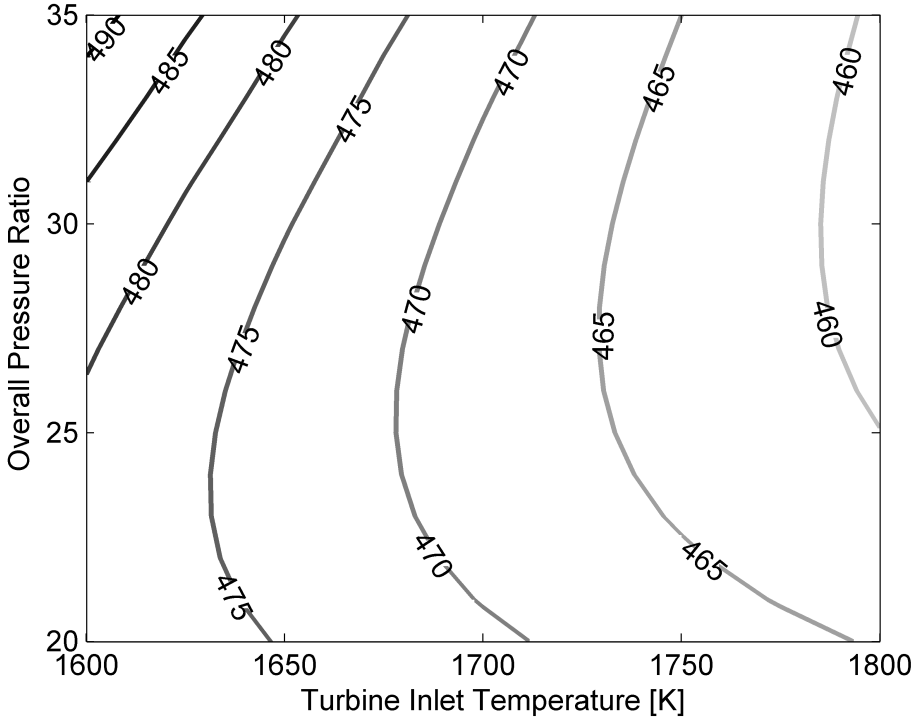

Figure 22: Isolated Engine Specific Thrust $[N/(kg/s)]$.

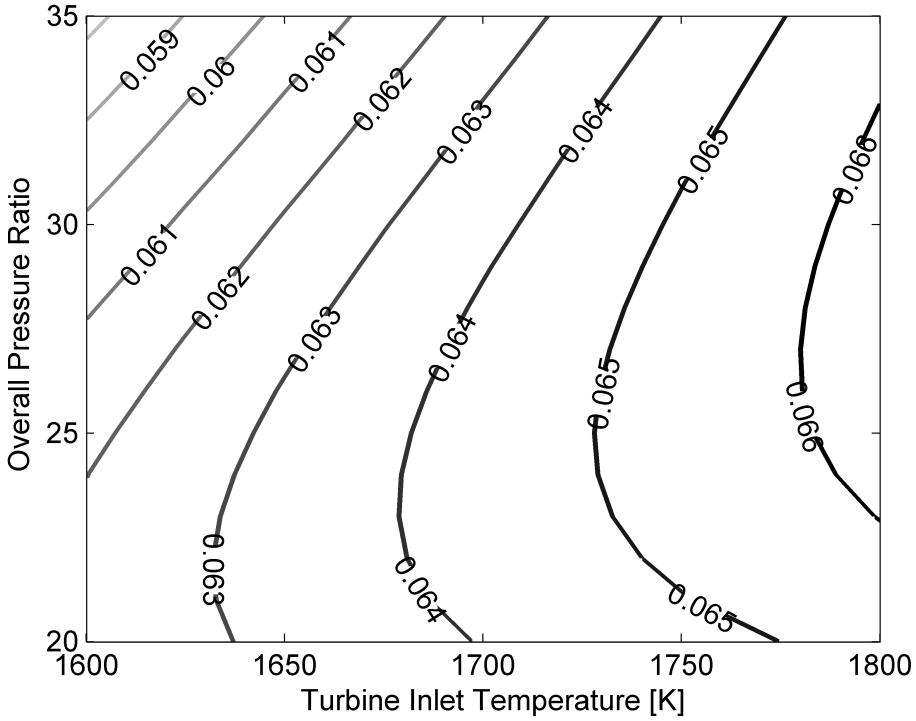

Figure 23: Isolated Engine Overall Efficiency.

These plots show that increasing the turbine inlet temperature increases the TSFC and efficiency of the cycle, but also reduces the specific thrust. This follows the discussion of Chapter II and highlights the basic tradeoff between thrust and fuel consumption in aircraft engine design. The results also show that there is an optimal overall pressure ratio for highest cycle efficiency that increases with temperature. In addition, it was also desired to investigate the impact of changes in engine component efficiencies on the overall engine performance. Figures 24-26 show the variation in performance due to fan and HPC adiabatic efficiency changes. Once again, the specific thrust, TSFC, and overall efficiency are illustrated.

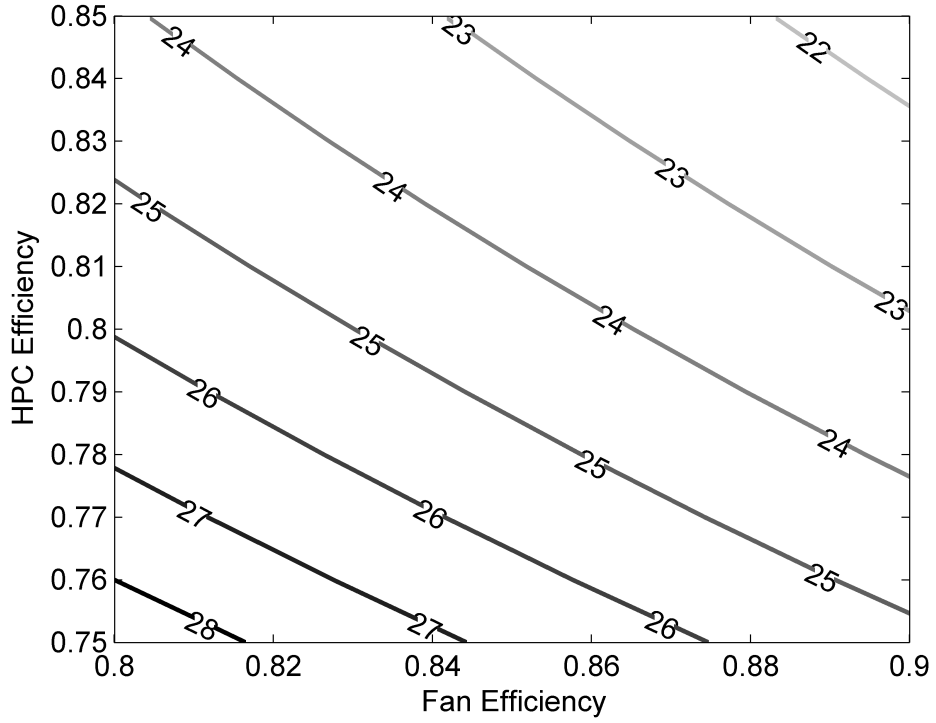

Figure 24: Isolated Engine Thrust Specific Fuel Consumption $[mg/s/N]$.

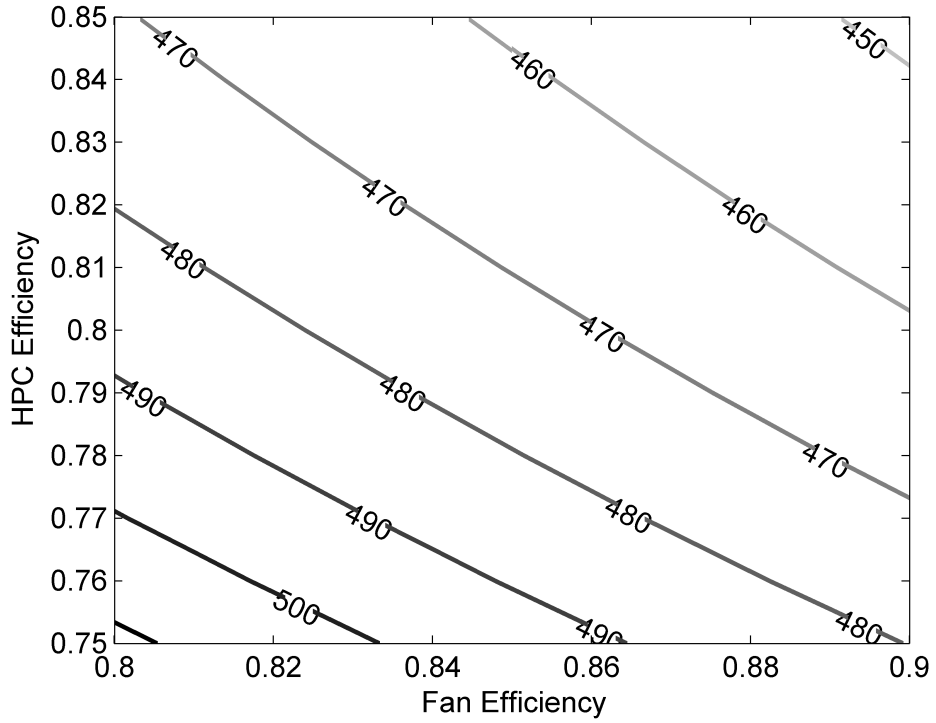

Figure 25: Isolated Engine Specific Thrust $[N/(kg/s)]$.

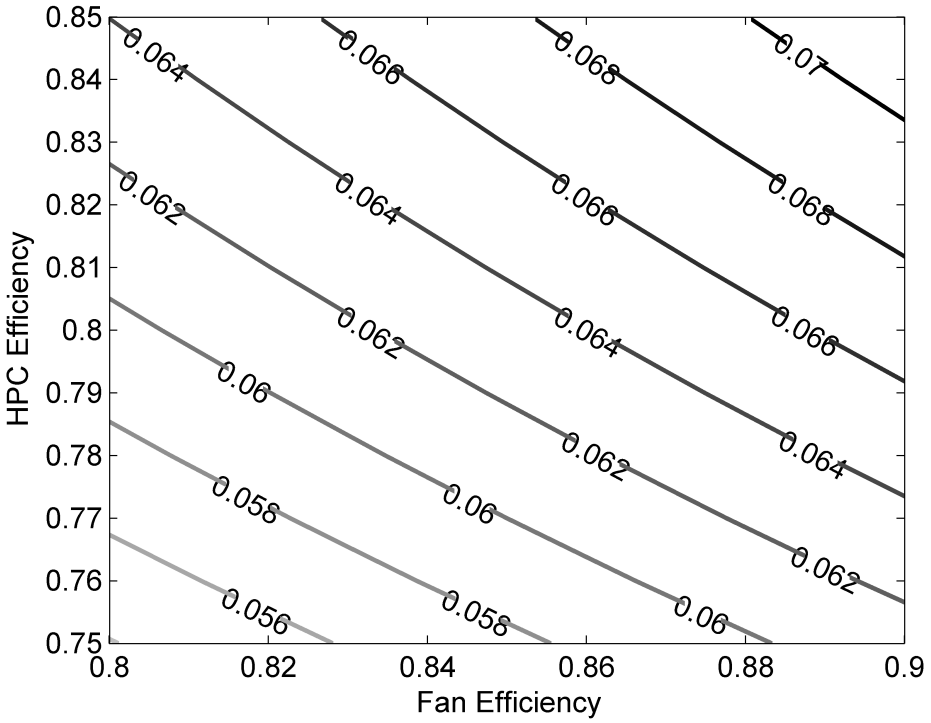

Figure 26: Isolated Engine Overall Efficiency.

These clearly show that increases in component efficiency result in a reduction in irreversible losses and an improvement in performance. The plots also show that the HPC efficiency has a larger effect on performance than the fan efficiency since it encounters the fluid at a higher temperature and pressure. This is an important observation that is further discussed in the next experiment in regards to the irreversibility characterization. The variation in compressor efficiencies also has a smaller impact on engine performance compared to the previously examined pressure ratio and turbine inlet temperature trades. Nevertheless, it is worth noting that the improvement in these efficiencies can sometimes be easier or cheaper than similar changes to the overall pressure ratio and turbine inlet temperature.

3.5.2 Case B: Integrated System

For Case B, the same analysis was performed as in Case A, except that the integrated system model was used in lieu of the previous assumptions. This allowed for the thermal management system models to provide the correct values to the propulsion system model at the four interaction points during the simulation. These values change as a result of changes in the engine itself, and the models are tightly coupled together. Furthermore, all of this changes in response to the heat loads in the two thermal management models and the temperature requirements of the systems. This is one substantial benefit of the integrated models: the ability to directly see the effects of thermal management load and temperature requirements on the propulsion system.

The integrated system was then run at the same design point as Case A using the assumptions outlined in the implementation section. The new engine performance parameters obtained at this design point for the integrated system are shown in Table 16. The engine cycle efficiencies are then shown in Table 17.

Table 16: Engine Performance Parameters (Integrated System).

Thrust	90.00 kN
Specific Thrust	468.13 N/(kg/s)
Air Mass Flow Rate	192.25 kg/s
HP Compressor Bleed Flow Rate	2.10 kg/s
Bypass Ratio	1.25
Exit Velocity	535.59 m/s
Initial Velocity	67.97 m/s
Fuel Mass Flow Rate	2.28 kg/s
Fuel-to-Air Ratio	0.0273
Thrust Specific Fuel Consumption	25.33 (mg/s)/N

The main change in performance for this case compared to the previous one is the reduction in both specific thrust and thrust specific fuel consumption. The thrust itself was constrained to remain the same in the system solver as outlined earlier.

Table 17: Engine Cycle Efficiencies (Integrated System).

Heat Input	100.34 MW
Power Output	27.16 MW
Thrust Power	6.12 MW
Thermal Efficiency	27.06%
Propulsive Efficiency	22.52%
Overall Efficiency	6.10%

The reduction in specific thrust makes sense, due to the increase in engine air flow required to power the air cycle machine for cooling. However, the reduction in TSFC is a little less intuitive. This is a result of the inclusion of the thermal loads in the thermal management systems. The heat transfer from the PTMS into the engine bypass stream, and the higher fuel temperature entering the combustor to a lesser extent, have a beneficial effect on the engine performance.

Similarly to the last case, the TSFC, specific thrust, and overall efficiency are examined next for a variation in the engine design parameters. Figures 27-29 show the results for the overall pressure ratio and turbine inlet temperature design space, and Figs. 30-32 show the variation due to changes in fan and HPC adiabatic efficiencies.

In these plots, the same trends are evident from Case A, although the overall efficiency, TSFC, and specific thrust are all degraded in this case due to the inclusion of the thermal management system. These reductions in efficiency clearly show that, even for traditional thermal management systems, there is a need to consider their effects during the design of the propulsion system. Although an experienced designer could somewhat remedy this by making better assumptions, this would be more difficult as the propulsion and thermal management system interactions increase. This phenomenon is further explored in the next two cases as the thermal load becomes more aggressive.

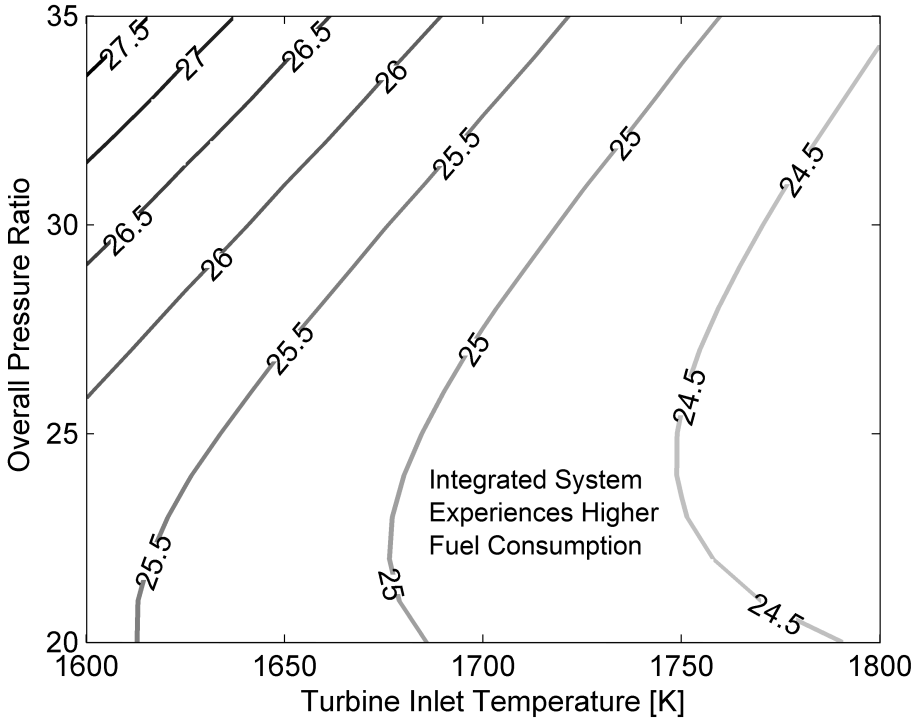

Figure 27: Integrated System Thrust Specific Fuel Consumption $[mg/s/N]$.

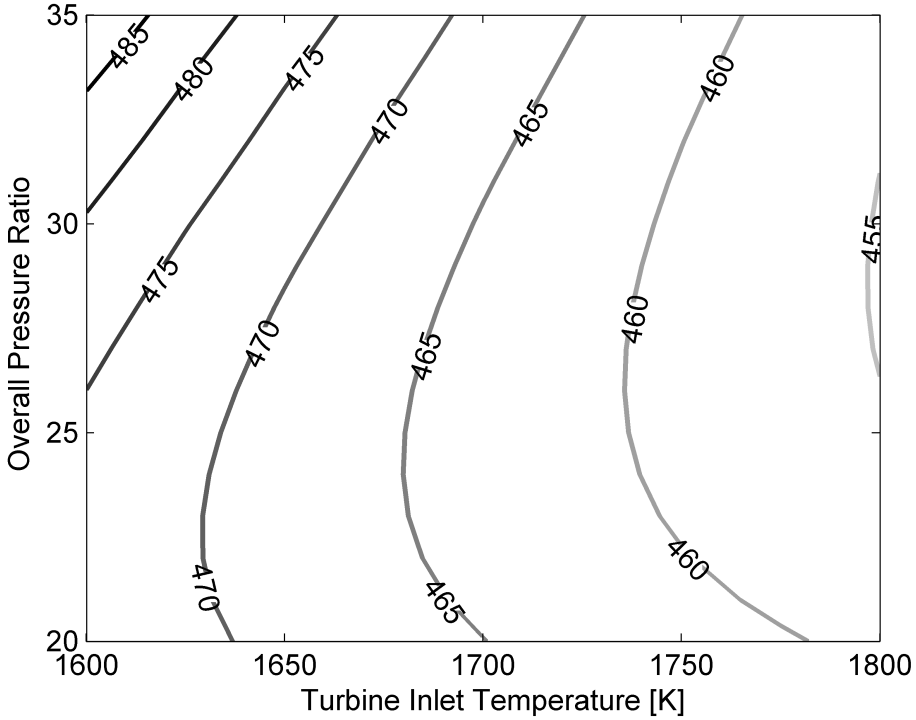

Figure 28: Integrated System Specific Thrust $[N/(kg/s)]$.

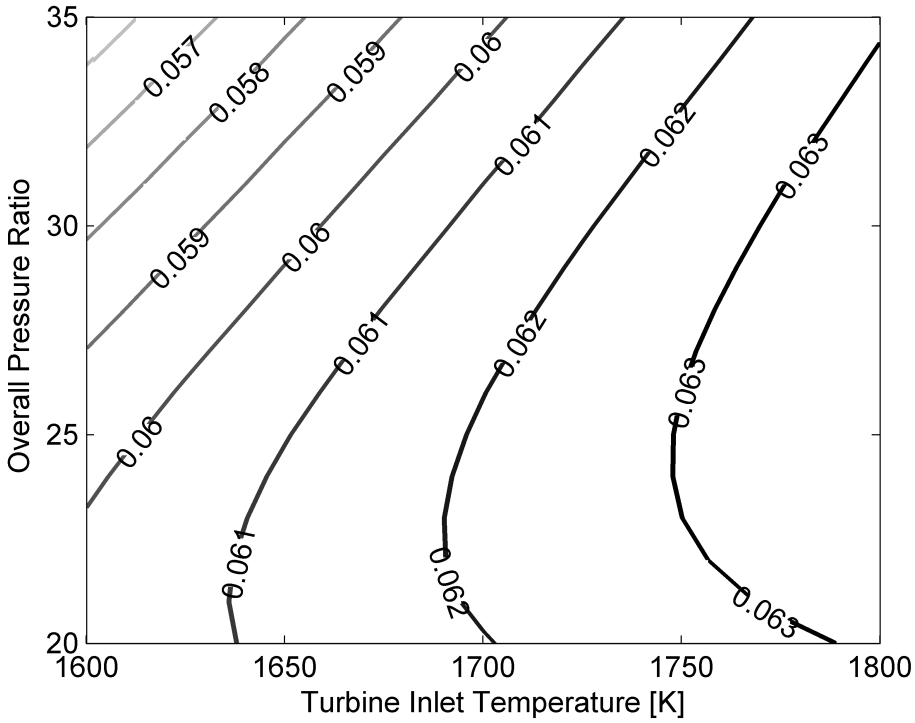

Figure 29: Integrated System Overall Efficiency

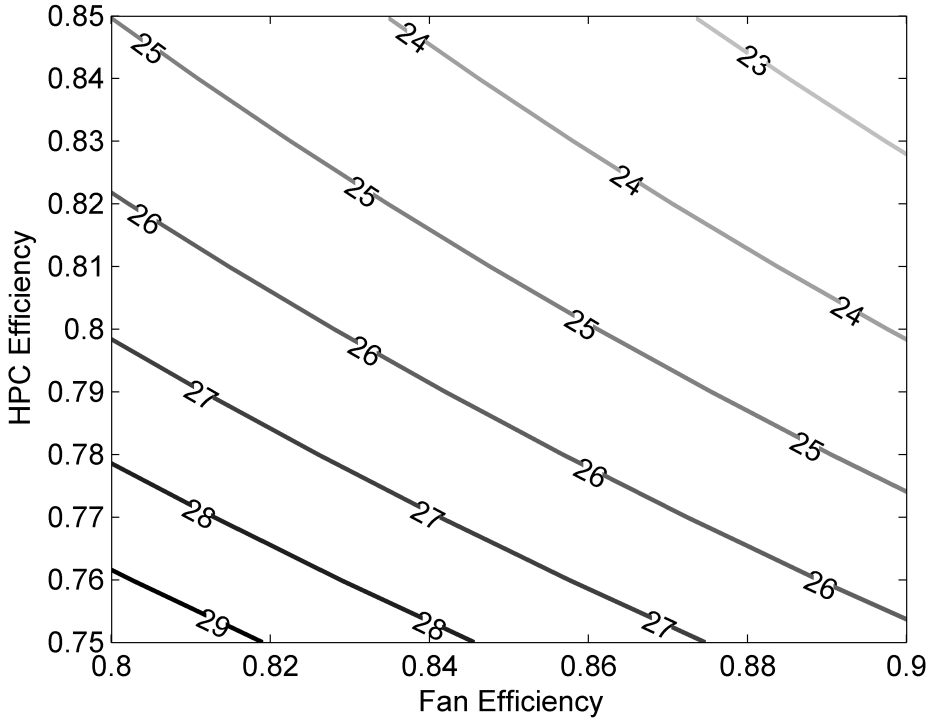

Figure 30: Integrated System Thrust Specific Fuel Consumption $[mg/s/N]$.

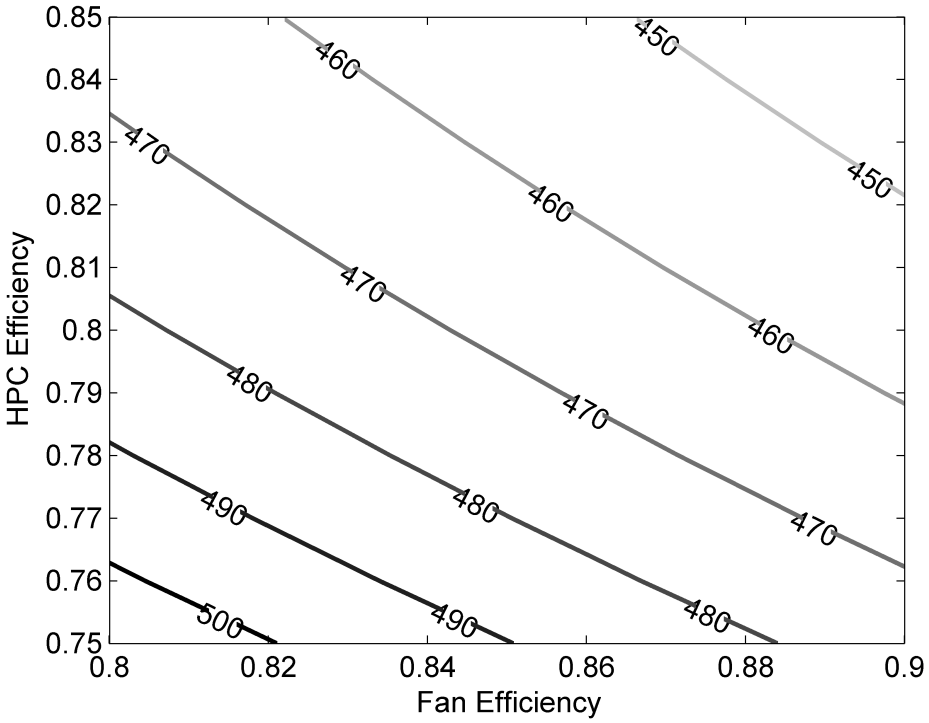

Figure 31: Integrated System Specific Thrust $[N/(kg/s)]$.

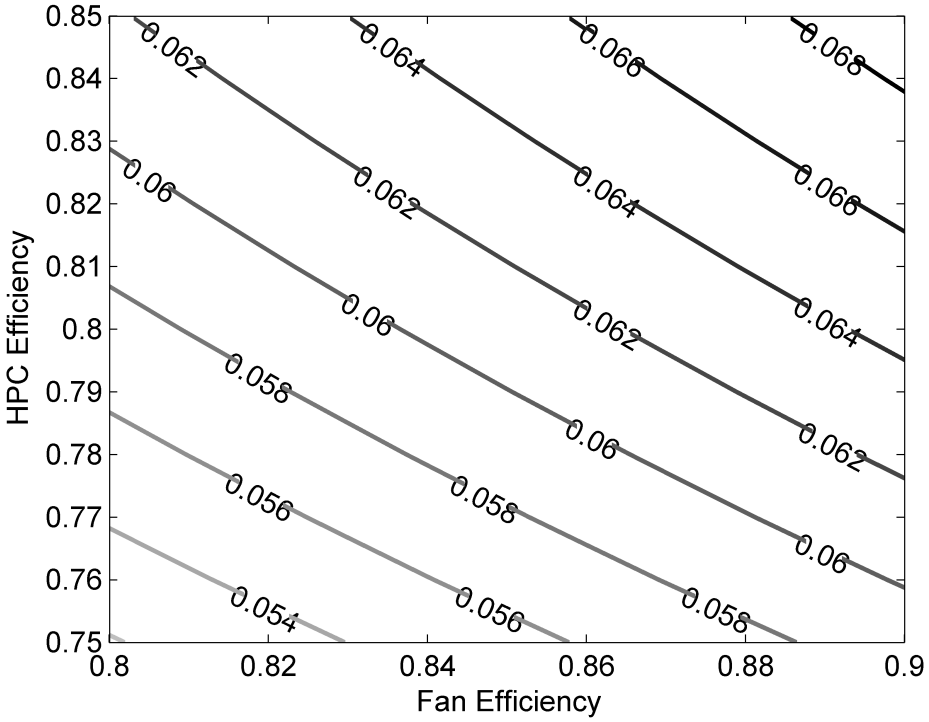

Figure 32: Integrated System Overall Efficiency.

3.5.3 Case C: Isolated Engine with High Heat Load

This case examines the propulsion system performance in the context of a higher PTMS thermal load. Since the thermal management subsystem models are unavailable in this case, the isolated engine model from Case A is once again used to indirectly explore this by varying the system interaction variables. Trades were conducted for the four main interactions that were previously outlined: compressor bleed, shaft power extraction, fuel temperature, and bypass heat transfer rate. These studies were conducted over ranges that are anticipated to result from thermal management system requirements.

Figure 33 illustrates the impact on engine performance resulting from changes in HPC bleed air requirements. From this, it is seen that the HPC bleed air extraction has a fairly substantial effect on both the TSFC and the specific thrust. Over the range of values examined, which are on the order of what would be required to provide cooling for the thermal management system, there is a slightly nonlinear reduction in both the TSFC and specific thrust. Results are next shown for fuel temperature in Fig. 34. As a reminder, this effect is due to the preheating of the fuel before it enters the combustor. The results show a nonlinear reduction in required fuel flow and TSFC with increasing fuel temperature as expected. However, this effect is much smaller than the previous case of the compressor bleed extraction. The third interaction parameter explored was the power extraction from the HP shaft and is shown in Fig. 35. This effect is larger than the fuel preheating effect, but still smaller than that which was seen with the compressor bleed extraction. The result shows a linear reduction in TSFC with increasing power extraction with a simultaneous increase in engine inlet air flow rate to maintain the required thrust. Finally, the bypass heat transfer rate is explored in Fig. 36. The results follow the same trend as the shaft power extraction, but have a larger magnitude.

An increase of 10 MW of heat addition into the fan stream results in an increase of around 20% in the bypass stream exit temperature.

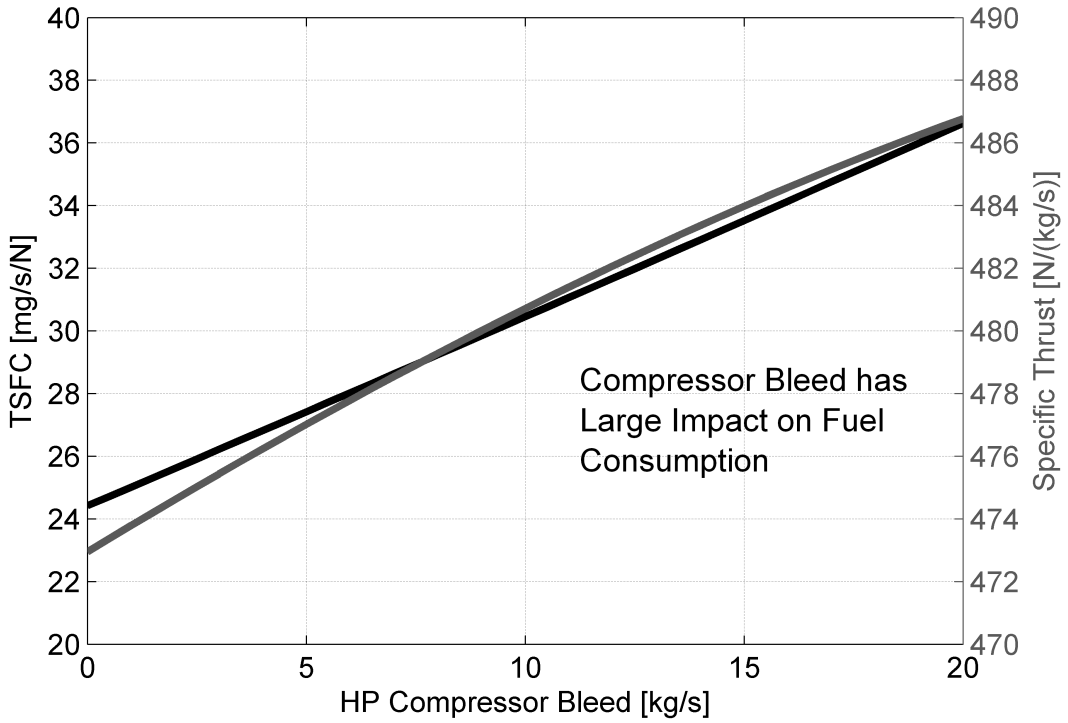

Figure 33: HPC Bleed Air Impact on Isolated MFTF Engine.

3.5.4 Case D: Integrated System with High Heat Load

The final case now merges both of the previous changes together: the increased heat load and the integrated propulsion and thermal management systems design. For this case, the same integrated system model from Case B is used. However, the PTMS thermal load heat rate is increased from 25 kW to 900 kW. This is intended to simulate the change from a traditional thermal load to a more ambitious one in anticipation of future requirements. A heat load of this magnitude could result from the waste heat from a directed energy weapon (DEW). This requires a substantial reconfiguration of the system solver in order to keep the thermal management system temperatures at their correct limits.

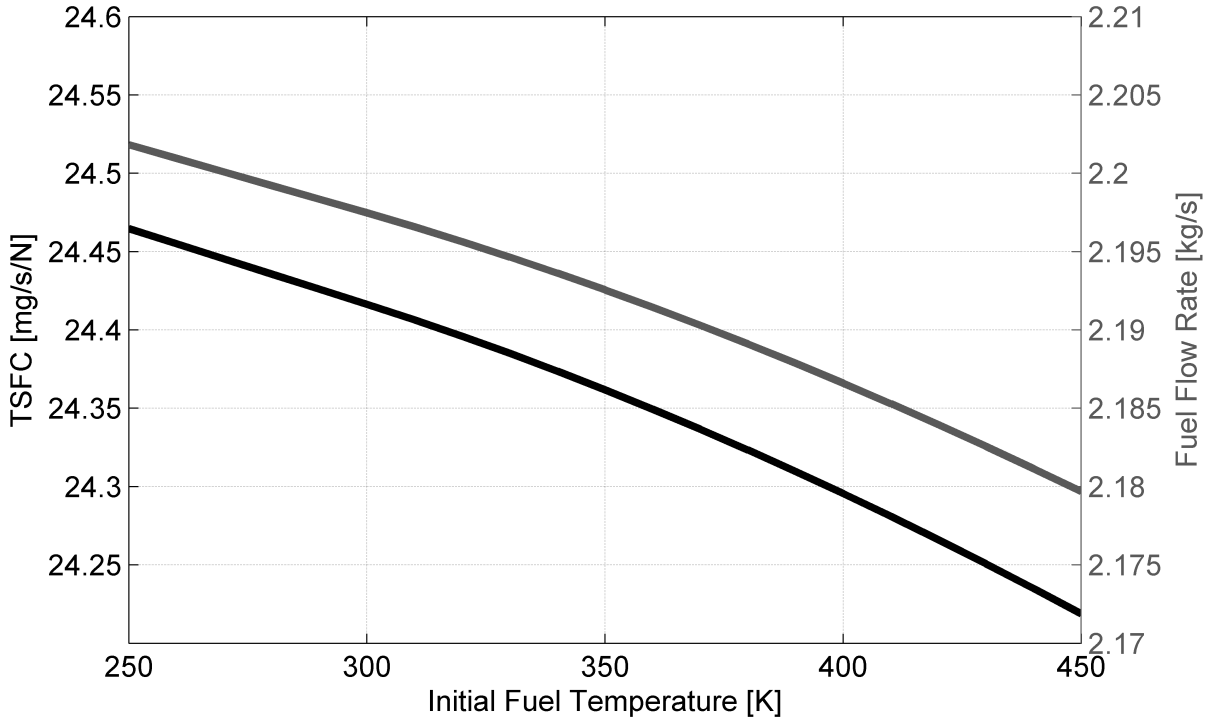

Figure 34: Fuel Temperature Impact on Isolated MFTF Engine.

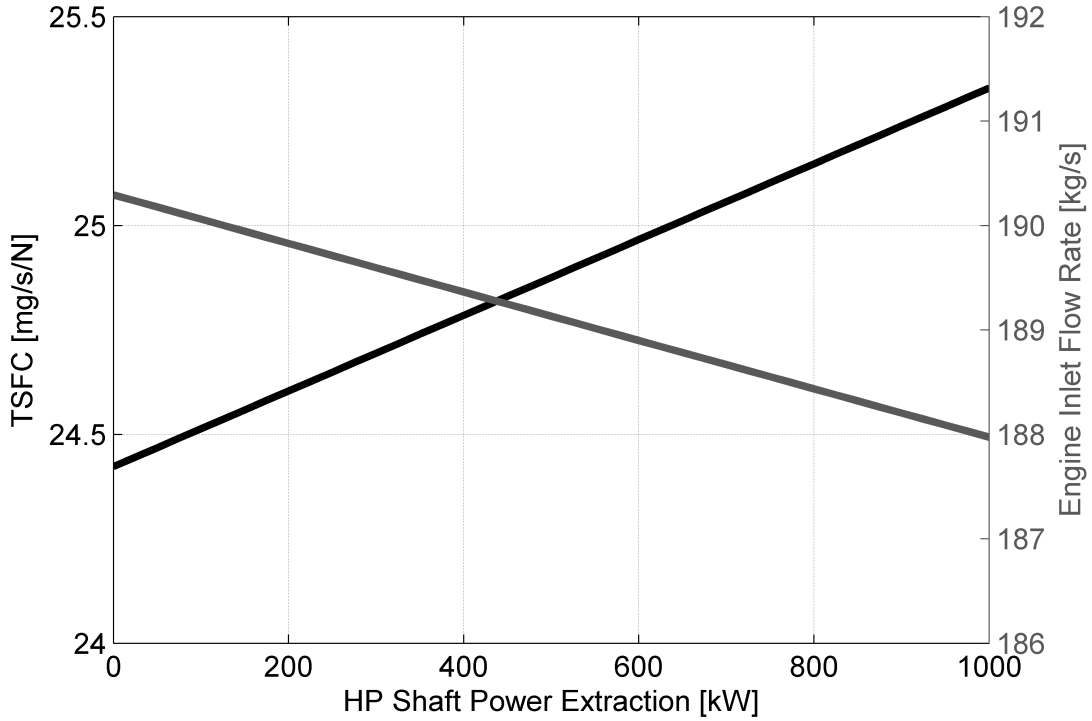

Figure 35: Shaft Power Extraction Impact on Isolated MFTF Engine.

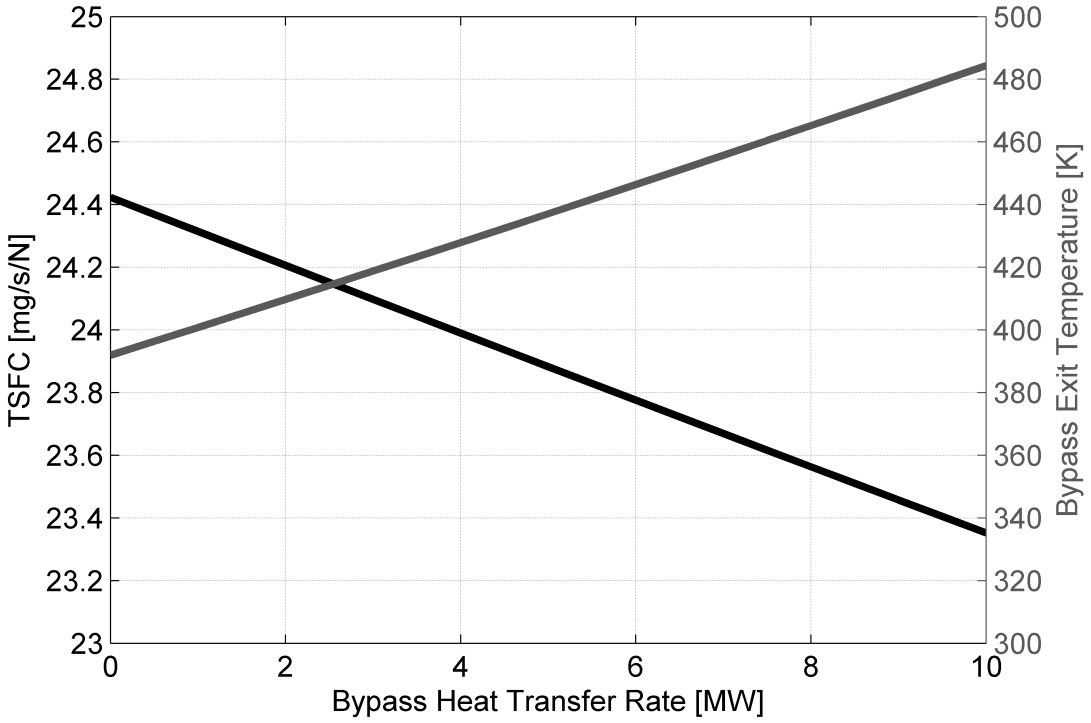

Figure 36: Bypass Heat Transfer Impact on Isolated MFTF Engine.

The new engine performance parameters obtained at the design point for the integrated system are shown in Table 18. The engine cycle efficiencies are then shown in Table 19. Comparing these results to those of the traditional load in Case B, it is seen that the required compressor bleed flow rate has now more than doubled from 2.10 kg/s to 4.64 kg/s. However, the additional heat transfer to the fan stream and fuel also has a balancing effect. As a result, the overall specific thrust and TSFC is slightly reduced.

Next, a trade study was conducted with respect to the heat transfer rate of the PTMS heat load in the context of the integrated system. The purpose of this is to investigate the relationship between the heat rate, engine design parameters, and system performance. Figures 37-39 show the TSFC, specific thrust, and overall efficiency variations resulting from changes in engine overall pressure ratio and PTMS heat load heat rate simultaneously.

Table 18: Engine Performance Parameters (Integrated System with High Heat Load).

Thrust	90.00 kN
Specific Thrust	474.33 N/(kg/s)
Air Mass Flow Rate	189.74 kg/s
HP Compressor Bleed Flow Rate	4.64 kg/s
Bypass Ratio	1.06
Exit Velocity	548.78 m/s
Initial Velocity	67.97 m/s
Fuel Mass Flow Rate	2.39 kg/s
Fuel-to-Air Ratio	0.0273
Thrust Specific Fuel Consumption	26.60 (mg/s)/N

Table 19: Engine Cycle Efficiencies (Integrated System with High Heat Load).

Heat Input	105.37 MW
Power Output	27.80 MW
Thrust Power	6.12 MW
Thermal Efficiency	26.38%
Propulsive Efficiency	22.01%
Overall Efficiency	5.81%

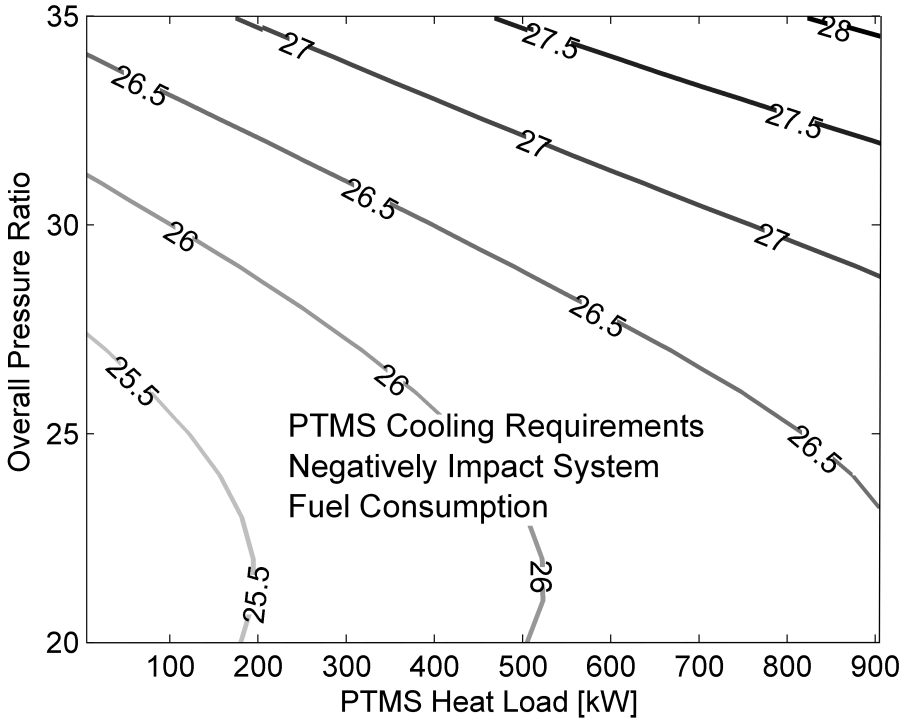

Figure 37: Integrated System Thrust Specific Fuel Consumption $[mg/s/N]$.

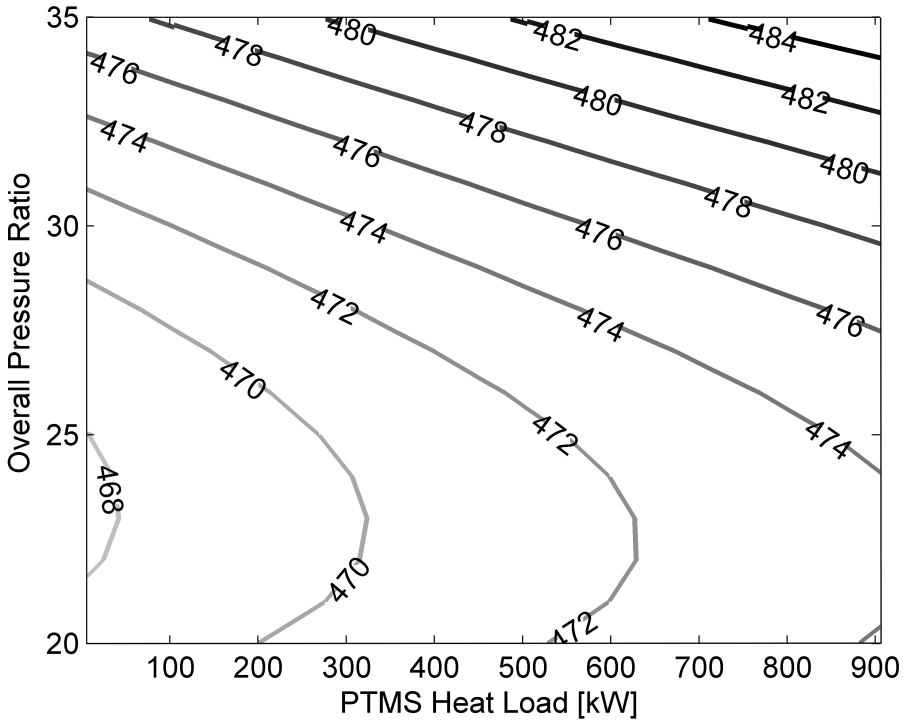

Figure 38: Integrated System Specific Thrust $[N/(kg/s)]$.

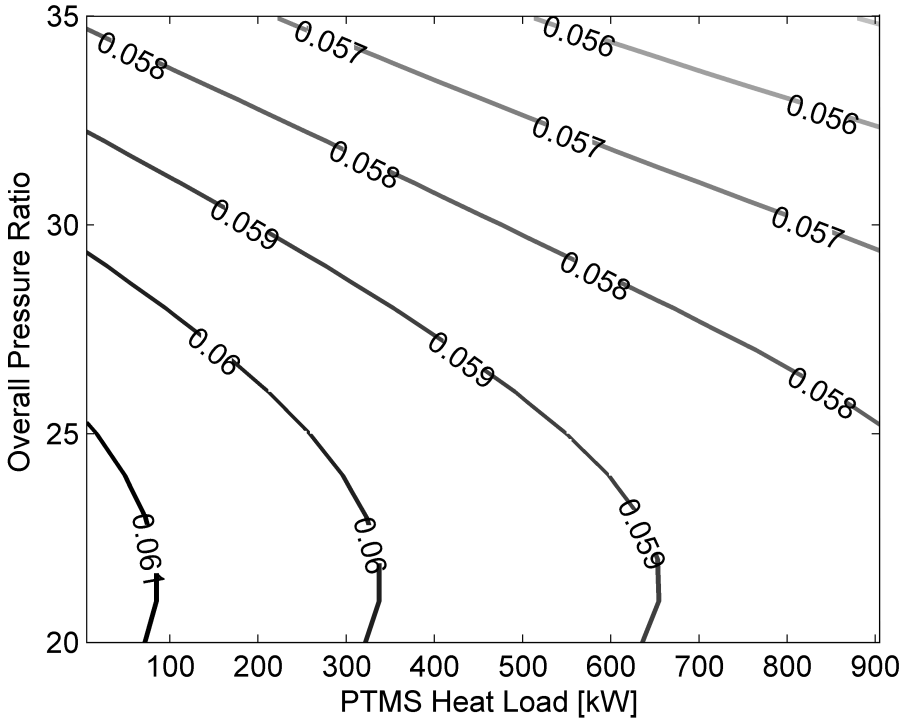

Figure 39: Integrated System Overall Efficiency

These plots show that the magnitude of the heat rate in the PTMS can actually have a fairly large effect on the optimal engine overall pressure ratio. As the PTMS thermal requirements change, the engine cycle parameters should also change so that the engine can operate at most efficiently.

3.6 Summary of Integrated Propulsion and Thermal Management Modeling and Simulation

For the first experiment, two different simulations were used for the design: first the isolated engine and then the integrated system. The isolated engine design was created without the benefit of leveraging the integrated system-level model. These two different approaches are compared for a traditional heat load and then compared again at a more aggressive heat load. This illustrates the differing impact on propulsion systems design between the two thermal environments.

The results show that taking the thermal management system interactions into account during the conceptual design of the engine have an impact on the design choices as expected. In fact, this trend becomes much more pronounced in the more challenging future thermal environments as was seen in Cases C and D. The coupled simulation rapidly predicts the interactions between the subsystems and estimates the impact on propulsion system performance as a result of thermal management requirements. The experiment showed that large cooling requirements can play an important role in the integrated design of the propulsion and thermal management systems. It is possible to redesign aspects of the propulsion system to minimize the irreversible losses due to the thermal system components.

CHAPTER IV

MAKING THE CASE FOR A SECOND-LAW-BASED FORMULATION

Now that the need for integrated modeling and simulation of the propulsion and thermal management systems has been demonstrated in the previous experiment, this second experiment is concerned with the usage of thermodynamic irreversibility to aid the conceptual engine designer. Although the irreversibility was neglected in the previous experiment, the direct quantification of the irreversibility is the main focus here.

The direct invocation of the second-law and the resulting irreversibility characterization is shown to give the designer a more complete picture of the trades present in the integrated propulsion and thermal management systems design. It allows the designer to partition all of the thermodynamic losses throughout the integrated system and identify them at the component-level. Then, the designer can rapidly visualize the relationship between engine component losses and thermal management performance.

4.1 Statement of Research Hypothesis #1b

Following the structure established in the previous chapter, a hypothesis for the second research question is first formally stated based on the background research of Chapter II. The hypothesis for Research Question 1b directly confronts the characterization of irreversibility in the integrated systems design. It is repeated here along with the statement of its corresponding hypothesis:

Research Question #1b: Is the characterization of the exergy destruction on a component basis able to provide the propulsion systems designer a more consistent and absolute metric to trade off the integrated performance of the propulsion and thermal management system?

Research Hypothesis #1b: A second-law analysis tracking the irreversibility in terms of exergy destruction within each of the subsystem components better identifies the key contributors that affect the thermodynamic performance of the integrated system design space than traditional energy techniques.

After demonstrating the need to consider the propulsion and thermal management systems together during the conceptual engine design through the previous experiment, the rest of the experiments will all use the integrated system simulation. It is hypothesized that the component irreversibility is a consistent and absolute measure of loss that can be used to put the two subsystems on equal footing. In this experiment, it is necessary to establish this for the case of integrated propulsion and thermal management systems design.

4.2 Experimental Approach

In order to perform this experiment it is necessary to calculate the entropy production and exergy destruction throughout the integrated system. This enables the direct characterization of the system irreversibility. From this, the advanced second-law techniques can be directly compared to the more-traditional energy balance only techniques. The key to this experiment is to show the differences between the two techniques for the system designer. It is of particular importance to highlight the differences in the two techniques with respect to clearly identifying the important trades for the designer.

Table 20 shows the experimental layout. Case A features the integrated system

simulation for the traditional heat load case using only the first law; Case B then utilizes the combined first and second laws and direct characterization of irreversibility. Like the previous experiment, Cases C and D then illustrate the difference for the high-heat load case.

Table 20: Experiment #1b: Irreversibility Characterization.

A	**B**
Integrated systems design Traditional heat load Energy balance	Integrated systems design Traditional heat load Exergy characterization
C	**D**
Integrated systems design High heat load Energy balance	Integrated systems design High heat load Exergy characterization

The summary of the steps to carry out this second experiment is as follows:

- Calculate exergy destruction across each component of the integrated propulsion and thermal management model
- From this information, construct a buildup of the irreversibility for the system
- Compare this absolute representation of irreversibility to the traditional approach used for engine cycle design: energy and perturbation techniques
- Demonstrate that the absolute irreversibility buildup enables the designer to more clearly identify the important trades than using the traditional techniques

4.3 Theory

The discussion now turns to the thermodynamic theory that is necessary to include in the integrated system-level modeling and simulation environment. This thermodynamic formulation is required to directly quantify the irreversibility within various components of the integrated system. This is pulled from the background discussion of Chapter II and is further elaborated upon here.

The second research hypothesis requires the inclusion of the combined first and second laws of thermodynamics. The first law representation is the straightforward conservation of energy that should already be present in any type of physics-based model. The second-law, however, is often not invoked directly in the development of the thermodynamic models. In the context of this research, this must be remedied to address the second and subsequent research questions.

4.3.1 Second-Law-Based Formulation

In this section, a derivation of the component-level second-law formulation is shown. This includes a discussion concerning entropy, exergy, and exergy destruction prediction. The concept of exergy is used to quantify the component irreversibility throughout the integrated system. As previously explained, it is a combined statement of the first and second laws of thermodynamics. The first law of thermodynamics is a statement of the conservation of energy in an isolated system [48]:

$$du = \Delta q - \Delta w \tag{66}$$

where internal energy is represented as u, heat as q, and work as w.

The second law, on the other hand, "postulates the existence of a state function called the entropy and defines the basic properties of this function" [174]. The second law can be stated mathematically as

$$ds \equiv \left(\frac{\Delta q}{T}\right)_{rev} \tag{67}$$

where s represents the entropy.

The exergy function is a measure of work potential and is derived through a combination of the first and second laws. This section follows the derivation of Camberos [32]. First, the first law is written in terms of heat and work transfer:

$$\int_t^{t_0} Q dt + \int_t^{t_0} W dt = \Delta U \tag{68}$$

The second law is used to define the heat term as a function of the entropy as

$$\int Q dt = T_0 \left(S_0 - S\right) \tag{69}$$

Likewise, the work term is written as

$$\int W dt = -\int P\dot{V} dt = -\int \left(P - P_0\right)\dot{V} dt - P_0 \int \dot{V} dt \tag{70}$$

Here the useful work term is

$$W_{\text{useful}} = \int \left(P - P_0\right)\dot{V} dt \tag{71}$$

while the other term is the flow work. Substituting Eqs. 69 and 70 into Eq. 68, leads to

$$T_0 \left(S_0 - S\right) - W_{\text{useful}} - P_0 \left(V_0 - V\right) = U_0 - U \tag{72}$$

and then rearranging for the useful work term,

$$W_{\text{useful}} = T_0 \left(S_0 - S\right) - \left(U_0 - U\right) - P_0 \left(V_0 - V\right) \tag{73}$$

By defining the thermodynamic quantity of exergy as this useful work, the exergy is

$$X \equiv T_0 (S_0 - S) - (U_0 - U) - P_0 (V_0 - V) \tag{74}$$

This is written in an intensive basis with respect to the ambient conditions as [143]:

$$x \equiv h - h_{amb} - T_{amb} (s - s_{amb}) \tag{75}$$

where the subscript *amb* represents the value of the property at the ambient dead state condition. h represents the enthalpy of the fluid and is defined as internal energy and flow work:

$$h \equiv u + pv \tag{76}$$

v is the specific volume, which is the reciprocal of the density ρ.

Using this information, the exergy destruction per component is then calculated as:

$$\dot{X}_D = \dot{X}_{in} - \dot{X}_{out} + \dot{Q}_{in} + \dot{W}_{in} \tag{77}$$

This equation allows for a characterization of the irreversibility throughout the entire system on a component basis. By calculating the flow properties entering and leaving the component and accounting for the heat and work transfer, the lost work is determined in terms of destroyed exergy. Application of this concept throughout the engine, thermal systems, and exhaust gives the systems designer a clear view of the loss distribution in a consistent and absolute manner.

4.3.2 Calculation of Thermodynamic Losses

The previous chapter proposed a lumped parameter model of an integrated propulsion and thermal management system abstraction. By stepping from station to station throughout the system and invoking the applicable thermodynamic relationships,

all of the requisite states were determined. This is now revisited in light of the thermodynamic properties of particular importance here: the entropy and exergy. The determination of these properties at each station is further discussed here. All of the station data is then used to characterize the irreversibility distribution for the system.

Each of the component models has the ability to calculate the entropy and exergy state variables at each station of the system model. For this work, air is assumed to behave as an ideal gas and fuel as an incompressible liquid. Tables are used for air and fuel specific heats as a function of temperature.

The specific entropy for the air is calculated as an ideal gas:

$$s - s_{ref} = c_p \, ln \left(\frac{T_0}{T_{ref}} \right) - R \, ln \left(\frac{p_0}{p_{ref}} \right) \tag{78}$$

where the reference conditions are defined at $p_{ref} = 101.325$ kPa and $T_{ref} = 273.15$ K. The fuel is modeled using the incompressible assumption

$$s - s_{ref} = c \, ln \left(\frac{T_0}{T_{ref}} \right) \tag{79}$$

The capability also exists within the CRATOS thermodynamic package to use thermodynamic tables for entropy calculations in place of the ideal gas and incompressible liquid assumptions. However, this additional complexity does little to affect the general results. In this case, entropy is tabulated as a function of temperature and pressure using the JANNAF thermodynamic tables [162]

$$s = s \left(T, p \right) \tag{80}$$

The intensive exergy at each station is then calculated as before:

$$x \equiv h - h_{amb} - T_{amb} \left(s - s_{amb} \right) \tag{81}$$

An extensive exergy rate is simply defined by:

$$\dot{X} = \dot{m}x \tag{82}$$

4.4 Implementation

The thermodynamic theory outlined in this chapter is now applied to the modeling and simulation environment from Chapter III. The physics-based formulations involving the concurrent usage of the first and second laws of thermodynamics are incorporated into the CRATOS environment so that the component-level losses can be directly characterized. The inclusion of this information leads to the direct prediction of the entropy generation distribution throughout the system, which helps give the propulsion systems designer a consistent and absolute view of the tradeoffs associated with the design of the entire integrated system [114, 61, 145].

4.4.1 Component Irreversibility Characterization

Once the exergy is calculated at each of the stations within the system, then the component-level exergy destruction can be calculated. Exergy destruction is calculated via conservation of energy considerations for each of the individual components according to the formulae in Table 21.

4.4.2 CRATOS Modeling and Simulation Environment

The previous chapter discussed the baseline elements of the CRATOS modeling and simulation environment. Once again, this environment was developed entirely from first principles in MATLAB; it was custom-built for the purpose of carrying out the experiments for this research. This tool combines all of the previously discussed components and subsystem models with an intuitive user interface, robust solver, and post processing and plotting capabilities. The irreversibility characterization posed in this chapter is included in the system-level modeling and simulation environment

Table 21: Component-Level Irreversibility Calculations in Terms of Exergy Destruction.

Component	Calculation
Inlet	$\dot{X}_D = \dot{X}_{in} - \dot{X}_{out}$
Compressor	$\dot{X}_D = \dot{X}_{in} - \dot{X}_{out} + \dot{X}_{bleed} + \dot{W}_{comp}$
Burner	$\dot{X}_D = \dot{X}_{in} - \dot{X}_{out} + \dot{Q}_{in}$
	$\dot{Q}_{in} = -\Delta h_f$
Turbine	$\dot{X}_D = \dot{X}_{in} - \dot{X}_{out} + \dot{W}_{turb}$
Mixer	$\dot{X}_D = \dot{X}_{in_{core}} - \dot{X}_{out_{core}} + \dot{X}_{in_{bypass}} - \dot{X}_{out_{bypass}}$
Nozzle	$\dot{X}_D = \dot{X}_{in} - \dot{X}_{out}$
Heat Exchanger	$\dot{X}_D = \dot{X}_{in_{cold}} - \dot{X}_{out_{cold}} + \dot{X}_{in_{hot}} - \dot{X}_{out_{hot}}$
Heat Load	$\dot{X}_D = \dot{X}_{in} - \dot{X}_{out} + \dot{Q}_{in}$
Fuel Pump	$\dot{X}_D = \dot{X}_{in} - \dot{X}_{out} + \dot{W}_{pump}$

implemented in Chapter III. It serves as an integral part of CRATOS due to the importance placed on the irreversibility allocation in the later experiments.

Figure 40 shows a snapshot of the CRATOS environment graphical user interface (GUI). As shown in the figure, the GUI is divided into five main sections for the designer to use. The upper right section contains illustrations of the subsystem architecture abstractions that were created in Chapter III, which can be toggled by the designer. Directly below these diagrams is a table featuring all of the pertinent thermodynamic station data for the selected subsystem. This includes the entropy and exergy prediction derived in the present chapter.

The design parameters for all aspects of the system are specified at the top of the page, while the important engine performance results are shown down the left-hand side. Finally, the most important section is the irreversibility allocation plot capability in the bottom left. This plot shows the irreversibility buildup for the entire system. This is a result of the thermodynamic calculations from this chapter. This can be viewed in several different formats as selected by the designer. For example, the irreversibility can be broken down to either the subsystem or component level and can be visualized in terms of intensive or extensive entropy production or exergy destruction.

This section of the GUI also has the capability of displaying the cost and weight results detailed in Chapter V.

Although the major foundation of the CRATOS environment stems from the modeling and simulation theory of the last chapter and the thermodynamic characterization of the present chapter, the next three chapters also add additional capabilities pertaining to the irreversibility allocation experiments. Chapter V adds the additional elements relating to cost and Chapter VI adds the mission performance elements. The foundation presented here is then used in conjunction with these two additional elements to perform the optimization and allocation in Chapter VII.

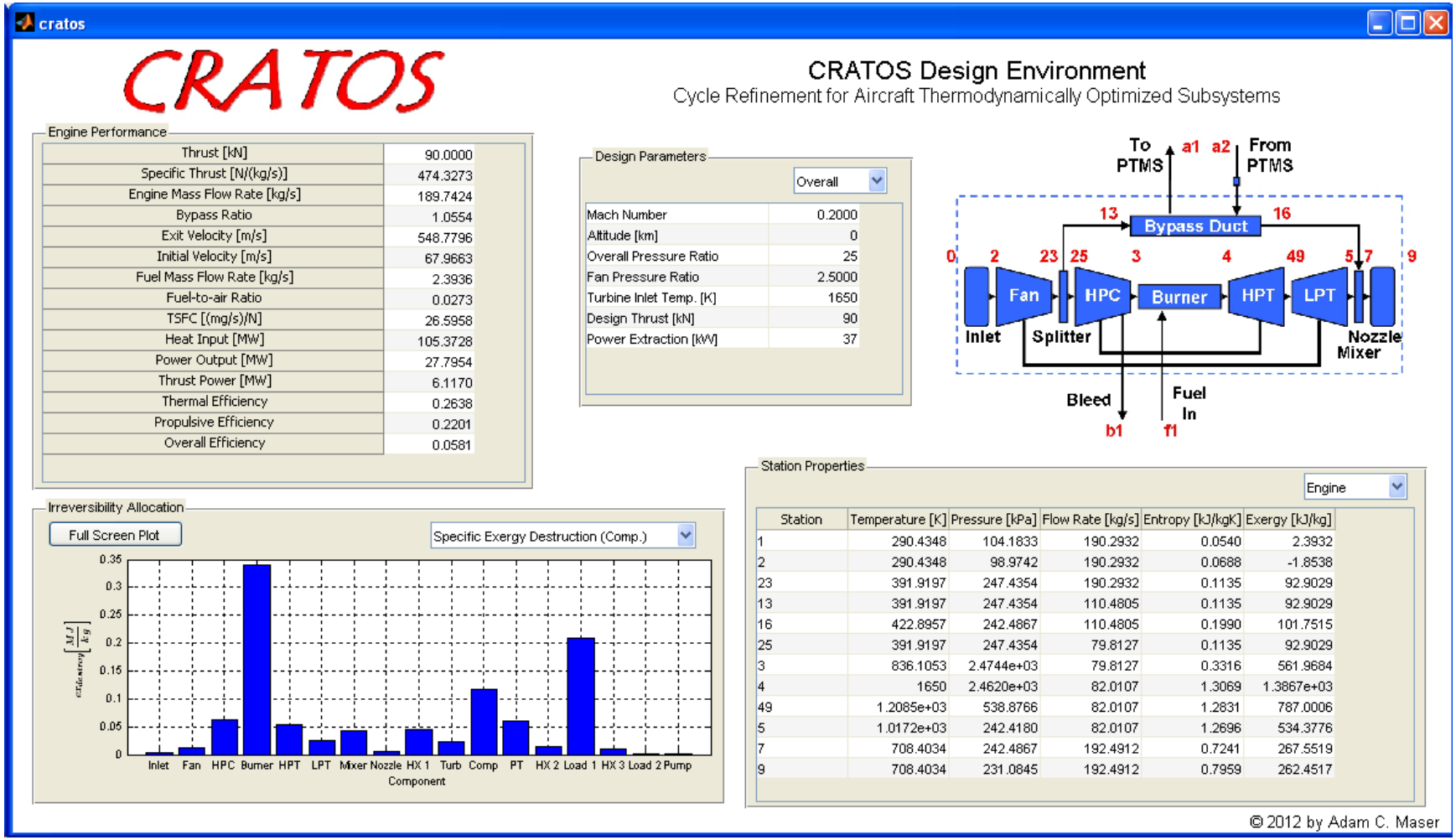

Figure 40: CRATOS Graphical User Interface.

4.5 Results: Irreversibility Comparison

The second experiment follows the same train of thought as the previous one with the important exception of now specifically focusing on the system irreversibility; the first experiment is reexamined using a second-law-based analysis. The examination of the exergy destruction on a component basis allows the designer to view all of the design trades on a specific and absolute footing. This is particularly beneficial in that it clearly demonstrates important features that are not as apparent without the direct application of the second-law. The graphical depiction of the four experimental cases is repeated in Table 22.

Table 22: Experiment #1b: Irreversibility Characterization.

A Integrated systems design Traditional heat load Energy balance	**B** Integrated systems design Traditional heat load Exergy characterization
C Integrated systems design High heat load Energy balance	**D** Integrated systems design High heat load Exergy characterization

4.5.1 Case A: Energy Balance (Fuel Burn)

Case A features the integrated system-level model at the traditional heat load. Since the first experiment has demonstrated the benefit of the integrated systems simulation, the rest of the experiments will focus exclusively on this system. This case

utilizes only a first-law energy balance as a counterpoint to the next case, which also includes a second-law-based formulation. This first case is identical to Case C from the previous experiment.

4.5.2 Case B: Exergy Characterization

Next, the effect of including an exergy-based analysis in the integrated systems design process is investigated. For Case B, the integrated systems design features the traditional heat load once again. To start off, the same design spaces examined in the first experiment are shown in terms of system-level exergy destruction. Figures 41 and 42 show this exergy destruction design space for the integrated system. Figure 41 shows the variation in compressor efficiencies, Fig. 42 the overall pressure ratio and turbine inlet temperature.

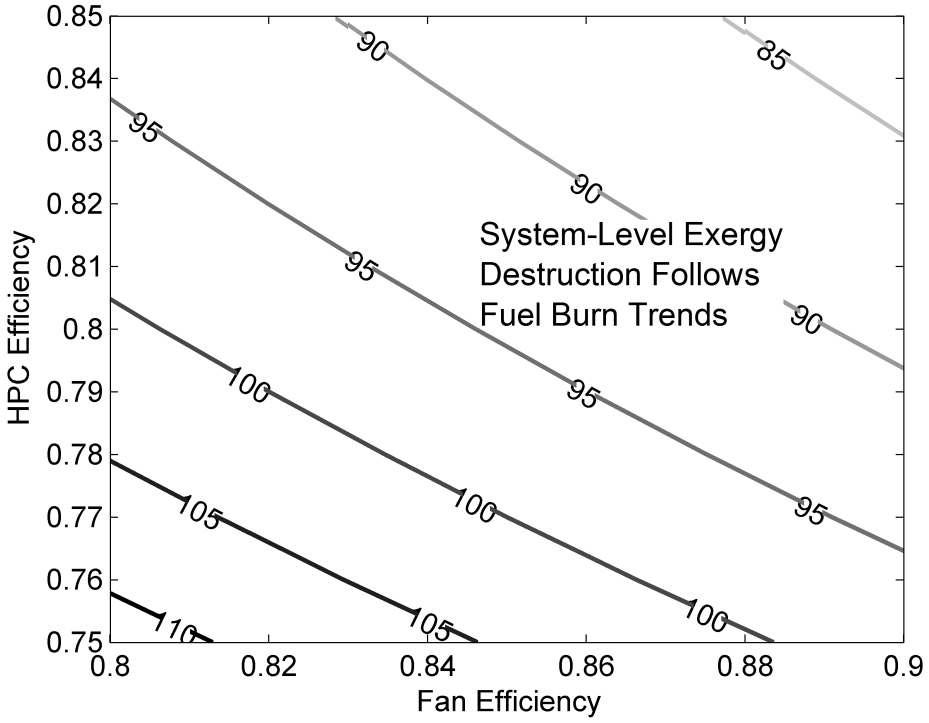

Figure 41: Integrated System Exergy Destruction Rate $[MW]$.

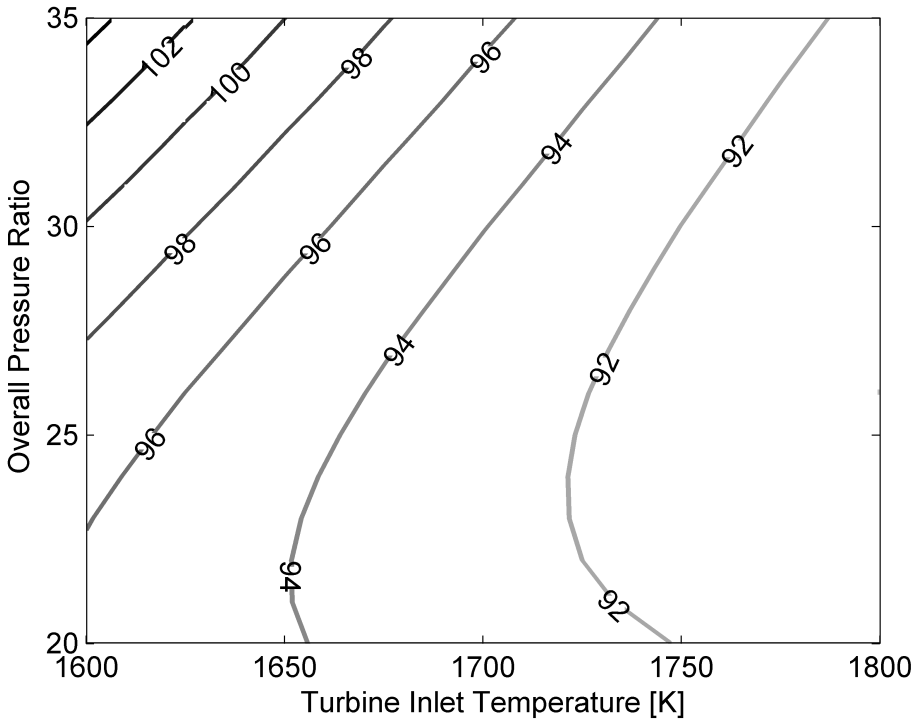

Figure 42: Integrated System Exergy Destruction Rate $[MW]$.

When compared to the previous case, these plots clearly show that at the system-level the exergy destruction metric behaves identically to the fuel consumption. In other words, designing a system for minimum fuel consumption is identical to designing a system for minimum exergy destruction. This confirms the earlier assertions by previous researchers highlighted in Chapter II. It also shows that it is consistent with an energy approach, while providing additional information about the system losses in absolute and consistent terms.

The major benefit of the exergy destruction perspective is that it then partitions the system fuel consumption amongst the individual components according to their respective irreversible losses. This distribution for the integrated system simulation at the design point is shown next. This is illustrated in Figs. 43-45 in terms of the extensive exergy rate. As shown in these figures, the engine components contribute a much larger amount of absolute exergy destruction due to the much larger mass flow

rates experienced through the engine as compared to the thermal subsystems.

Figures 46-48 then show the exergy destruction on an intensive basis. Since these results have been normalized by their respective mass flow rates, the results are much closer in magnitude. The PTMS air cycle machine, and the power turbine in particular, then become major contributors of exergy destruction if their mass flow rate difference are taken into account.

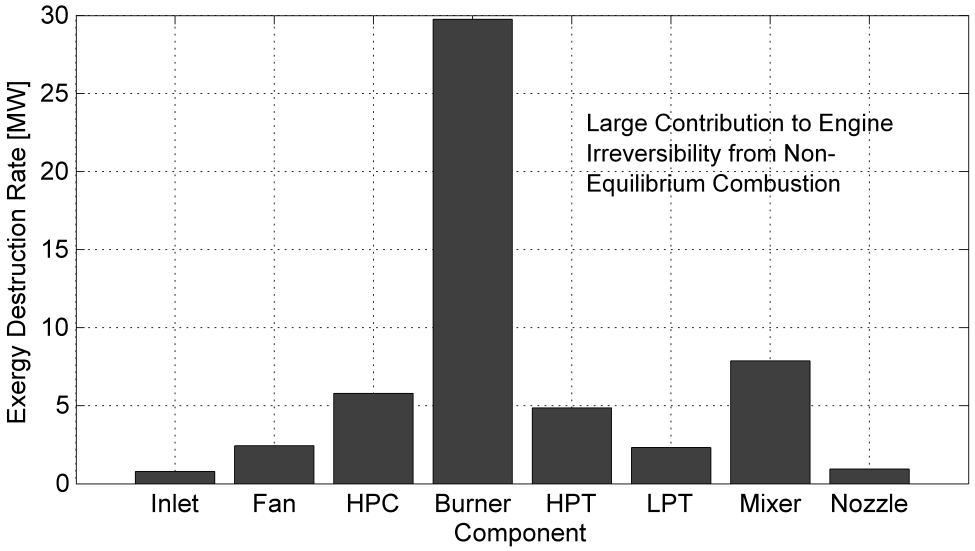

Figure 43: Exergy Destruction Rate Engine Distribution.

The linkage between component design parameters, exergy destruction, and system-level performance is now investigated in greater detail. In order to show this, several components were investigated for a range of design parameters choices. Figures 49-54 illustrate the sensitivities of the PTMS compressor efficiency, PTMS power turbine efficiency, PTMS/bleed heat exchanger effectiveness, bleed/PTMS heat exchanger pressure drop, engine high pressure turbine efficiency, and nozzle velocity coefficient, respectively. Each of these shows the change in the exergy destruction at the component level on the left axis and the change in system-level fuel consumption on the right.

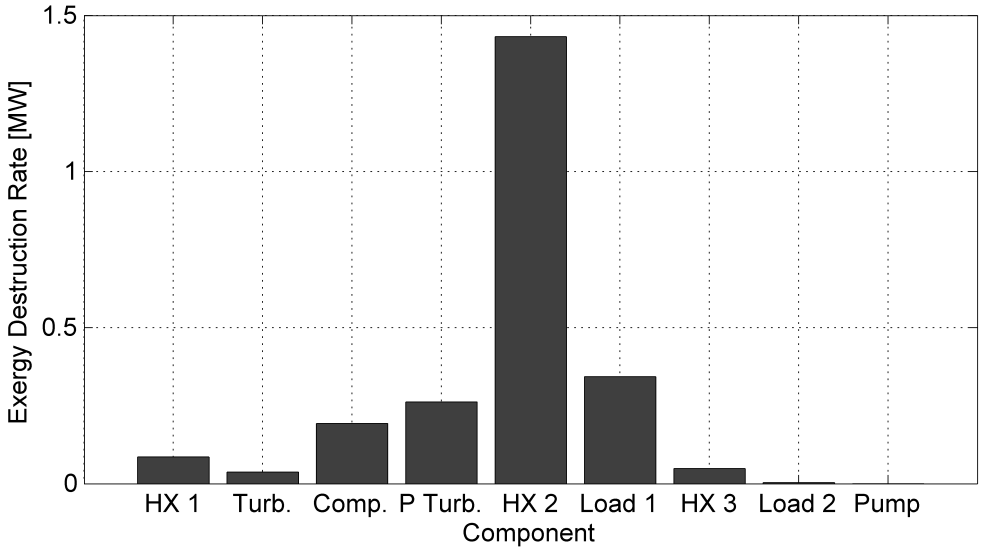

Figure 44: Exergy Destruction Rate Thermal Management Distribution.

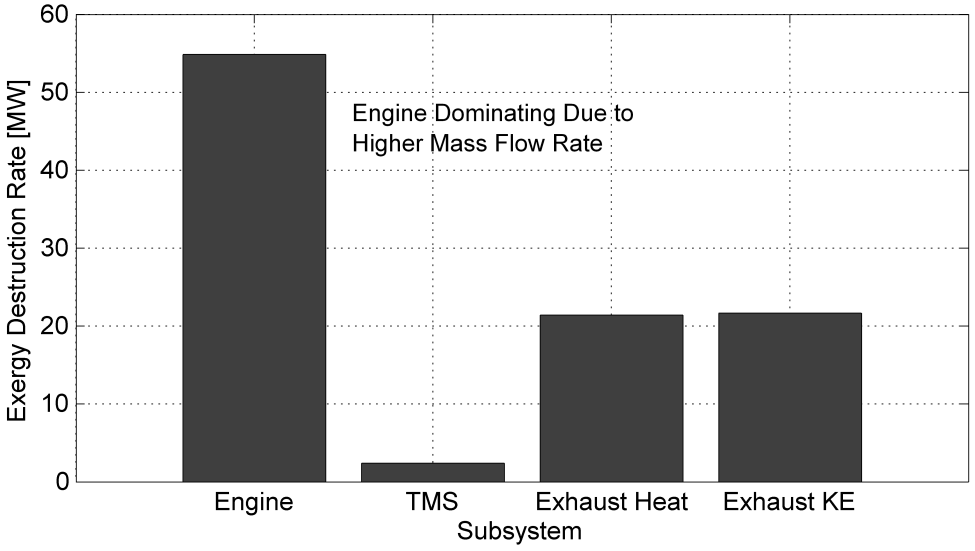

Figure 45: Exergy Destruction Rate System Distribution.

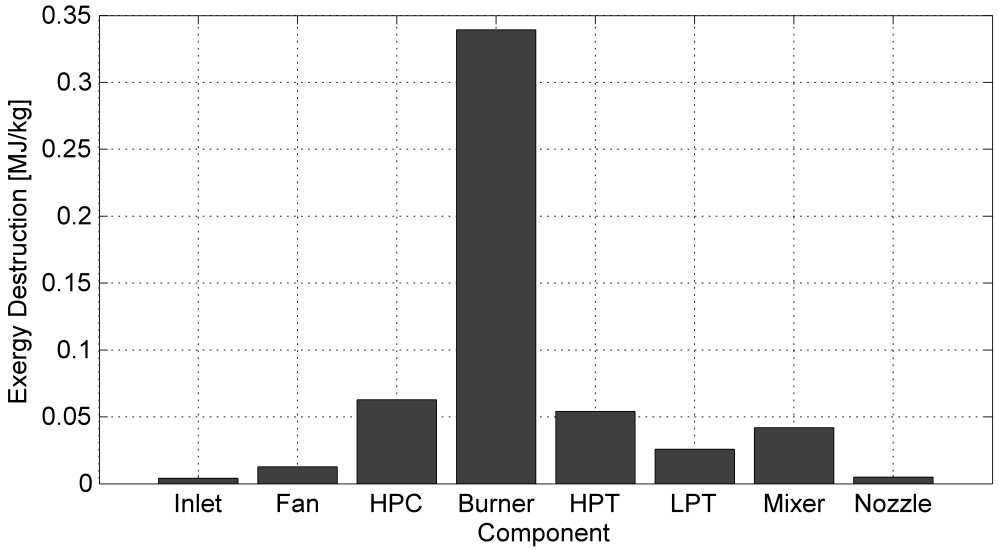

Figure 46: Intensive Exergy Destruction Engine Distribution.

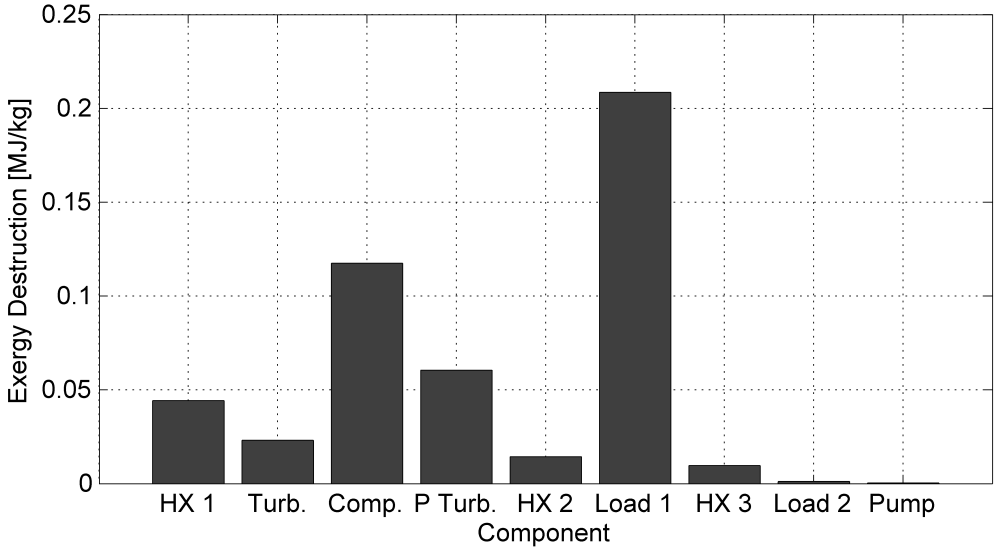

Figure 47: Intensive Exergy Destruction Thermal Management Distribution.

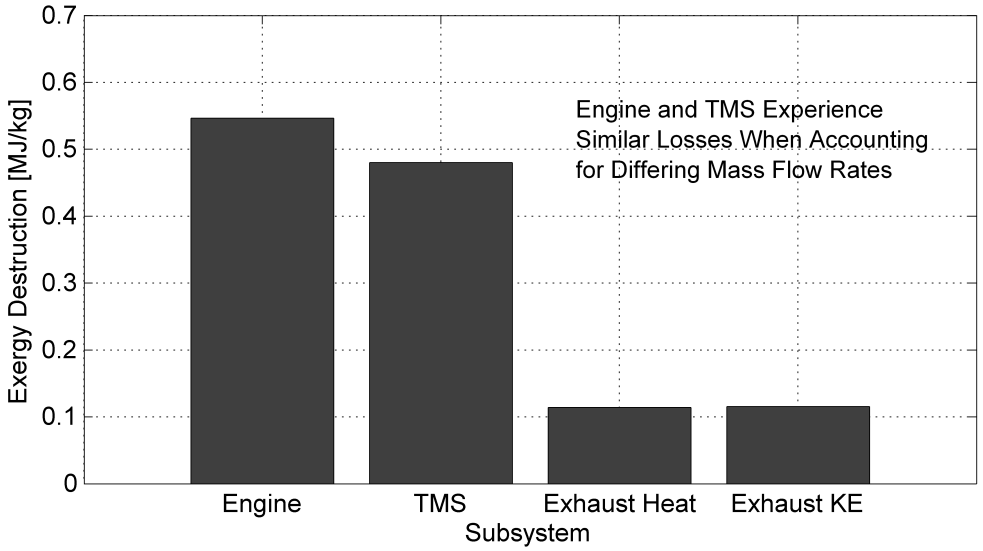

Figure 48: Intensive Exergy Destruction System Distribution.

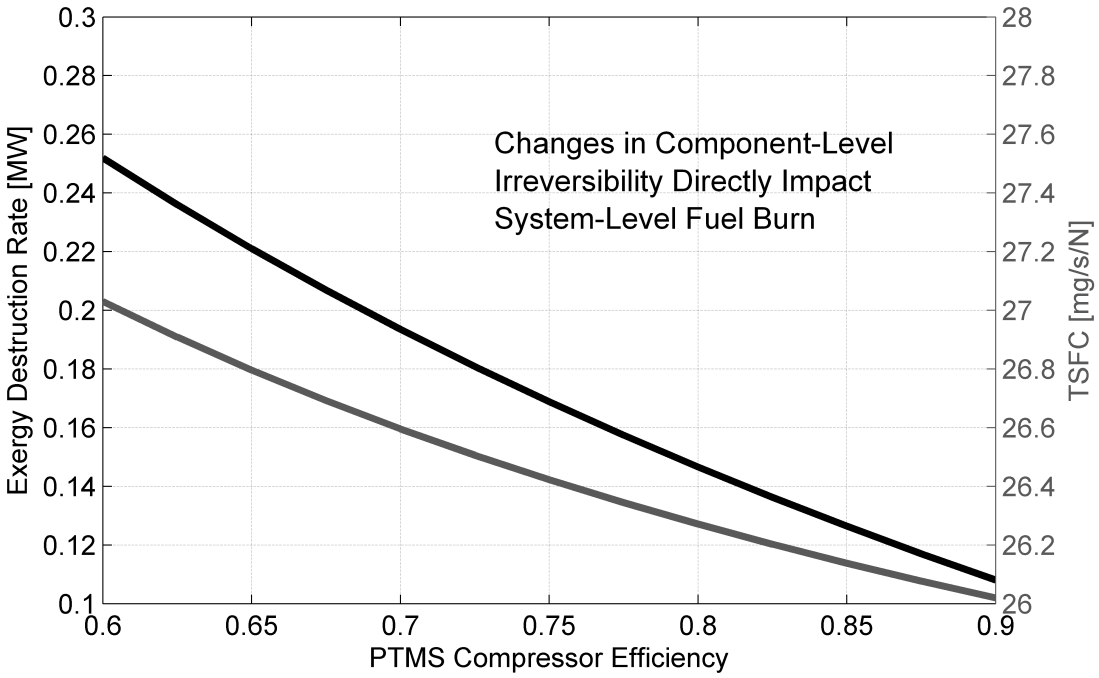

Figure 49: Component and System Effects of PTMS Compressor Efficiency.

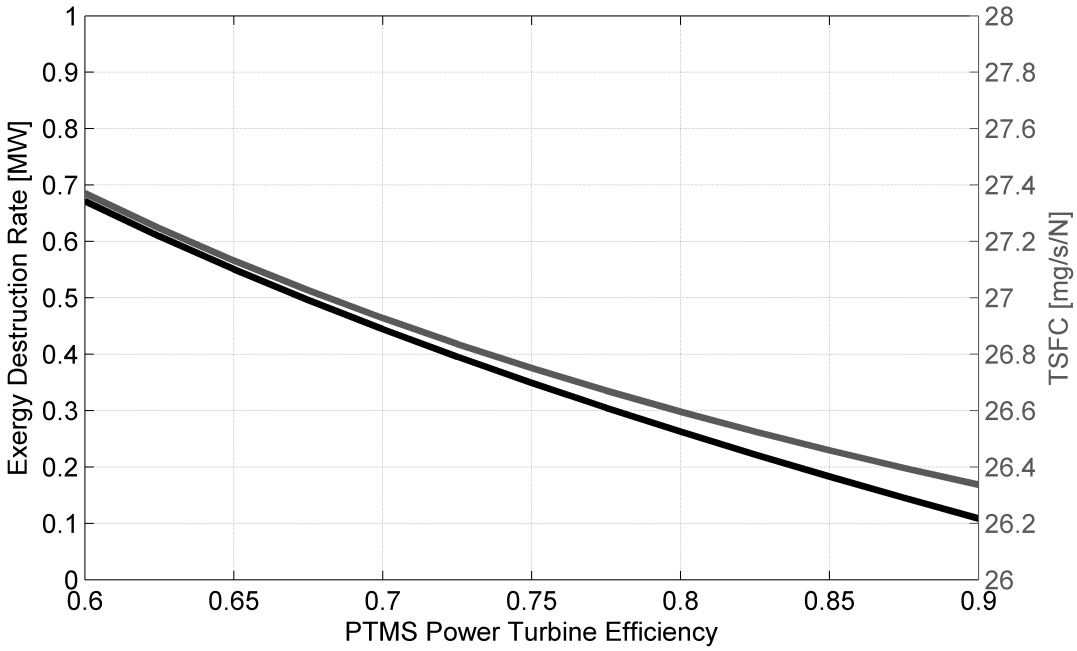

Figure 50: Component and System Effects of PTMS Power Turbine Efficiency.

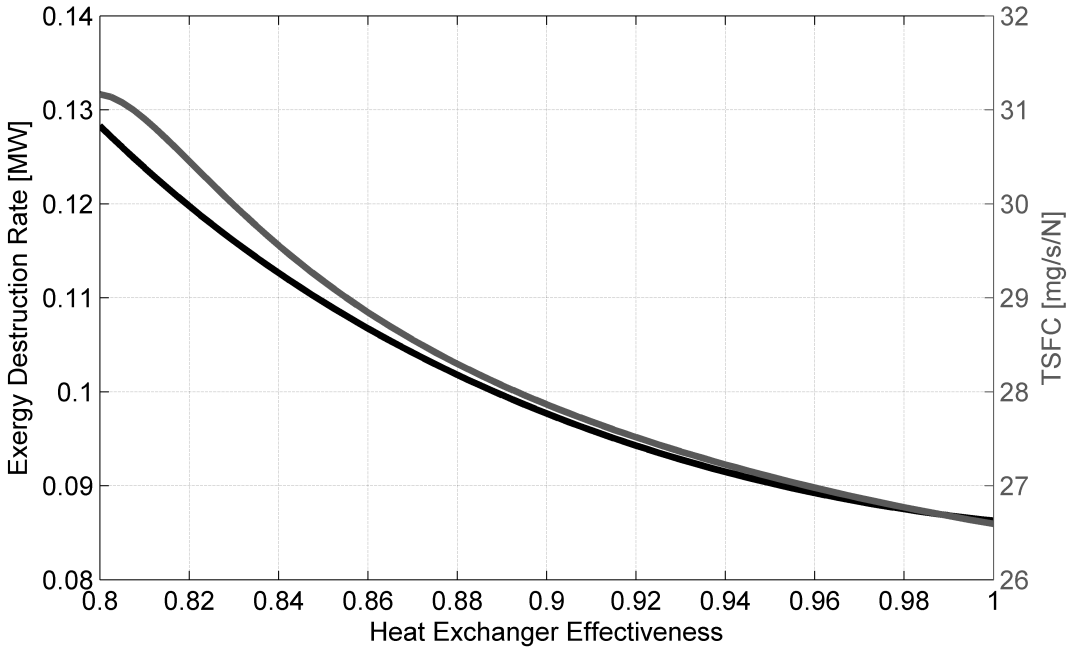

Figure 51: Component and System Effects of Bleed/PTMS Heat Exchanger Effectiveness.

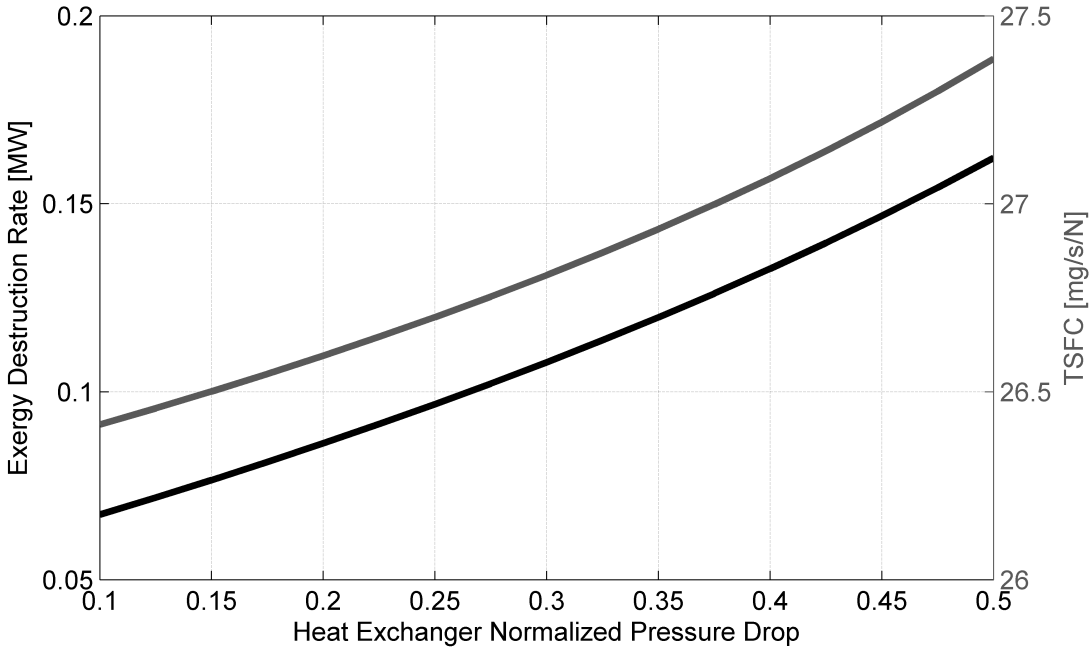

Figure 52: Component and System Effects of Bleed/PTMS Heat Exchanger Pressure Drop.

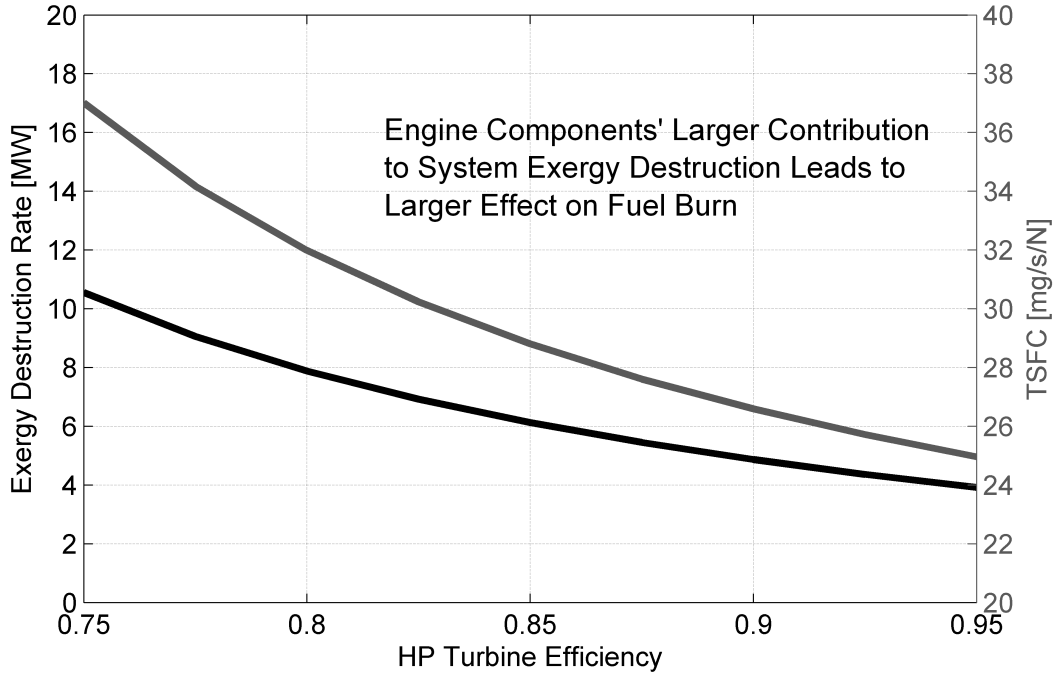

Figure 53: Component and System Effects of Power Turbine Efficiency.

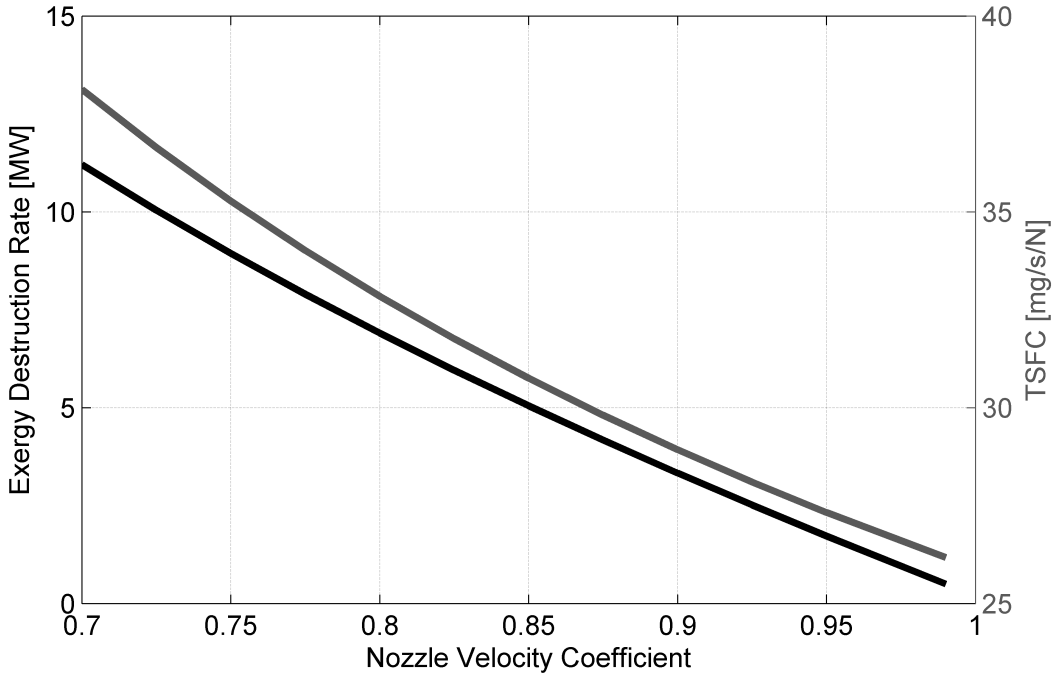

Figure 54: Component and System Effects of Nozzle Velocity Coefficient.

All of these trends demonstrate a reduction in fuel burn for improvements in component efficiencies as expected. This reduction is also seen for increases in heat exchanger effectiveness, while an increase in fuel burn is experienced for increases in component pressure losses. The individual component exergy destruction rates follow the same trends as the system-level engine fuel burn results. Another important aspect to note is the difference in magnitudes of the exergy destruction rates for the various components. Engine component improvements result in much larger destruction rates as was previously shown for the design point in Figs. 43 and 44.

4.5.3 Case C: Energy Balance with High Heat Load

This case, like Case A, is simply the result of the previous experiment for the integrated system with the higher PTMS heat load. This is so that this first-law-based case can then be compared to the exergy-based design.

It was previously seen that the interactions between the subsystems are even more significant due to the higher heat load.

4.5.4 Case D: Exergy Characterization with High Heat Load

It is now time to reexamine the results of the high heat load case from Experiment 1a from the perspective of exergy destruction. Once again, like in Case B, the exergy destruction distributions are presented, but the higher PTMS heat load is used. Figs. 55-57 illustrate the extensive exergy destruction distribution for the high heat load compared side by side with the previous results from Case B. A few important observations can be made by comparing these two different distributions. First, it is seen that the higher thermal load directly results in an increase in exergy destruction for the PTMS load component, since the pressure drop across the component now has a larger effect due to the higher temperature. Also, the relative impacts of the engine components remain essentially the same, but they all increase in magnitude due to the higher thermal load. There is also an increase in the exergy destruction resulting from the waste heat in the engine exhaust; however, the destruction in the wasted exhaust kinetic energy remains unchanged.

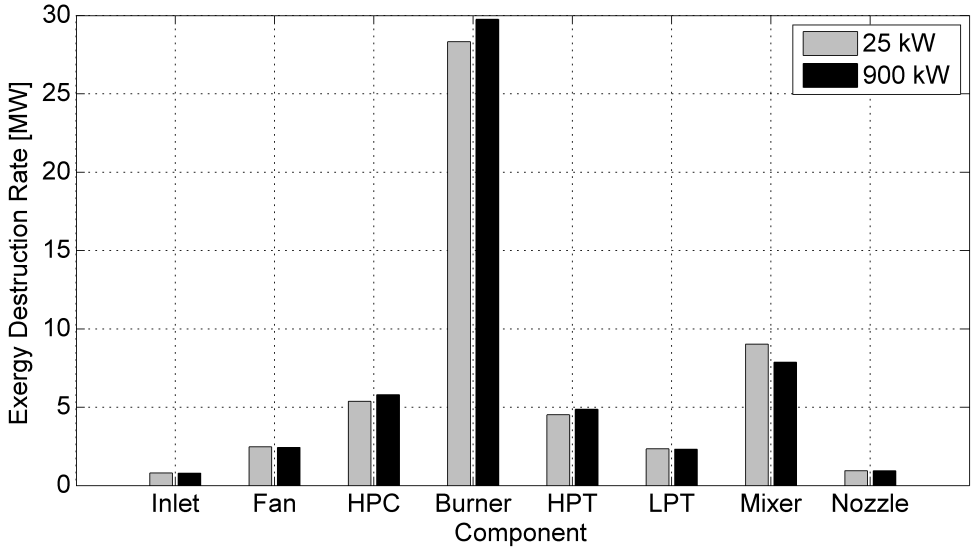

Figure 55: Exergy Destruction Rate Engine Distribution with High Heat Load.

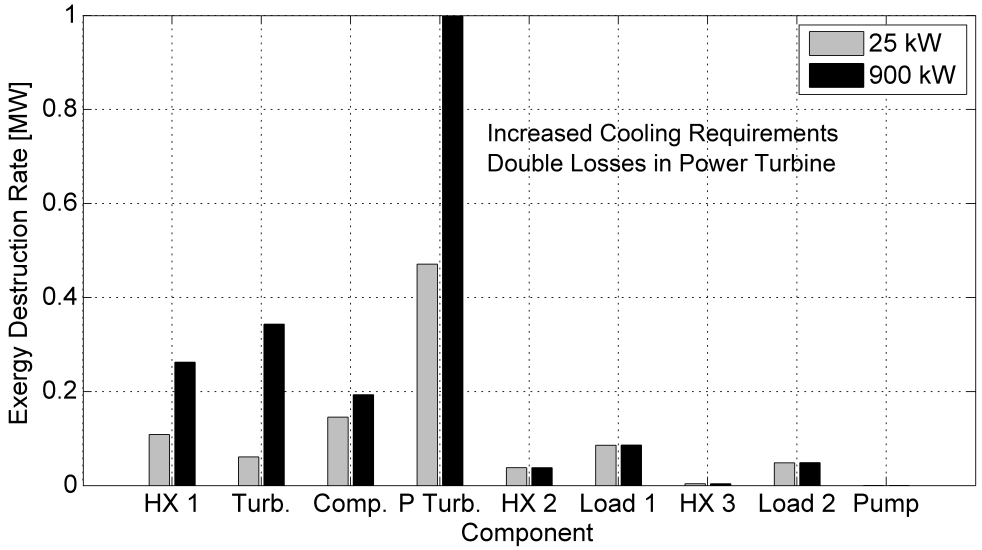

Figure 56: Exergy Destruction Rate Thermal Management Distribution with High Heat Load.

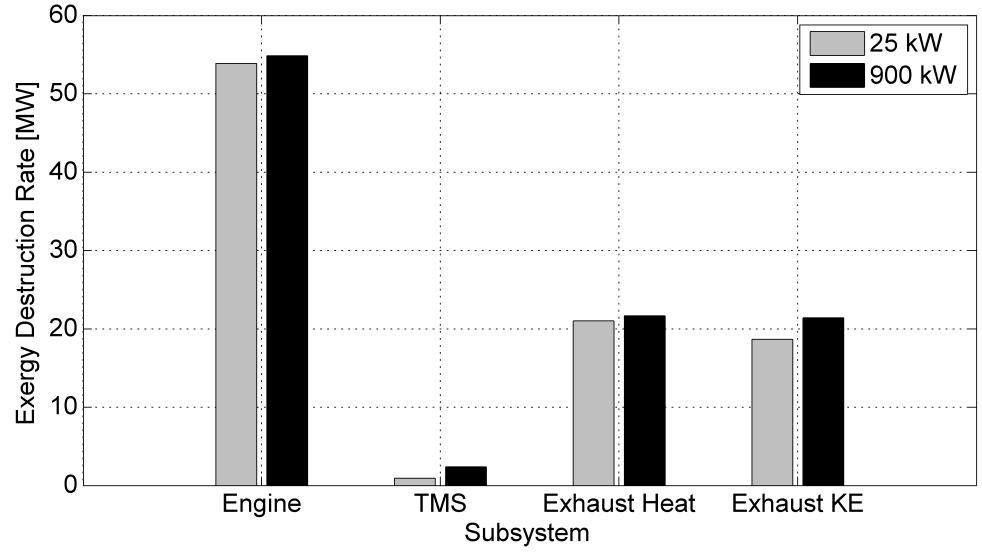

Figure 57: Exergy Destruction Rate System Distribution with High Heat Load.

4.6 Direct Comparison of Exergy Destruction and Fuel Burn as Design Metrics

As a final point to underscore the benefit of the exergy destruction metric's incorporation into the systems design process, a direct comparison of exergy destruction and fuel burn as design metrics is made here. This is done through the examination of the fuel burn and exergy destruction sensitivities with respect to the various design parameters presented in this chapter.

First, the fuel burn sensitivity is examined; this is essentially the traditional approach of Cases A and C. For this, the sensitivity vector is expressed as:

$$\nabla \bar{F}\left(\vec{\bar{X}}\right) = \left[\frac{\partial \bar{F}}{\partial \bar{X}_1} \quad \cdots \quad \frac{\partial \bar{F}}{\partial \bar{X}_n}\right] \tag{83}$$

where X represents the design parameters such as pressure drop and component efficiency and F represents the overall system fuel burn. These are expressed here in non-dimensional terms by dividing the variables by their design point values:

$$\frac{\partial \bar{F}}{\partial \bar{X}} = \frac{X_{\text{design}}}{F_{\text{design}}}\frac{\partial F}{\partial X} \tag{84}$$

This fuel burn gradient is shown at the system design point in Fig. 58. The design parameters are listed in Table 23. This was created by individually perturbing each of the design variables through a finite difference: $\vec{X_0} + \vec{h}$ where $\vec{h}$ is very small. The figure clearly shows the effect of each of the system design parameters on the overall fuel burn at the design point. The coloring of each block represents the value of a specific element of the sensitivity vector. The lighter colors represent larger positive values (an increase in the parameter increases the fuel burn), while the darker colors represent larger negative values (an increase in the parameter decreases the fuel burn).

This shows pictorially the strong positive relationship between fan pressure ratio and fuel and the strong negative relationship between the turbine inlet temperature and component efficiencies. As far as the TMS goes, the heat exchanger parameters have the greatest impact.

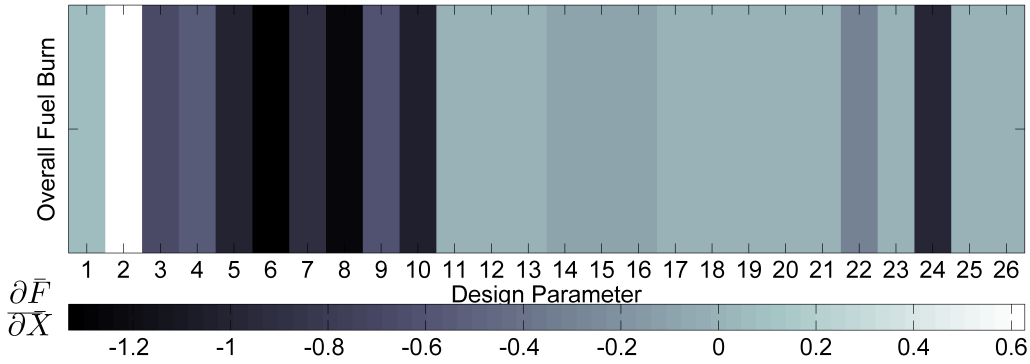

Figure 58: Fuel Burn Gradient at Design Point.

Next, a similar approach is taken for the irreversibility characterization approach demonstrated in Cases B and D. For this, the exergy destruction is used in lieu of fuel burn. This then allows the design parameters to directly affect the individual components of the system exergy destruction. This means that the previous sensitivity vector now becomes a two-dimensional matrix. The sensitivities are expressed in a matrix with respect to each of the individual component losses as:

$$J_{\vec{\bar{F}}}\left(\vec{\bar{X}}\right) = \begin{bmatrix} \frac{\partial \bar{F}_1}{\partial \bar{X}_1} & \cdots & \frac{\partial \bar{F}_1}{\partial \bar{X}_n} \\ \vdots & \ddots & \vdots \\ \frac{\partial \bar{F}_m}{\partial \bar{X}_1} & \cdots & \frac{\partial \bar{F}_m}{\partial \bar{X}_n} \end{bmatrix} \tag{85}$$

X still represents the n design parameters. This time, however, $\vec{F}$ is a vector that contains each of the m component losses in terms of exergy destruction. Like the previous plot of the fuel burn gradient, the exergy destruction Jacobian is illustrated in Fig. 59. Once again, the corresponding design parameters are listed in Table 23.

Table 23: System Design Variables Illustrated in Fuel Burn Gradient and Exergy Destruction Jacobian.

1	Overall Pressure Ratio	14	PTMS Compressor Efficiency
2	Fan Pressure Ratio	15	PTMS Turbine Efficiency
3	Turbine Inlet Temperature	16	PTMS Power Turbine Efficiency
4	Inlet Efficiency	17	Fuel Loop Minimum Pressure
5	Fan Efficiency	18	Recirculation Mass Flow Rate
6	HPC Efficiency	19	FTMS Heat Load Pressure Drop
7	Burner Efficiency	20	Fuel Pump Efficiency
8	HPT Efficiency	21	Heat Exchanger 1 Pressure Drop
9	LPT Efficiency	22	Heat Exchanger 1 Effectiveness
10	Nozzle Velocity Coefficient	23	Heat Exchanger 2 Pressure Drop
11	PTMS Closed Loop Pressure Ratio	24	Heat Exchanger 2 Effectiveness
12	PTMS Turbine Outlet Pressure	25	Heat Exchanger 3 Pressure Drop
13	PTMS Heat Load Pressure Drop	26	Heat Exchanger 3 Effectiveness

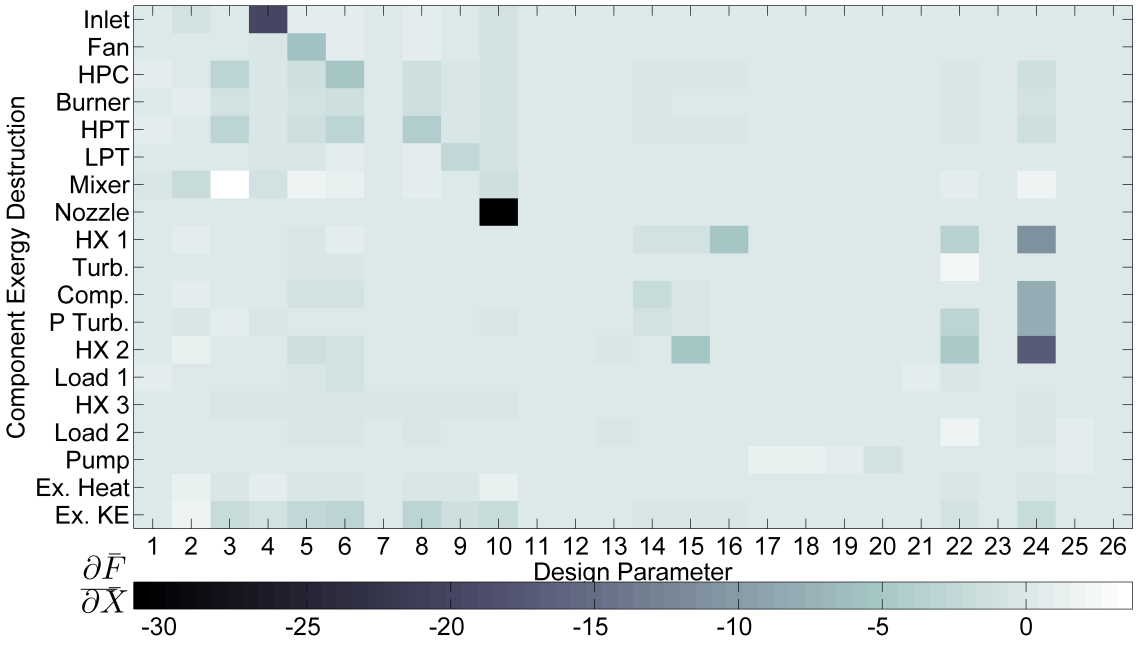

Figure 59: Exergy Destruction Jacobian at Design Point.

The direct comparison of Figs. 58 and 59 shows a great advantage of the irreversibility characterization of the system. It enables a quick view of the losses throughout the system and how they change throughout the design space in response to the design parameters. This takes the fuel burn down to the component-level and shows exactly how it is spent and for what purpose. This clearly gives the designer more insight into the integrated systems design. The computation of the design variable sensitivities with respect to component exergy destruction is further explored in more detail in Chapter VI in the context of the irreversibility allocation design.

4.7 Summary of Irreversibility Characterization

The results of this investigation are an initial indication of the benefits of designing in terms of irreversibility allocation. This formulation allows for an absolute and consistent buildup of system losses. It is absolute in the sense that it expresses the amount of loss from the thermodynamic ideal and does not require a perturbation in design parameters to quantify it. The formulation is consistent in the sense that all of the losses can be directly compared: An increase of 1 MW of exergy destruction in the engine is identical to 1 MW in the PTMS. Furthermore, the exergy destruction follows the same trend as the system-level fuel burn metric since all of the system work is extracted from the fuel.

CHAPTER V

BRINGING SYSTEM COST INTO THE MIX

The previous two experiments focused on providing the foundation for the irreversibility allocation research. The first dealt with the idea of integrated propulsion and thermal management modeling and simulation. This was proposed as a means of better meeting the thermal system requirements during the conceptual design of the aircraft engine. This also led to the creation of the foundation for the CRATOS modeling and simulation environment. The second experiment built on this by making the case for the irreversibility characterization and led to significant upgrades to the CRATOS modeling and simulation environment.

The next two chapters start to focus on the proper way of allocating the unavoidable thermodynamic losses throughout the entire integrated system. They each concentrate on an additional element (first economics and then mission performance) that is brought into the fold along with the thermodynamics. Later, all of these are used concurrently to perform the actual irreversibility allocation. This experiment begins down this path by exploring the relationship between cost and thermodynamics. Specifically, the thermoeconomic research question from Chapter II is addressed. This enables the designer to directly consider the financial repercussions of his or her thermodynamic design decisions.

5.1 Statement of Research Hypotheses #2a

The hypothesis to Research Question 2a based on the thermoeconomic literature review of Chapter II is stated as:

Research Question #2a: Does the posing of the integrated thermal management systems design problem in thermoeconomic terms enable the designer to quantitatively identify more favorable system-level designs?

Research Hypothesis #2a: The application of thermoeconomic techniques to integrated propulsion and thermal management systems design provides a quantifiable means of finding a system-level solution with the most value in terms of thermodynamics and cost; however, it is unable to directly account for changes in vehicle mission performance capability.

To test this hypothesis, an experiment was designed to compare the irreversibility allocation using thermodynamics alone to the case where non-thermodynamic criteria are also taken into account. For this experiment, this is represented as a cost, which is related to component design parameters. It is then shown that by taking cost into account the designer will arrive at a much different system-level solution.

5.2 Experimental Approach

Table 24 illustrates this experiment graphically. Both experiments, as well as the remainder of the experiments in this research, utilize the integrated system-level simulation in the high heat load configuration. Case A then uses a second-law-based design approach relying on thermodynamics exclusively. Case B expands on this by directly capturing the component-level costs as a function of performance.

The steps to this experiment are summarized as:

- Include costing equations for the components by incorporating data fits of weight and cost estimating relationships
- Compare the favorable irreversibility allocations obtained using both thermodynamics and cost to those only considering thermodynamics

- Demonstrate that the variation of costs of the system due to the changes in thermodynamic performance have a large influence on design decisions

Table 24: Experiment #2a: Cost Formulation.

A	**B**
Integrated systems design	Integrated systems design
High heat load	High heat load
Thermodynamics (Exergy)	Thermodynamics and cost

5.3 Theory

Next, the requisite theory to enable the second component of the resource allocation triad is discussed. This allows for the cost prediction capability required to appropriately trade off irreversibility during the conceptual propulsion systems design process. The theory of this section stems from the thermoeconomic background laid out in Chapter II.

5.3.1 Thermoeconomic Formulation

It was shown in Chapter II that the designer cannot properly allocate irreversibility based on thermodynamic metrics alone since the results are meaningless if they do not take into account the financial costs of improvement. Although cost data is difficult to obtain for aircraft propulsions systems, one option is to include component weight and degree of implementation difficulty as surrogates for financial cost. The system-level optimization procedure must allow for the incorporation of these additional metrics and their change with respect to changes in the thermodynamic performance of the system.

This is similar to the thermoeconomic notion of concurrently considering exergy and cost that was previously discussed. In the overall thermoeconomic formulation,

this data is combined with scaling coefficients, and a system-level metric is achieved. This combined metric is then minimized:

$$\min J = \sum_i (c_D D_i + c_z z_i) \tag{86}$$

where D_i represents the exergy destruction for component i and z_i the cost. The coefficients c_D and c_z then convert these to a total cost (production and operating) of the component. The overall system cost is then obtained by adding up the costs of all of the components.

The main element that needs to be incorporated in the previous modeling and simulation approach is the estimation of a representative cost for each individual component of the system. This can be estimated in numerous ways depending on the data available. In the case of aircraft engine component costs, the data that is publicly available is relatively small.

If financial cost data is unavailable, other metrics such as degree of implementation difficulty or weight could also be used as a surrogate. This approach is frequently used in the aerospace industry. Another approach might be to look at cost in a more holistic manner, i.e. aircraft life cycle cost. However, this was not considered here due to the difficulty in obtaining this data and relating it down to the component-level. It was desired to use the most transparent techniques available to model cost to clearly illustrate the process in this research.

5.3.2 Component Cost Estimating Relationships

One way to estimate the cost of individual components is by creating cost estimating relationships (CERs) that link component performance to cost. These relationships are obtained by regressing component cost data to key performance parameters such as pressure ratio and mass flow rate. El-Sayed used the following formulation in his thermoeconomic writings [56]. First, a representative area is predicted using a data

fit of up to three performance parameters:

$$A = k{x_1}^{n_1}{x_2}^{n_2}{x_3}^{n_3} \tag{87}$$

From this area data fit, a component cost is then estimated using a constant c_a that varies from component to component

$$z_i = c_{ai}A_i \tag{88}$$

A similar approach could just as easily be used for weight in the case of aircraft engines if this is desired, since weight is often more representative than area for aerospace applications. In this case, this parameter would be used in the data fits in place of the area

$$W = k{x_1}^{n_1}{x_2}^{n_2}{x_3}^{n_3} \tag{89}$$

If the necessary data is available, then c_a constants can be used to relate component weight to financial cost. Since this is also difficult to obtain for aircraft engines, an alternative approach is to relate total engine weight to production cost.

Using either of these approaches enables the designer to directly link a change in component performance to a change in component cost and ultimately a change in system-level cost. This then allows for an investigation of the financial repercussions of system efficiency improvements. This will play a large role in the ultimate irreversibility allocation process of Chapter VII.

5.3.3 Ground-Based Power Area Curve Fits and Cost Coefficients

Before leaving the theory section and heading into the discussion of the actual implementation of the cost prediction within the modeling and simulation environment, the cost relationships used by El-Sayed in [56] are examined in a little more detail. The relationships were created for the specific purpose of ground-based power systems

design. These ground-based power systems are of a much larger size than the aircraft engines of interest here. As a result, these relationships are not directly applicable to aircraft engine design. Instead, they are simply shown to illustrate their form; new relationships for aircraft engine design will then be obtained in the implementation section.

Once again, the component cost was defined as a product of the component area and a component cost-to-area coefficient:

$$z_i = c_{ai} A_i \tag{90}$$

The cost coefficient is held constant for each component, but the component area is obtained through a curve fit of key performance parameters as

$$A = k {x_1}^{n_1} {x_2}^{n_2} {x_3}^{n_3} \tag{91}$$

The cost coefficients are listed in Table 25; the corresponding area curve fits are presented for each of the components in Table 26. All of the units are in terms of kg, m, and s, except for the pressures and heat rates; the pressures are in kPa and the heat rates are in kW.

Table 25: Ground-Based Power Component Cost Coefficients [56].

Component	Coefficient [$\$K/m^2$]
Axial Compressor	538
Combustor	2.15
Gas Turbine	538
Mixing Chamber	1060
General Heat Exchanger	0.430
Feed Pump	32.0

Table 26: Ground-Based Power Component Representative Area Curve Fits [56].

Component	Representative Area $[m^2]$
Axial Compressor	$0.0063\,(\dot{m})\,(PR)^{0.45}\left(\frac{\eta}{1-\eta}\right)^{0.45}$
Combustor	$0.261\,(\dot{m})^{0.5}\,(p_{in})^{0.24}\,(dp)^{-0.75}$
Gas Turbine	$0.0135\,(\dot{m})\,(PR)^{-0.5}\left(\frac{\eta}{1-\eta}\right)^{0.85}$
Mixing Chamber	1
General Heat Exchanger	$0.8\,\dot{Q}\,(T_{inhot}-T_{incold})^{-1}\,(dp_{hot})^{0.15}\,(dp_{cold})^{-0.15}$
Feed Pump	$0.000435\,(\dot{m})^{0.55}\,(p_{out}-p_{in})^{0.55}\left(\frac{\eta}{1-\eta}\right)^{1.05}$

5.4 Implementation

Now that the modeling and simulation requirements and the second-law thermodynamic implementation have been explained, the cost component relating to Research Question 2a is discussed. Next, the CRATOS software was upgraded to include a cost prediction capability. This was achieved by including the component weight curve fits and cost estimating relationships in the system model.

It was necessary to include prediction for component cost as described in Chapter II; the implementation of this follows the approach outlined in the last section.

5.4.1 Propulsion System Weight Estimation

As previously explained in the theory section, one problem with the cost estimating relationships used by El-Sayed in his thermoeconmic formulation [56] is that the curve fits were specifically developed for large ground-based power systems. As a result, they are not completely applicable to smaller aerospace engine applications. Additionally, information is lacking for some of the necessary engine components that are not present in ground-based systems, such as the nacelle and nozzle. Therefore, new curve fits were created using the Weight Analysis of Turbine Engines (WATE++) weight estimation software [166].

The WATE++ software is part of the NPSS propulsion system modeling framework that was previously detailed in Chapter II. This software uses the thermodynamic data from NPSS to construct a detailed buildup of the engine that is then used to estimate the physical properties like size and weight. To use this software to create weight prediction equations for the baseline propulsion system, it was first necessary to create a propulsion system model in NPSS. This model was comparable to the isolated engine model previously created in Chapter III. Using this model, combined with a generic WATE++ model of component properties, a mass breakdown for the engine was obtained at the system design point. Next, the major design parameters were varied over reasonable ranges to investigate the weight sensitivities. Using the data from all of these different engine design runs, a least squares regression was performed on the data for each of the components to obtain the coefficients for the following equation [118]:

$$f\left(\vec{x}_i, \vec{\beta}\right) = \beta_0 {x_1}^{\beta_1} {x_2}^{\beta_2} {x_3}^{\beta_3} \tag{92}$$

where f represents the dependent variable (weight in this case), x represents the independent variables (performance parameters such as mass flow rate and pressure ratio), and the β variables are the coefficients obtained from the regression. To do this curve fitting, the sum of squares of the error residuals is minimized

$$S = \sum_{i=1}^{n} {r_i}^2 \tag{93}$$

The residuals are the errors between the actual and predicted values for each point used in the curve fitting:

$$r_i = y_i - f\left(\vec{x}_i, \vec{\beta}\right) \tag{94}$$

where f is the predicted value and y is the actual value. Table 27 shows the component

mass prediction relationships that were obtained using the WATE++ model and the least squares regression.

Table 27: Propulsion System Component Mass Estimation Relationships.

Component	Mass $[kg]$
Inlet and Nacelle	$0.81\,(\dot{m}_0)^{1.01}\,(\eta)^{-0.79}$
Fan	$0.57\,(\dot{m}_2)^{1.17}\,(\eta)^{0.18}\,(PR)^{0.43}$
Swan Neck Duct	$0.33\,(\dot{m}_{25})^{1.30}$
HP Compressor	$2.45\,(\dot{m}_{25})^{1.06}\,(\eta)^{-0.11}\,(PR)^{0.23}$
Burner	$23.73\,(\dot{m}_3)^{0.47}$
HP Turbine	$0.50\,(\dot{m}_4)^{1.42}\,(\eta)^{0.38}\,(PR)^{0.86}$
Interstate Turbine Transition (ITT) Duct	$0.17\,(\dot{m}_{49})$
LP Turbine	$0.13\,(\dot{m}_{49})^{1.63}\,(\eta)^{-1.95}\,(PR)^{0.63}$
Turbine Exit Guide Vane (TEGV) Duct	$0.08\,(\dot{m}_5)$
Bypass Duct	$0.02\,(\dot{m}_{13})^{1.38}$
Mixer	$0.10\,(\dot{m}_7)$
Tailpipe	$0.33\,(\dot{m}_7)^{0.50}$
Nozzle	$0.04\,(\dot{m}_7)$
LP Shaft	$0.02\,(\dot{m}_0)^{1.50}$
HP Shaft	$0.33\,(\dot{m}_0)^{0.98}$
Engine Mount	$0.10\,(\dot{m}_0)^{1.16}$

For these relationships, $\dot{m}$ is the mass flow rate in kg/s, η is the component efficiency, and PR is the pressure ratio across the component. The subscripts correspond to the stations of the propulsion system model listed in Chapter III.

5.4.2 Jet Engine Unit Cost Estimation

After the prediction of the component weights for a specific configuration, the total propulsion system weight is then easily obtained. This weight is an excellent predictor of the production cost of the engine. Younossi provides a cost estimation relationship (CER) for unit production cost as a function of rotor inlet temperature, dry weight, and unit production number [186]. These relationships also take into account the learning curve effects that reduce the cost of each engine due to the knowledge of the

previously produced engines. After the cost stabilizes around unit 375, this unit cost is predicted as [186]

$$\ln T_{375} = -10.40 + 1.162 \ln (ritf) + 0.482ab + 0.262 \ln (drywt) \tag{95}$$

where $ritf$ is the rotor inlet temperature in °F, $drywt$ is the total engine dry weight in lb, and T_{375} is the production price for unit number 375 in \$M FY2001. ab is a switch that is set as 1 for afterburning engines and 0 for non-afterburning engines.

For a non-afterburning engine in metric units, this equation becomes

$$\ln z = -10.40 + 1.162 \ln \left\{ \left[\frac{9}{5} (T_4 - 273) \right] + 32 \right\} + 0.262 \ln (2.205W) \tag{96}$$

where z now represents the production price, T_4 the turbine inlet temperature in K, and W the system mass in kg. This system mass is the sum of the individual components of the propulsion system

$$W = \sum_i W_i \tag{97}$$

It is then assumed that the cost of the thermal management systems is negligible compared to the engine itself and is neglected in this work. The main cost repercussions resulting from thermal management system design modifications arise from downstream changes to the engine cycle. For example, a reduction in compressor bleed air results in a reduction in overall engine mass flow. This, in turn, leads to a reduction in engine component weight and cost.

5.4.3 Combining Operating and Production Costs

The weight prediction fits and the costing equation of the previous section enables an overall cost estimation based on the system performance. This new information can be combined with the previous exergy destruction information from Chapter IV to arrive at an overall objective to minimize. In this case, the exergy destruction

represents the operating cost from the fuel burn that is then added to the production cost. These metrics are combined as discussed previously as

$$\min J = c_D \sum_i (D_i) + c_z z_i \tag{98}$$

This is written slightly differently from before since the costing equation used computed the overall system cost as a function of the total weight.

To complete this optimization, values for c_D and c_z must be estimated. If it is assumed that D_i is the total fuel burn for one mission, then

$$c_D = \frac{price * mission}{\rho} \tag{99}$$

where *price* is the current price of jet fuel per volume, *mission* is the average number of missions per year, and ρ is the density of the fuel. The current cost of jet fuel was assumed to be \$3.228 per gallon [78] and the density was assumed to be 3.104 kg per gallon. Finally, it was assumed that there are 300 missions per year for the fighter engine baseline.

Similarly, the cost coefficient is calculated as

$$c_z = \frac{i}{years} \tag{100}$$

where *years* is the number of years that the engine is used and i is the inflation factor. For a fighter engine, 10 years was chosen as the depreciation factor. In other words, a purchased engine will remain in service for an average of 10 years. The inflation factor is used to convert between FY2001 dollars predicted using the CER and current FY2012 dollars; it was determined to be 1.29 [168].

5.5 Results - Cost Trades

Now that the benefits of the direct characterization of irreversibility for the integrated propulsion and thermal management system have been demonstrated, the next goal of the research is to bring this concept into the realm of conceptual propulsion systems design. In this experiment, the distribution of irreversibility throughout the system is examined concurrently with its effect on the system's developmental cost.

The objective is then to minimize both irreversibility and cost simultaneously, which can be difficult since these two metrics are often at odds with one another. An increase in component efficiency can lead to a reduction in system exergy destruction, but is also accompanied by a corresponding increase in the total development cost of the system.

Table 28 illustrates the two distinct cases for this experiment. The first case further explores the results of the last two experiments by only considering thermodynamic losses in the design of the system. This is in some ways akin to the concept of entropy generation minimization (EGM) technique discussed earlier. Then, Case B takes a look at the inclusion of the cost data, which follows the thermoeconomic literature.

Table 28: Experiment #2a: Cost Formulation.

A	**B**
Integrated systems design	Integrated systems design
High heat load	High heat load
Thermodynamics	Thermodynamics and cost

5.5.1 Case A: Thermodynamics (Exergy)

The consideration of thermodynamics in isolation is the approach that was taken in the previous two experiments. Optimizing the system for minimum exergy destruction

or overall fuel burn results in a design of perfect component efficiencies and maximum performance parameters since the optimization is unconstrained. This points the designer towards the extremes of the design space plots shown in the previous experiments and is a fairly intuitive result. It is also not physically realistic since it does not consider the full repercussions of these changes. One way to remedy this is through the introduction of additional constraints on the design problem. In the final experiment, Experiment 2c, the system is optimized for a minimum fuel burn under performance constraints. The approach taken in the next case is through the direct consideration of cost and performance instead.

5.5.2 Case B: Thermodynamics and Cost

The cost prediction data is now included in the integrated model for this case. Using this data, it is now possible to directly explore the tradeoffs in regards to production cost and system irreversibility. First, the design point from the previous experiments is reexamined in light of the resulting cost information. Figure 60 shows the weights associated with each component at the system design point.

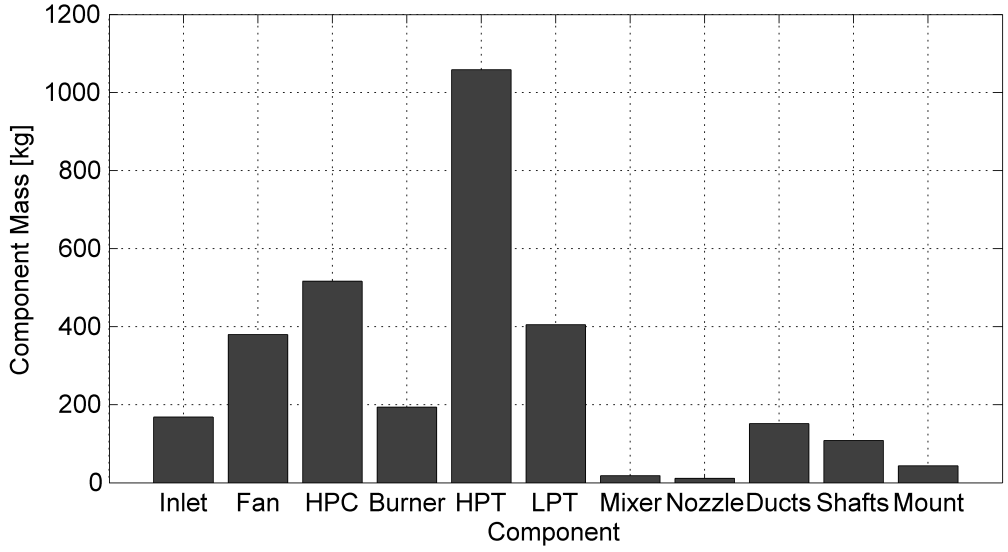

Figure 60: Propulsion System Mass Breakdown.

This figure demonstrates that the relative component contributions to system weight (and in turn production cost) are not proportional to their respective exergy destruction rates. The heavy hitters that have the most influence on the system weight are also shown to be the turbomachinery components. Combining this component information together results in a propulsion system mass of 3058 kg and a production cost of $3.53M. Rather than simply examining the weight and cost information at the design point in isolation, it is much more enlightening to revisit the trades that were investigated in Experiments 1a and 1b. Using the new cost relationships, the cost impact of the compressor efficiency trades are quantified and compared to the exergy destruction. Figures 61 and 62 present these results for a range of fan and HP compressor efficiency values. The first plot shows the propulsion system mass variation across the space, while the second translates this into system production cost.

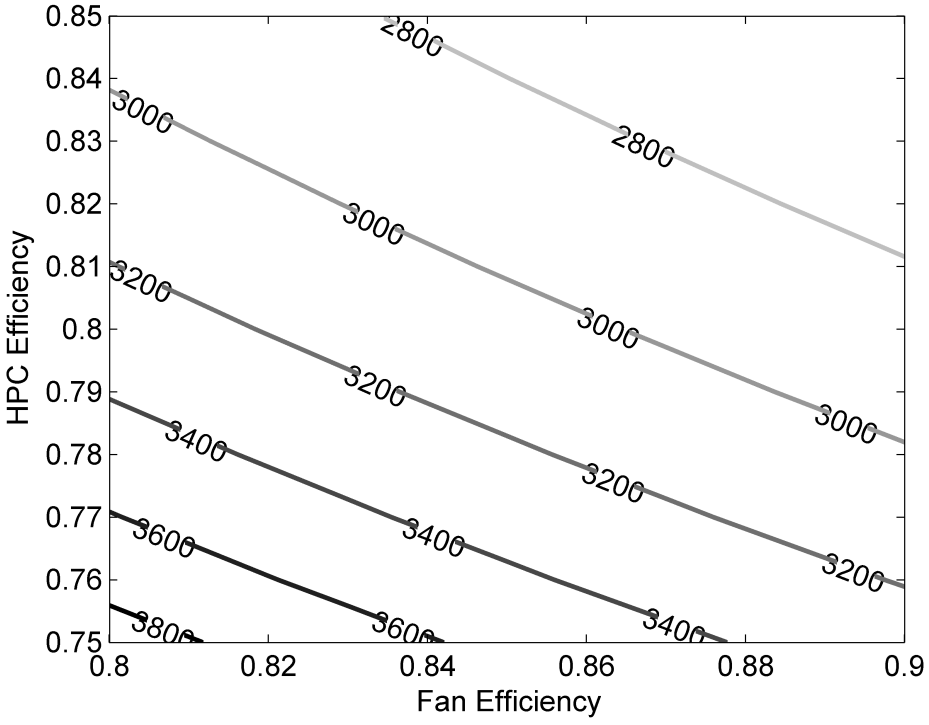

Figure 61: Total Propulsion System Mass $[kg]$.

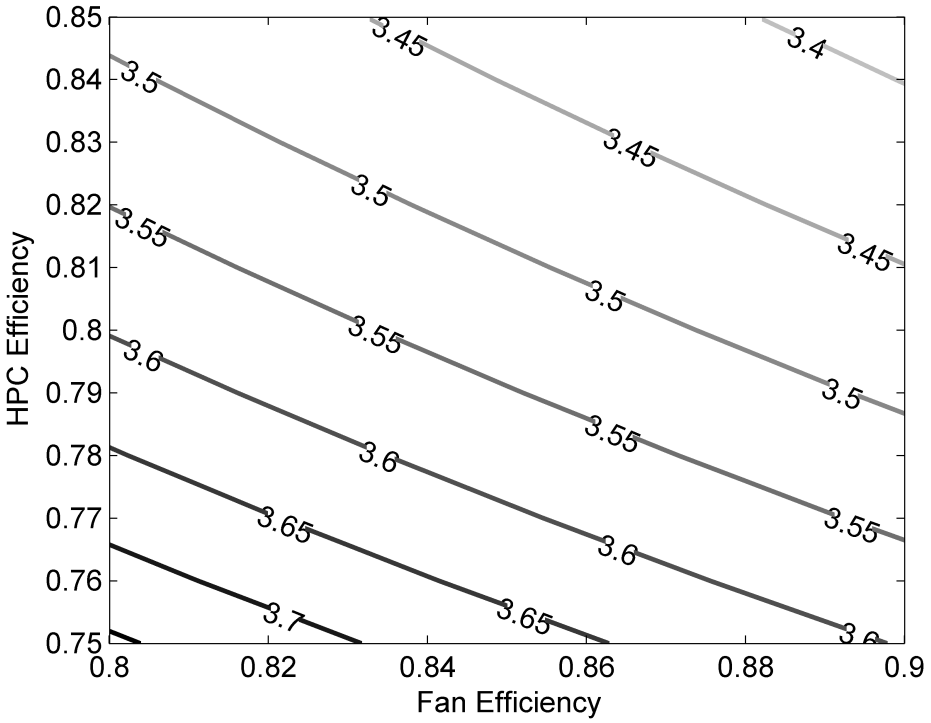

Figure 62: Production Cost [$\$M$FY2012].

The overall pressure ratio and turbine inlet temperature trades are now revisited in light of the cost prediction. Figures 63 and 64 show the results for these trades. Once again, the first shows the mass variation and the second the cost variation across the OPR and T4 design space. Comparing these plots to the results from Experiment 1b, it is seen that increases in these parameters result in both irreversibility and cost increases. However, it is also well know that increases in these parameters leads to an increase in thrust and mission performance as was explained in Chapter II. For these trades, mission performance must be taken into account to reach a more conclusive decision.

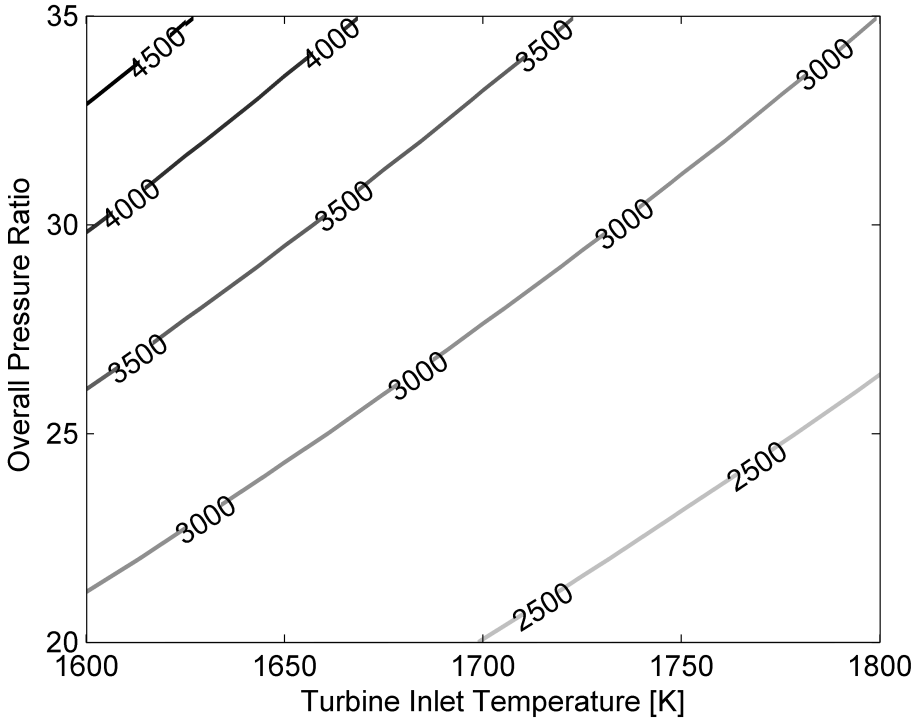

Figure 63: Total Propulsion System Mass $[kg]$.

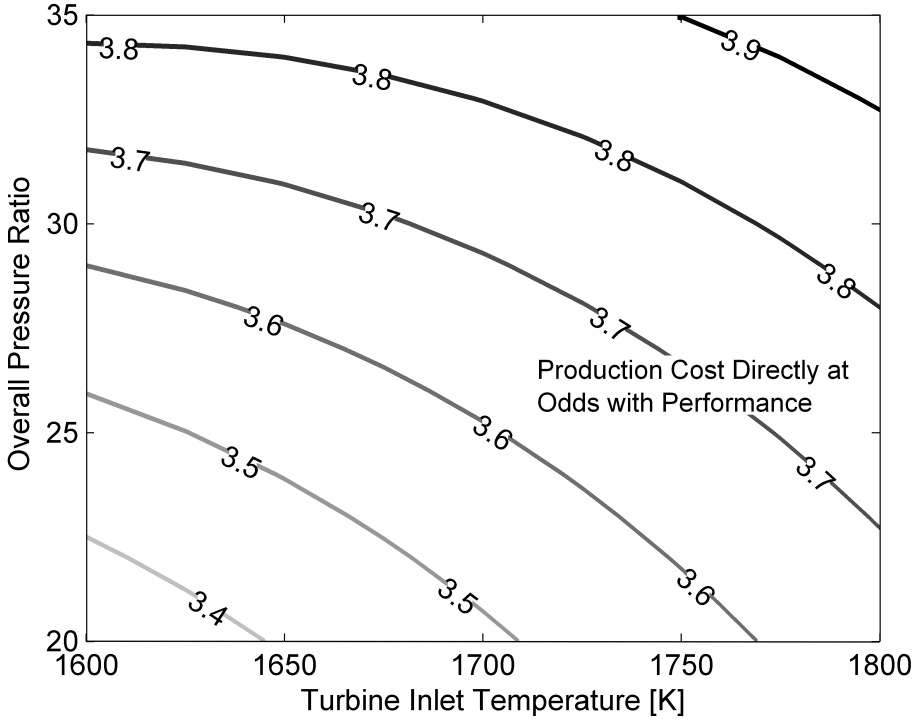

Figure 64: Production Cost [$\$M$FY2012].

5.6 Summary of Thermoeconomic Formulation

In this experiment, the thermoeconomic approach (exergy destruction and cost) was compared to the entropy generation minimization approach (exergy destruction). It was shown that at a specific point the continuation of the irreversibility minimization within the system no longer makes sense. Eventually the cost of increased efficiency simply becomes too large to justify the continued minimization of exergy destruction due to its diminishing returns. It was also seen that the cost of improvement for the thermal management system was significantly less than the engine; however, the resulting improvement at the system-level is also smaller. Finally, it was shown that for some parameters a decrease in irreversibility occurs with an additional decrease in cost. In this case, however, the system performance is degraded as well.

CHAPTER VI

ACCOUNTING FOR MISSION PERFORMANCE REQUIREMENTS

The last chapter concentrated on bringing cost prediction into the irreversibility allocation discussion. Similarly, the concentration in this chapter is on the incorporation of mission performance considerations within the irreversibility allocation process. As first explained in the household power consumption analogy of Chapter I, it is often desired to minimize power consumption while simultaneously considering the financial and performance implications of this minimization. The irreversibility and cost elements were previously added to the modeling and simulation environment in Chapters IV and V. Mission performance is investigated in the same manner here before finally considering the system optimization and allocation itself in the next chapter.

6.1 Statement of Research Hypotheses #2b

The fourth hypothesis rounds out the triad of thermodynamics, cost, and performance. It is formally stated here in response to the background literature of Chapter II:

Research Question #2b: How can the design process be modified so that the designer can explicitly take vehicle mission performance into account along with thermodynamics and cost for the integrated propulsion and thermal management problem?

Research Hypothesis #2b: The inclusion of vehicle mission performance through a third design criterion in addition to thermodynamics and cost by flying each design through a variety of missions allows the designer to quantifiably trade off thermodynamics, cost, and vehicle performance in a structured manner.

This experiment continues to use the same modeling and simulation platform as the previous experiments. The environment must be expanded to take mission performance effects into account through the inclusion of an off-design simulation capability. This then enables the simulation of the entire aircraft mission profile, which is accomplished through the quasi-steady-state simulation at a series of off-design points. In this manner, mission performance data can be collected for the entire mission.

A mission profile can then serve as a constraint on the design, and the mission integrated exergy destruction can provide component-level information to the designer. This additional information is expected to impact the design decisions due to mission performance constraints.

6.2 Experimental Approach

It is now time to modify the previous approach to better address aerospace applications. This research question specifically deals with vehicle mission performance and its complementary inclusion in the design process next to thermodynamics and cost.

The graphical representation of this experiment is shown in Table 29. In this experiment, Case A represents the combined thermodynamics and cost baseline from the previous experiment. Then, Case B builds on this through the direct consideration of overall mission performance.

The steps for this experiment are summarized as:

- Include the capability to examine the off-design points in the modeling and simulation environment

- Fly each design through a mission profile to collect the necessary performance data
- Compare the favorable irreversibility allocations for the thermodynamics and cost case to the upgraded case that includes vehicle mission performance
- Demonstrate the significance of considering this additional knowledge and its effect on the favorable irreversibility allocations

Table 29: Experiment #2b: Mission Performance Considerations.

A	**B**
Integrated systems design	Integrated systems design
High heat load	High heat load
Thermodynamics and cost	Thermodynamics, cost, and vehicle mission performance

6.3 Theory

Following the organizational structure of the preceding chapters, it is now time to outline the necessary theory required for the implementation of the vehicle mission performance experiment. This additional vehicle performance capability provides the final element for the irreversibility allocation as outline in Chapter II.

One of the primary differences between aircraft systems design and the traditional design of ground-based power systems is the off-design operation across the mission profile. Therefore, it is anticipated that it is not appropriate to examine a single design point in isolation when performing the second-law-based design. As a result, the mission requirements need to be brought directly into consideration during the allocation process.

6.3.1 Extension to Aircraft Design by Including Mission Requirements

Hypothesis 2b suggested that vehicle mission performance could be captured by tracking the necessary performance parameters throughout the execution of a constrained mission profile. The integrated system performance constraints can vary depending on the specific situation, but many of the important metrics in the investigation of the thermal management challenge involve the vehicle mission and the resulting thermal limits. These result in performance requirements at both the vehicle-level and the individual subsystem-level. In this research, the vehicle performance is captured in terms of thrust available and mission maneuver capability. The subsystem performance is expressed as cockpit temperature and flow rate, air cooled machine or vapor cooling flow rates, fuel temperature, and heat loads within the air and fuel systems.

There are two possible ways to simulate the entire mission. The first is through a quasi-steady-state simulation of a series of mission segment points. In this situation, the simulation is still constructed in a steady-state manner, but the conditions are allowed to change for each execution. This assumes that the time constants in the simulation are much smaller than the mission itself. The second way is to perform a full transient simulation, where some of the states are calculated with differential equations at each time step. This has the potential of providing a more accurate simulation, but also adds more complexity and increases the execution time. Either way, a mission integrated exergy destruction can be calculated and a time history of component temperatures is obtained. These temperature limits can then be treated as constraints on the problem as shown for cockpit temperature in Fig. 65 from Maser [102].

This approach then gives the designer three separate and important metrics to aid in the allocation of irreversibility within the system: thermodynamics, cost, and performance. The next chapter then deals with this system-level optimization.

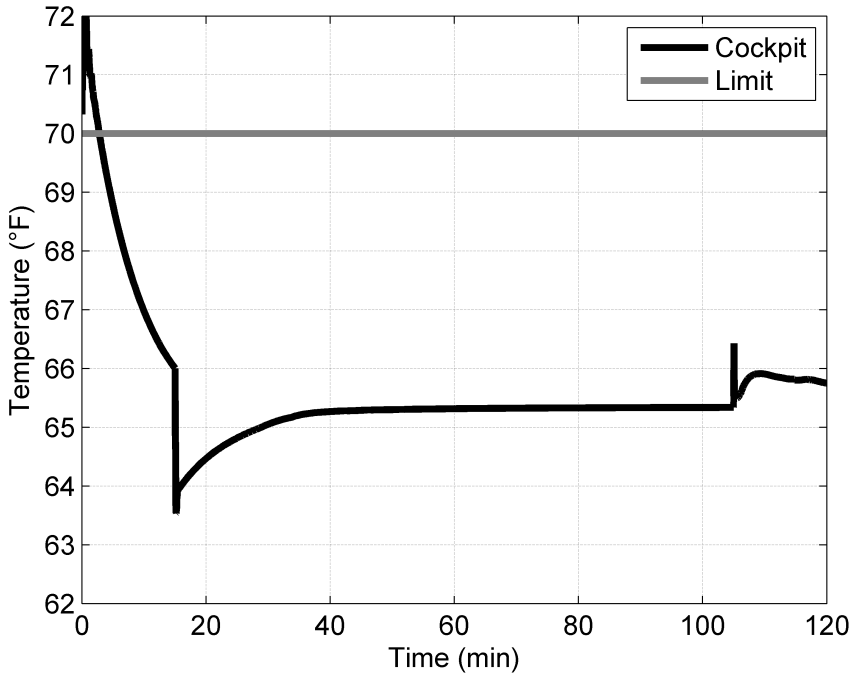

Figure 65: Component-Level Temperature Time History [102].

6.3.2 Off-Design Performance Modeling

The formulations up until this point were of an on-design (parametric) nature. This allows the designer to scale the engine for a specific design point. However, without including additional capability the models are unable to correctly predict the performance at off-design points as is required to simulate a complete aircraft mission. It is therefore essential to add this off-design (performance) capability to the component models, especially the engine and thermal management turbomachinery. The off-design functionality is accomplished using standard turbomachinery maps. These maps are normally defined using special non-dimensional parameters, so that they can be used over a wide range of conditions. The non-dimensionalized pressure and temperature are first defined as [104]

$$\delta = \frac{p}{p_{ref}} \tag{101}$$

and

$$\theta = \frac{T}{T_{ref}} \tag{102}$$

From these parameters, the non-dimensionalized parameters needed for the turbomachinery maps are defined. The corrected flow and speeds are defined as

$$W_c = \frac{\dot{m}\sqrt{\theta}}{\delta} \tag{103}$$

and

$$N_c = \frac{N}{\sqrt{\theta}} \tag{104}$$

Three parameters are then obtained using the compressor maps. These are the corrected flow, pressure ratio, and efficiency as a function of an arbitrary R-line and the corrected speed:

$$W_c = W_c\left(R, N_c\right) \tag{105}$$

$$PR = PR\left(R, N_c\right) \tag{106}$$

$$\eta = \eta\left(R, N_c\right) \tag{107}$$

The turbine maps are similarly defined; however, since the flows and and speeds can be uniquely defined by two points due to the shape of the turbine maps, only two maps are required and the arbitrary R-line is no longer necessary. The corrected flow and efficiency is defined as a function of pressure ratio and corrected speed:

$$W_c = W_c\left(PR, N_c\right) \tag{108}$$

$$\eta = \eta\left(PR, N_c\right) \tag{109}$$

Scale factors are used to scale the maps to the specific design point desired. These are expressed as

$$SF_x = \frac{x_{design}}{x_{map}} \tag{110}$$

This enables the maps to be used parametrically over a wide range of designs and is a frequently used approach in conceptual propulsion systems design. Scale factors are applied to the compressor and turbine pressure ratios, efficiencies, corrected speeds, and corrected flows.

6.3.3 Linking Mission Requirements to Thermal Performance via a Vehicle Model

The vehicle model is based on the method proposed by Mattingly in [104]. This is an energy method that calculates the drag and vehicle acceleration at each point in the mission to determine a thrust requirement. The remainder of this section outlines this approach.

Vehicle speed is first calculated using a Mach number demanded by the mission profile and the ambient conditions:

$$V = Ma = M\sqrt{\gamma RT} \tag{111}$$

The vehicle drag polar characteristics are expressed as

$$C_D = C_{D0} + K\,{C_L}^2 \tag{112}$$

where C_D is the drag coefficient, C_L the lift coefficient, and C_{D0} and K are constants defined by [142]

$$C_{D0} = \frac{f}{S} \tag{113}$$

and

$$K = \frac{1}{AR\, e\, \pi} \tag{114}$$

where f is a frictional coefficient, S is the wing area, AR is the aspect ratio, and e is an efficiency factor. The aspect ratio is defined as

$$AR = \frac{b^2}{S} \tag{115}$$

where b is the wingspan. Then, the lift coefficient is calculated as:

$$C_L = \frac{nW}{qS} \tag{116}$$

where W is the weight and q is the dynamic pressure, which is defined as

$$q = \frac{1}{2}\rho V^2 \tag{117}$$

From this, drag is defined by

$$D = qSC_D \tag{118}$$

Finally, the required thrust at each point in the mission is calculated from an energy balance [104]:

$$\left[T - (D + R)\right] V = W\frac{dh}{dt} + \frac{W}{g}\frac{d}{dt}\left(\frac{V^2}{2}\right) \tag{119}$$

This is rearranged to solve for the thrust requirement as:

$$T_{req} = D + W\left(\frac{1}{g}\frac{dV}{dt} + \frac{1}{V}\frac{dh}{dt}\right) \tag{120}$$

Here g is the gravitational acceleration, V is the velocity, and h is the altitude.

The vehicle weight is updated at each mission segment using the fuel burn of the previous segment

$$\Delta W = -\dot{m}_f g \Delta t \tag{121}$$

6.4 Implementation

Now it is necessary to upgrade the CRATOS modeling and simulation environment to handle the vehicle mission performance requirements. This essentially requires three new features: a component off-design performance capability, an air vehicle model, and an off-design system-level solver. By including these additional features into the environment, the designer is then able to predict the performance repercussions due to irreversibility allocation decisions much like was done with cost in the previous chapter.

6.4.1 Turbomachinery Performance Maps

The off-design performance capability outlined in the theory chapter was added to the turbomachinery components. This was achieved through the use of generic turbomachinery maps. For each individual engine design, these maps are automatically rescaled based on the system design point for that case. The compressor maps used for the system model are illustrated in Figs. 66-68. These are generic turbomachinery maps from [84].

The turbine maps used for the system model are illustrated in Figs. 69 and 70.

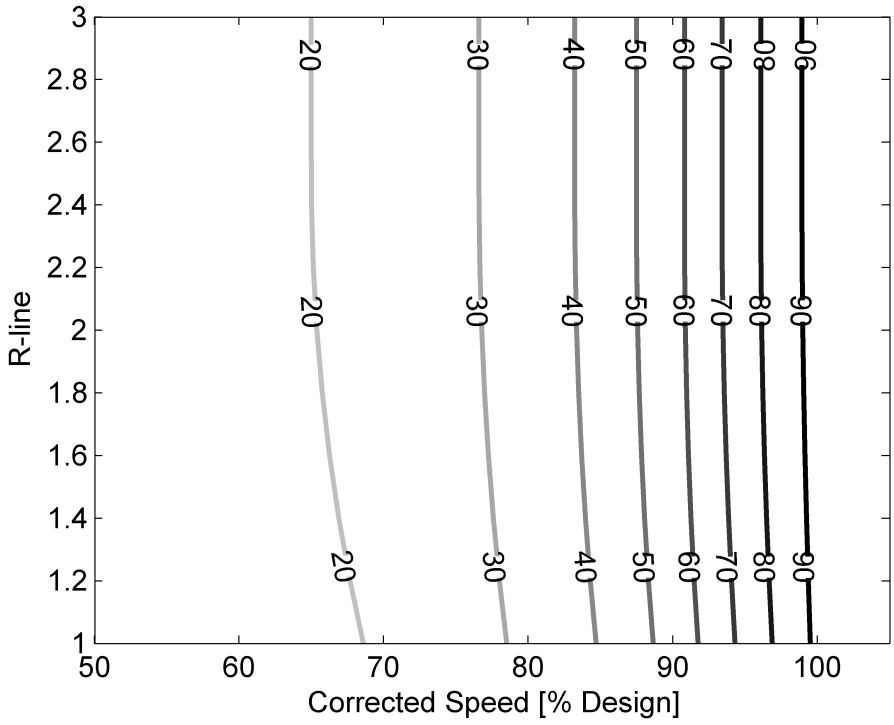

Figure 66: Compressor Corrected Flow Performance Map [kg/s].

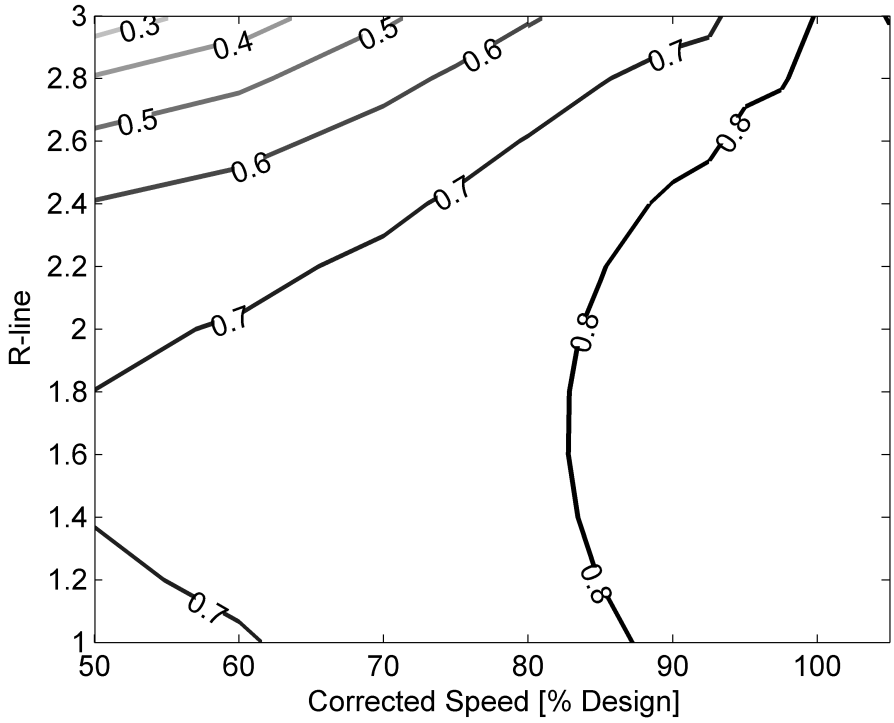

Figure 67: Compressor Adiabatic Efficiency Performance Map.

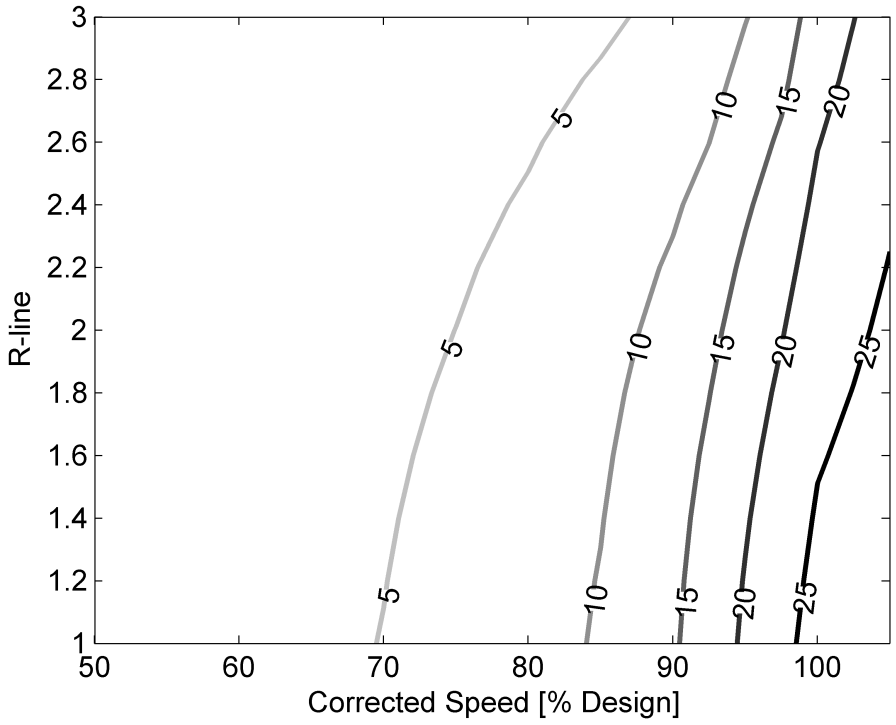

Figure 68: Compressor Pressure Ratio Performance Map.

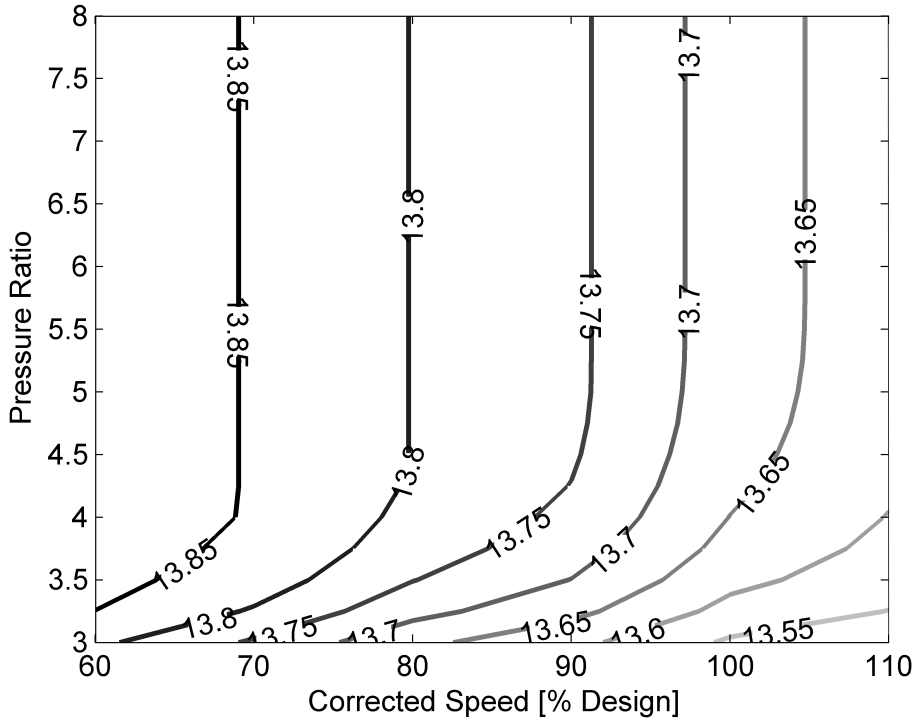

Figure 69: Turbine Corrected Flow Performance Map [kg/s].

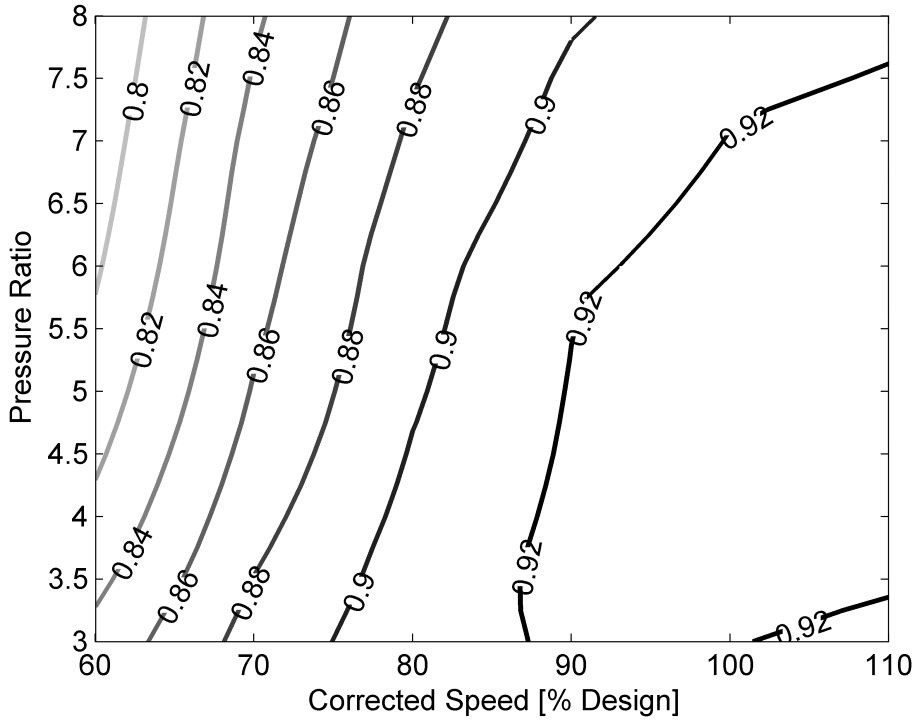

Figure 70: Turbine Adiabatic Efficiency Performance Map.

6.4.2 Nominal Vehicle Model and Mission Profile

Two additional and critical ingredients to enable the simulation of the full aircraft mission is a model of the air vehicle and a specified mission profile. The air vehicle model is required to calculate the thrust requirement at each point in the mission. This allows the vehicle to fly through a series of quasi-steady-state off-design points to arrive at an integrated fuel burn and component exergy destruction over the entire mission.

The mission profile used for this research is shown in Fig. 71; this is a shortened version of the mission profile that was used by Roberts, Eastbourn, and Maser in [139]. It provides the required Mach number and altitude as a function of time. Using a standard atmosphere model, the altitude is directly converted to a pressure and temperature, which specifies the ambient environment.

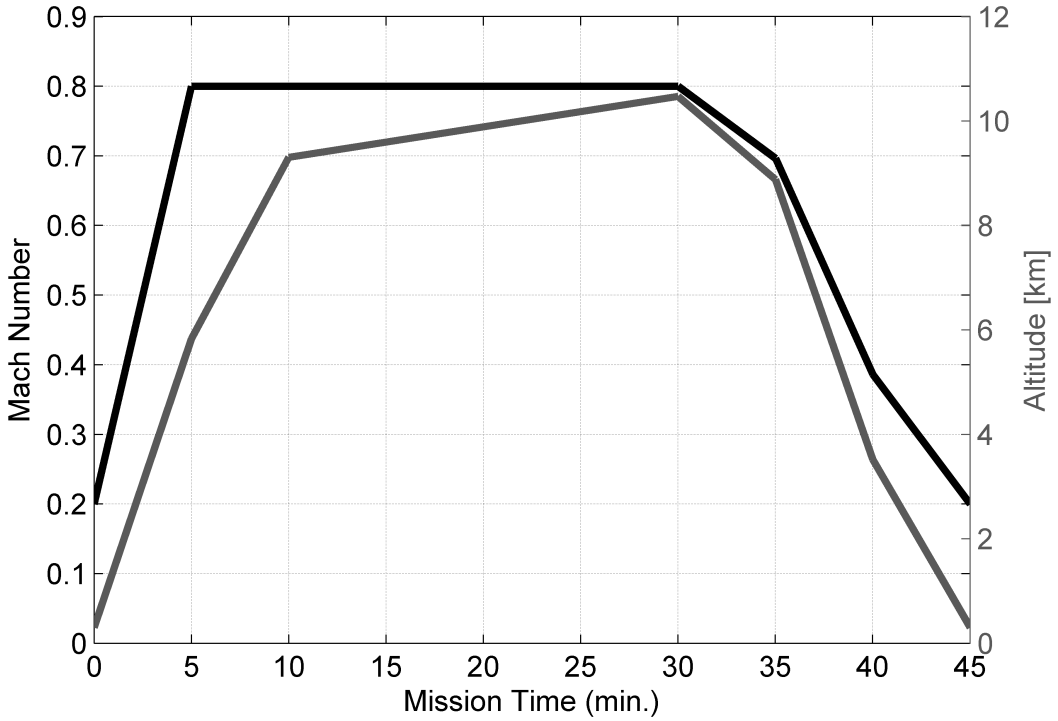

Figure 71: Vehicle Mission Profile Used for Off-Design Operation.

The vehicle model was based on a single engine fighter aircraft, and it was intentionally kept as generic as possible. Table 30 shows the overall vehicle parameters used in the construction of the vehicle model. Some of these values are obtained from a generic fighter in [142], while others are based on data for the F-16 in [81].

Table 30: Air Vehicle Parameters [81, 142].

Empty Mass	8573 kg
Initial Fuel Mass	7000 kg
Takeoff Gross Weight (TOGW)	162,600 N
Wing Area	30.0 m^2
Wing Span	10.0 m
Aerodynamic Efficiency	0.800
Friction Factor	0.980 m^2

6.4.3 Integrated System Off-Design Solver

Now that the simulation includes components with performance maps and off-design operating capabilities and a vehicle model to link the mission requirements to the propulsion and thermal management system performance, a third and final element is needed to perform the simulation in the off-design (performance) mode. This final addition to the CRATOS modeling and simulation is the inclusion of a system-level solver capability for off-design. The same solver framework and approach from Chapter III is used here. However, a new (and lengthier) set of solver constraints is necessary to operate the solver in off-design mode.

The solver independents and dependent constraints for off-design operation are listed in Tables 31 and 32. The off-design solver requires additional constraints to match the predicted environment with the performance maps.

The first eight constraints are carried over from the on-design solver. The next 11 constraints are required for turbomachinery map convergence. There are two constraints for each turbine in the model corresponding to the corrected flow and pressure ratio, and there is one constraint for each compressor corrected flow. The solver changes the operating points on the maps until the predicted thermodynamic values match the values obtained with the maps. The final constraint varies the engine turbine inlet temperature so that the nozzle corrected flow is constrained to the design point.

The previously discussed system-level solver theory from Chapter III and used for the on-design mode was updated to include the additional constraints.

6.4.4 Mission Simulation Execution

The mission simulation begins with the execution of the system design point. This sizes the engine in the same manner as previously explained in Chapter III. After the on-design solver has converged, the CRATOS modeling and simulation environment

Table 31: Integrated System Solver Independents for (Performance) Off-Design.

	Independent		Independent
1	Engine Mass Flow Rate	11	PTMS Compressor R-Line
2	Engine Bypass Ratio	12	LP Turbine Pressure Ratio
3	Bleed Mass Flow Rate	13	LP Shaft Speed
4	Station d1 Temperature	14	HP Turbine Pressure Ratio
5	Station d1 Pressure	15	HP Shaft Speed
6	Station d1 Mass Flow Rate	16	PTMS Turbine Pressure Ratio
7	Station e1 Temperature	17	PTMS Shaft Speed
8	Station e1 Mass Flow Rate	18	PTMS Power Turbine Pressure Ratio
9	HP Compressor R-Line	19	PTMS Turbine Outlet Pressure
10	Fan R-Line	20	Engine Turbine Inlet Temperature

Table 32: Integrated System Solver Dependents for (Performance) Off-Design.

	Dependent LHS	Dependent RHS
1	Engine Thrust	Design Thrust
2	Station 16 Static Pressure	Station 5 Static Pressure
3	PTMS Compressor Power	PTMS Turbine Power
4	Station d1 Temperature	Station c2 Temperature
5	Station d1 Pressure	Station c2 Pressure
6	Station b5 Temperature	Cockpit Design Temperature
7	Station e1 Temperature	Station e4 Temperature
8	Station e4 Mass Flow Rate	Recirculation Design Mass Flow Rate
9	HP Compressor WC (Actual)	HP Compressor WC (Map)
10	Fan WC (Actual)	Fan WC (Map)
11	PTMS Compressor WC (Actual)	PTMS Compressor WC (Map)
12	HP Turbine PR (Actual)	HP Turbine PR (Map)
13	HP Turbine WC (Actual)	HP Turbine WC (Map)
14	LP Turbine PR (Actual)	LP Turbine PR (Map)
15	LP Turbine WC (Actual)	LP Turbine WC (Map)
16	PTMS Turbine PR (Actual)	PTMS Turbine PR (Map)
17	PTMS Turbine WC (Actual)	PTMS Turbine WC (Map)
18	PTMS Power Turbine PR (Actual)	PTMS Power Turbine PR (Map)
19	PTMS Power Turbine WC (Actual)	PTMS Power Turbine WC (Map)
20	Nozzle WC	Nozzle WC Design Point

switches to its off-design mode. The on-design point supplies all of the necessary performance map scale factors as well as the nozzle design point data. Also, the production cost data is still calculated using the on-design point data only. The mission profile is then broken up into a series of quasi-steady-state points. Each of these points is executed in CRATOS using the off-design solver. After all of the points have executed, overall fuel burn, exergy destruction, and other important parameters are integrated for the duration of each mission segment.

6.5 Results - Performance Trades

Until this point, all of the results from the previous experiments have examined a single design point and have neglected to directly consider performance. As previously explained, this is rarely appropriate for aircraft design applications due to the frequent change throughout the mission. Here, the mission performance is finally taken into account. As a result, the variation in the irreversibility distribution throughout the mission must now be accounted for. Also, there are thermal constraints throughout the vehicle that cannot be violated and specific maneuvers that must be made possible. The actual thermal environment is tracked and compared to the thermal constraints throughout the mission.

Table 33 illustrates the two different cases for this experiment. The first case, Case A, is a continuation of the last experiment, where the design is strictly a matter of irreversibility and cost. Case B then explores the addition of important performance metrics, such as vehicle thrust and component temperature limits.

Table 33: Experiment #2b: Mission Performance Considerations.

A	**B**
Integrated systems design	Integrated systems design
High heat load	High heat load
Thermodynamics and cost	Thermodynamics, cost, and vehicle mission performance

6.5.1 Case A: Thermodynamics and Cost

As was seen in the previous experiment, the investigation of thermodynamics and cost led to the two often being at odds to design decisions. This is due to the fact that an initial monetary investment is required to increase the efficiency of the system and avoid additional irreversibility. Several trades were shown in the previous experiment to demonstrate the case of simultaneously considering thermodynamics and cost.

However, the previous study still fails to directly account for changes in mission or thermal performance. One way that this could be indirectly accounted for is to include performance constraints. The goal would then be to satisfy these performance constraints while concurrently reducing the exergy destruction and cost. The final experiment, Experiment 2c, does this by using a system-level optimization to minimize thermodynamics and cost, while treating performance as a constraint. Alternatively, these performance metrics can be directly included in the thermodynamics and cost trades; this is the approach taken in Case B.

6.5.2 Case B: Thermodynamics, Cost, and Vehicle Mission Performance

By building off of the results from the previous experiments, the mission trades are now investigated. In the context of this study, two main types of performance metrics were considered. The first was thermal performance; thermal attributes of the system include heat load heat rates and thermal system temperatures. The second was

mission performance. This is established by specifying a mission profile and then examining the mission integrated exergy destruction per component. The maximum thrust capability and TSFC are also considered.

To first take a look at and better understand the impact of thermal performance on the system, several trade studies were examined. The first trade investigated was the effect of varying the magnitude of the PTMS heat load heat transfer rate from 5 to 100 kW. It was found that increasing this heat rate results in a linear increase of the PTMS closed loop maximum temperature. The temperature variation due to the PTMS heat load heat transfer rate is

$$T\,[K] = 1.224\,\dot{Q}\,[kW] + 875.7 \tag{122}$$

This additional heat is ultimately transferred from the PTMS loop into the engine fan stream through the fan air heat exchanger. When this fan stream heat transfer is examined in isolation, it is seen that an increase in heat transfer to the stream results in a small decrease in the thrust specific fuel consumption. A trade was conducted by varying this heat transfer rate from 1 to 2 MW. The variation of engine TSFC as a function of heat transfer from the thermal system into the engine fan stream is

$$TSFC\left[\frac{mg}{sN}\right] = -0.1085\,\dot{Q}\,[MW] + 24.42 \tag{123}$$

The variation of the fuel loop temperature limit was also investigated through a third trade study and its results are illustrated in Fig. 72. The effect of increasing the maximum fuel temperature results in a nonlinear reduction in the required compressor bleed and a corresponding reduction in engine fuel burn. This is a result of the reduction in the air cycle cooling requirements and the additional enthalpy available in the fuel stream.

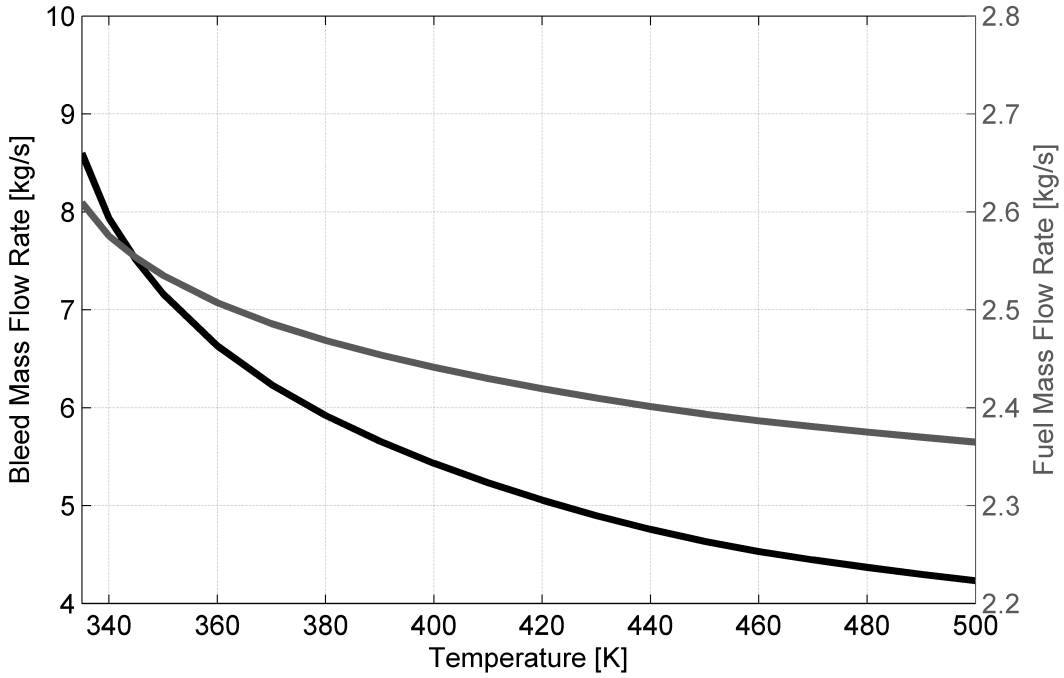

Figure 72: Increasing Fuel Temperature Limit Lowers Bleed and Fuel Burn Requirements.

A fourth trade study was conducted on the heat transfer rate of the FTMS heat load. The heat transfer rate was varied between 5 and 100 kW similarly to the previous case of the PTMS heat load. These ranges are reasonable estimates for fuel-cooled electronics. For the fuel loop to remain at the desired temperature during this heat rate increase, a corresponding linear increase in engine compressor power extraction must also occur. Specifically, the compressor bleed mass flow rate varies as

$$\dot{m}_{bleed}\left[\frac{kg}{s}\right] = 0.0155\,\dot{Q}\,[kW] + 4.256 \tag{124}$$

Next, the mission performance was investigated. For this, the integrated propulsion and thermal management system was sized at the system design point. The

vehicle model was then flown through the mission profile shown previously. The combination of the vehicle model and the mission profile then provided a thrust requirement and corresponding Mach number and ambient conditions for separate mission segments. These mission thrust requirements are shown in Fig. 73.

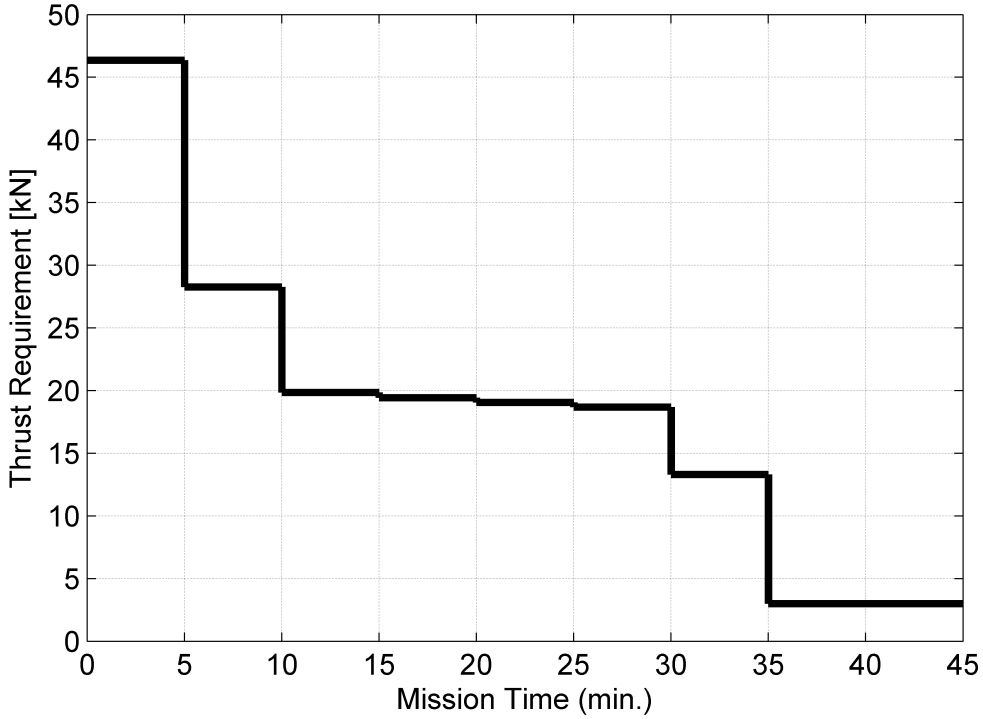

Figure 73: MFTF Thrust Requirement Variation over Mission.

The execution of each of these mission segments in an off-design mode then allowed for the calculation of the system irreversibility over each segment. From this information, mission integrated exergy destruction was calculated by considering the length of each segment. These mission integrated irreversibility results are illustrated in Figs. 74-76.

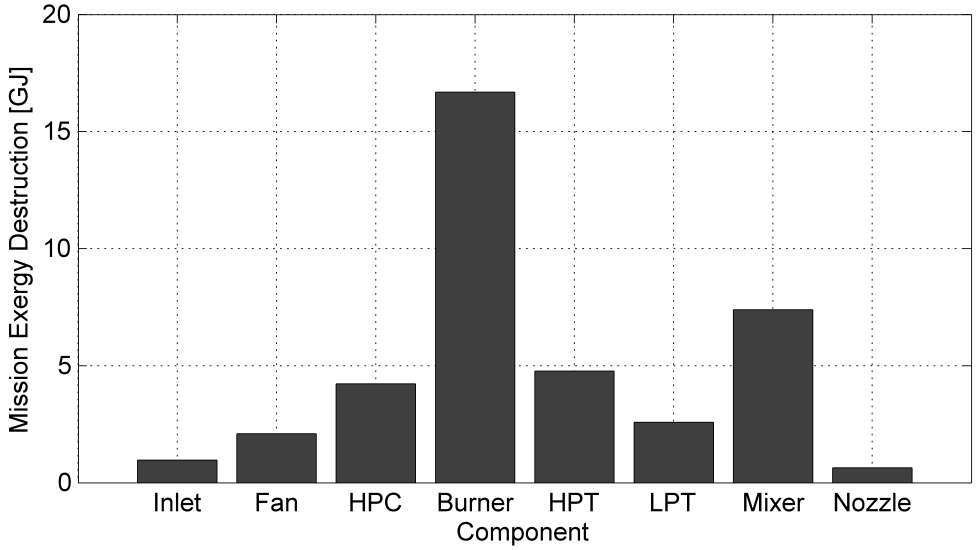

Figure 74: Engine Component Irreversibility over Mission.

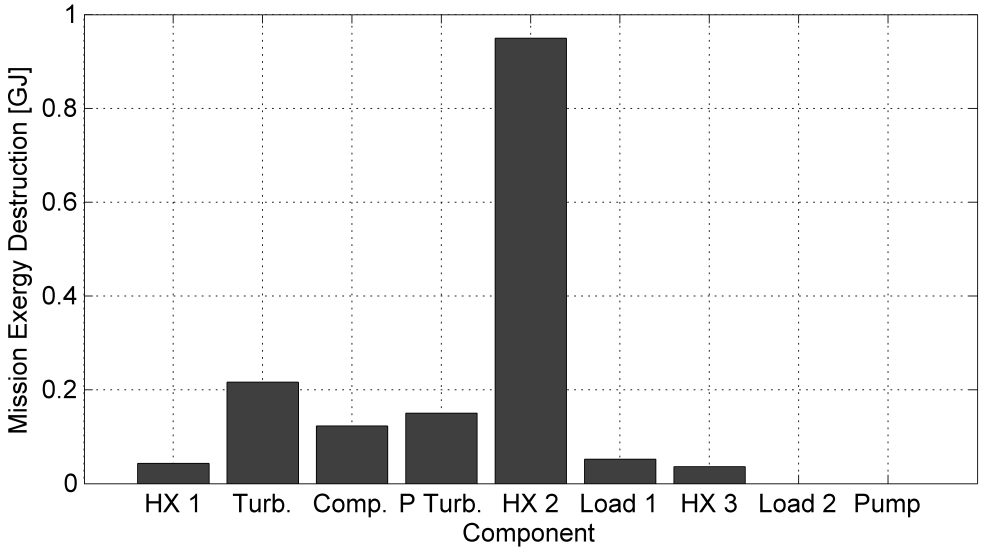

Figure 75: Thermal Management Component Irreversibility over Mission.

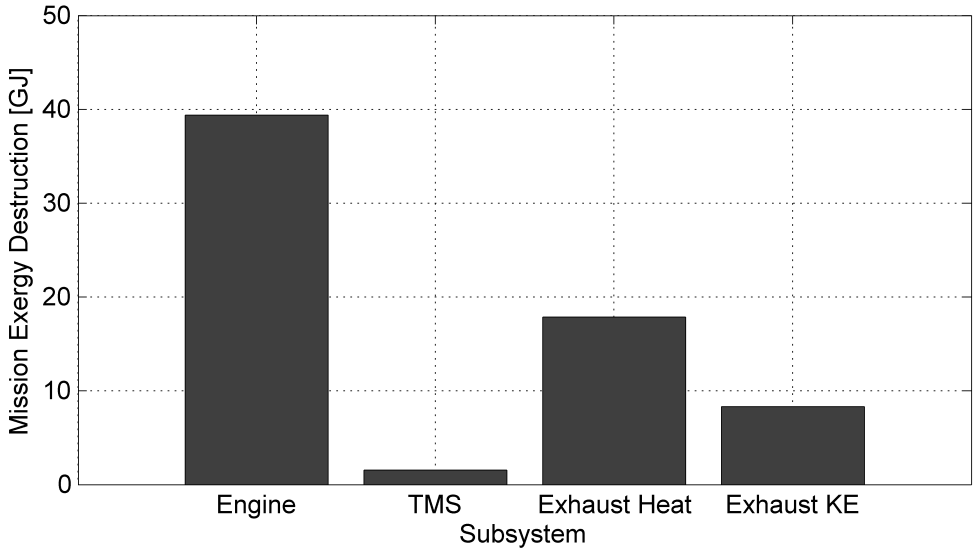

Figure 76: Subsystem Irreversibility over Mission.

These results show that the mission integrated results are much different than the results that were simply shown for the design point. This difference highlights that the aircraft mission and performance must be considered due to the unsteady nature of aircraft flight. Unlike ground-based power production systems which operate continuously at a specified design point, aircraft power production is continuously changing to match the mission requirements and ambient conditions. The results again show the engine and its exhaust dominate the system-level exergy destruction.

6.6 Summary of Mission Performance Considerations

Once mission performance requirements are considered, it then becomes readily apparent that the favorable allocations of irreversibility change. The allocation of component irreversibility at the system design point is different than the mission integrated exergy destruction allocation. This is important because it is directly analogous to the mission integrated fuel burn, which is an extremely important metric in propulsion system design. There are now instances when an allocation of irreversibility with a higher system-level exergy destruction at the design point and higher cost is

desired due to its improved mission integrated exergy destruction and thermal performance. The next experiment will take a closer look at the specific trades encountered between the three metrics: thermodynamics, cost, and performance.

CHAPTER VII

INVESTIGATION OF SYSTEM IRREVERSIBILITY ALLOCATION

The first experiment, Experiment 1a, was focused entirely on demonstrating the need for conducting integrated propulsion and thermal management simulations during conceptual engine design. After making the case for the integrated design, Experiment 1b then showed the benefits of applying second-law-based design techniques to the design of the integrated system. These first two experiments served as the foundation for the remainder of the work.

Next, Experiment 2a investigated the irreversibility and cost tradeoffs inherent in the design of thermodynamic systems and began the search for an appropriate means of taking this into account. Experiment 2b continued the trend of the previous experiment by directly accounting for aircraft mission performance. This was the final ingredient needed for the allocation process.

The final and culminating experiment, Experiment 2c, now brings all of this together. This experiment investigates the advantages of using an allocation bartering technique to directly allocate irreversibility during the conceptual design process as opposed to conducting a strict numerical optimization at the system-level.

7.1 Statement of Research Hypothesis #2c

The final research question addresses the appropriate method of searching for an optimal design configuration in the context of thermodynamics, cost, and performance. This technique must feature some type of system-level exploration, but the essence of the question is whether this consists of a strictly numerical optimization or if the

problem formulation in terms of irreversibility characterization lends itself better to a different, less point design, approach.

The final hypothesis in response to Research Question 2c is now formally stated:

Research Question #2c: Can the designer improve upon a strict numerical optimization of the integrated propulsion and thermal management systems by directly allocating the component irreversibility with regards to cost and vehicle performance?

Research Hypothesis #2c: The direct allocation of irreversibility provides the designer with a consistent and absolute means of directly trading off system thermodynamics, performance, and cost, and it is more effective in achieving favorable system-level irreversibly distributions and performance than a strict numerical optimization.

This hypothesis results from the multiple design criteria and the complexity of the design space. The comparison is made between the numerical minimization of a combined cost metric to the direct allocation of irreversibility with respect to cost and performance.

7.2 Experimental Approach

Table 34 graphically shows the two different cases for this experiment. They both use the baseline modeling and simulation environment of the previous experiments: the integrated propulsion and thermal management model in the high heat load configuration. The first, Case A, uses a strict minimization of a combined thermodynamic and cost metric with performance constraints. Case B then utilizes a resource allocation approach to barter for an improved system-level solution.

The real benefit of the second approach is that it allows the designer to allocate the irreversibility in a consistent and absolute way while accounting for cost and performance without burying all of the information in a single metric. Using this

more transparent technique, the designer is much less dependent on the weighting of the design metrics, and the decision making process becomes much more intuitive.

Table 34: Experiment #3c: Irreversibility Allocation.

A	**B**
Integrated systems design	Integrated systems design
High heat load	High heat load
Thermodynamics, cost, and vehicle mission performance	Thermodynamics, cost, and vehicle mission performance
System-level numerical optimization	Irreversibility allocation design

The summary for this last experiment is then:

- Develop the allocation tradeoff capability in the CRATOS modeling and simulation environment
- Compare the allocation approach to the direct application of a system-level numerical optimizer
- Show the connection between the allocation of irreversibility, cost, and mission performance
- Demonstrate that the results of the strict numerical optimization are not as valuable to the designer due to the complexity of the design space, the multiple design criteria (thermodynamics, cost, and performance), and uncertainty in the cost data

7.3 Theory

The last research hypothesis is the culmination of all of the previous work to this point. The other hypotheses concentrated on a specific element of the irreversibility allocation process, so that they could be experimentally tested independently. This final hypothesis now focuses directly on the allocation itself, while leveraging the previously tested elements.

Hypothesis 2c deals with the concurrent consideration of the cost and performance metrics during the allocation of irreversibility. As a result, the allocation design criteria is a combination of mission integrated exergy destruction, system cost, and mission performance. It is important to treat these three metrics simultaneously. The approach used in this study is to treat the vehicle mission profile as a constraint and then seek a minimum exergy destruction while accounting for cost and performance. The irreversibility allocation is the process that the designer uses to explore the way that the unavoidable system losses should flow down to the individual subsystems and components for specific performance and cost requirements.

7.3.1 Design of Experiments and Surrogate Modeling to Enable Rapid Optimization

The approach taken in the first case is to calculate a system-level cost that is a combination of the production and operating costs. This was the thermoeconomic formulation that was shown in Chapter V and serves as a good baseline with which to compare and contrast the irreversibility allocation approach. In this case, mission performance and thermal requirements are accounted for through constraints on the problem. Next, the system design parameters are chosen in such a way to achieve the minimum cost. There are a few difficulties associated with this approach as discussed at the end of Chapter II. These involved the difficulty of running the system-level model for a large number of cases and the presence of multiple local optima. The two techniques discussed earlier to remedy each of these challenges were surrogate

modeling and stochastic optimization.

The surrogate modeling approach enables simple, empirical equations to be created for each of the required responses. This can include fuel burn and component exergy destruction. A design of experiments is used to vary the simulation design parameters in such a way as to obtain the most information about the behavior of the system with the least amount of model executions [185]. The design of experiments accomplishes this by changing multiple design variables at one time in specific combinations. These combinations are chosen so that all of the first-order effects of the design variables, called the main effects, are still captured by the model, while unimportant secondary effects resulting from changes in multiple variables concurrently are ignored.

The data from the resulting design of experiments runs is then fitted using a least squares regression. This was also done earlier to create the weight data fits in Chapter V. This time, however, the form of the equations is the second order response surface [118]

$$\eta = \beta_0 + \sum_{i=1}^{k} \beta_i x_i + \sum_{i=1}^{k} \beta_{ii} x_i^2 + \sum_{i=1}^{k-1} \sum_{j=i+1}^{k} \beta_{ij} x_i x_j \tag{125}$$

Surrogate models are later created for system-level exergy destruction rate, fuel burn, and production cost.

7.3.2 Genetic Algorithm for Global Optimization

The actual system-level optimization is then performed on the resulting responses using a genetic algorithm [133]. Execution of the genetic algorithm with the variation of all of the design variables then results in values for exergy destruction and cost on a component basis for each of the cases. This data is rapidly computed since the response surface equations are evaluated nearly instantaneously compared to the much lengthier direct execution of the integrated system-level solver.

The genetic algorithm is important since it has a better chance of finding a global optimum than more traditional gradient-based algorithms. Although gradient-based algorithms are mathematically guaranteed to locate an optimum, this will often be only local if the design space has many such local optima. This was previously explained in the background of Chapter II. The genetic algorithm works by first converting each design variable into a string of binary code. For example, if a pressure ratio needs to be explored from a low value of 2 to a high value of 10, then '000000' would represent 2 and '111111' would represent 10 if six binary bits are used. More or fewer bits can be used depending on the degree of discretization desired. Using this approach, all of the design variable values for a case can be represented as a single string of binary bits. If there are 10 design variables each with a discretization of six bits, then all of the design variables would be represented by a string of 60 binary bits.

A large population of these design strings are initially randomly created to start the algorithm. Each of the design cases within the population is run through the modeling and simulation environment to obtain its associated fitness value, which is the reciprocal of the value to be minimized. Then, a series of operations, termed selection, crossover, and mutation, is performed on the population resulting in a new population. In the selection phase, strings are randomly chosen two at a time using a weighted spinner based on the strings' fitness value, i.e. it is more likely that better design strings will be chosen. Next, there is the possibility that a crossover will occur between the two strings. This means that the two strings will switch their second halves at a random bit. Finally, a random mutation can occur to any of the bits in the string based on some predetermined probability. After these three operations, the resulting strings are added to the new population. This continues until the new population has reached the same size as the previous population.

The genetic algorithm finally converges once the best fitness value within the population stabilizes for a predetermined number of populations.

7.3.3 Irreversibility Allocation

In this study, a comparison is made between the thermoeconomic minimization approach just discussed and the direct allocation of the thermodynamic losses, which is used in Case B. This is enabled through the prediction of the irreversibility distribution within the canonical integrated propulsion and thermal management system. The main emphasis here is the impact of propulsion system design modifications on the irreversibility distribution; specifically, the effects of key engine cycle design parameter variations are investigated.

The major idea in regards to the irreversibility allocation is that it should allow the component irreversibility to drive the system design. This is done by reversing the way that the designer thinks about the traditional analysis. Instead of the exergy destruction distribution simply resulting from the system design, the design starts with a desired component exergy destruction and then works backwards to find the design parameters that provide this result:

$$\dot{X}_D \rightarrow \{\eta, \Delta p, \dot{m}, \text{etc.}\} \tag{126}$$

This enables the systems level designer to directly utilize the allocation of unavoidable system losses to achieve a system design that better meets the requirements. In addition, this allows the exergy destruction to serve as a true common currency with which the individual components and subsystems can barter amongst themselves to obtain system improvement as shown in Fig. 77.

7.3.4 Analogy to Resource Allocation

The formulation of the preceding section stated the systems design process as an event where the irreversibility is utilized as a system-level currency that is used to

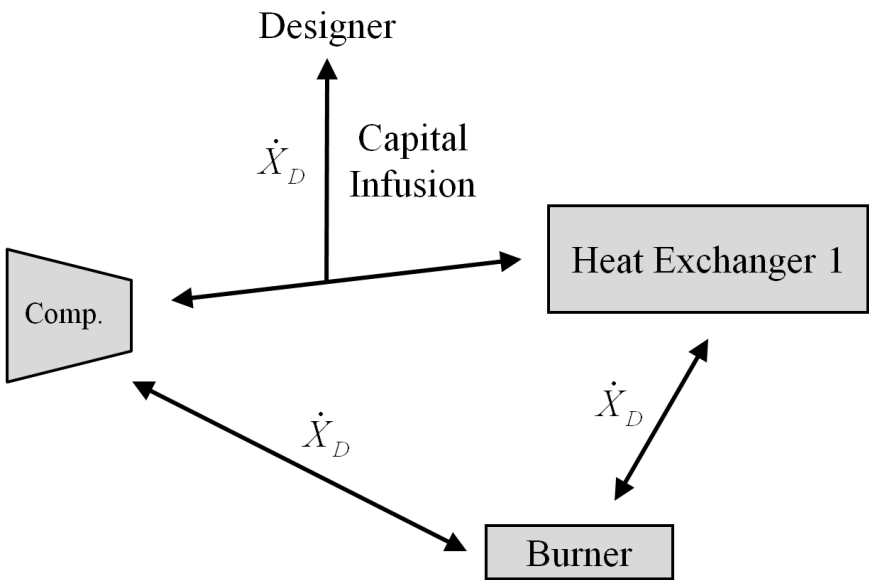

Figure 77: Component Irreversibility Bartering Concept.

purchase improvements in performance and cost in an effort to better meet the system requirements. This is also very similar to the concept of resource allocation, which is a common activity in other fields such as economics, finance, and computing [35, 64, 92]. Therefore, techniques from these disciplines were investigated to develop a way to perform the integrated propulsion and thermal management systems irreversibility allocation. This section will detail some of the work into resource allocation in these other disciplines. This formulation can then be included in the system-level modeling and simulation as a means of seeking the optimal irreversibility allocation.

The approach taken in this research in the search for the optimal allocation is to use a technique analogous to the concept of resource allocation in the field of economics. In this approach, the components are set up to barter for improvement using exergy destruction as the currency. The system irreversibility distribution amongst the various components is then investigated to determine the optimal allocation of the irreversibility inventory throughout the system. The designer can then obtain system-level improvement by infusing capital to cover the additional irreversibility costs incurred.

Of particular interest to this research is the application of economics-based resource allocation to computing [111]. The question of resource allocation has received significant attention lately in this field and has demonstrated substantial improvement. This includes the particular areas of memory management [158], bandwidth allocation [187], and processor resources [59].

Resource allocation has improved the real-time decision making of wireless networks in the multiplexing the various user signals according to a limited supply of bandwidth. A popular resource allocation method is orthogonal frequency-division multiple access (OFDMA) [90, 91]. This method is proposed for future wireless communications protocols. This multiple access method rapidly allocates the various users according to a real-time scheme. This involves dynamic resource allocation, through the use of proportional fairness and water-filling algorithms [66, 156].

7.3.5 Irreversibility Allocation Formulation

The next question concerns how the allocation should actually be conducted. The optimal allocation could be obtained through a global optimization at the system-level as shown in Case A. However, the ultimate goal is to directly trade off propulsion systems performance in terms of exergy destruction for improved design.

The allocation formulation is outlined here by following the nomenclature from signal processing [59]. Using this nomenclature, it is assumed that there are m components. These components are sharing one resource: exergy destruction. Essentially, each of the various members of the system can purchase reductions in cost or improvements in performance through an expenditure of exergy destruction. This directly follows the idea that "there is nothing wrong with expending exergy if something useful is obtained in return" [16].

The allocation of resources to each component is represented as a two-dimensional matrix ω. The set off all possible ω allocation schemes is then represented by the three-dimensional matrix:

$$\Omega = \begin{bmatrix} \omega_1 & \cdots & \omega_z \end{bmatrix} \tag{127}$$

A particular allocation matrix consists of m components denoting each of the components:

$$\omega = \begin{bmatrix} r_1 & \cdots & r_m \end{bmatrix} \tag{128}$$

Additionally, there is a total budget constraint on exergy destruction that is imposed by the system-level designer. This can be thought of as the main system-level constraint on exergy destruction:

$$\sum_{i=1}^{m} x_i \leq \dot{X}_{D_{\text{system}}} \tag{129}$$

The approach taken in this research is to then allow the designer to decide on the relative importance of each of the metrics during the design process to perform the allocation. This can then be changed on the fly as assumptions and conditions change. This approach was taken in this study since it was seen to be transparent and useful to the designer.

Alternatively, a commodities market or auction approach could be taken for the irreversibility allocation [60, 163, 183]. This would then help to automate the allocation process. Using the price anticipating mechanism, the subsystems or components can submit bids for each of the resources desired. In this case, the various subsystems bid for a specific amount of exergy destruction. If each bid is represented as x_i, then the price of the exergy destruction is calculated as

$$Y = \sum_{i=1}^{m} x_i \tag{130}$$

One standard way to then allocate the resources is through the proportional share mechanism. In this case, the resources are allocated based on the total amount bid by all of the subsystems:

$$r_i = \frac{x_i}{Y} \tag{131}$$

The main challenge in using this automated approach is the determination of how the individual subsystems will judge the relative utility of their individual performance and cost metrics. The simplest way to do this is through a linear utility function

$$U_i\left(r_{i1}, \ldots, r_{in}\right) = W_{i1} r_{i1} + \ldots + W_{in} r_{in} \tag{132}$$

The problem with this is that it still assumes weightings on the metrics like the OEC discussed in Chapter II. The benefit is that it brings it down to the component-level like other multi-level optimization approaches.

7.3.6 Irreversibility Allocation for Improved Cost and Performance

The conclusion of the irreversibility allocation theory blends the resource allocation approach just discussed with the earlier work by restating it in terms of irreversibility, cost, and mission performance. The key focus here is on allowing the irreversibility allocation to drive the conceptual design of the propulsion system.

The allocation vector is formally stated as

$$\omega = \begin{bmatrix} \dot{X}_{D_1} & \cdots & \dot{X}_{D_m} \end{bmatrix} \tag{133}$$

The Jacobian matrix of partial derivatives of cost and performance with respect to component exergy destruction is

$$J = \begin{array}{c} \\ \text{Comp. 1} \\ \\ \text{Comp. m} \end{array} \begin{array}{c} \begin{array}{cccc} \text{Perform. 1} & & \text{Perform. n-1} & \text{System Cost} \end{array} \\ \begin{pmatrix} \frac{\partial y_1}{\partial \dot{X}_{D_1}} & \cdots & \frac{\partial y_{n-1}}{\partial \dot{X}_{D_1}} & \frac{\partial y_n}{\partial \dot{X}_{D_1}} \\ \vdots & \ddots & \vdots & \vdots \\ \frac{\partial y_1}{\partial \dot{X}_{D_m}} & \cdots & \frac{\partial y_{n-1}}{\partial \dot{X}_{D_m}} & \frac{\partial y_n}{\partial \dot{X}_{D_m}} \end{pmatrix} \end{array} \tag{134}$$

where $\vec{y}$ represents the performance and cost metrics.

The characterization of system-level improvement in terms of exergy expenditures enables the designer to quickly perform trade studies. The types of questions that the irreversibility allocation procedure can answer include:

- What is the cheapest component modification that will result in a 1% reduction in fuel burn?
- What is the cost of increasing the air-cooled thermal load by 5 kW?
- If 4 kW of exergy destruction is allocated to the power turbine to modify the air cycle, then how do the other components respond?

This essentially results in component irreversibility costs associated with each improvement gain; this concept is shown in Fig. 78.

The allocation approach provides powerful and insightful information concerning the optimal design of the propulsion system in the context of thermal management challenges. The rapid allocation process can illustrate the effects of a wide range of design cases to create an engine design that is robust to thermal management system modifications.

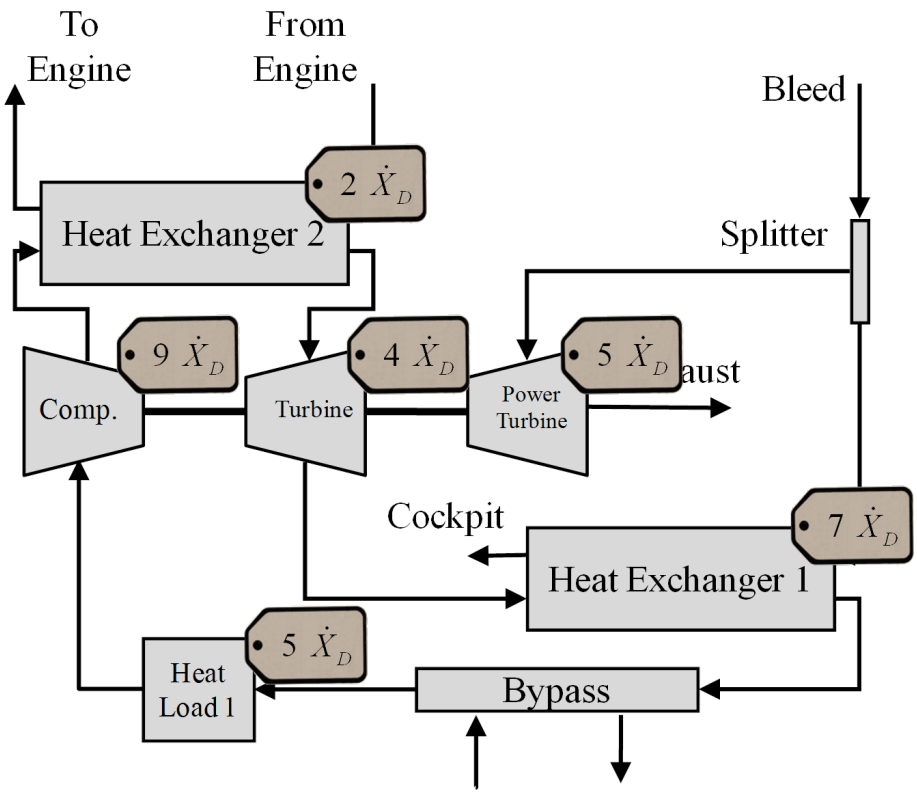

Figure 78: Economic View of System-Level Irreversibility Costs.

7.3.7 Filtered Monte Carlo and Inverse Design for Allocation of Irreversibility

The final question with regards to the allocation approach is how the inverse design is conducted. Two different approaches are used here as a means of aiding the designer in his or her decision making. The first is to use an optimizer to individually vary the performance parameters until a specified change in system-level exergy destruction is obtained. This optimization can be conducted through the use of a gradient-based optimizer. This then allows the designer to view the change in each performance and cost resulting from the "buying" or "selling" of a specific quantity of exergy destruction. This buying and selling market be discussed further in the implementation section.

The advantage to this approach over the previous system-level optimization is

that it allows the designer to specifically view the cost and performance repercussions of reallocating the exergy destruction throughout the system. It does not bury the individual contributions of thermodynamics and cost inside of a combined cost metric and no longer requires the performance to be constrained. Instead, it provides a clear view of component exergy destruction, cost, and performance. As a result, it gives the designer more freedom and information to arrive at an informed decision.

The principal disadvantage to this approach is that it requires a separate optimization for each performance and cost metric and it also does not yield any information regarding the sensitivities of the design variables and allocation. A different way to perform the inverse design is through the use of filtered Monte Carlo techniques. In this Monte Carlo approach, no optimizers are used at all; instead, a large number of random points throughout the design space are executed. This information is then visualized to provide the designer with a bird's-eye view of the overall behavior of the system across the space.

To perform this Monte Carlo, the surrogate model responses are first created for all of the major responses, including exergy destruction, cost, and performance as a function of the design variables. This allows for the necessary number of cases to be quickly executed. The cases are then randomly chosen from a uniform distribution of each design parameter over a reasonable range of values. A large number of cases (on the order of 10,000) are then run and their responses obtained. All of the cases are plotted as individual points in the exergy destruction vs. cost vs. performance space.

From this information, the designer then has additional information that was not available from the previous performance optimization. First, the boundary of the design space, known as the Pareto frontier, is readily available. The points along this boundary are dominant points that result in the best result for some combination of one or more design metrics. The other points are dominated by the Pareto frontier,

which means that one or more of the metrics can be improved without a resulting decrease in the others. The Monte Carlo results also allow the designer to rapidly locate favorable designs by filtering out points by imposing additional constraints on the space, such as a maximum allowable component temperature, cost, or exergy destruction.

7.4 Implementation

The theory of the previous section is now implemented within the system-level CRATOS design environment. Two additional capabilities were needed: the system-level optimization that was first discussed and then the irreversibility allocation. This section goes deeper into the specifics of each of those. Specifically, the mechanics of the genetic algorithm and response surface creation are explained for system-level optimization and the buy and sell markets for the irreversibility allocation.

7.4.1 System-Level Optimization

A major contribution from this research is not simply the irreversibility characterization of a single design point, but instead the capability to rapidly conduct system-level trade studies. To enable a system-level optimization, it is first necessary to set up the modeling environment to operate in an automated batch mode. This allows for an automatic variation of the input parameters. From this, the appropriate variables are selected and their ranges established.

A DOE is used to obtain surrogate models in the form of response surface equations for the metrics of interest. These include exergy destruction rate, system production cost, fuel burn, integrated exergy destruction, and system weight. Sphere Packing and Latin Hypercube DOE tables were explored for this study. The major system design variables are listed in Table 35 along with their selected ranges.

Using the metric responses, a system-level optimization was then conducted through the use of a genetic algorithm. The probability of a crossover occurrence was 80%,

and the probability of a mutation was 50%. The optimization featured the 26 design variables, and four binary bits were used to encode each variable. This allowed for a farily small discretization for the design variables, while still allowing the crossover and mutation oparations to work effectively. The total population size was 10 times the total chromosome length; the population was considered to have converged after 50 cases of no improvement in the objective function for any member of the population.

Several different optimization scenarios were explored and are discussed in the experimental results section. These scenarios include a minimization of fuel burn, production cost, and finally a combined production and operating cost.

Table 35: System Design Variables and Ranges.

Variable	Low Value	High Value
Overall Pressure Ratio	20.0	30.0
Fan Pressure Ratio	2.00	3.00
Turbine Inlet Temperature [K]	1600	1750
Design Thrust [kN]	75.0	150
Inlet Efficiency	0.85	0.99
Fan Efficiency	0.80	0.90
HPC Efficiency	0.80	0.90
Burner Efficiency	0.85	0.99
HPT Efficiency	0.85	0.99
LPT Efficiency	0.85	0.99
Nozzle Velocity Coefficient	0.95	0.99
PTMS Closed Loop Pressure Ratio	12.0	18.0
PTMS Turbine Outlet Pressure [kPa]	101	152
Cockpit Mass Flow Rate [kg/s]	0.10	0.30
Cockpit Temperature [K]	290	305
PTMS Heat Load Heat Rate [kW]	10.0	100
PTMS Heat Load Pressure Drop	0.25	0.35
PTMS Compressor Efficiency	0.80	0.99
PTMS Turbine Efficiency	0.85	0.99
PTMS Power Turbine Efficiency	0.85	0.99
Fuel Loop Minimum Pressure [MPa]	4.00	5.00
Recirculation Mass Flow Rate [kg/s]	0.500	2.00
Design Fuel Temperature [K]	450	550
FTMS Heat Load Heat Rate [kW]	10	100
FTMS Heat Load Pressure Drop	0.15	0.20
Fuel Pump Efficiency	0.80	0.99
Heat Exchanger 1 Pressure Drop	0.15	0.20
Heat Exchanger 1 Effectiveness	0.90	1.0
Heat Exchanger 2 Pressure Drop	0.15	0.20
Heat Exchanger 2 Effectiveness	0.90	1.0
Heat Exchanger 3 Pressure Drop	0.15	0.20
Heat Exchanger 3 Effectiveness	0.47	0.53

7.4.2 System-Level Irreversibility Allocation

This capability leverages the previous system-level optimization framework, but is improved using the allocation theory. First, it is important to remember that the irreversibility, i.e. exergy destruction, distribution throughout the system is used here to drive the design. In this case, the designer thinks about the exergy destruction as the input for each component, and the actual component parameters are varied to achieve this irreversibility allocation.

The key feature of the allocation approach is the market selling and buying capability. For this, an optimization is performed to enable the solution of the inverse design problem. This allows the designer to see the results of the allocation of a specific quantity of irreversibility in various forms. In addition, cost and performance calculations must also be performed on the fly. These pricing options are then used by the system-level designer to perform the actual allocation. Finally, the system must take into account the effects of rebalancing the system after each purchase of performance improvement or sale of component design parameter modification due to the integrated nature of the components and their effects on one another.

7.4.3 Irreversibility Buy and Sell Markets

The approach of the previous chapters with respect to system-level optimization is then applied to this new formulation of the problem. The important results now include the component-level irreversibility, the system-level cost, and subsystem performance metrics. The specific formulation for this research investigates seven different engine design parameters for the sell market: overall pressure ratio, fan pressure ratio, turbine inlet temperature, and fan, HPC, HPT, and LPT efficiencies. In effect, these seven parameters can be improved to supply the designer with a specific quantity of irreversibility (exergy destruction). This irreversibility can then be saved to provide fuel-savings and increased efficiency for the aircraft or it can be used to purchase

system performance improvements through the buy market. For this research, the buy market consists of six different system performance metrics: cockpit temperature, cockpit mass flow rate, PTMS thermal load heat rate, fuel temperature, FTMS thermal load heat rate, and engine thrust. Since all of these parameters have intentionally been included in the system design solver, they are treated by the allocation optimizer in a similar fashion to the engine design parameters. After the designer purchases their improvement with a fixed quantity of irreversibility, the solver automatically finds the new performance and quickly readjusts the overall irreversibility allocation of the system.

From this direct allocation of irreversibility, the relationship between the irreversibility distribution, cost, and performance is directly compared. The system-level designer then has the capability of allocating the irreversibility expenditures amongst the three subsystems to obtain the best compromise of exergy destruction, cost, and performance. In effect, the destruction of exergy serves as a true system-level currency for design.

7.4.4 Overall Allocation Design Methodology

Now that the all of the main elements of the approach have been formally covered, it is important to lay out the overall design methodology more systematically. This gives the propulsion systems designer a straightforward series of steps to apply to his or her problem. The steps to the methodology are listed here:

1. Define the system-level requirements
2. Outline the system-level architecture under consideration for the study
3. Develop physics-based models of the critical subsystem models
4. Include prediction of exergy destruction at the component-level
5. Add component cost estimation and other non-thermodynamic design criteria

6. Include off-design turbomachinery performance and component maps
7. Develop vehicle model and include relevant mission profiles
8. Create system-level solver for on-design and off-design performance
9. Execute on-design points and corresponding mission cases for system configurations
10. Obtain cost data and exergy destruction per component for entire mission
11. Run a design of experiments and develop surrogate models of irreversibility, cost, and performance
12. Use surrogate models to perform filtered Monte Carlo simulations
13. Implement system-level irreversibility allocation in terms of subsystem performance metrics
14. Utilize the direct allocation of irreversibility to meet requirements and improve the conceptual design of the engine

7.5 Results - Optimal Allocation

The final experiment examines techniques for identifying the optimal irreversibility allocation. This is a challenging proposition due to the mixed nature of the metrics: thermodynamics, cost, and performance. The simplest technique for accounting for this fact is using a combined cost metric with performance constraints. This is the approach taken for Case A as shown in the illustration of the experiment in Table 36. This case builds on the results of the last experiment with the additional focus of the system-level numerical optimization. Then, Case B considers the direct application of irreversibility and explores the promise that it brings.

Table 36: Experiment #2c: Irreversibility Allocation.

A	**B**
Integrated systems design	Integrated systems design
High heat load	High heat load
Thermodynamics, cost, and vehicle mission performance	Thermodynamics, cost, and vehicle mission performance
System-level numerical optimization	Irreversibility allocation design

7.5.1 Case A: System-Level Numerical Optimization

The results necessary to perform the system-level numerical optimizations were previously presented in Chapters IV, V and VI. Three different scenarios are examined here in particular. The first one features a minimization of the design point fuel burn. The second optimization examines the minimization of production cost by bringing in the prediction capability from Chapter V. Finally, the last optimization brings all of the previous work together. This optimization utilizes a combined production and operating cost metric. This also uses the mission profile to obtain a mission fuel burn for each of the cases. This fuel burn is converted to an annual operating cost which is combined with the depreciated production cost.

Table 37 lists the performance requirements for the optimization. These specific variables were defaulted to the required values within the optimization. The other 26 design variables then played a part in the optimization.

The minimization functions were created using data from response surface equation surrogate models, which are in turn obtained from a design of experiments. The design of experiments for this optimization contained the 26 design variables; it was

Table 37: Performance Requirements for System-Level Numerical Optimizations.

Performance Variable	Required Value
Design Thrust	90 kN
Cockpit Mass Flow Rate	0.30 kg/s
Cockpit Temperature	300 K
PTMS Heat Load Heat Rate	25 kW
Design Fuel Temperature	450 K
FTMS Heat Load Heat Rate	25 kW

a spherical space-filling design of 100 separate runs. Responses were created for overall system exergy destruction rate, fuel burn rate, system production cost, mission integrated exergy destruction, and mission integrated fuel burn.

The responses from the design of experiments were then used to perform the three optimizations as previously noted. The first of these optimizations attempts to minimize design point fuel burn. The fuel burn minimization is written as

$$\min\ J_A = \dot{w}_f \tag{135}$$

A second system-level optimization scenario is performed where the goal is to minimize the production cost of the system. This can be expressed as

$$\min\ J_B = z_{\text{system}} \tag{136}$$

Finally, in this case, the goal is to minimize the combined exergy and cost metric. This is essentially the same as attempting to minimize the life cycle cost of the system. The exergy destruction is converted to an annual fuel cost, and the system development cost is depreciated annually over the expected life of the system. This is expressed mathematically in thermodynamic terms as a combination of operating and production costs:

$$\min\ J_C = \left(c_D \int_0^t \dot{w}_f dt + c_z z_{\text{system}} \right) \tag{137}$$

A genetic algorithm was used to perform the system-level optimizations on the surrogate models for each of the different cases. The performance parameters for all four cases are shown in Tables 38-40. The allocation results associated with these four optimized cases are then shown in Figs. 79-81.

Table 38: Comparison of Engine Performance for Optimized Cases.

Parameter	Opt. A	Opt. B	Opt. C	Design
Specific Thrust [N/(kg/s)]	341.8	441.1	427.6	468.1
Air Mass Flow Rate [kg/s]	263.3	204.1	210.5	192.3
HP Comp. Bleed Flow Rate [kg/s]	1.169	1.787	1.214	2.097
Bypass Ratio	4.343	1.486	1.796	1.246
Exit Velocity [m/s]	408.6	507.5	493.5	535.6
Fuel-to-Air Ratio	0.0395	0.0298	0.0288	0.0273
TSFC [(mg/s)/N]	21.13	26.58	23.69	25.33

Table 39: Comparison of Engine Cycle Efficiencies for Optimized Cases.

Parameter	Opt. A	Opt. B	Opt. C	Design
Heat Input [MW]	72.67	92.40	92.82	100.34
Power Output [MW]	21.43	25.89	25.25	27.16
Thrust Power [MW]	6.117	6.117	6.117	6.117
Thermal Efficiency [%]	29.50	28.02	27.20	27.06
Propulsive Efficiency [%]	28.54	23.63	24.23	22.52
Overall Efficiency [%]	8.417	6.620	6.590	6.096

Table 40: Comparison of System-Level Performance for Optimized Cases.

Parameter	Opt. A	Opt. B	Opt. C	Design
Exergy Destruction Rate [MW]	67.10	86.66	87.12	94.54
Fuel Mass Flow Rate [kg/s]	1.902	2.392	2.132	2.279
Production Cost [$M]	3.431	3.290	3.474	3.475
Exergy Destruction [GJ]	95.52	104.00	67.26	67.16
Fuel Burn [kg]	2823	2968	1660	1677
Total 10-Year Cost [$M]	12.24	12.55	8.653	8.707

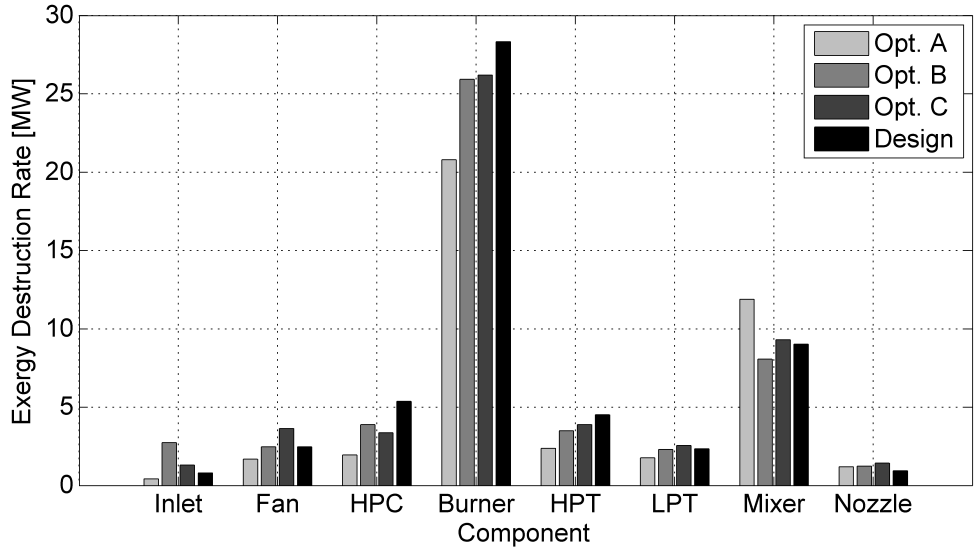

Figure 79: Engine Irreversibility Distribution for Optimizations.

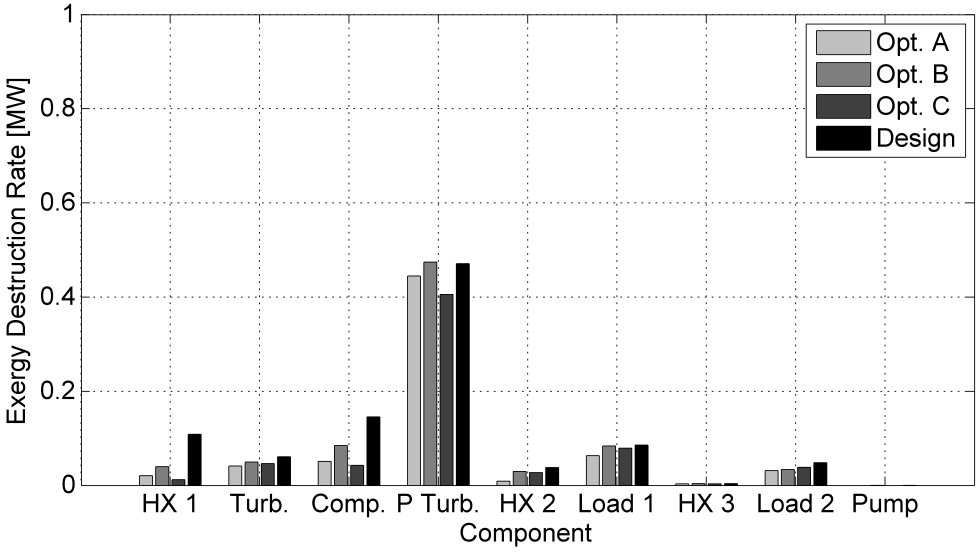

Figure 80: TMS Irreversibility Distribution for Optimizations.

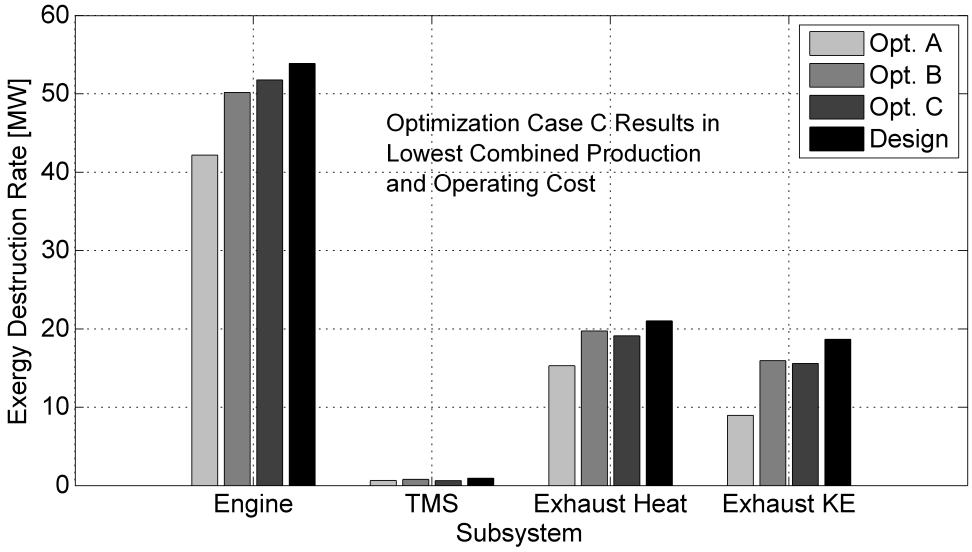

Figure 81: System Irreversibility Distribution for Optimizations.

These plots clearly demonstrate the differences between the three optimization scenarios. The first scenario results in an engine design that has concentrated on a low fuel burn rate as required. Also, a key aspect of keeping the fuel burn and exergy destruction low is the reduction of the air mass flow rate through the engine and a small bypass ratio. The overall efficiency of the engine is also relatively low compared to the design point.

When focusing on production cost in the second case, a much different engine design begins to take shape. For this optimized design, a much larger thrust specific fuel consumption is apparent; the engine inlet mass flow rate has also dramatically increased. All of this has led to a reduction in the overall efficiency of the engine. This more inefficient engine has the upside of having a lower production cost. The fuel burn and production cost minimizations essentially bound the minimization; the relationship between them is dictated by their relative importance.

In the last case, the tradeoff on fuel burn and production cost is realized. In this case, these are combined through three parameters: the price of fuel, number of missions per year, and lifetime of the engine. This design is also closest to the initial

design point. A reasonable specific thrust and thrust specific fuel consumption is seen. Also, it is worth noting that the overall efficiency of the engine in this scenario is the highest out of the the other two scenarios and the initial design point.

The differences between these three cases show a fairly significant change in the solution by shifting the focus between production and operating costs. Also, the combined cost minimization fails to directly incorporate changes in performance. Case B will attempt to remedy these problems through the use of the irreversibility allocation approach. A second problem with the system-level optimization is that it fails to directly capitalize on the one major benefit of exergy-based design: the consistent and absolute measure of system losses. Instead, the system optimization simply lumps the irreversibility together at the system-level; this is similarly achieved by tracking the system fuel consumption. The next case capitalizes on this idea idea by instead using the irreversibility as the main currency in obtaining an optimal allocation.

7.5.2 Case B: Irreversibility Allocation Design

Next, the irreversibility allocation approach outlined earlier in which thermodynamics, cost, and performance are concurrently considered is applied to the integrated propulsion and thermal management systems simulation. The benefits of this approach are then directly compared to the previous automated optimization. For this allocation, a market is established as a means of demonstrating the upside of framing the problem in economic terms.

First, a sell market, which is comprised of several different engine performance parameters, is examined. Through the sale of thermodynamic improvement of these parameters, the designer can obtain additional irreversibility capital. This can be used in turn to purchase mission performance improvements or it can be saved in the form of a more efficient (fuel-saving) system. Specifically, seven major engine cycle parameters are presented: overall pressure ratio, fan pressure ratio, turbine

inlet temperature, and the fan, HPC, HPT, and LPT efficiencies.

A Monte Carlo simulation is initially performed to get a better feel for the exergy destruction distribution across the entire sell market design space. As explained in the theory section, the Monte Carlo was conducted by creating responses of the exergy destruction for each of the subsystems. These responses are produced from a design of experiments similarly to the system optimization of Case A. Once the exergy destruction responses were created, the Monte Carlo is performed by running 10,000 random cases across the design space. Figures 82 and 83 illustrate the variation of the system-level exergy destruction and fuel consumption resulting from the Monte Carlo simulation. Note that the original design point is also represented in the design space plots in red. The first plot shows a fairly large variation in overall system exergy destruction and the system production cost; the Pareto frontier is along the lower left portion of the ellipse. This means that the minimum exergy destruction could vary between 60 and 80 kW and the minimum cost between \$3.1M and \$3.5M depending on their relative importance to the designer. The second fuel consumption plot simply shows the strong relationship between fuel burn and system exergy destruction. This confirms the early experiments showing that a minimum fuel burn design is the same as a minimum exergy destruction design. The true power of the irreversibility characterization is its ability to quickly and consistently break the losses down to the subsystem or component level. The next four plots, Figs. 84-87, do just that. These four plots break the system exergy destruction down into four parts: the destruction occurring within the engine, thermal management system, exhaust heat, and exhaust kinetic energy. As shown in the plots, each of these behave differently across the design space. The first shows that the engine exergy destruction has a variation between 37-63 kW. The variation is quite large at the upper end of the system exergy destruction space, but the variation goes away towards the lower end of the space. The second plot shows that there is not a strong relationship between the TMS

and system exergy destruction, which means that the design has a decent amount of independent control over the losses within the TMS although they are smaller in magnitude. Finally, an interesting observation are the exhaust stream design spaces. The first is the waste heat, which has a strong relationship with exhaust temperature. This plot shows a non-linear relationship between the system and exhaust heat exergy destruction; the variation, however, at any given system-level destruction is small. The kinetic energy plot shows a much larger variation alerting the designer of the possibility of shifting the losses between the exhaust kinetic energy and the rest of the system.

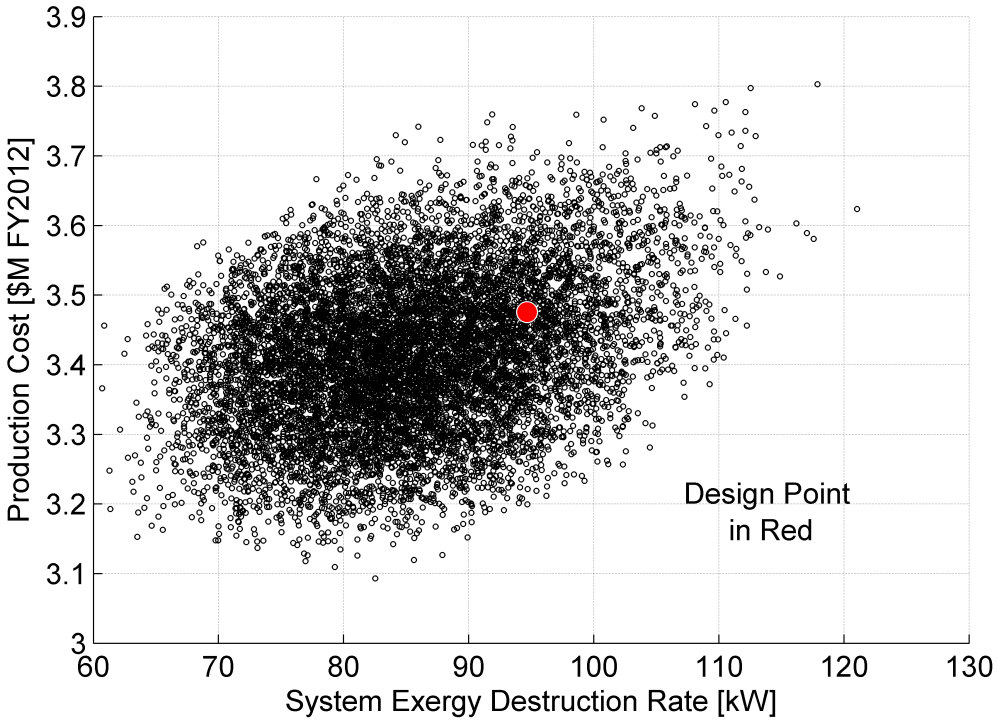

Figure 82: System Exergy Destruction Design Space for Sell Market.

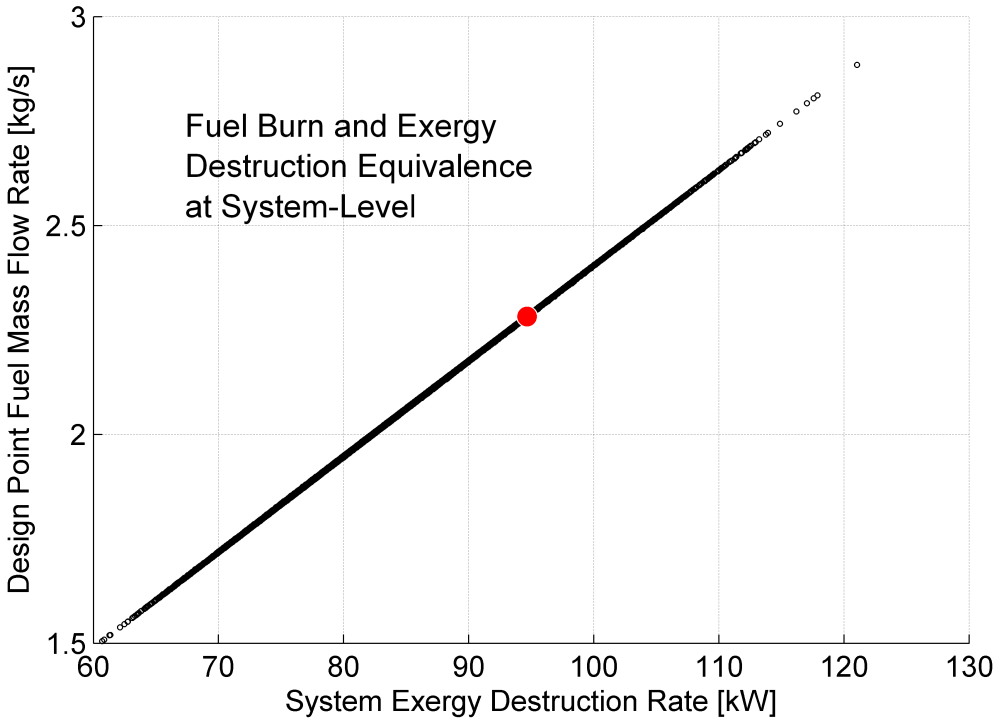

Figure 83: Fuel Consumption Design Space for Sell Market.

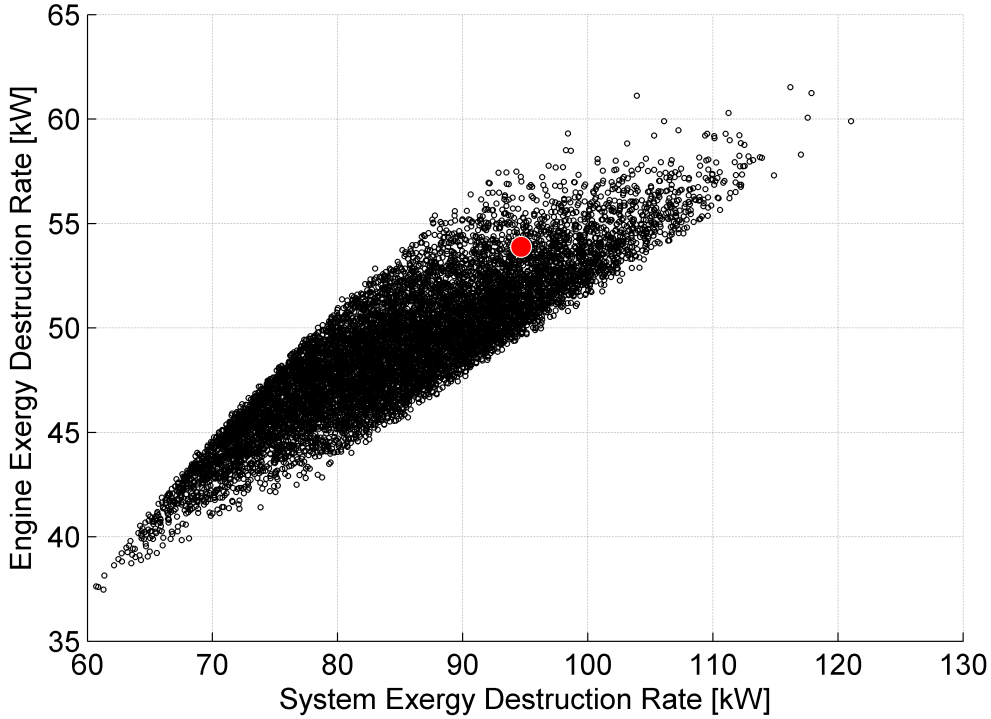

Figure 84: Engine Exergy Destruction Design Space for Use Case Sell Market.

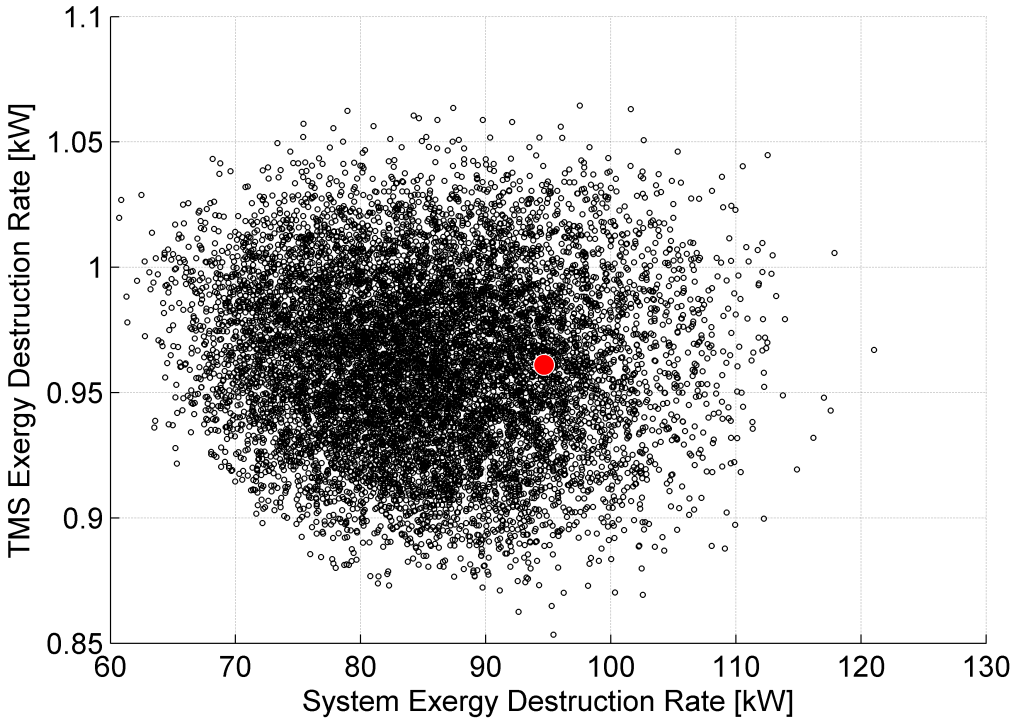

Figure 85: TMS Exergy Destruction Design Space for Use Case Sell Market.

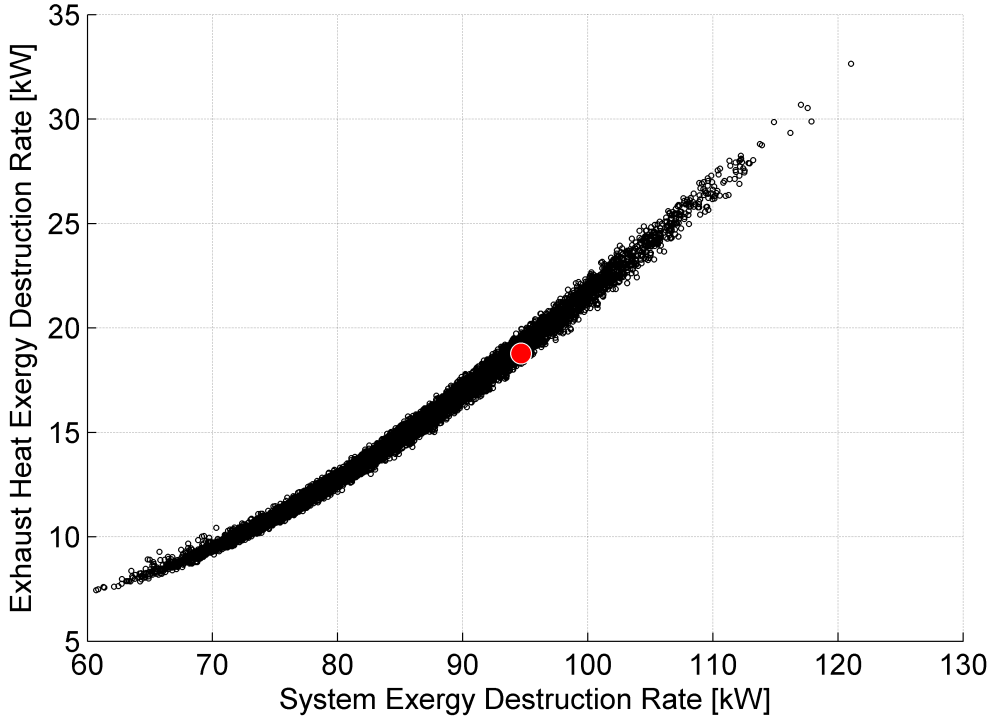

Figure 86: Exhaust Heat Exergy Destruction Design Space for Use Case Sell Market.

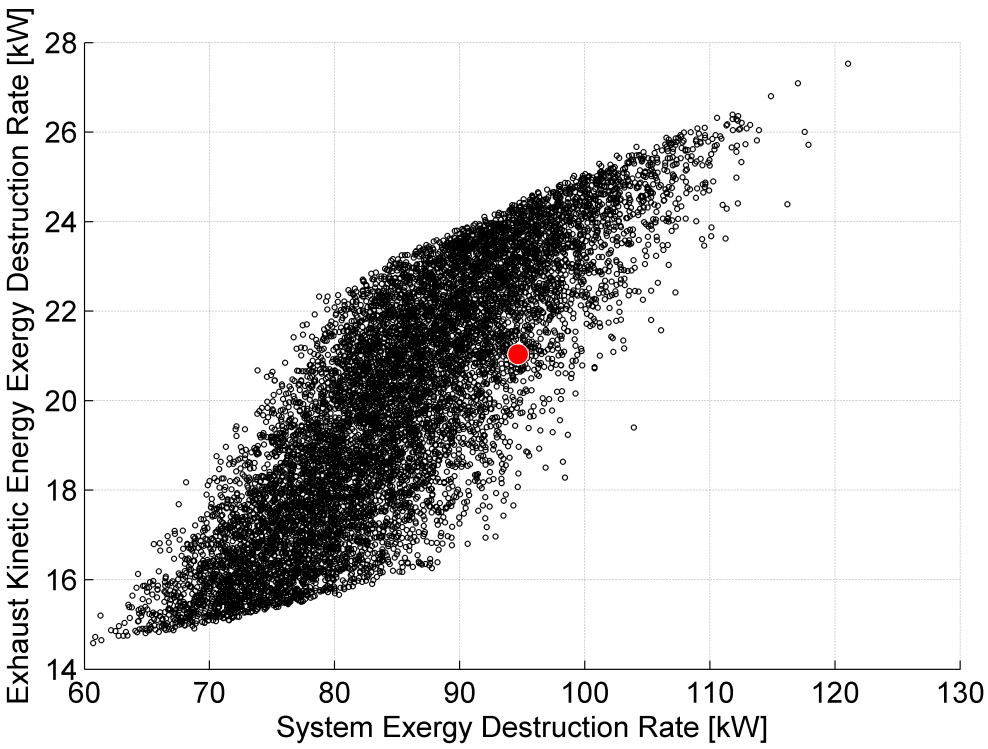

Figure 87: Exhaust Kinetic Energy Exergy Destruction Design Space for Use Case Sell Market.

Now, the designer can also zoom into the design space to see the direct results of changes to the design point. For example, assume the system-level designer wishes to reduce the exergy destruction by 500 kW at the design point through the sell market. The engine design parameter sale options are shown in Fig. 88; each of these sales results in a gain of 500 kW of irreversibility reduction. As the figure shows, the particular change to the parameters themselves varies greatly due to their relationship with the other components and their placement in the system. For the designer to obtain additional irreversibility, the efficiencies and turbine inlet temperature must be increased. On the other hand, the overall and fan pressure ratios are decreased as was shown in the first experiment.

Also, not only are the parameter adjustments unequal, but so are the production cost and mission fuel burn. This was demonstrated previously in Experiments 2a and 2b, respectively. A comparison of the production costs required for each of the sales

is shown in Fig. 89. This shows that the majority of the component changes work in various degrees to lower the overall system production cost with the exception of the turbine inlet temperature which raises this cost. Finally, the mission fuel burn differences are shown in Fig. 90. Decreases in the two pressure ratios result in significant increases to the mission fuel burn, while the turbine inlet temperature and component efficiencies do just the opposite. Keep in mind that the design point exergy destruction change is the same for each sale; this was set as a reduction of 500 kW. The differences in fuel burn arise from the mission flight and the simple fact that the system operating point is constantly changing, which affects the ambient conditions and thrust requirements of the engine.

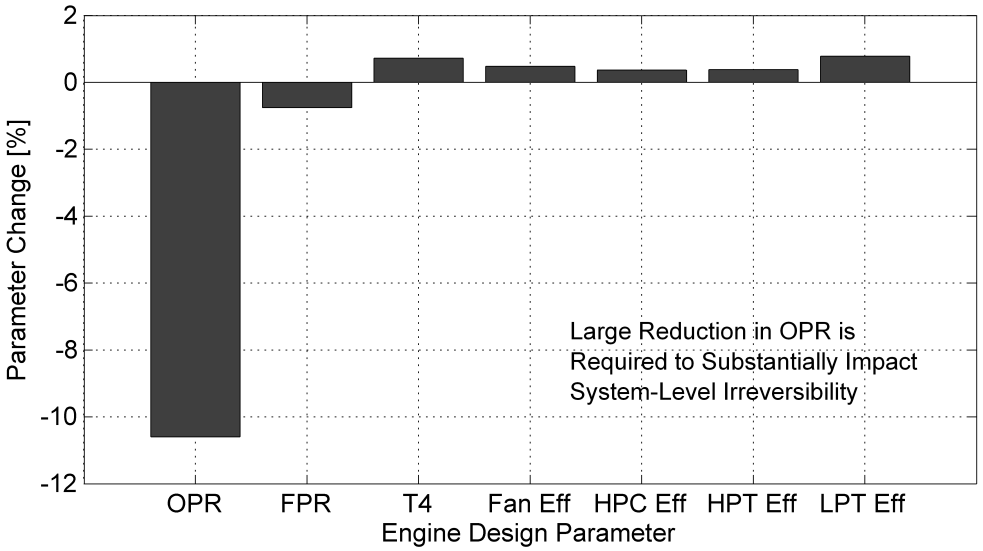

Figure 88: Engine Design Sale Options for 500 kW of Additional Irreversibility.

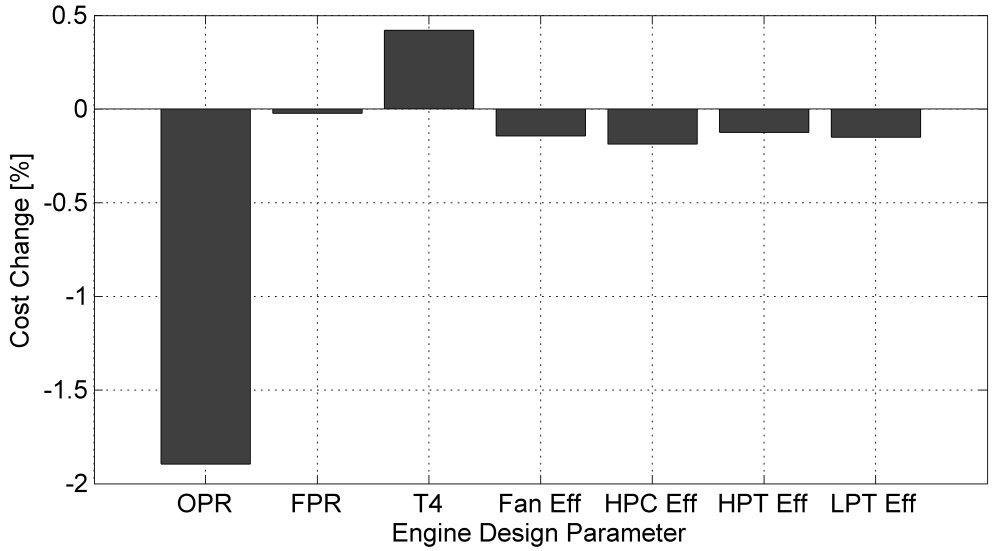

Figure 89: System Cost Repercussions of Engine Design Sales.

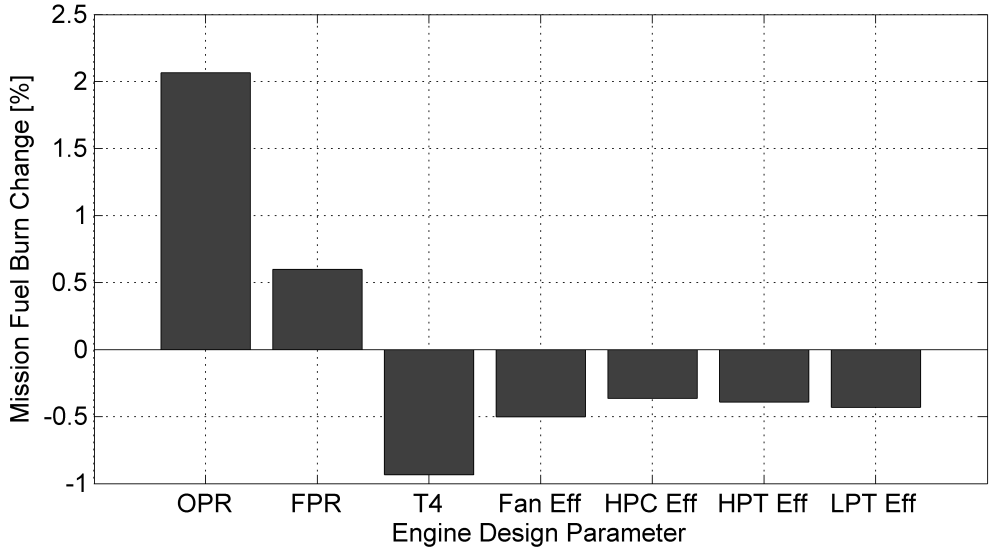

Figure 90: Mission Fuel Burn Repercussions of Engine Design Sales.

Next, consider the case where the designer wishes to obtain 500 kW of irreversibility (in the form of reduced system exergy destruction) through the previously listed sales. It is important to remember that this 500 kW is not removed directly from the particular component nor is it removed uniformly throughout the system. Instead, it is removed in such a way that this system remains balanced as required by the system solver. This redistribution of system irreversibility for each of the sales is illustrated in Figs. 91-93.

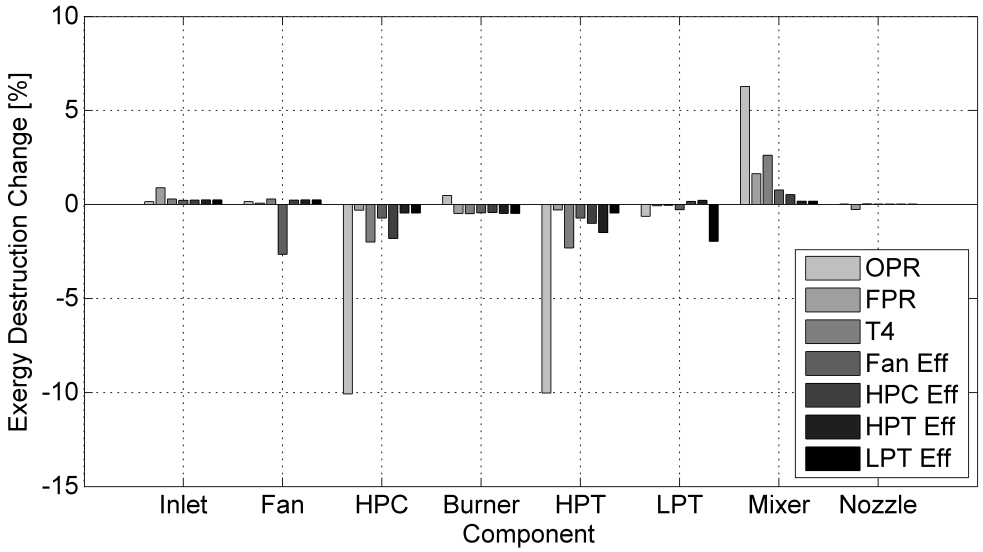

Figure 91: Changes in Engine Irreversibility Allocation for Sell Options.

These plots show that the overall pressure ratio has the largest effect on the engine and TMS distributions, while the turbine inlet temperature is the major player in reducing the exhaust heat. All of the changes have somewhat similar impacts on the exhaust kinetic energy destruction except the overall pressure ratio which has little effect.

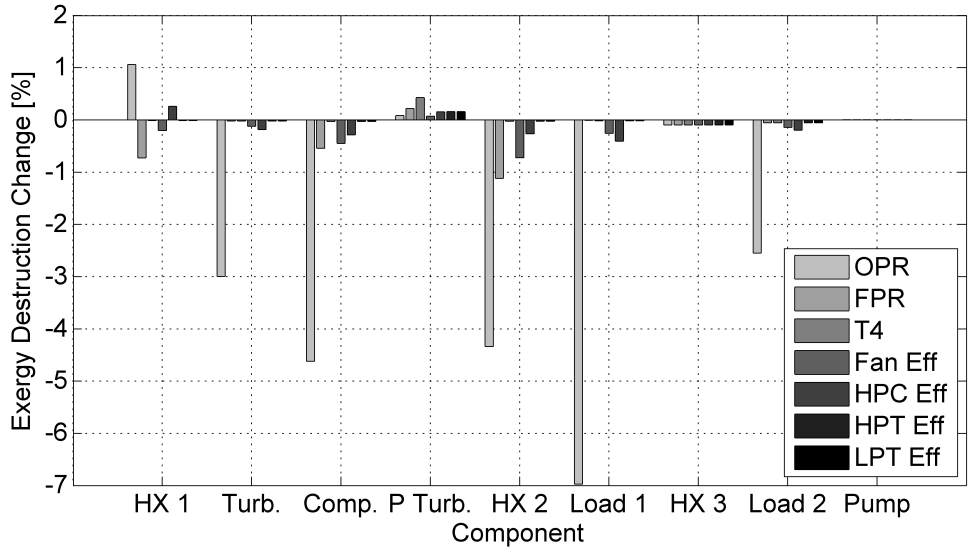

Figure 92: Changes in TMS Irreversibility Allocation for Sell Options.

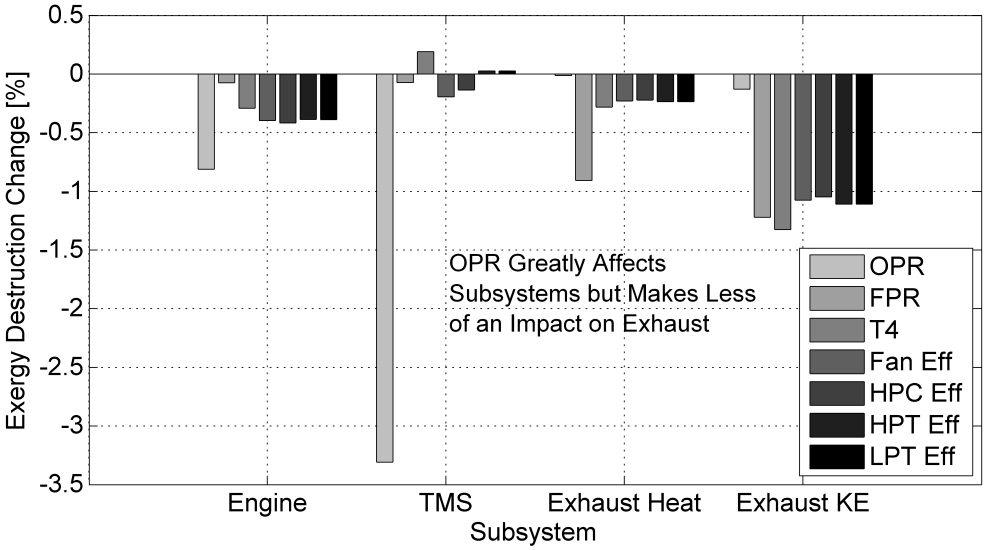

Figure 93: Changes in System Irreversibility Allocation for Sell Options.

The distributions illustrate one of the major benefits of the irreversibility characterization. It allows the designer to quickly visualize the changes in the distribution of losses as the result of design changes. This second distribution shows that the OPR sale reduces the exergy destruction throughout the core of the engine. It has the largest impact on reducing the loss in the HP compressor itself and the HP turbine which is directly connected via the engine shaft. However, there is also a conflicting increase in exergy destruction in the mixer component due to the changed nature of its two input streams. Although the changes in the thermal management systems are smaller, the biggest impact is on the PTMS load and its cooling power turbine which is powered directly by the bleed air from the HP compressor. One of the most interesting results of this allocation is shown in Fig. 93. Here it is seen that the change in percentage exergy destruction is quite large for the exhaust stream, in terms of both waste heat and kinetic energy. This clearly demonstrates the importance of considering the engine exhaust in the irreversibility allocation. On the other hand, the importance of the exhaust stream is very minimal in the case of ground-based power systems.

For the opposite case, the purchase of mission performance improvement through a buy market, is considered. The process is identical to the previous one with the difference of irreversibility addition instead of reduction. Once again, the overall design space is examined through the use of a Monte Carlo and then the focus is around the design point where an amount of irreversibility equal to 500 kW of exergy destruction is considered. This fixed standard amount of exergy destruction is reallocated throughout the system to achieve an increase in performance.

First, PTMS performance is considered by taking a look at three different metrics: cockpit temperature, cockpit mass flow rate, and the heat rate of the PTMS thermal load. For the FTMS, two different performance metrics are investigated: a reduction in maximum fuel temperature and an increase in thermal load heat rate

capability. Finally, the engine thrust capability is examined as a means of including the propulsion system performance.

This mission performance improvements can be purchased directly with the capital obtained through the improvement of the engine cycle parameters just presented. Alternatively, instead of reallocating irreversibility within the system, the designer may wish to infuse additional capital at the expense of reduced system efficiency. In this case, there will be a fuel penalty associated with this purchase.

Figures 94 and 95 illustrate the variation of the exergy destruction, fuel burn, and production cost resulting from the Monte Carlo simulation for the buy market. The next four plots, Figs. 96-99, then break the exergy destruction down into four parts as was previously done with the sell market: the destruction occurring within the engine, thermal management system, exhaust heat, and exhaust kinetic energy.

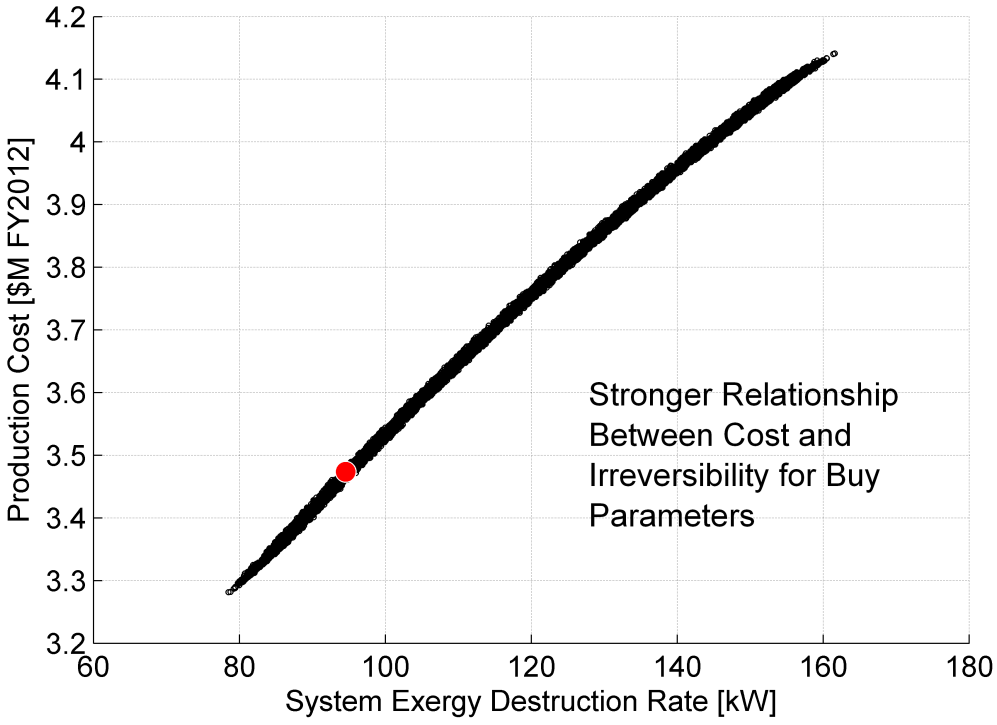

Figure 94: System Exergy Destruction Design Space for Buy Market.

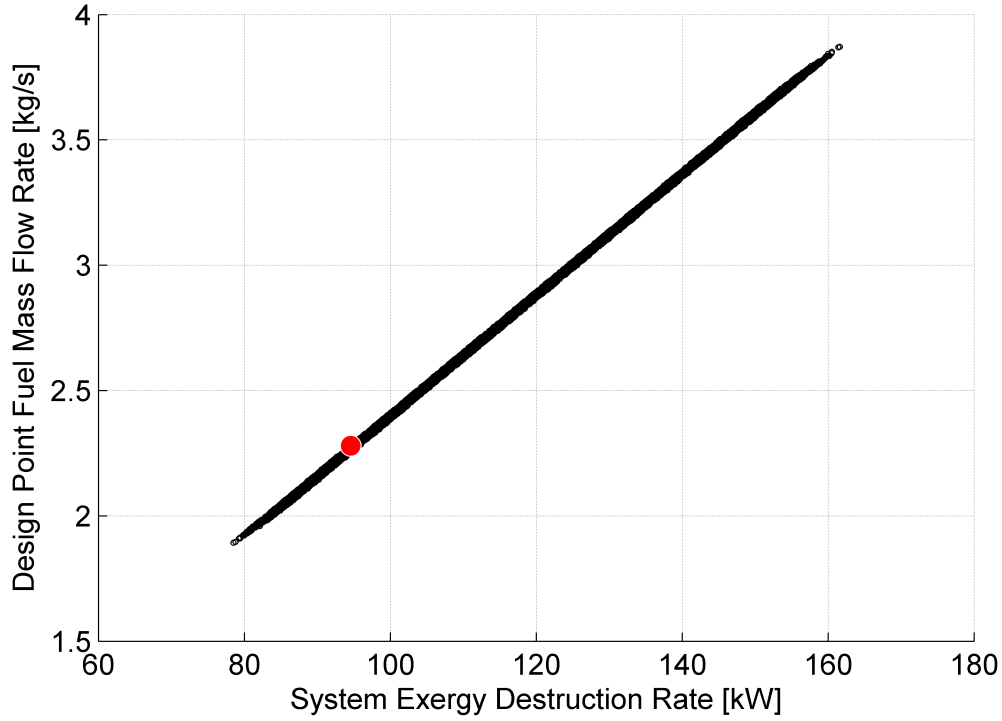

Figure 95: Fuel Consumption Design Space for Buy Market.

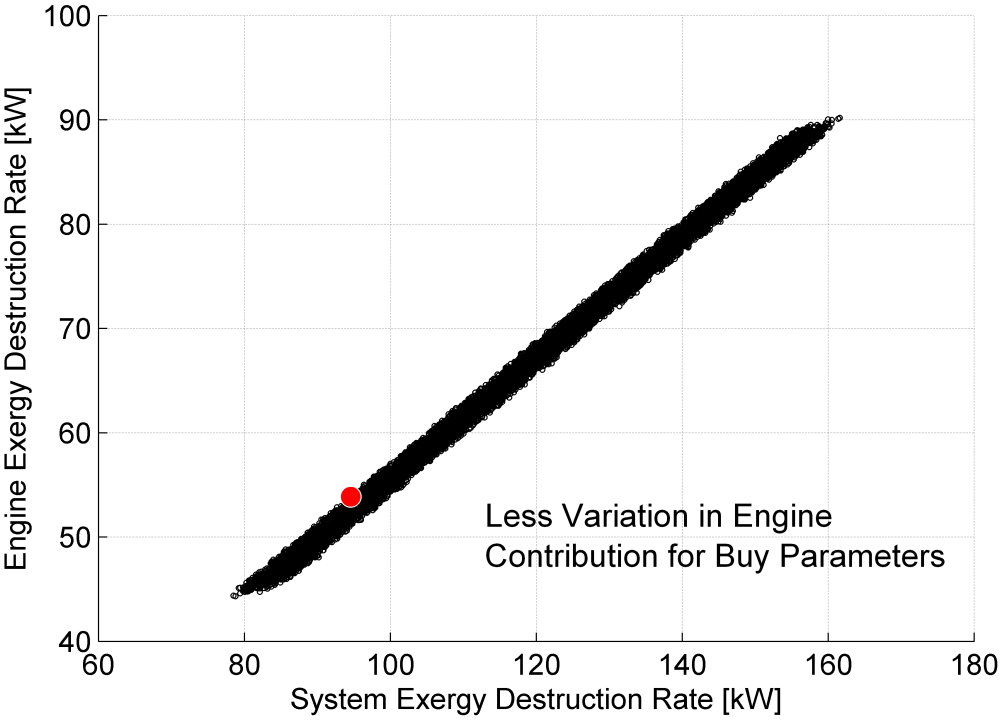

Figure 96: Engine Exergy Destruction Design Space for Buy Market.

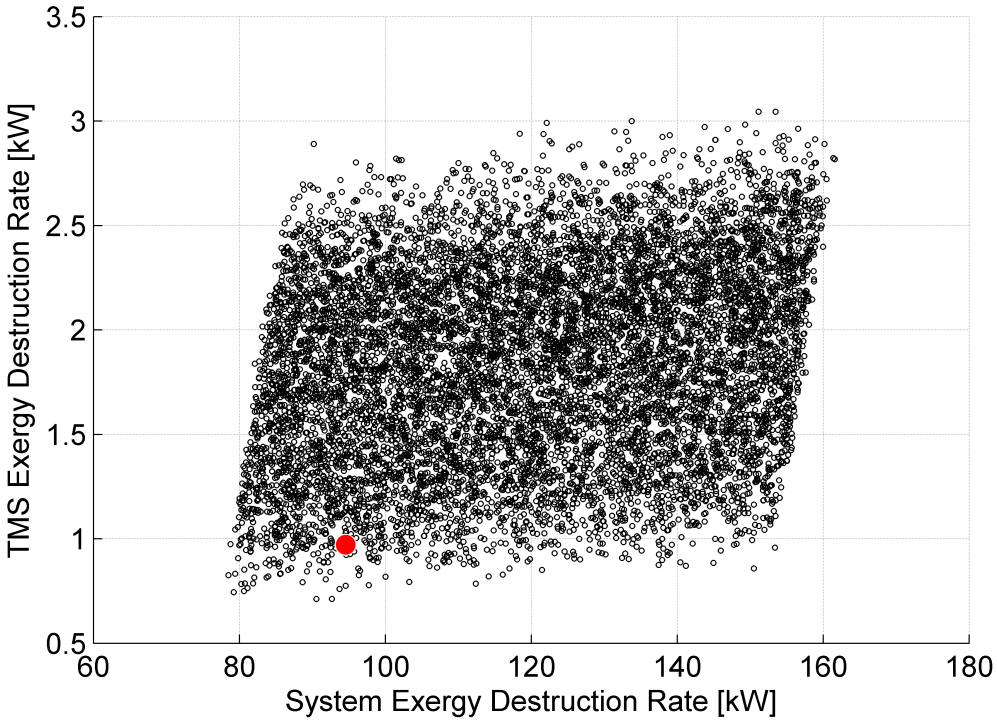

Figure 97: TMS Exergy Destruction Design Space for Buy Market.

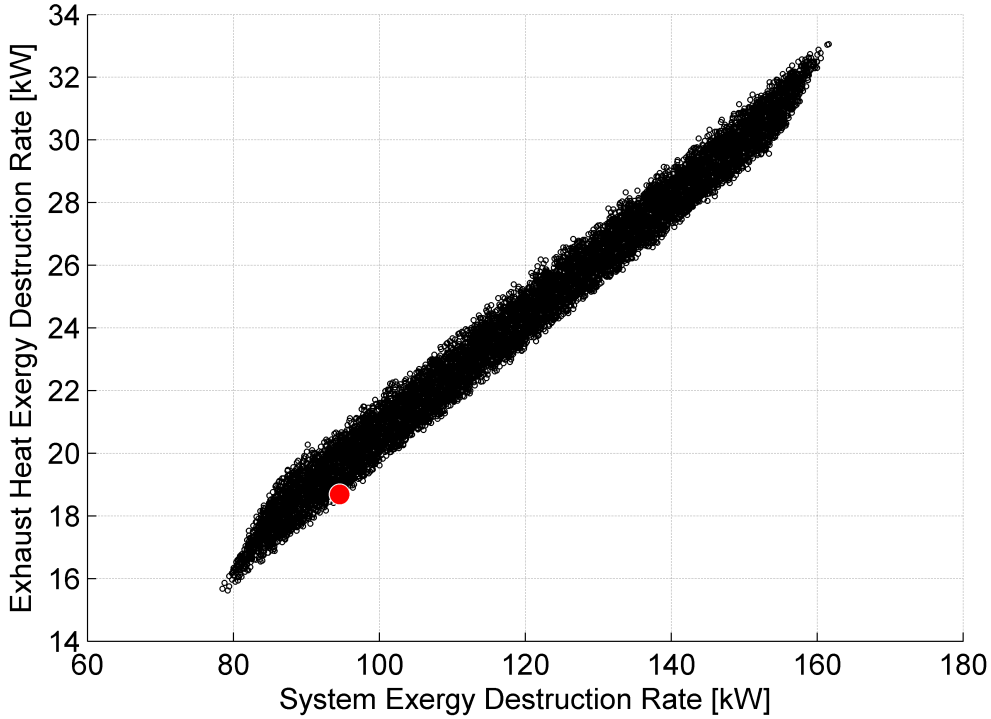

Figure 98: Exhaust Heat Exergy Destruction Design Space for Buy Market.

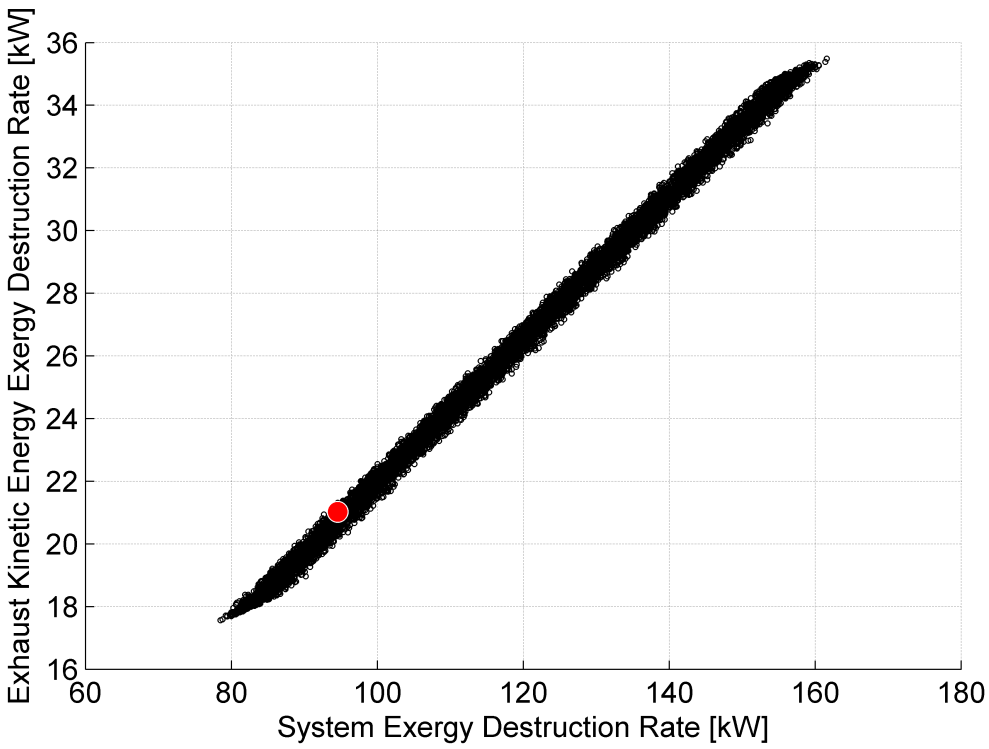

Figure 99: Exhaust Kinetic Energy Exergy Destruction Design Space for Buy Market.

The results for the buy market are actually quite different from the previous sell market. Taking a look at the first two plots shows that the production cost and exergy destruction are not at odds, although they are both at odds with performance improvement. For example, increasing the allowable PTMS heat load has a detrimental effect on both production and operating costs. The subsystem plots show a fairly linear relationship between the system exergy destruction and the subsystem exergy destruction. This time the designer has the most control over shifting the destruction to and from the exhaust waste heat through changes in the buy market.

Now, the focus turns to improvements exclusively around the design point as was done in the previous case. The available performance improvement purchase options are illustrated in Fig. 100. An additional amount of 500 kW of irreversibility is infused into the system to cover the expense of each of these purchases. As shown in the figure, the addition of irreversibility into the system results in a reduction in

cockpit and fuel temperatures, but an increase in the other performance metrics. Also worth noting is the fact that the cockpit mass flow rate and the two heat loads result in the largest percentage change, while the thrust increase is very minimal for 500 kW of additional exergy destruction.

The subsequent cost effects are shown in Fig. 101 and the mission fuel burn effects are shown in Fig. 102. The cost results show that all six of these performance improvements result in a small increase in the system cost. These increases are all roughly of the same order of magnitude as was seen in the Monte Carlo portion of the study. The mission fuel burn does show distinct differences between the metrics due to the effects of the mission profile and demonstrates the need to take this into consideration. The heat loads, especially the large PTMS load, increase the mission fuel burn the most; it takes a significant amount of cooling to keep the large PTMS load within the appropriate limits.

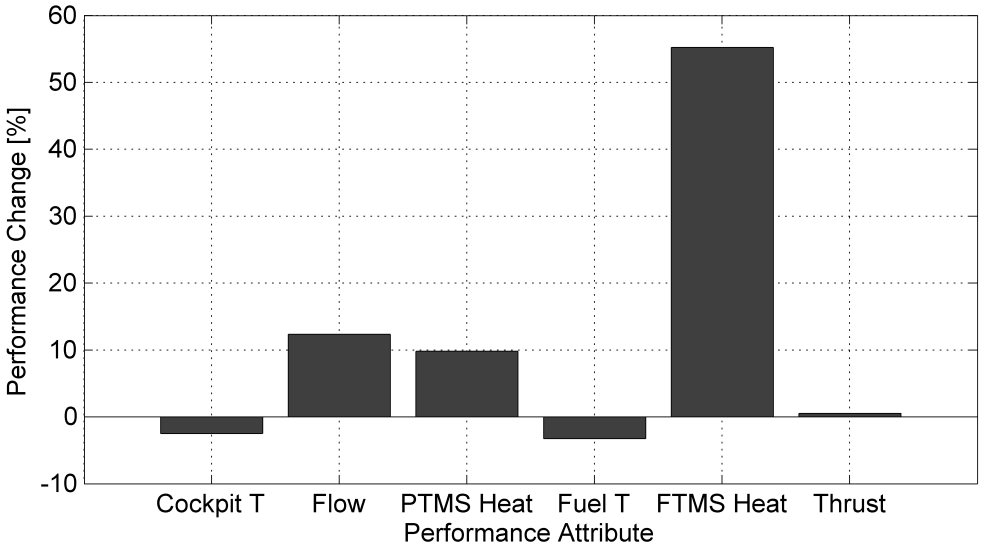

Figure 100: Performance Improvements Purchase Options Available for 500 kW of Additional Irreversibility.

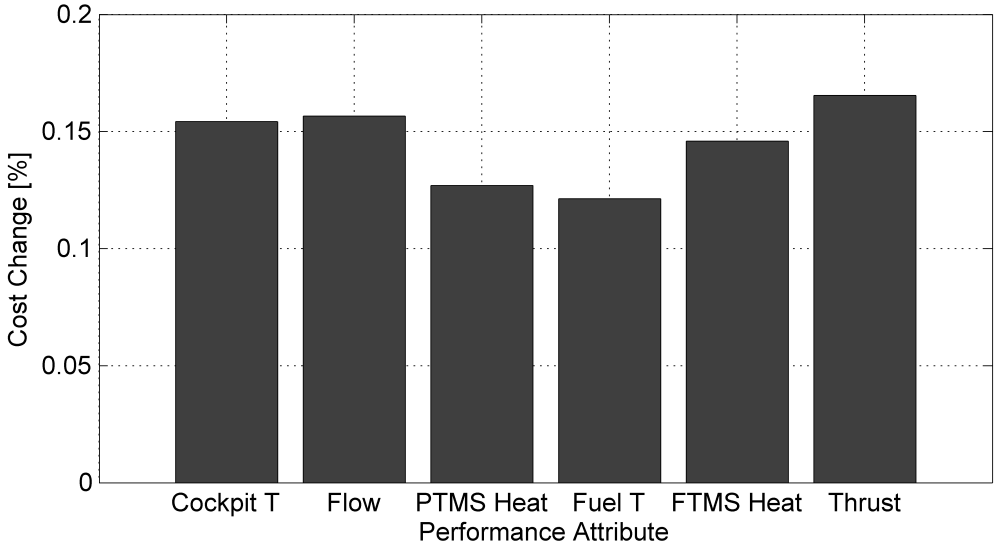

Figure 101: System Cost Repercussions of Performance Improvement Purchases.

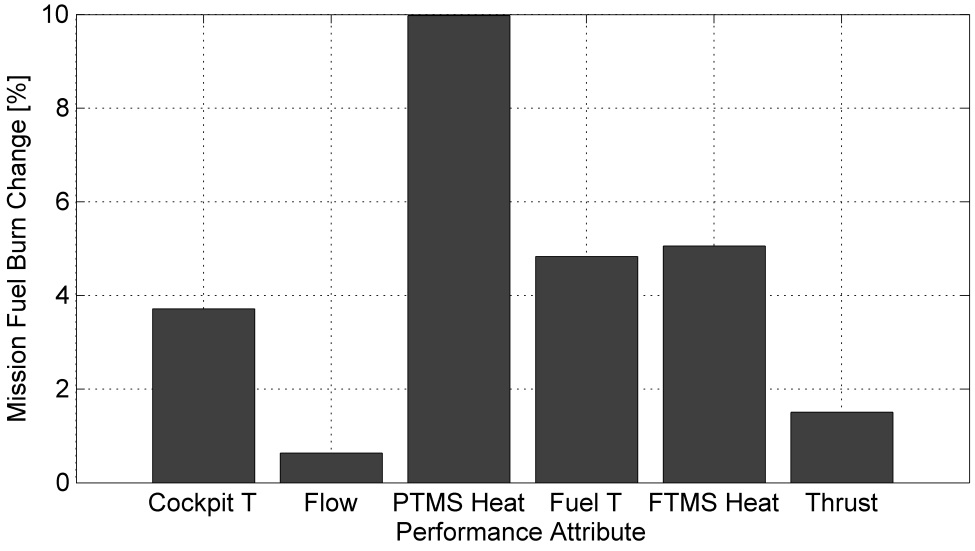

Figure 102: Mission Fuel Burn Repercussions of Performance Improvement Purchases.

Consider that an additional 500 kW of exergy destruction is infused into the system through the purchase of a performance improvement. The resulting change in the system-level allocation due to this infusion of irreversibility is illustrated for all of the buy options in Figs. 103-105.

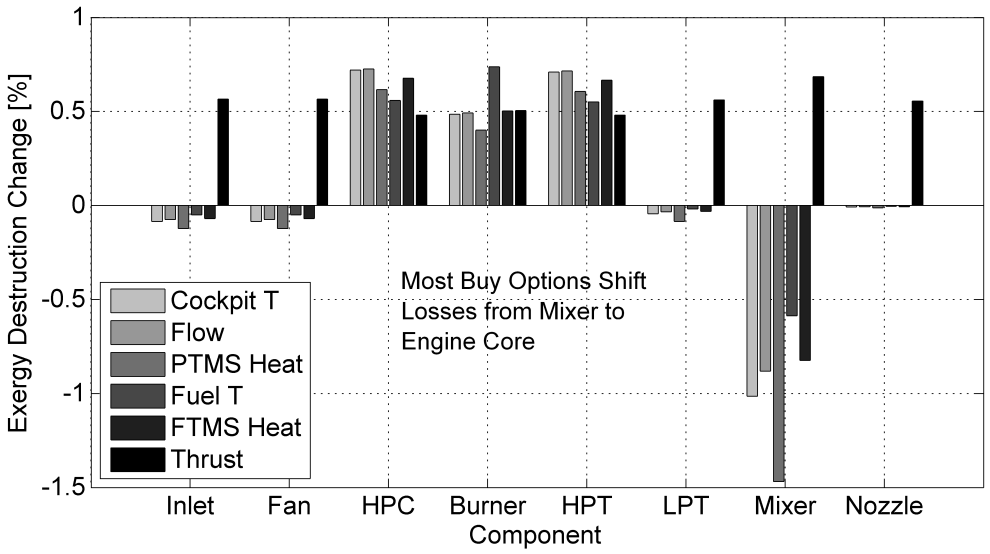

Figure 103: Changes in Engine Irreversibility Allocation for Buy Options.

This reallocation of irreversibility also affects the entire system as noted in the case of the sell market. This time, however, there is a much more pronounced change in the thermal management systems, especially for the FTMS thermal load. The impact on the engine is the reverse of the previous case, where now the core components see an increase in irreversibility and the mixer sees a substantial decrease. It should still be kept in mind that the magnitude of the exergy destruction in the engine and exhaust is much larger than the PTMS and FTMS. Taking a look at Fig. 105, it is once again seen that the exhaust has a large impact on the irreversibility allocation change.

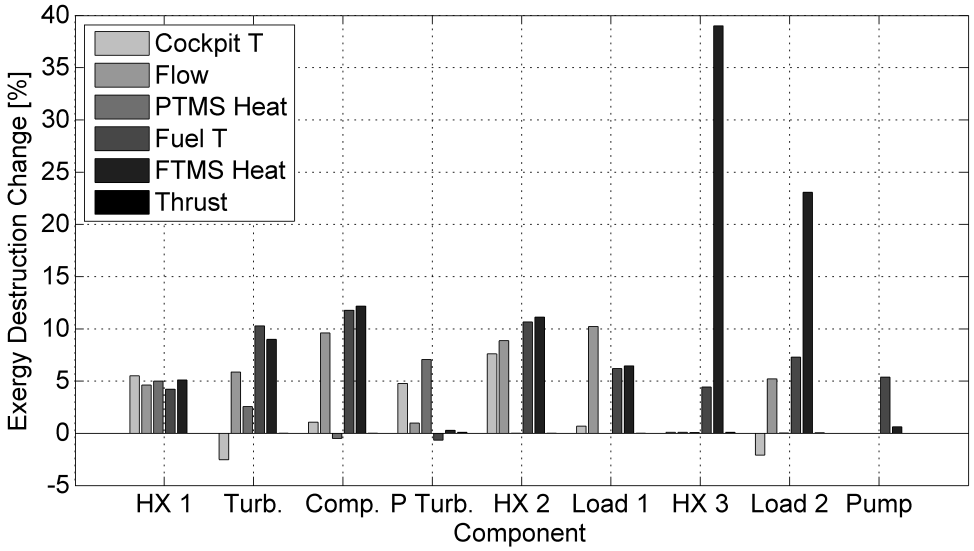

Figure 104: Changes in TMS Irreversibility Allocation for Buy Options.

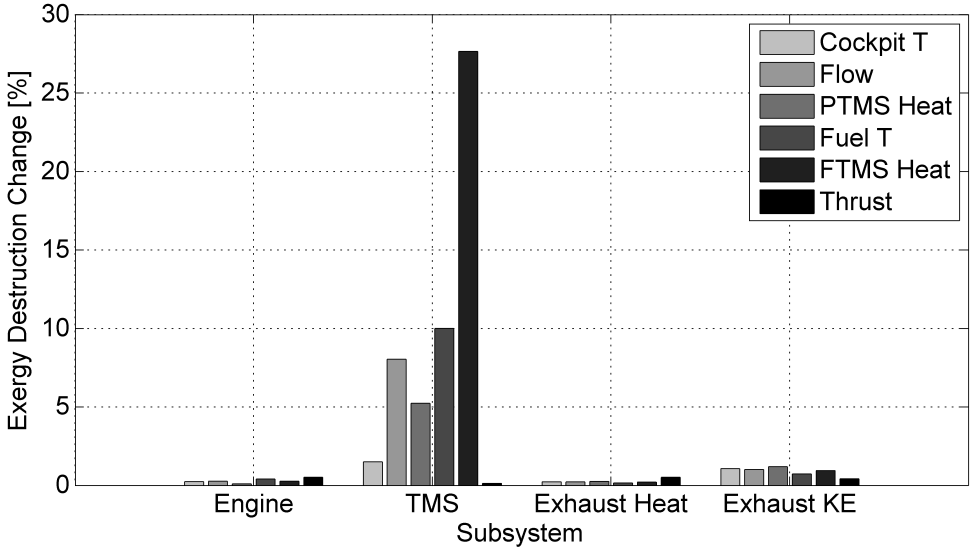

Figure 105: Changes in System Irreversibility Allocation for Buy Options.

7.6 Examination of Exergy Destruction Sensitivities

Finally, it also important to now investigate the exergy destruction sensitivities for the buy and sell markets. This is done in a similar manner as as to what was done in Chapter IV when the the fuel burn and exergy destruction metrics were compared. This is also done at two different operating points to demonstrate the consistency of the modeling environment and the irreversibility allocation approach.

The first case shows the sensitivities with respect to the component exergy destructions at the initial design point used throughout the study. For this first point, the design variables were perturbed through a finite difference to calculate their sensitivities with respect to component exergy destruction. The finite difference perturbation of the design variables was $\vec{X}_0 + \vec{h}$ where $\vec{h}$ is very small. As before, this information can be presented in the form of an m-by-n Jacobian matrix, where m is the number of components and production cost and n is the number of design variables:

$$J_{\vec{\bar{F}}}\left(\vec{\bar{X}}_0\right) = \begin{bmatrix} \frac{\partial \bar{F}_1}{\partial \bar{X}_1} & \cdots & \frac{\partial \bar{F}_1}{\partial \bar{X}_n} \\ \vdots & \ddots & \vdots \\ \frac{\partial \bar{F}_m}{\partial \bar{X}_1} & \cdots & \frac{\partial \bar{F}_m}{\partial \bar{X}_n} \end{bmatrix} \tag{138}$$

Once again, the variables are normalized by their values at the design point:

$$\frac{\partial \bar{F}}{\partial \bar{X}} = \frac{X_{\text{design}}}{F_{\text{design}}} \frac{\partial F}{\partial X} \tag{139}$$

The design point irreversibility Jacobian with respect to the buy and sell parameters is shown in Fig. 106. The buy and sell parameters are listed in Table 41. The visualization of this Jacobian can quickly give the designer an overall view of the system's local behavior. The first relationship that is readily obvious from the plot is the strong positive correlation between turbine inlet temperature and the mixer exergy destruction. The strongest negative correlations are between the compressor and turbine efficiencies and their corresponding component irreversibility. The sell

market also has a significant effect on the exhaust irreversibility, especially the kinetic energy. The buy market illustrates a strong relationship between the thrust and engine and exhaust irreversibility. On the other hand, the other five parameters serve to mostly affect the allocation within the TMS itself.

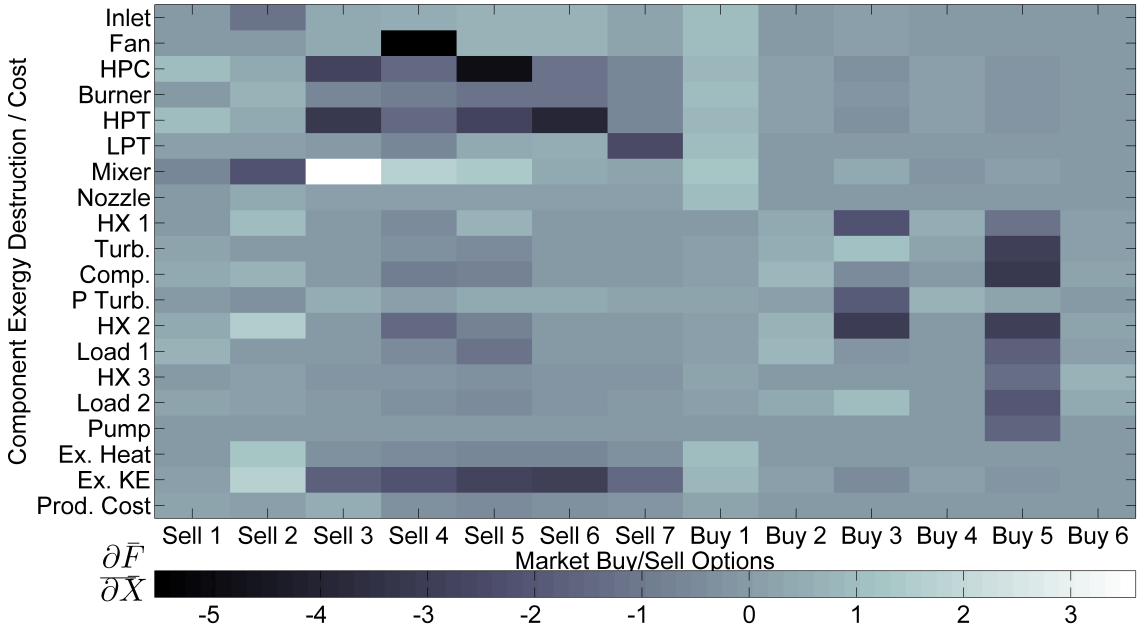

Figure 106: Exergy Destruction vs. Buy/Sell Jacobian at Design Point.

Table 41: Buy and Sell Parameters listed in Exergy Destruction Jacobian.

	Sell		Buy
1	Overall Pressure Ratio	1	Thrust
2	Fan Pressure Ratio	2	Cockpit Mass Flow Rate
3	Turbine Inlet Temperature	3	Cockpit Temperature
4	Fan Efficiency	4	PTMS Load Heat Rate
5	HPC Efficiency	5	Fuel Temperature
6	HPT Efficiency	6	FTMS Load Heat Rate
7	LPT Efficiency		

For the second case, the exergy destruction sensitivities are reexamined at a new design point, which has a thrust requirement that is 3% greater than the original design point. Once again, the sensitivities are obtained through a finite difference of the design variables: $\vec{X_1} + \vec{h}$ where $\vec{h}$ is very small.

The new Jacobian for this point is written as

$$J_{\vec{F}}\left(\vec{X}_1\right) = \begin{bmatrix} \frac{\partial \bar{F}_1}{\partial \bar{X}_1} & \cdots & \frac{\partial \bar{F}_1}{\partial \bar{X}_n} \\ \vdots & \ddots & \vdots \\ \frac{\partial \bar{F}_m}{\partial \bar{X}_1} & \cdots & \frac{\partial \bar{F}_m}{\partial \bar{X}_n} \end{bmatrix} \tag{140}$$

The results at the new design point are shown in Fig. 107; this new Jacobian is almost identical to the original design point. There is an overall lightening across the space with a slightly larger effect across the thrust column, which is the design point value that was increased. Since the design space shows a similar increase between the two design points, it is assumed that the modeling environment and irreversibility allocation approach are well behaved in the local neighborhood of the design points.

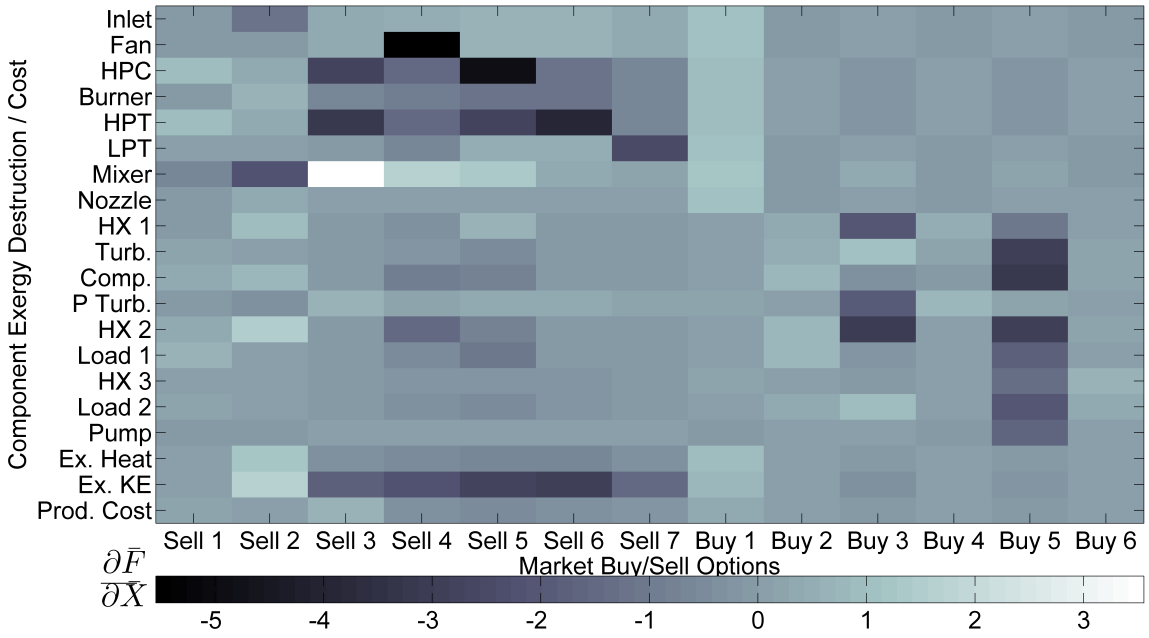

Figure 107: Exergy Destruction vs. Buy/Sell Jacobian at New Design Point.

7.7 Designer Use Case to Demonstrate Benefits of Approach

It is now time to bring all of the previous elements together and fully illustrate the benefits of the irreversibility allocation approach to the system-level designer. This is demonstrated most effectively through the posing of two use cases which are based on typical design decisions that might be encountered by the designer. The irreversibility allocation approach presented in this chapter is then applied to each case in an effort to clearly compare and contrast it with traditional design techniques. It is shown that the irreversibility allocation is beneficial to the designer in that it yields new information to support the designer in her or her decision making in regards to the system-level requirements.

The designer use cases presented here feature the same propulsion and thermal management system architecture that was previously used for the individual experiments throughout the rest of the study. They build on the observations in the optimization and allocation sections of this chapter by highlighting some of the ways that this information can then influence design choices. The first one presents the case of a system-level designer trying to properly satisfy competing requirements; the second one then deals with a scenario where several different design improvements exist and the designer must choose between them.

7.7.1 Using the Irreversibility Allocation to Better Satisfy System-Level Requirements

As a result of the demands discussed in the motivation, the subsystem designers often desire a cooling system that is capable of dealing with ever-increasing thermal loads because it enables them to utilize higher-performing, high power electrical systems. On the other hand, designers responsible for the low observability of the aircraft are concerned mostly with the stealth capabilities of the system and view these increasing thermal loads negatively. It is, therefore, the job of the system-level designer to

balance these competing demands and satisfy the requirements in such a way as to create the best overall *system*.

For this first use case, the designer must decide how to appropriately address the system requirements regarding the internal and external heating and cooling loads. This tradeoff is encountered when the designer is simultaneously trying to accommodate larger thermal loads within the thermal management system while also keeping the exhaust temperature low in an effort to reduce the infrared signature. Assume that the designer needs to investigate a range of PTMS thermal loads and exhaust temperatures to strike the appropriate balance while concurrently deciding on the appropriate engine design parameters, achieving a target thrust, and meeting a system production cost limit. Table 42 lists the ranges for the two thermal parameters of interest along with the thrust and cost requirements.

Table 42: Requirements for Thermal Sensitivity Use Case.

PTMS Thermal Load Heat Rate	50-500 kW
Exhaust Temperature	600-680 K
Maximum Thrust	90.0 kN
System Production Cost	<$3.55M

To start to look at these internal versus external heat trades, an overview of the design space around these requirements is beneficial. Figures 108 and 109 show the relationship between the PTMS thermal load and the propulsion system exhaust temperature and design parameters; Fig. 108 looks at a variation of the overall pressure ratio and a constant turbine inlet temperature, while Fig. 109 holds the pressure ratio constant and varies the turbine inlet temperature.

Next, five points are highlighted on these two plots to discuss their respective advantages and disadvantages. Note that α appears in both plots because it has an overall pressure ratio of 25 and a turbine inlet temperature of 1650 K, which are the constant values for the plots.

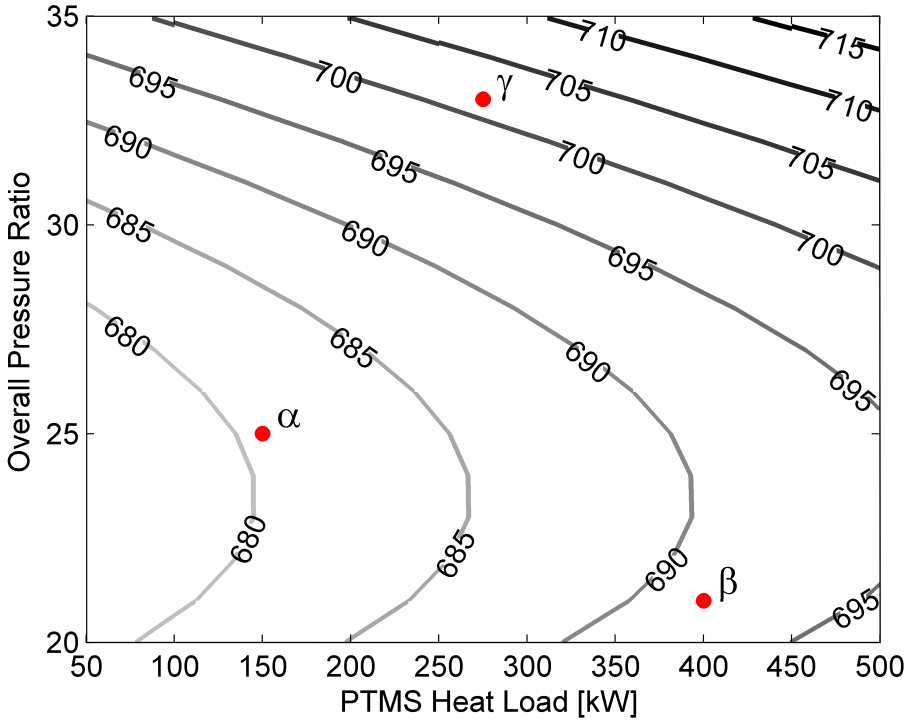

Figure 108: Engine Exhaust Temperature [K] (T4 = 1650 K).

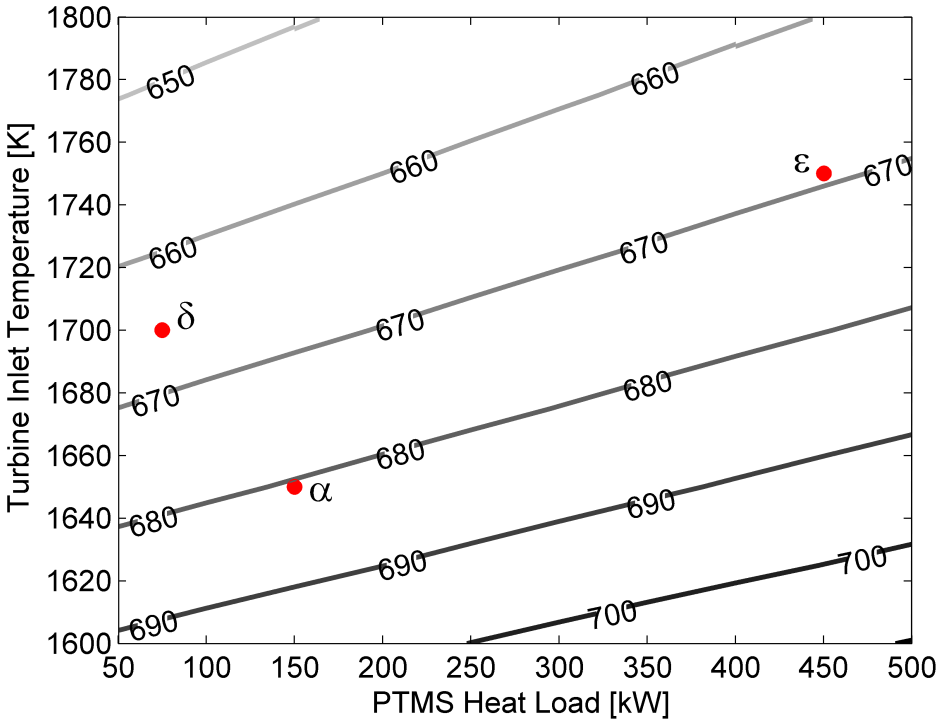

Figure 109: Engine Exhaust Temperature [K] (OPR = 25).

From this visualization of the design space, it is also worth noting that the typical exhaust temperature values range from 650-715 K; this means that it is not possible to achieve the lower limit of the exhaust temperature range by varying the two engine parameters and thermal load.

Now that the designer has a general idea of the behavior of the design space, the irreversibility allocation approach is useful in aiding the designer by illuminating the losses on a consistent and absolute basis while also accounting for cost and performance. The designer can start this investigation by viewing the changes in the system's irreversibility distribution across the five parameters within the design space. Of particular importance is the relationship between the TMS heat loads, exhaust heat and kinetic energy, and fuel burn and all of their implications on propulsion system performance. The five different irreversibility distributions are shown in Figs. 110-112. Table 43 then compares the irreversibility, cost, and performance for these five cases.

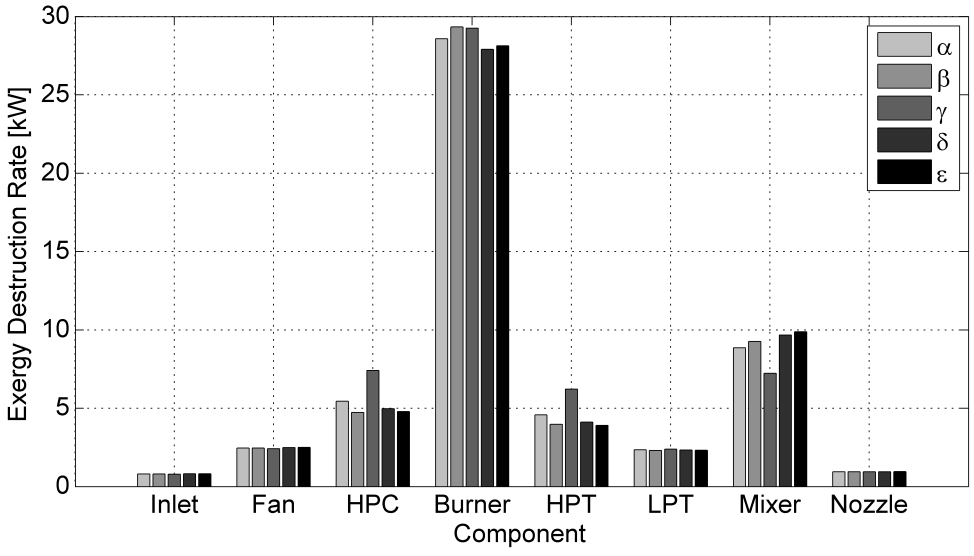

Figure 110: Engine Irreversibility Distributions for Tradeoff Cases.

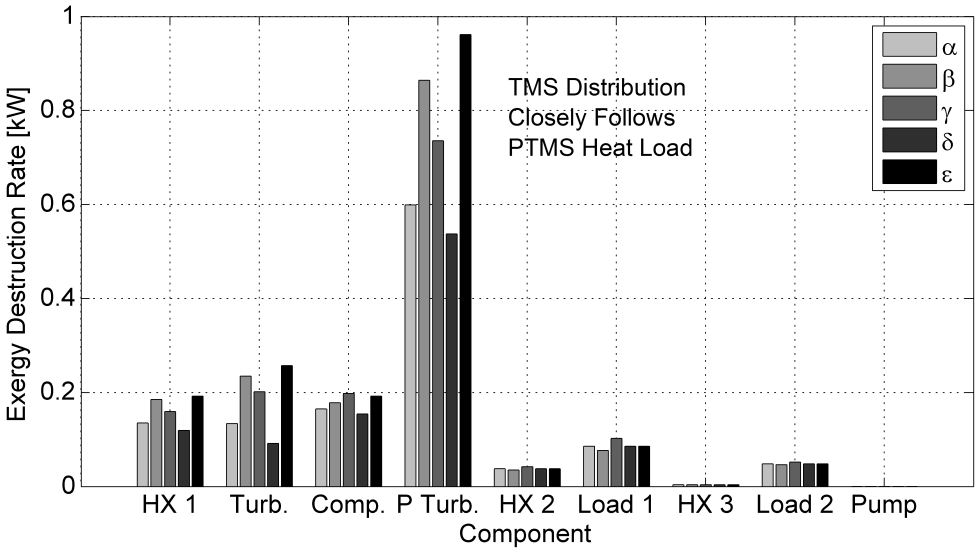

Figure 111: TMS Irreversibility Distributions for Tradeoff Cases.

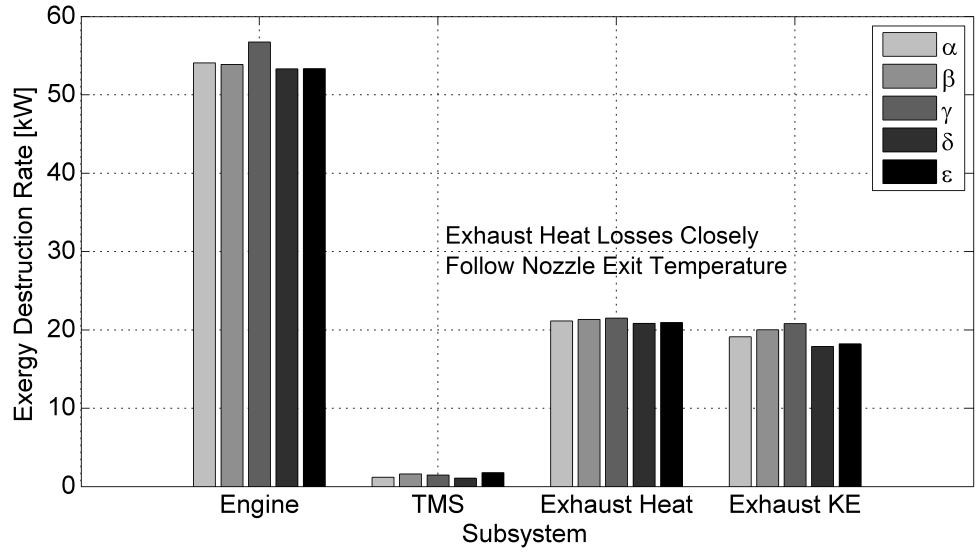

Figure 112: System Irreversibility Distributions for Tradeoff Cases.

Table 43: Irreversibility, Cost, and Performance for Tradeoff Cases.

Case	Exergy Dest. (Total) [kW]	Exergy Dest. (Exh. Heat) [kW]	Exh. Temp [K]	Cost [$M]	Heat Load [kW]
α	95.53	19.12	680.6	3.48	150
β	96.86	20.02	691.6	3.41	400
γ	100.5	20.81	701.5	3.72	275
δ	93.12	17.90	665.3	3.55	75.0
ϵ	94.27	18.22	669.2	3.64	450

By formulating the problem in this way, the designer then has all of the information visually available to make his or her decision easier. There are a few important points to note from the data in Table 43. The first point is that higher turbine inlet temperatures and lower PTMS heat loads achieve more favorable exhaust temperatures. Also, for a specific turbine inlet temperature and heat load combination, there is an optimal overall pressure ratio for minimum exhaust temperature. One limit to high values of the engine design parameters is the production cost; it is important to realize that the δ case lies right at the edge of the constraint, while both γ and ϵ are too expensive. This is because the γ case has a relatively high overall pressure ratio and the ϵ case has a high value for both turbine inlet temperature and PTMS heat load.

It is important to realize that all of the pertinent information is also present in the irreversibility distribution plots. First, the overall exergy destruction is directly related to the system fuel burn as shown previously. Secondly, the PTMS heat load has a substantial effect on the allocation of the TMS irreversibility and the power turbine irreversibility in particular. As a result, the TMS distribution can be used as a surrogate for the PTMS heat load as shown in Fig. 111. Finally, the exhaust temperature, which is one of the most important tradeoffs in this example, is directly related to the exergy destruction in the exhaust waste heat. This correspondence is demonstrated in Table 43 and illustrated in Fig. 112.

7.7.2 Using the Irreversibility Allocation to Make Designs More Robust to Future Requirements

Now a second use case is shown to highlight an additional benefit of directly characterizing and allocating the component irreversibility. In this case, it is shown that the differing irreversibility distributions of the various designs can impact future design requirements. As a means of highlighting this fact, consider the options in Table 44.

This table features four different choices to improve the system performance; in addition to the listed performance change, there is also a cost associated with the implementation of each option.

Table 44: Options for Cooling Requirements Exploration Use Case Example.

Option #1:	
Compressor Material Improvement	
Additional Cost	$1.00M
HPC Efficiency Change	+3%
Option #2:	
Fuel Temperature Limit Increase	
Additional Cost	$750K
Fuel Temperature Change	+7%
Option #3:	
Decreased Cockpit Cooling Needs	
Additional Cost	$250K
Mass Flow Rate Change	-5%
Option #4:	
Turbine Material Improvement	
Additional Cost	$500K
Allowable T4 Change	+2%

Traditional techniques in isolation can be used by the designer to reach a decision in regards to these options, but it is especially enlightening to examine the additional information gleaned from the irreversibility reallocations in response to these design changes. Figures 113-115 do just that; they examine the distributions for these four different designs and highlight this important fact. As seen in these figures, Option #1 results in a large decrease in exergy destruction in the high pressure compressor component and due to the resulting interactions also has the largest decrease in system exergy destruction of the four options by far. The drawback of this option is its high implementation cost. Next, Option #2 results in a fairly substantial improvement as well for a reduced cost. An important feature of this option, which focusing on achieving the higher fuel temperature, is its large impact on the TMS irreversibility. The reduction in irreversibility for this specific subsystem can be an

important consideration due to its potential to affect future design decisions. This single reduction at the present time can have a multiplying effect in the future as thermal design requirements change. The third case, although featuring a 5% reduction in the cockpit mass flow requirement, has a minimal effect on the overall system's irreversibility distribution; however, its implementation cost is also smaller than the others. Finally, like Option #2, the final option has a substantial effect on a specific segment of the system, in this case the wasted kinetic energy of the exhaust. It also achieves a reasonable reduction in system-level exergy destruction for a moderate cost.

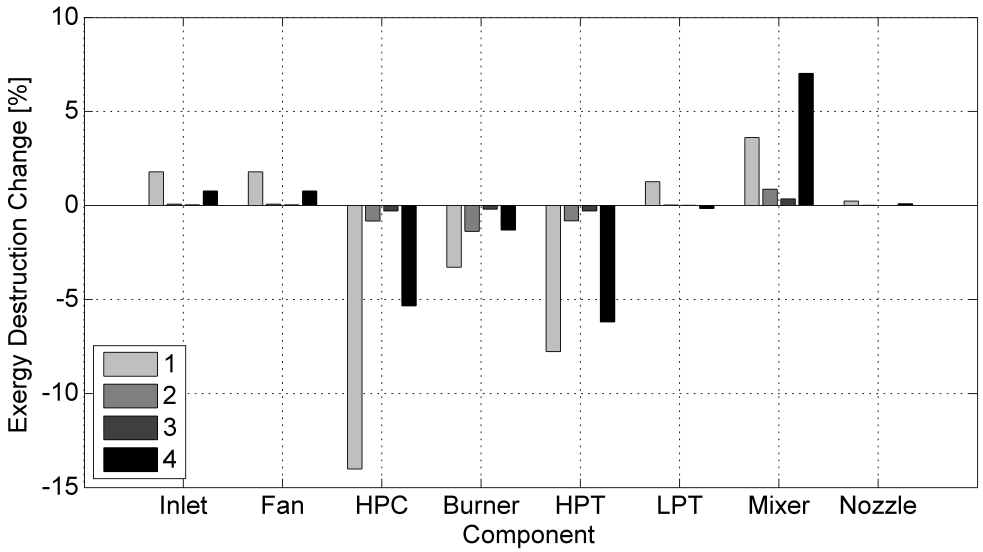

Figure 113: Changes in Engine Irreversibility Allocation for Improvement Options.

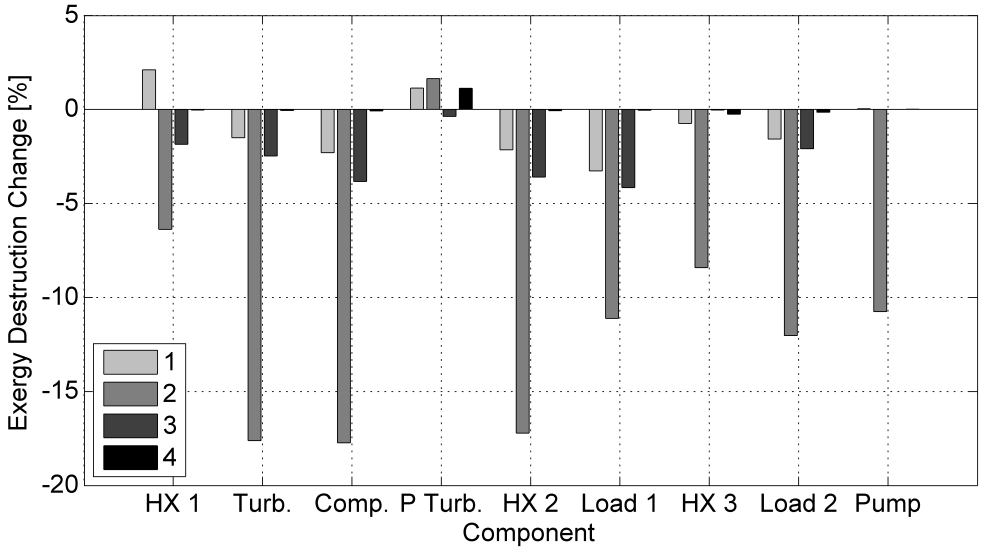

Figure 114: Changes in TMS Irreversibility Allocation for Improvement Options.

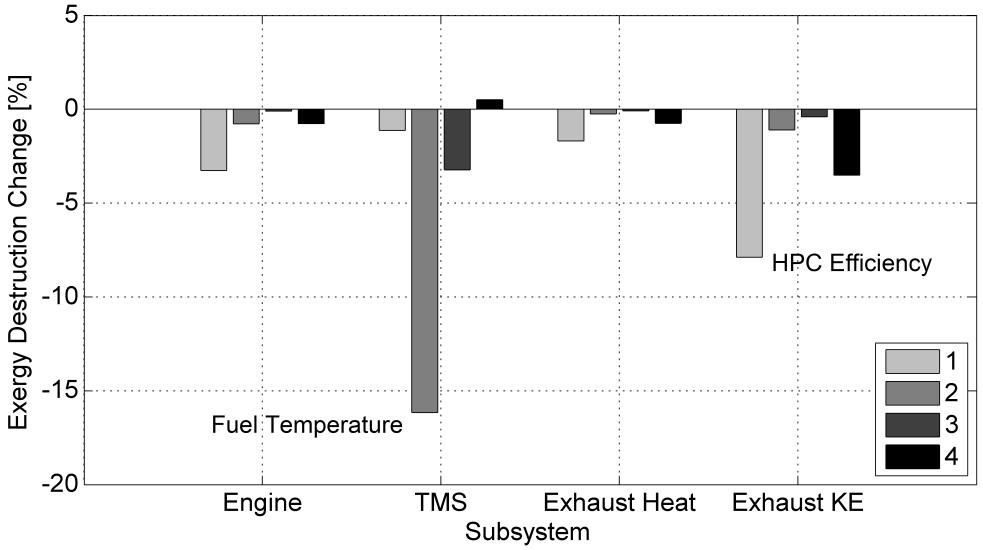

Figure 115: Changes in System Irreversibility Allocation for Improvement Options.

7.7.3 Improved Designer Decision Making

The additional information from the irreversibility allocation directly improves the decision making process for the propulsion systems designer by highlighting the relationships between the system losses and design decisions. As shown earlier, one of the important differences between the irreversibility allocation approach and simply using the overall fuel burn is that the designer can now see how the losses move around the system at the various design points.

The irreversibility distributions can also clearly denote multiple design tradeoffs simultaneously as shown in the first use case that dealt with the thermal sensitivities. There it was shown that the overall fuel burn, exhaust temperature, PTMS cooling requirements, and engine design parameters were all clearly visualized in the distributions for the five different design points. Then, the cooling requirements exploration use case demonstrated the additional capability of allowing the designer to consider the irreversibility allocation's impact on future design requirements. For example, a change in the fuel temperature requirement affected the irreversibility distribution by reducing it in the manner shown previously in Fig. 114. This new distribution shifts the losses towards the PTMS air cycle loop, which means that a change in the PTMS compressor and turbine performance or a new cooling requirement in the future can now have a larger effect on the performance of the overall performance in this new configuration.

7.8 Summary of Irreversibility Allocation

As this last experiment has shown, the principle benefit of approaching integrated propulsion and thermal management systems design as a process of directly allocating unavoidable irreversibility is the absolute and consistent illustration of the inherent tradeoffs between thermodynamic losses, cost, and performance. The problem with the direct application of a numerical optimizer to the combined metric is that it masks

these important factors. Although the same solutions existed in that case, they were buried under complexity and unapparent to the system-level designer.

The irreversibility allocation option is also especially enlightening because it makes no assumptions regarding the relative importance of the various metrics. This is useful for the engineer because it is most illustrative of the possible design choices. Instead of arriving at a single design point through a plethora of assumptions, the allocation approach allows the designer to clearly visualize the entire trade space and identify numerous "optimal" allocations. This allows the designer to better tradeoff and satisfy requirements at the system-level in regards to performance and cost.

CHAPTER VIII

CONCLUSIONS AND FUTURE WORK

Increasing thermal loads require a greater emphasis on the integrated performance of aircraft propulsion and thermal management systems during the conceptual design of the gas turbine engine to ensure that the requirements are satisfied. This work investigates the integrated system performance through thermodynamic modeling and simulation with a particular focus on directly characterizing the individual component losses throughout the system.

An integrated model and simulation environment for a canonical aircraft propulsion and thermal management system was created to investigate the system irreversibility distribution. This model was created entirely from first principles and is meant to capture all of the salient aspects of a typical system. It contains a combination of the first and second laws of thermodynamics as a means of directly characterizing the irreversibility in terms of exergy destruction. The characterization of the integrated system in terms of component irreversibility allows for a consistent and absolute measure of overall performance that can aid in these tradeoffs and lead to the design of an improved engine cycle.

This proper allocation of the irreversibility throughout the integrated system was then considered at length. First, it was shown that cost and performance must also be taken into account during the allocation process. Cost formulations and mission performance capabilities were implemented within the modeling and simulation environment. Then, the direct allocation of irreversibility with the simultaneous consideration of cost and performance was compared to a numerical system-level optimization approach to assess its benefits.

8.1 Experiments Revisited and Discussion of Results

Chapter III through VII outlined the entire experimental plan for this study. The sequence of experiments tested each individual aspect of the allocation approach in order to build up to the final objective: a technique for directly allocating irreversibility to the integrated propulsion and thermal management system in the context of cost and performance considerations.

8.1.1 Experiment 1a: Integrated Propulsion Systems Design

The first experiment laid the foundation for the entire effort by making the case for integrated propulsion and thermal management systems design. It was shown that as the complexity and challenges of thermal management systems design increases, it must be taken into account during the conceptual design of the jet engine. This was done through the integrated modeling and simulation of the propulsion and thermal management systems. The results of the first experiment showed that the thermal management requirements could actually impact the selection of propulsion systems design parameters. Additionally, it was seen that the interactions between the two systems continued to rise as the thermal load requirement was increased.

8.1.2 Experiment 1b: Irreversibility Characterization

The second experiment directly confronted the irreversibility characterization concept and demonstrated its ability to absolutely and consistently partition the system losses amongst the individual components. Although the results followed those obtained with the first-law, the characterization of the integrated system losses in terms of second-law metrics was shown to enable the designer to observe the propulsion and thermal management interactions much more clearly. Although the losses in the propulsion system were significantly larger than those in the thermal management system, it was shown that changes in the thermal management system design could affect the propulsion system losses.

8.1.3 Experiment 2a: Cost Formulation

This experiment then investigated the first of two additional metrics that were identified as important players in the irreversibility allocation. The formulation related the design parameters to component weights, which then enabled a build-up of the system-level weight. This system weight was then related to the production cost through a cost estimating relationship. It was shown that the cost results were often in opposition to the thermodynamic losses, since increases in efficiency usually require capital expenditures. As a result, it was determined that the systems designer must take cost into account along with the irreversibility characterization to determine the economics associated with a reduction in exergy destruction.

8.1.4 Experiment 2b: Mission Performance Considerations

In a similar manner, this experiment then investigated the second additional metric needed for the irreversibility allocation: mission performance. It was shown that one of the major differences between aerospace power systems and the ground-based power systems, where thermoeconomics is traditionally applied, is the constantly changing operating conditions. Due to the unsteady nature of aircraft mission operations, the design point performance is not sufficient by itself and the mission must also factor into the design process. This is accomplished through the inclusion of a mission profile that is then used to relate vehicle performance, propulsion system design features, and thermal management temperature constraints.

8.1.5 Experiment 2c: Irreversibility Allocation

Finally, the process of allocating the irreversibility throughout the integrated system was investigated. This allocation was conducted by simultaneously considering the thermodynamics, cost, and mission performance. The first approach was to treat performance as a constraint, combine the fuel burn and production cost into an overall cost metric, and then conduct a system-level optimization to search for the proper

distribution of the losses. Although this provided some useful information, it also presented problems since the exact cost information is unknown and the treatment of an overall cost as a single evaluation criterion masks many of the benefits of the second-law-based formulation. As an alternative, the direct allocation of irreversibility in the context of cost and performance was investigated. This was conducted using an economic approach to address the problem by treating the irreversibility as the system currency, which can then be used by the designer to buy improvements in performance. The benefit to this approach is that it provides the designer with a transparent metric to perform quick allocation trade studies, while also visualizing the cost and performance repercussions of allocation decisions. At the conclusion of the final experiment, two use cases were then presented to showcase the power of the irreversibility allocation approach in helping the designer meet the system-level requirements.

8.2 Limitations of Current Research and Suggestions for Future Work

During the course of this research several different paths for future research were identified. These include the consideration of transient effects, investigation of additional architectures and subsystems, model order reduction to enable higher-fidelity simulations, and architecture uncertainty. These areas are discussed in greater detail in the following sections to aid future researchers wishing to continue in the direction of this research.

8.2.1 Investigation of Transient System Interactions

An important element in the study of propulsion and thermal management systems design is the investigation of their transient responses. As the interconnectivity and complexity of aircraft subsystems increases, so does the importance of considering dynamic effects therein. As an example, consider the effect of the *on-demand* nature of

the more electric subsystems. When one of these electrical loads is suddenly switched on, this results in an increase in electrical power demand from the generator. The generator power is created from an increase in power extraction from the engine shaft and a change in engine performance. None of these events are instantaneous, and they require some duration of time to react. There can be negative consequences of these events such as changes in available thrust, engine stall, or voltage transients [42].

Previous research has demonstrated the need to capture the transients that the system experiences during particular events [102, 139, 101]. Transient, time-domain models are required to properly simulate these interactions during the integrated engine design efforts. This research has concentrated on steady-state physics to prevent further complications from masking the essential effects; however, an important extension of this work is its application to transient simulations.

8.2.2 Investigation of Additional Architectures and Subsystems

Another limitation of this research is the use of simplified and canonical subsystem model abstractions. This has the benefit of clearly demonstrating the irreversibility allocation approach in an academic environment where industrial data was unavailable. However, through the utilization of higher fidelity models of irreversibility, cost, and performance, more meaningful results could be obtained.

In addition, this work has intentionally focused on the propulsion and thermal management systems in isolation to clearly illustrate the improved capability. Nevertheless, once the process is better refined, it should be expanded to include other systems, such as electrical, hydraulic, pneumatic, and flight controls.

8.2.3 Utilizing Higher Fidelity Simulations through Model Order Reduction

If the subsystem models are upgraded to include higher-fidelity, dynamic analyses, then the resulting simulation can become complex and have the effect of masking the most important contributors to the system design. Model order reduction has been identified as an appropriate approach to more clearly simulate the important integrated subsystem effects, while still retaining the required physics and time-domain behavior. It is important to identify the subsystem analyses that have the largest influence on the design of the propulsion system, and it is necessary to clearly and rapidly visualize the interactions between the propulsion and thermal management systems to focus on the pertinent subsystem characteristics.

Model order reduction methods are different from traditional surrogate modeling techniques as they preserve the physical representation of the system. These techniques are frequently used in the control systems design field to simplify plant models. Model order reduction techniques have also been applied to power [36, 54] and thermal simulations [5]. Essentially, the ordinary differential equations that represent the physical system are reduced to a smaller number of equations by extracting only the essential information from the model in order for it to serve its purpose. These reduced models must retain the dynamic characteristics of the original system within an "admissible error" [6]. Schilders summarizes model order reduction "as the task of reducing the dimension of the state space vector, while preserving the character of the input-output relations" [150].

Model order reduction methods have been shown to be beneficial in many types of large scale finite element analyses [2]. They have also been implemented in many

aspects of aerospace design, particularly computational fluid dynamics [71] and aeroelastic simulations [96]. Although they are usually constrained to these types of high-fidelity modeling efforts, there has also been significant research recently in the application of model order reduction to object-oriented modeling environments similar to those that have been created for the current research.

8.2.4 Accounting for Architecture Uncertainty

Future research in integrated propulsion systems design should address the impact of changes to the system architecture as well. Usually the system-level models are created for a specific baseline architecture, as was the case for this study. The capability of examining various system architectures, especially in regards to thermal management, is necessary to conduct the appropriate architecture trade studies. Therefore, it was determined that a systematic and rapid approach is needed to better trade off these architecture modifications.

The field of probabilistics has the potential of providing a solution to this problem. This use of probabilistics within the aerospace design community has become widespread [7, 47]. Probabilistic design has also been used in the design of a thermal management system [135] and a hypersonic thermal protection system, which are directly relevant to this research [122].

Although probabilistic methods are a well established way to systematically account for uncertainty, the application to architecture uncertainty is somewhat more complicated. The key difference and the critical challenge when addressing architecture uncertainty is that probability distributions cannot be directly applied to the integrated model. This is because a change in architecture requires a physical change to the layout of the system. For example, if it was desired to compare a vapor cycle cooling approach to an air cycle, the designer would need to go into the modeling

environment, swap out the components, and reconfigure the system for the new components. This type of approach would then need to be applied for every architecture change. As a result, architecture decisions are normally made through subjective techniques such as a morphological matrix [4, 46]. This could be more deeply investigated using probabilistic design techniques to yield additional information for the designer at the expense of additional time and complexity.

8.3 Summary of Research Contributions

The contributions of this research to the state-of-the-art are now summarized here:

- Methodology to better satisfy system-level requirements through the characterization of the system irreversibility distribution
- Conceptual propulsion systems design in the context of thermal management challenges
- Integrated propulsion and thermal management modeling and simulation, including both on-design (parametric) and off-design (performance) capabilities
- Application of thermoeconomic principles to aerospace vehicles
- Posing of aircraft engine design effort in irreversibility allocation terms
- Investigation of optimal solutions to the system-level irreversibility allocation problem
- Economic formulation of irreversibility allocation while concurrently considering cost and vehicle mission performance

8.4 Final Thoughts

This research grew out of the observation that higher heat loads in future aircraft and the resulting thermal challenges require that the propulsion and thermal management systems no longer be designed in isolation. The investigation of their integrated performance during the conceptual design process is necessary for the designer to better meet the system requirements. The present research demonstrated the benefit of integrated modeling and simulation in this context and specifically showed that vehicle-level thermal performance requirements can affect the design of the propulsion system.

The major focus of this research was the irreversibility characterization and the subsequent investigation of its optimal allocation. It was shown that the characterization of the system in terms of component exergy destruction enables the designer to quickly obtain an absolute and consistent view of the system losses. This is important because it essentially allows the total fuel consumption to be partitioned accordingly across the system to aid the designer in his decision-making with regards to system improvement. One problem with this approach, however, is that it does not explicitly account for non-thermodynamic criteria, such as cost or mission performance considerations.

The concurrent consideration of thermodynamics, cost, and mission performance was then shown to be a solution to this, but this is a challenge in its own right. Traditional system-level optimization was examined as one possible way to address this, but there are two major faults with this approach. First, this requires that the performance serve as a constraint and the fuel burn and cost be combined into a single objective function. This poses the problem of determining the relative importance of the production and operating costs, which greatly affects the final optimum, and it does not allow the designer to actively trade off the performance requirements. The second problem is that this approach also masks the most important benefit of the

irreversibility characterization: the ability to absolutely and consistently partition the losses.

Instead, it was shown that giving the designer the freedom to directly allocate the losses within the system in the context of cost and performance was much more effective. The specific approach described here was to pose the problem in economic terms by treating the exergy destruction as a true common currency to barter for improved efficiency, cost, and performance. This allowed the designer to quickly and clearly visualize the impact of her choices on the losses throughout the system. By treating the decision making process as a task of directly allocating the irreversibility to the various components, the propulsion systems designer is able to gain a deeper understanding of the important relationships between the system losses and the design requirements; the designer can then also see how the losses move around the system and settle into different equilibria at the various design points. The overall result and final takeaway of this work is that the additional information obtained from the irreversibility distributions can then aid the designer in better satisfying the system-level requirements.

APPENDIX A

TACTICAL FIGHTER MODELING ENVIRONMENT

As discussed in Chapter III, the development of the system-level modeling and simulation environment used in this research was based on two previous efforts by the author. It is useful to examine these in more detail here to better explain the modeling foundation for this research. The first, the tactical fighter model, is discussed in greater detail here; the second, the generic tip-to-tail, is discussed in Appendix B.

The integrated modeling and simulation environment of the tactical fighter modeling environment was published by Maser, Garcia, and Mavris in [102]. This simulation includes subsystem models of propulsion, power, and thermal management subsystems that are integrated together and linked to an air vehicle model, a mission profile, and a system controller. All of this work was conducted in Simulink with the exception of the engine model, which is in NPSS. An overview of the system-level tactical fighter model is shown in Fig. 116. In this integrated model, propulsion, power, and thermal management subsystem models are included and integrated together with an air vehicle model and mission profile [102].

As shown in the figure, there are six subsystem level blocks contained within the Simulink model. Starting at the upper left of Fig. 116 is the yellow Mission Profile block. This block handles all of the mission level data for the simulation and passes it to the other subsystems at each time step. Progressing to the right of the Mission Profile block is the blue Air Vehicle model. This block keeps track of important vehicle parameters such as weight, drag, and lift. Additionally, this subsystem uses an energy balance to determine the thrust required for the vehicle to operate throughout the flight envelope.

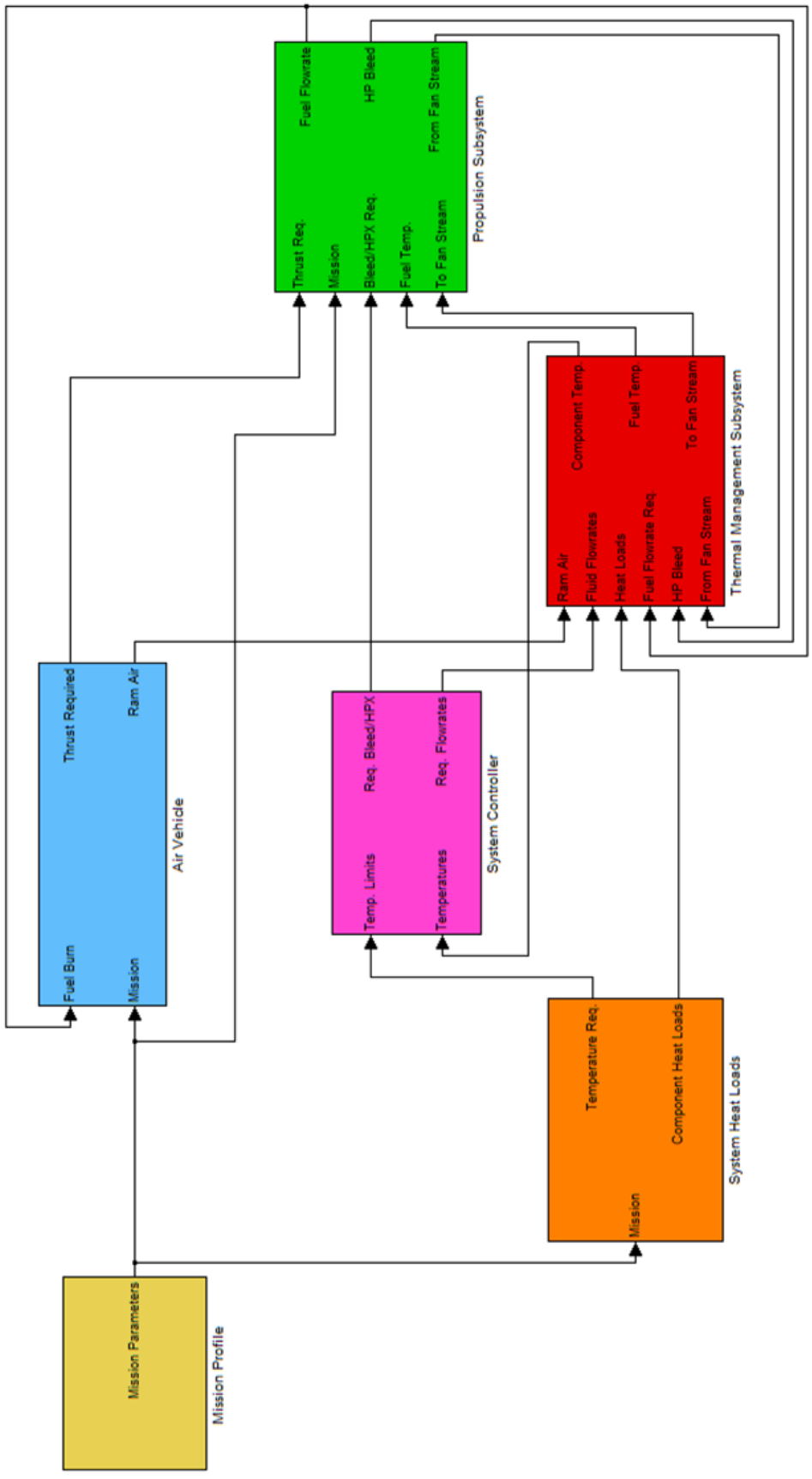

Figure 116: Integrated-System Level Model [102].

Continuing in a clockwise fashion around the model brings one to the green Propulsion Subsystem model. This block is responsible for calculating the engine thrust and fuel burn throughout the mission. This is accomplished using information from both the mission profile and air vehicle as well as important information from the Thermal Management Subsystem (TMS) model, which is represented as the red block within Simulink. There are several important and intimate connections between the propulsion subsystem and TMS in the model. This is particularly important since shaft power extraction and compressor bleed requirements from the thermal management system affect the engine performance. The final blocks illustrated in the system-level model are the System Heat Loads block, which is colored orange, and the System Controller, which is colored magenta. The Systems Heat Loads block keeps track of the heat loads and temperature requirements of the various components over the mission profile. The System Controller uses this temperature information to control the propulsion and thermal management systems throughout the mission.

A.1 Propulsion Subsystem

The propulsion subsystem model is represented as the green block in the system-level Simulink model on the right of Fig. 116. However, the actual engine is modeled separately using the NPSS software. NPSS is the industry standard gas turbine cycle analysis software and has many capabilities in the domain of engine component modeling in addition to a very robust solver. This NPSS engine model is then directly linked to the Simulink model in order to enable its seamless functionality in the system-level simulation. It was decided to model the engine in NPSS due to the complexities of engine performance modeling and its on-design sizing and off-design performance capabilities. Additionally, it was important to model the engine at a high fidelity since there is such a great amount of interaction between the engine and TMS.

The propulsion subsystem model is illustrated in Fig. 117. This Simulink model is responsible for enabling the proper communication between NPSS and Simulink and for controlling the fuel flow rate. This fuel control is accomplished by first converting the thrust demand from the air vehicle into a required HP shaft speed. The actual speed of the HP shaft of the transient engine model is then tracked by the engine FADEC and is used to adjust the fuel flow rate. The LP shaft speed imposes limits on the fuel flow rate in order to maintain a proper compressor surge margin.

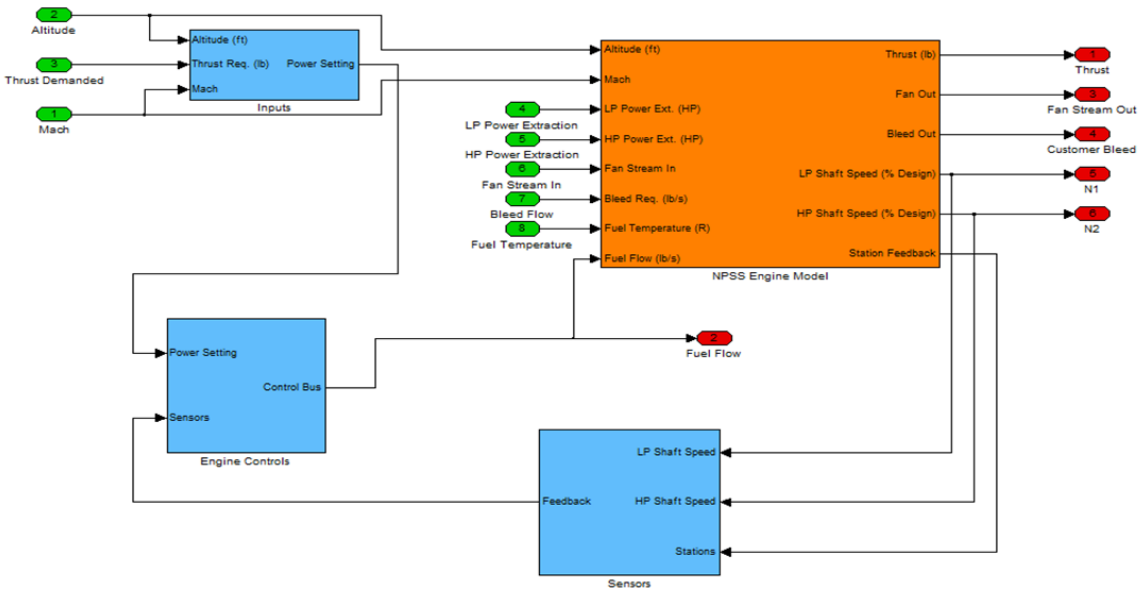

Figure 117: Propulsion Subsystem Model [102].

A.2 NPSS Engine Model

The engine model represents the transient performance of a twin-spool mixed-flow turbofan (MFTF) engine and is composed entirely of public domain data. The NPSS component level model of the engine is illustrated in Fig. 118 using the NPSS visual based syntax.

This model includes HPC, HPT, and LPT size effects, technology levels, component Reynolds effects, turbine cooling flows and leakages, compressor loading, and variable nozzle areas. In addition, cooled cooling air technology is modeled by utilizing a heat exchanger to cool the compressor discharge air with the fan bypass duct.

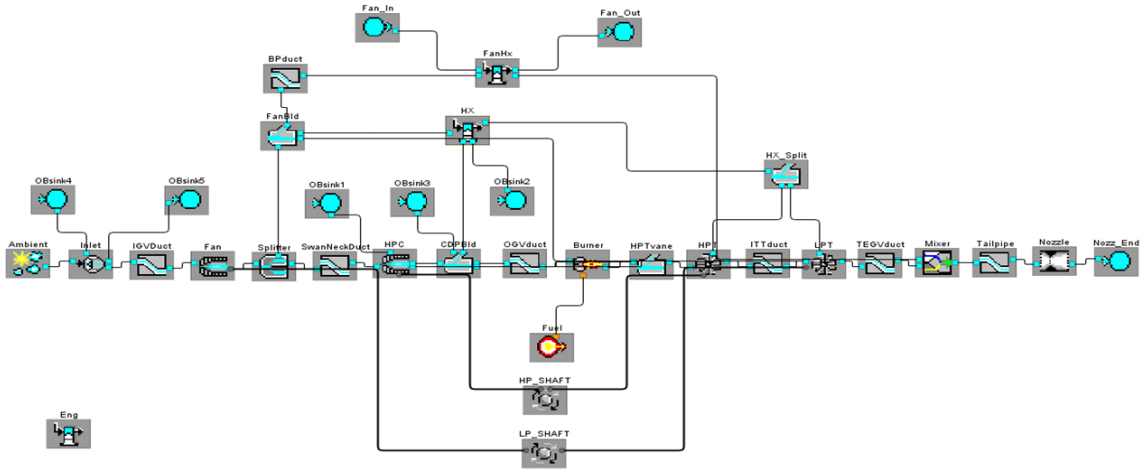

Figure 118: NPSS Engine Model Schematic [102].

A.3 Tactical Fighter Example System Temperature Results

Figures 119 and 120 illustrate results along the fan stream of the integrated tactical fighter simulation. These results are included to help illustrate the type of information that is available from the simulation.

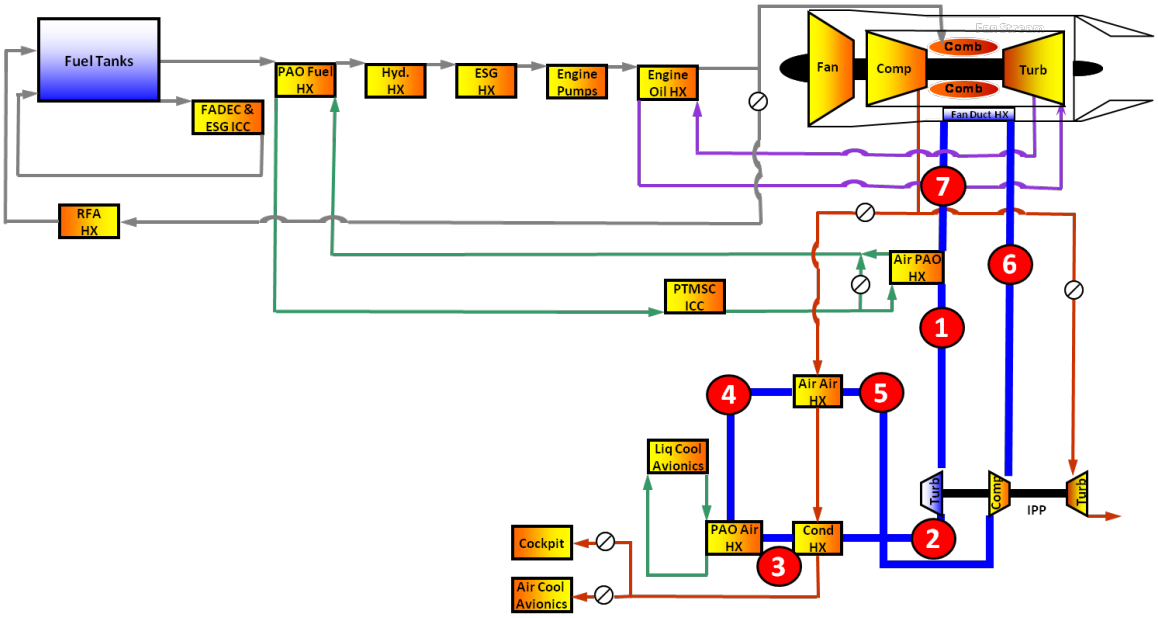

Figure 119: Tactical Fighter Fan Stream Temperature Locations [102].

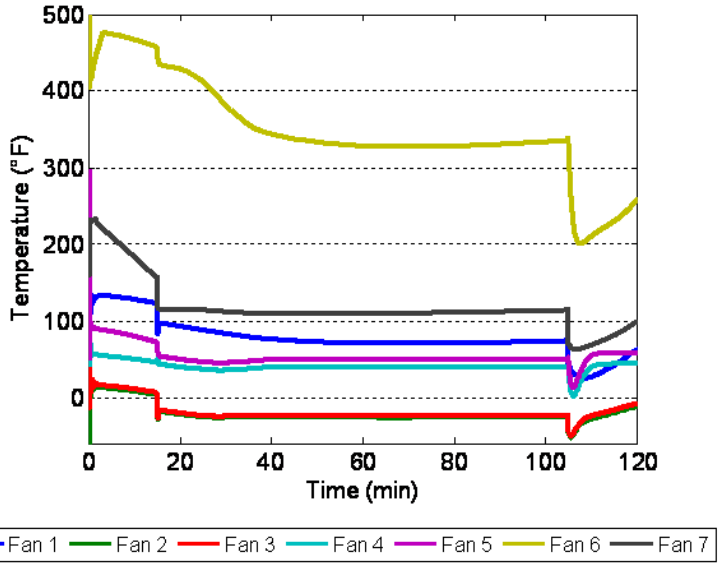

Figure 120: Tactical Fighter Temperatures over Mission [102].

APPENDIX B

GENERIC TIP-TO-TAIL MODELING ENVIRONMENT

The system-level tactical fighter model developed by Maser, Garcia, and Mavris and discussed in Appendix A was later transitioned into a more-capable generic tip-to-tail aircraft model. This generic model leveraged elements of both the tactical fighter model as well as subsystem models previously created by researchers at AFRL. This work was published by Roberts, Eastbourn, and Maser in [139].

The integrated tip-to-tail model was created by using the tactical fighter model as a baseline and then upgrading various subsystem elements. Additionally, the system-level model was reorganized to make it more user-friendly and to better match modeling standards previously developed at AFRL. Significant upgrades to the fuel and power thermal management subsystems and the air vehicle were also made. Physics-based models of the engine oil, fuel pump, oil pump, and generator components were created in order to better estimate these heat loads. Also, a more-detailed model of the vehicle fuel tanks was included. An improved control system was developed to measure various temperatures throughout the system and then use this information to adjust several control valves. By adjusting these flow rates, it was possible to maintain all of the system components at their appropriate temperatures. The one drawback with respect to the tip-to-tail model is the engine. This model does not contain an on-design capability, which makes resizing and cycle modification very difficult.

The generic tip-to-tail model is shown in Fig. 121. As seen in this model overview, there are seven different subsystem blocks present. The two red blocks are the Fuel and Power Thermal Management Systems (FTMS and PTMS) and are an upgraded

version of the tactical fighter thermal management system that was previously discussed. The two orange blocks, the Robust Electrical Power System and the High Performance Electric Actuation System are simply a reorganized version of the System Heat Loads block from the tactical fighter model. The green Engine block and the blue Air Vehicle System block are more-capable AFRL models that have been incorporated and are discussed in more detail in the next section.

Finally, the magenta System Controller block is an upgraded version of the previously discussed System Controller and includes all of the controllers needed to operate the thermal management systems and the Integrated Power Package (IPP). The inclusion of the AFRL vehicle and engine models greatly improved the fidelity of the system-level simulation. The other significant upgrades to the system-level model focused on the PTMS and FTMS models. A high-fidelity, transient model of the Integrated Power Pack (IPP) was created and integrated into the PTMS model. The PTMS model was also refined in order to include better dynamics and higher-fidelity heat exchangers. Finally, the volume dynamics at the engine and PTMS interfaces were included in order to achieve proper model convergence and performance. The FTMS model was greatly enhanced by including higher-fidelity fuel tank models and including the proper fuel tank drain sequencing. Additionally, the FTMS model was upgraded to include physics-based engine oil and fuel pump components in place of the previous lookup tables.

An integrated control scheme was developed for the tip-to-tail model and it was shown to be capable of maintaining all of the appropriate component temperatures. Once completed, the generic tip-to-tail thermal model was exercised over the course of a notional mission profile.

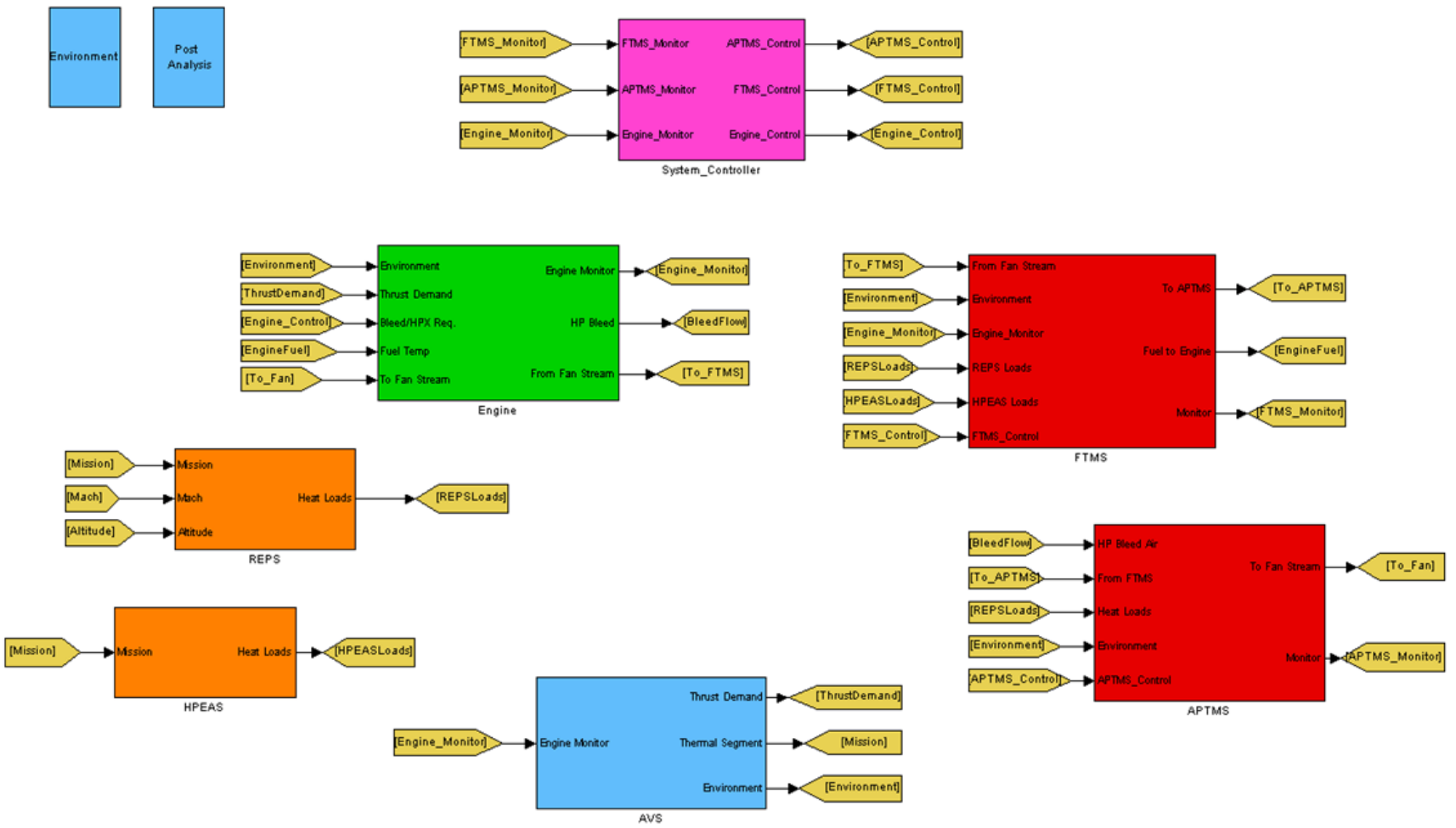

Figure 121: Overview of Generic Tip-to-Tail Model.

B.1 Tip-to-Tail Engine Model

The engine model was developed by AFRL from previous work [112]. The model is completely built in Simulink and rated at 20,000 lb thrust class. The model represents the performance of a twin-spool low bypass turbofan engine. A lumped element approach is used to represent each component of the engine. This enables the model to be very modular and easily modifiable. The model syntax is similar to the standard adopted by NPSS. A generic, previously published version of the engine model is shown in Fig. 122.

Each of the individual components is physics-based and enforces the conservation of mass, momentum, and energy. Although the compressor, fan, and turbine turbomachinery components may contain multiple physical stages, they are modeled as single elements and rely on performance maps. Transient inertial effects are included in the engine shaft components that are used within the complete engine model. All other components are assumed to be zero-dimensional and quasi-steady-state. However, there is also a transfer function on the fuel flow rate in order to simulate the lag in the fuel pump.

The engine model is equipped with its own controls that modulate fuel flow to meet a demanded thrust. The model does this by first mapping the required thrust to an engine power setting level and then to a high-pressure (HP) spool rotational speed. A simple feedback controller is then used to vary the fuel flow rate to obtain this HP rotational speed. Additionally, there are limits in place to restrict the low-pressure (LP) rotational speed in order to retain the necessary compressor surge margin. A generic, dynamic propulsion system model was later developed by Eastbourn in [52] that allows for much faster integrated model execution.

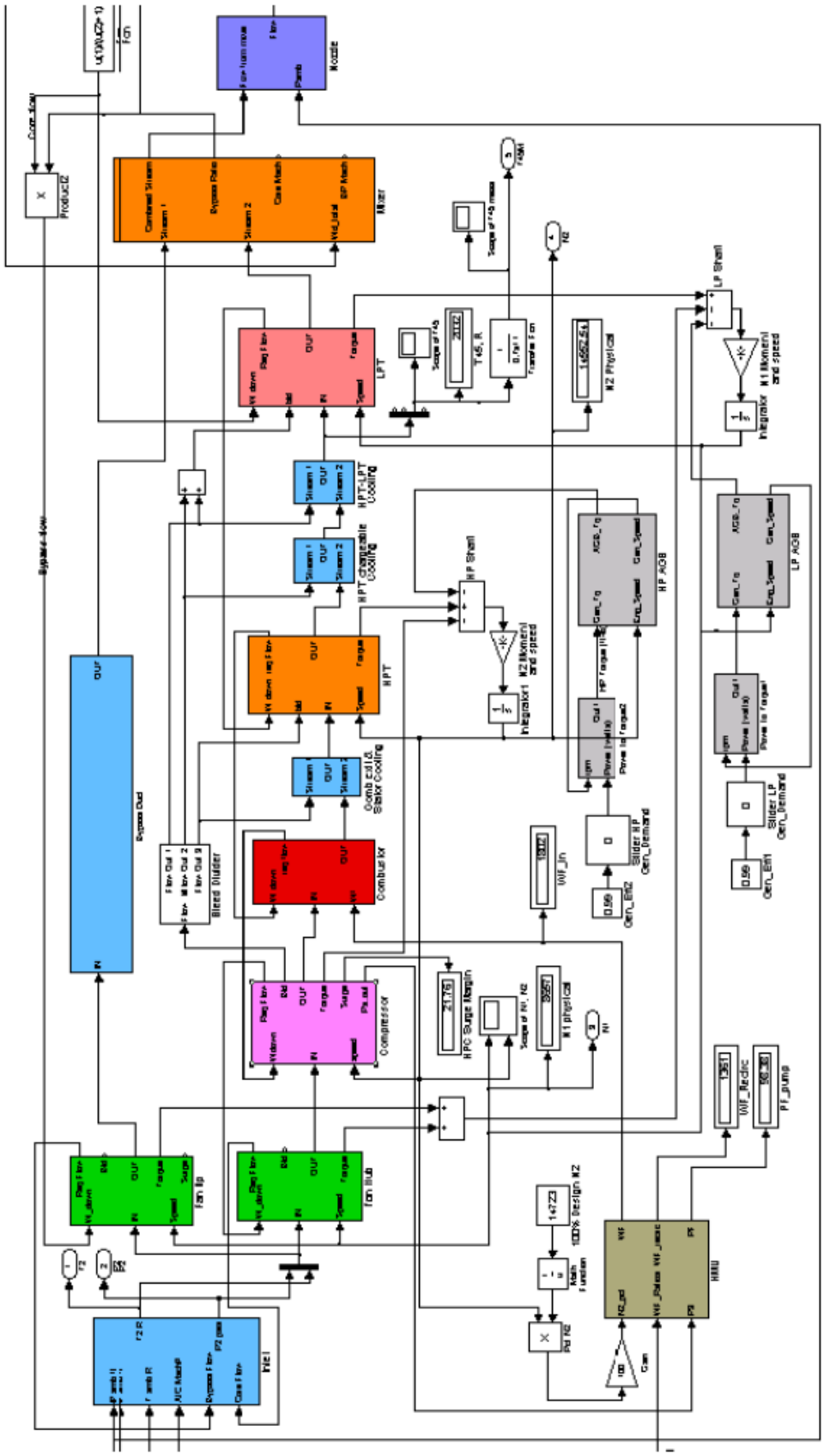

Figure 122: Generic Simulink Engine Model [112].

B.2 Tip-to-Tail Vehicle Model

The air vehicle model was developed by AFRL from previous work [25]. The model is completely built in Simulink for a long range strike vehicle. At the heart of the AVS model is the numerical integration of the six degrees-of-freedom equations of motion:

$$\vec{F}_b = \begin{bmatrix} F_x \\ F_y \\ F_z \end{bmatrix} = m\left(\dot{\vec{V}}_b + \vec{\omega} \times \vec{V}_b\right) + \dot{m}\vec{V}_b \tag{141}$$

$$\vec{M}_b = \begin{bmatrix} L \\ M \\ N \end{bmatrix} = I\dot{\vec{\omega}} + \vec{\omega} \times (I\vec{\omega}) + \dot{I}\vec{\omega} \tag{142}$$

where $\vec{F}_b$ represents the force vector, $\vec{M}_b$ the moment vector, $\vec{\omega}$ the rotational velocity, and I the moment of inertia.

Aircraft weight, inertia, and centers of gravity are constantly updated throughout the flight. The aerodynamics are included in the form of lookup tables and were created from a previously developed aerodynamic database. A diagram of the aircraft plant and its associated controls is shown in Fig. 123.

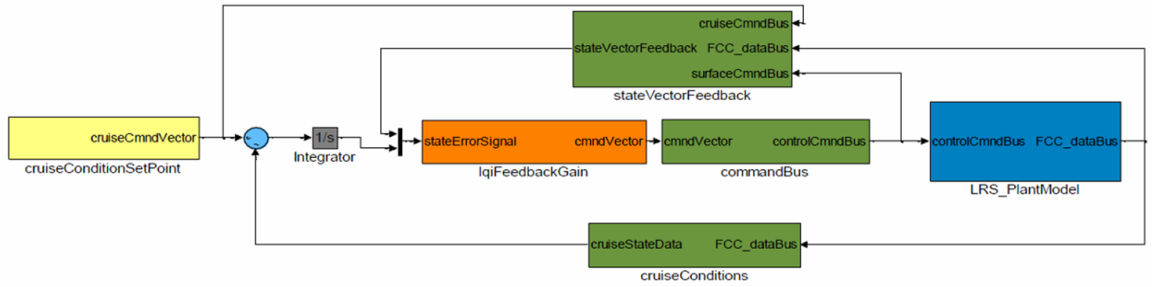

Figure 123: Simulink Vehicle Model and Controls [25].

The mission profile required for AVS operation is input as a series of Mach and altitude waypoints. The AVS model is equipped with its own controls that then modulate the control surfaces and calculate a thrust demand needed to fly the predefined flight profile. The feedback gains required for the controller are properly scheduled throughout the mission as a function of weight and dynamic pressure.

REFERENCES

[1] Ahern, J. E., "Thermal Management of Air-Breathing Propulsion Systems," in *AIAA Paper*, AIAA, 1992.

[2] Amsallem, D. and Farhatbui, C., "Interpolation Method for Adapting Reduced-Order Models and Application to Aeroelasticity," *AIAA Journal*, vol. 46, pp. 1803–1813, Jul 2008.

[3] Arce, D. F. R., "A Decomposition Strategy Based on Thermoeconomic Isolation Applied to the Optimal Synthesis/Design and Operation of an Advanced Fighter Aircraft System," Master's thesis, Virginia Polytechnic Institute and State University, 2003.

[4] Armstrong, M., "A Process for Function Based Architecture Definition and Modeling," Master's thesis, Georgia Institute of Technology, Apr 2008.

[5] Augustin, A., Hauck, T., Maj, B., Czernohorsky, J., Rudnyi, E., and Korvink, J., "Model Reduction for Power Electronics Systems with Multiple Heat Sources," tech. rep., Freescale Semiconductor, 2006.

[6] Bai, Z. and Skoogh, D., "Krylov Subspace Techniques for Reduced-Order Modeling of Nonlinear Dynamical Systems," tech. rep., University of California, 2002.

[7] Bandte, O., *A Probabilistic Multi-Criteria Decision Making Technique for Conceptual and Preliminary Aerospace Systems Design.* PhD thesis, Georgia Institute of Technology, Sep 2000.

[8] Barrett, M. J. and Johnson, P. K., "Performance and Mass Modeling Subtleties in Closed-Brayton-Cycle Space Power Systems," in *AIAA Paper*, Glenn Research Center and Analex Corporation, AIAA, 2005. NASA/TM2005-213985.

[9] Bartel, M. and Young, T. M., "Simplified Thrust and Fuel Consumption Models for Modern Two-Shaft Turbofan Engines," *Journal of Aircraft*, vol. 45, pp. 1450–1456, Jul-Aug 2008.

[10] Bayraktar, I., "Time Dependent Simulation Methods for Vehicle Thermal Management," in *Ground Vehicle Systems Engineering and Technology Symposium (GVSETS)*, Oshkosh Corporation, 2009.

[11] Beam, J., "Heat Sink Options for a More Electric Aircraft Thermal Management System," in *SAE*, 1997.

[12] Bejan, A. and Haynsworth, P., "The Natural Design of Hierarchy: Basketball Versus Academics," *Int. J. of Design & Nature and Ecodynamics*, vol. 7, no. 1, pp. 14–25, 2012.

[13] Bejan, A., *Entropy Generation Minimization: The Method of Thermodynamic Optimization of Finite-Size Systems and Finite-Time Processes*. CRC Press, 1996.

[14] Bejan, A., *Advanced Engineering Thermodynamics*. John Wiley & Sons, Inc., 2nd ed., 1997.

[15] Bejan, A., "A Role for Exergy Analysis and Optimization in Aircraft Energy-System Design," in *Proceedings of the ASME Advanced Energy Systems Division*, 1999.

[16] Bejan, A., *Thermodynamic Optimization of Complex Energy Systems*. Kluwer Academic Publishers, 1999.

[17] Bejan, A., *Shape and Structure, from Engineering to Nature*. Cambridge University Press, 2000.

[18] Bejan, A., "Constructal Theory: Tree-Shaped Flows and Energy Systems for Aircraft," *Journal of Aircraft*, vol. 40, pp. 43–48, Jan-Feb 2003.

[19] Bejan, A., Jones, E. C., and Charles, J. D., "The Evolution of Speed in Athletics: Why the Fastest Runners are Black and Swimmers White," *Int. Journal of Design & Nature.*, vol. 5, no. 3, pp. 199–211, 2010.

[20] Berry, R., Kazakov, V., Sieniutycz, S., Szwast, Z., and Tsirlin, A., *Thermodynamic Optimization of Finite-Time Processes*. John Wiley & Sons, Ltd., 2000.

[21] Bevilaqua, P. M., "Joint Strike Fighter Dual-Cycle Propulsion System," *Journal of Propulsion and Power*, vol. 21, pp. 778–783, Sep-Oct 2005.

[22] Blanding, D., "Subsystem Design and Integration for the More Electric Aircraft," in *5th International Energy Conversion Engineering Conference and Exhibit (IECEC)*, (St. Louis, Missouri), Boeing Phantom Works, AIAA, 25 - 27 Jun 2007.

[23] Bodden, D., Eller, B., and Clements, S., "Integrated Electrical and Thermal Management Sub-system Optimization," in *SAE Power Systems Conference*, 2 Nov 2010.

[24] Bodie, M., "Power Thermal Management System Design for Enhanced Performance in an Aircraft Vehicle," in *SAE Power Systems Conference*, 2 Nov 2010.

[25] Bodie, M., Russell, G., McCarthy, K., Lucus, E., Zumberge, J., and Wolff, M., "Thermal Analysis of an Integrated Aircraft Model," in *48th AIAA Aerospace Sciences Meeting Including the New Horizons Forum and Aerospace Exposition*, (Orlando, Florida), PC Krause and Associates, Inc. and Air Force Research Laboratory, AIAA, 4 - 7 Jan 2010.

[26] Braun, R. D., Moore, A. A., and Kroo, I. M., "Collaborative Approach to Launch Vehicle Design," *Journal of Spacecraft and Rockets*, vol. 34, pp. 478–486, Jul-Aug 1997.

[27] Braun, R., Moore, A., and Kroo, I., "Use of the Collaborative Optimization Architecture for Launch Vehicle Design," in *AIAA Paper*, NASA Langley Research Center and Stanford University, AIAA, 1996.

[28] Braun, R., *Collaborative Optimization: An Architecture for Large-Scale Distributed Design*. PhD thesis, Stanford University, Jun 1996.

[29] Bretscher, O., *Linear Algebra with Applications*. Prentice Hall PTR, 2004.

[30] Brown, D., Squier, S., and Smith, G., "Integrated Thermal Energy (I-TEM) - An Evaluation Tool for Aircraft," in *SAE Paper*, 1993.

[31] Butzin, E. L., Johnson, P. K., and Creekmore, R. E., "Airframe Thermal Management System Modeling in NPSS," in *43rd AIAA/ASME/SAE/ASEE Joint Propulsion Conference & Exhibit*, (Cincinnati, OH), Wolverine Ventures, Inc., AIAA, 8 - 11 Jul 2007.

[32] Camberos, J. A., "Revised Interpretation of Work Potential in Thermophysical Processes," *Journal of Thermophysics and Heat Transfer*, vol. 14, pp. 177–185, Apr-Jun 2000.

[33] Camberos, J. A. and Moorhouse, D. J., *Exergy Analysis and Design Optimization for Aerospace Vehicles and Systems*. AIAA, 2011.

[34] Cengel, Y. and Boles, M., *Thermodynamics: An Engineering Approach*. McGraw-Hill, 2008.

[35] Chambers, R. G. and Quiggin, J., "Resource Allocation and Asset Pricing," tech. rep., The University of Maryland, College Park, 2002.

[36] Chaniotis, D. and Pai, M. A., "Model Reduction in Power Systems Using Krylov Subspace Methods," *IEEE Transactions on Power Systems*, vol. 20, pp. 888–894, May 2005.

[37] Chen, W.-Z., Lin, T., and Hill, B. P., "Thermal Modelling of a Flight-Critical Electrohydrostatic Actuator," in *SAE Paper*, 1995.

[38] Cipollone, R. and Villante, C., "Vehicle Thermal Management: A Model-Based Approach," in *Proceedings of ICEF04*, 24-27 Oct 2004.

[39] Cipollone, R. and Villante, C., "A Fully Transient Model for Advanced Engine Thermal Management," in *SAE Vehicle Thermal Management Systems Conference and Exhibition*, (Toronto Canada), SAE, May 10-12 2005.

[40] Clarke, J. M. and Horlock, J. H., "Availability and Propulsion," *Journal of Mechanical Engineering Science*, vol. 17, no. 4, pp. 223–232, 1975.

[41] Clough, J. A., Starkey, R. P., Lewis, M. J., and Lavelle, T. M., "Integrated Propulsion and Power Modeling for Bimodal Nuclear Thermal Rockets," in *43rd AIAA/ASME/SAE/ASEE Joint Propulsion Conference & Exhibit*, (Cincinnati, OH), University of Maryland and NASA Glenn Research Center, AIAA, 8 - 11 Jul 2007.

[42] Corbett, M., Lamm, P., McNichols, J., Boyd, M., and Wolff, M., "Effects of Transient Power Extraction on an Integrated Hardware-in-the-Loop Aircraft/Propulsion/Power System," in *SAE 2008 Power Systems Conference*, (Bellevue, Washington), Air Force Research Laboratory and PC Krause and Associates, Inc., SAE, 11-13 Nov 2008.

[43] Corbett, M. W., Lamm, P. T., Miller, K. L., Wolff, J. M., and Walters, E. A., "Transient Analysis of an Aircraft/Propulsion System with Hardware-in-the-Loop Power Extraction," in *43rd AIAA/ASME/SAE/ASEE Joint Propulsion Conference & Exhibit*, (Cincinnati, OH), Air Force Research Laboratory and PC Krause and Associates, Inc., AIAA, 8 - 11 Jul 2007.

[44] Corbett, M. W., Lamm, P. T., Owen, P. R., Phillips, S. D., Blackwelder, M. J., Alt, J. T., McNichols, J. M., Boyd, M. A., and Wolff, J. M., "Transient Turbine Engine Modeling with Hardware-in-the-Loop Power Extraction," in *6th International Energy Conversion Engineering Conference (IECEC)*, (Cleveland, Ohio), Air Force Research Laboratory and Rolls-Royce Corporation and PC Krause and Associates, Inc., AIAA, 28 - 30 Jul 2008.

[45] Dalton, J. S. and Behbahani, A., "An Integrated Approach to Conversion, Verification, Validation and Integrity of AFRL Generic Engine Model and Simulation," in *42nd AIAA/ASME/SAE/ASEE Joint Propulsion Conference & Exhibit*, (Sacramento, California), AVETeC Inc. and Air Force Research Laboratory, AIAA, 9 - 12 Jul 2006.

[46] de Tenorio, C., Armstrong, M., and Mavris, D., "Architecture Subsystem Sizing and Coordinated Optimization Methods," in *47th AIAA Aerospace Sciences Meeting Including The New Horizons Forum and Aerospace Exposition*, (Orlando, Florida), Georgia Institute of Technology, 5 - 8 Jan 2009.

[47] DeLaurentis, D. A., *A Probabilistic Approach to Aircraft Design Emphasizing Stability and Control Uncertainties*. PhD thesis, Georgia Institute of Technology, Nov 1998.

[48] Denbigh, K., *The Principles of Chemical Equilibrium*. Cambridge University Press, 1981.

[49] Denton, J., "Loss Mechanisms in Turbomachines," *Journal of Turbomachinery*, vol. 115, pp. 621–651, 1993.

[50] Dieter, G. E., *Engineering Design*. McGraw-Hill, 2000.

[51] Dincer, I. and Rosen, M. A., *Exergy: Energy, Environment and Sustainable Development*. Elsevier, 2007.

[52] Eastbourn, S. M. and Roberts, R. A., "Modeling and Simulation of a Dynamic Turbofan Engine Using Simulink," in *47th AIAA/ASME/SAE/ASEE Joint Propulsion Conference & Exhibit*, 2011.

[53] Eberth, J. F., Wagner, J. R., Afshar, B. A., and Foster, R. C., "Modeling and Validation of Automotive "Smart" Thermal Management System Architectures," in *SAE Paper*, 2004.

[54] El-Nahas, I. A., *Model Reduction Methods Applied to Power Systems*. PhD thesis, McMaster University, 1983.

[55] El-Sayed, Y. M., "Thermodynamics and Thermoeconomics," *International Journal of Applied Thermodynamics*, vol. 2, pp. 5–18, Mar 1999.

[56] El-Sayed, Y. M., *The Thermoeconomics of Energy Conversion*. Pergamon, 2003.

[57] Faleiro, L., "Beyond the More Electric Aircraft," tech. rep., Aerospace America, Sep 2005.

[58] Fang, R., Jiang, W., Monti, A., Zerby, M., Anderson, G., Bernotas, P., and Khan, J., "System-Level Dynamic Thermal Modeling and Simulation for an All-Electric Ship Cooling System in VTB," in *IEEE Paper*, pp. 462–469, University of South Carolina and Naval Surface Warfare Center, IEEE, 2007.

[59] Feldman, M., Lai, K., and Zhang, L., "The Proportional-Share Allocation Market for Computational Resources," *IEEE Transactions nn Parallel and Distributed Systems*, vol. 20, pp. 1075–1088, Aug 2009.

[60] Ferguson, D. F., Nikolaou, C., Sairamesh, J., and Yemini, Y., "Economic Models for Allocating Resources in Computer Systems," tech. rep., IBM T.J. Watson Research Center, 1996.

[61] Figliola, R. S., Tipton, R., and Li, H., "Exergy Approach to Decision-Based Design of Integrated Aircraft Thermal Systems," *Journal of Aircraft*, vol. 40, pp. 49–55, Jan-Feb 2003.

[62] Figliola, R. and Tipton, R., "An Exergy-Based Methodology for Decision-Based Design of Integrated Aircraft Thermal Systems," in *SAE*, 2000.

[63] Fischer, A. J., "Design of a Fuel Thermal Management System for Long Range Air Vehicles," in *3rd International Energy Conversion Engineering Conference*, (San Francisco, California), Universal Technology Corporation Air Force Research Laboratories, AIAA, 15 - 18 Aug 2005.

[64] Fozzard, A., "The Basic Budgeting Problem Approaches to Resource Allocation in the Public Sector and their Implications for Pro-Poor Budgeting," tech. rep., Centre for Aid and Public Expenditure, 2001.

[65] Freeh, J. E., Pratt, J. W., and Brouwer, J., "Development of a Solid-Oxide Fuel Cell/Gas Turbine Hybrid System Model for Aerospace Applications," NASA Technical Memorandum NASA/TM2004-213054, Glenn Research Center and University of California, May 2004.

[66] Gao, J., Vorobyov, S. A., and Jiang, H., "Cooperative Resource Allocation Games Under Spectral Mask and Total Power Constraints," *IEEE Transactions on Signal Processing*, vol. 58, pp. 4379–4395, Aug 2010.

[67] German, B., "A Tank Heating Model for Aircraft Fuel Thermal Systems with Recirculation," in *AIAA Aerospace Sciences Meeting Including the New Horizons Forum and Aerospace Exposition*, 2011.

[68] Gerstler, W. D. and Bunker, R. S., "Aircraft Engine Thermal Management: The Impact of Aviation Electric Power Demands." ASME Global Gas Turbine News, Dec 2008.

[69] Grierthuysen, V. J. V., Glickstein, M. R., and Hodge, E. S., "Integrating Subsystems and Engine System Assessments," *Journal of Engineering for Gas Turbines and Power*, vol. 125, pp. 263–269, Jan 2003.

[70] Grierthuysen, V. J. V., Issacci, F., and Farr, J., "A Modeling Approach for Integrated Thermal Management System Analysis of Aircraft," in *SAE*, 1997.

[71] Hall, K. C., Thomas, J. P., and Dowell, E. H., "Proper Orthogonal Decomposition Technique for Transonic Unsteady Aerodynamic Flows," *AIAA Journal*, vol. 38, pp. 1853–1862, Oct 2000.

[72] Heltzel, A. J., "Simulation of Emerging Heat Exchanger Technologies for Progressive Aerospace Platforms," in *48th AIAA Aerospace Sciences Meeting Including the New Horizons Forum and Aerospace Exposition*, (Orlando, Florida), PC Krause and Associates Inc., AIAA, 4 - 7 Jan 2010.

[73] Hill, P. and Peterson, C., *Mechanics and Thermodynamics of Propulsion*. Addison-Wesleyl, 1992.

[74] Hodge, E. S. and Glickstein, M. R., "Thermal System Analysis Tools (TSAT)," AFRL Final Report AFRL-PR-WP-TR-2002-2013, Modelogics, Inc., Kennesaw, GA, Jan 2002.

[75] Homitz, J., Scaringe, R. P., Cole, G. S., Fleming, A., and Michalak, T., "Comparative Analysis of Thermal Management Architectures to Address Evolving Thermal Requirements of Aircraft Systems," in *SAE 2008 Power Systems Conference*, (Bellevue, Washington), Mainstream Engineering Corporation and Air Force Research Laboratory, SAE, 11-13 Nov 2008.

[76] Iden, S. M., "Integrated Vehicle Energy Technology INVENT Program Overview." Presentation, 8 Sep 2008.

[77] Iden, S. M., Sehmbey, M. S., and Borger, D. P., "MW Class Power System Integration in Aircraft," in *SAE Paper*, 2004.

[78] International Air Transport Association, "Jet Fuel Price Monitor." `http://www.iata.org/whatwedo/economics/fuel_monitor/Pages/index.aspx`, 24 Aug 2012.

[79] Issacci, F., John L. Farr, J., Wassel, A. T., and Griethuysen, V. V., "An Integrated Thermal Management Analysis Tool," in *IEEE*, (Torrance, California), Science Applications International Corp. and Wright Paterson Air Force Base, 1996.

[80] Issacci, F. and Traci, R., "Integrated Thermal Management of Advanced Aircraft," phase i sbir: af97-174 final report, UNISTRY Associates, Inc., Mar 1998.

[81] Jackson, P., ed., *Jane's All the World's Aircraft*. Sampson Low, Marston & Co., 2009.

[82] Jang, H.-Y., "Innovative Optimal Control Methodology of Heat Dissipation in Electronic Devices," *Journal of Thermophysics and Heat Transfer*, vol. 22, pp. 563–571, Oct-Dec 2008.

[83] Johnson, P. K. and Mason, L. S., "Performance and Operational Characteristics for a Dual Brayton Space Power System with Common Gas Inventory," in *AIAA Paper*, Analex Corporation and Glenn Research Center, AIAA, 2006. NASA/TM2006-214393.

[84] Jones, S. M., "An Introduction to Thermodynamic Performance Analysis of Aircraft Gas Turbine Engine Cycles Using the Numerical Propulsion System Simulation Code," tech. rep., NASA/TM2007-214690, 2007.

[85] Kanne, E. C., *Engine Thermomanagement for Fuel Consumption Reduction*. PhD thesis, Swiss Federal Institute of Technology Zurich, 2000.

[86] Kays, W. M. and London, A. L., *Compact Heat Exchangers*. New York: McGraw-Hill, Inc., 1984.

[87] Kestner, B., *Model Predictive Control (MPC) Algorithm for Tipjet Reaction Drive Systems*. PhD thesis, Georgia Institute of Technology, 2009.

[88] Khire, R., Becz, S., Reeve, H., and Zeidner, L., "Assessing Performance Uncertainty in Complex Hybrid Systems," in *10th AIAA Aviation Technology, Integration, and Operations (ATIO) Conference*, 13-15 Sep 2010.

[89] Klatt, N. D., "On-Board Thermal Management of Waste Heat from a High-Energy Device," Master's thesis, Air Force Institute of Technology, Mar 2008.

[90] Ksairi, N., Bianchi, P., Ciblat, P., and Hachem, W., "Resource Allocation for Downlink Cellular OFDMA SystemsPart I: Optimal Allocation," *IEEE TRANSACTIONS ON SIGNAL PROCESSING*, vol. 58, pp. 720–734, Feb 2010.

[91] Ksairi, N., Bianchi, P., Ciblat, P., and Hachem, W., "Resource Allocation for Downlink Cellular OFDMA SystemsPart II: Practical Algorithms and Optimal Reuse Factor," *IEEE Transactions on Signal Processing*, vol. 58, pp. 735–749, Feb 2010.

[92] Lai, K., Huberman, B. A., and Fine, L., "Tycoon: a Distributed Market-based Resource Allocation System," tech. rep., HP Labs, 2008.

[93] Lazarovich, D. and Lee, S.-J., "Approach for an Integrated Multi-Domain Aircraft Energy Model," in *SAE 2008 Power Systems Conference*, (Bellevue, Washington), Honeywell, SAE, 11-13 Nov 2008.

[94] Levenspiel, O., *Understanding Engineering Thermo.* Prentice Hall, 1996.

[95] Li, Y., Balchanos, M., Nairouz, B., Weston, N., and Mavris, D., "Modeling and Simulation of Integrated Intelligent Systems," in *Winter Simulation Conference*, pp. 1225–1223, 2008.

[96] Lieu, T. and Farhat, C., "Adaptation of Aeroelastic Reduced-Order Models and Application to an F-16 Configuration," *AIAA Journal*, vol. 45, pp. 1244–1257, Jun 2007.

[97] Liscouet-Hanke, S., Mare, J.-C., , and Pufe, S., "Simulation Framework for Aircraft Power System Architecting," *Journal of Aircraft*, vol. 46, pp. 1375–1380, Jul-Aug 2009.

[98] Louviere, J. A., "Thermal Issues of an Integrated Subsystem," in *SAE*, 1997.

[99] Lytle, J. K., "The Numerical Propulsion System Simulation: A Multidisciplinary Design System for Aerospace Vehicles," Tech. Rep. NASA TM-1999-209194, NASA, Sep 1999.

[100] Mahefkey, T., Yerkes, K., Donovan, B., and Ramalingam, M. L., "Thermal Management Challenges for Future Military Aircraft Power Systems," in *SAE Paper*, 2004.

[101] Maser, A. C., Garcia, E., and Mavris, D. N., "Thermal Management Modeling for Integrated Power Systems in a Transient, Multidisciplinary Environment," in *45th AIAA/ASME/SAE/ASEE Joint Propulsion Conference & Exhibit*, (Denver, Colorado), Georgia Institute of Technology, AIAA, 2 - 5 Aug 2009.

[102] Maser, A. C., Garcia, E., and Mavris, D. N., "Facilitating the Energy Optimization of Aircraft Propulsion and Thermal Management Systems through Integrated Modeling and Simulation," in *SAE 2010 Power Systems Conference*, (Fort Worth, Texas), Georgia Institute of Technology, SAE, 2 - 4 Nov 2010.

[103] Maser, A. C., Garcia, E., and Mavris, D. N., "Characterization of Thermodynamic Irreversibility for Integrated Propulsion and Thermal Management Systems Design," in *Aerospace Sciences Meeting 2012*, (Nashville, Tennessee), Georgia Institute of Technology, AIAA, 9-12 Jan 2012.

[104] Mattingly, J. D., *Elements of Propulsion: Gas Turbines and Rockets*. AIAA, 2006.

[105] Mattingly, J. D., Heiser, W. H., and Pratt, D. T., *Aircraft Engine Design*. Reston, VA: AIAA, 2002.

[106] Mavris, D. N., DeLaurentis, D. A., Bandte, O., and Hale, M. A., "A Stochastic Approach to Multi-disciplinary Aircraft Analysis and Design," in *36th Aerospace Sciences Meeting & Exhibit*, AIAA 98-0912, (Reno, NV), Georgia Institute of Technology, AIAA, 12-15 Jan 1998.

[107] McCarthy, K., Walters, E., Heltzel, A., Elangovan, R., Roe, G., Vannice, W., Schemm, C., Dalton, J., Iden, S., Lamm, P., Miller, C., and Susainathan, A., "Dynamic Thermal Management System Modeling Electric Aircraft," in *SAE 2008 Power Systems Conference*, (Bellevue, Washington), P.C. Krause and Associates, Inc. and Boeing and Lockheed Martin and Avetec and USAF, SAE, 11-13 Nov 2008.

[108] McCarthy, K., Heltzel, A., Walters, E., Roach, J., Iden, S., and Lamm, P., "A Reduced-Order Enclosure Radiation Modeling Technique for Aircraft Actuators," in *SAE Power Systems Conference*, 2 Nov 2010.

[109] McKinley, T. L. and Alleyne, A. G., "Real-Time Modeling of Liquid Cooling Networks in Vehicle Thermal Management Systems," in *SAE 2008 Power Systems Conference*, (Bellevue, Washington), Cummings, Inc. and University of Illinois at Urbana-Champaign, SAE, 11-13 Nov 2008.

[110] McNichols, J., Barnes, C., Wolff, M., Baudendiste, T., Corbett, M., and Lamm, P., "Hardware-in-the-Loop Power Extraction Using Different Real-Time Platforms," in *6th International Energy Conversion Engineering Conference (IECEC)*, (Cleveland, Ohio), PC Krause and Associates, Inc. and Air Force Research Laboratory, AIAA, 28 - 30 Jul 2008.

[111] Mills, K. L. and Dabrowski, C., "Can Economics-based Resource Allocation Prove Effective in a Computation Marketplace?," *Journal of Grid Computing*, vol. 1, pp. 1–21, 2007.

[112] Mink, G. and Behbahani, A., "The AFRL ICF Generic Gas Turbine Engine Model," in *41st AIAA/ASME/SAE/ASEE Joint Propulsion Conference & Exhibit*, (Tucson, Arizona), Scientific Monitoring, Inc and Air Force Research Laboratory, AIAA, 10 - 13 Jul 2005.

[113] Moir, I. and Seabridge, A., *Aircraft Systems: Mechanical, Electrical and Avionics Subsystems Integration*. Wiley, 2008.

[114] Moorhouse, D. J., "Proposed System-Level Multidisciplinary Analysis Technique Based on Exergy Methods," *Journal of Aircraft*, vol. 40, pp. 11–15, Jan-Feb 2003. U.S. Air Force Research Laboratory.

[115] Moorhouse, D. J. and Pratt, D. M., "Review of Methods for Thermal Management and to Design for Energy Efficiency," tech. rep., US Air Force Research Laboratory, 2010.

[116] Mudawar, I., "Assessment of High-Heat-Flux Thermal Management Schemes," *IEEE Transactions on Components and Packaging Technologies*, vol. 24, pp. 122–141, Jun 2001.

[117] Munoz, J. R. and von Spakovsky, M. R., "Decomposition in Energy System Synthesis/Design Optimization for Stationary and Aerospace Applications," *Journal of Aircraft*, vol. 40, pp. 35–42, Jan-Feb 2003.

[118] Myers, R. H. and Montgomery, D. C., *Response Surface Methodology: Process and Product Optimization Using Designed Experiments*. John Wiley & Sons, Inc., 2002.

[119] Nagano, H. and Ku, J., "Capillary Limit of a Multiple-Evaporator and Multiple-Condenser Miniature Loop Heat Pipe," *Journal of Thermophysics and Heat Transfer*, vol. 21, pp. 694–701, Oct-Dec 2007.

[120] Numerical Propulsion System Simulation Consortium, "NPSS User Guide Version 2.3.0," tech. rep., The Ohio Aerospace Institute, 2010.

[121] O'Connell, T. C., Lui, C., Walia, P., and Tschantz, J., "A Hybrid Economy Bleed, Electric Drive Adaptive Power and Thermal Management System for More Electric Aircraft," in *SAE Power Systems Conference*, 2 Nov 2010.

[122] Ordaz, I., *A Probabilistic and Multi-Objective Conceptual Design Methodology for the Evaluation of Thermal Management Systems on Air-Breathing Hypersonic Vehicles*. PhD thesis, Georgia Institute of Technology, Dec 2008.

[123] Osterbeck, P., Butzin, E. L., and Johnson, P., "Air Vehicle Sizing and Performance Modeling in NPSS," in *45th AIAA/ASME/SAE/ASEE Joint Propulsion Conference & Exhibit*, (Denver, Colorado), Belcan Corporation and Wolverine Ventures, Inc., AIAA, 2 - 5 Aug 2009.

[124] Page, R. W., Hnatczuk, W., and Kozierowski, J., "Thermal Management for the 21st Century Improved Thermal Control & Fuel Economy in an Army Medium Tactical Vehicle," in *SAE Paper*, 2005.

[125] Paiva, R. M., Carvalho, A. R. D., Crawford, C., and Suleman, A., "Comparison of Surrogate Models in a Multidisciplinary Optimization Framework for Wing Design," *AIAA Journal*, vol. 48, pp. 995–1006, May 2010.

[126] Parker, K. I., Felder, J. L., Lavelle, T. M., Withrow, C. A., Yu, A. Y., and Lehmann, W. V., "Integrated Control Modeling for Propulsion Systems Using NPSS," NASA Technical Memorandum NASA/TM2004-212945, Glenn Research Center and Modern Technologies Corporation, Cleveland, Ohio, Feb 2004.

[127] Paulus, D. M. and Gaggioli, R. A., "Rational Objective Functions for Vehicles," *Journal of Aircraft*, vol. 40, pp. 27–34, Jan-Feb 2003.

[128] Pellegrini, L. F., Politcnica, E., Gandolfi, R., da Silva, G. A. L., Politcnica, E., and de Oliveira Jr., S., "Exergy Analysis as a Tool for Decision Making in Aircraft Systems Design," in *45th AIAA Aerospace Sciences Meeting and Exhibit*, (Reno, Nevada), University of So Paulo and Embraer Empresa Brasileira de Aeronutica and University of So Paulo and Escola Politcnica, AIAA, 8 - 11 Jan 2007.

[129] Perrett, B., "F-35 May Need Thermal Management Changes." `http://www.aviationweek.com/aw/generic/story.jsp?id=news/F35-031209.xml&headline=F-35%20May%20Need%20Thermal%20Management%20Changes&channel=defense`, 12 Mar 2009.

[130] Pratt, D., Fingers, R., Moorhouse, D., and Nairus, J., "Thermal System Challenges from a United States Air Force Research Laboratory Perspective." Presentation, 21 Sep 2007.

[131] Ramalingam, M., Mahefkey, T., and Donovan, B., "Fuel Savings Analysis and Weapon Platform Thermal Management Options in a Tactical Aircraft," in *Proceedings of IMECE03*, 15-21 Nov 2003.

[132] Rancruel, D. F. and von Spakovsky, M. R., "Decomposition with Thermoeconomic Isolation Applied to the Optimal Synthesis/Design of an Advanced Tactical Aircraft System," *Int. J. Thermodynamics*, vol. 6, pp. 93–105, Sep 2003. Virginia Polytechnic Institute and State University.

[133] Rao, S. S., *Engineering Optimization - Theory and Practice*. John Wiley & Sons, 2009.

[134] Raymer, D. P., *Aircraft Design: A Conceptual Approach*. AIAA, 2006.

[135] Reeve, H. M. and Finney, A. M., "Probabilistic Analysis for Aircraft Thermal Management System Design and Evaluation," in *46th AIAA Aerospace Sciences Meeting and Exhibit*, (Reno, Nevada), United Technologies Research Center, AIAA, 7 - 10 Jan 2008.

[136] Richard, J. C., "Unsteady Quasi-One-Dimensional Nonlinear Dynamic Model of Supersonic Through-Flow Fan Surge," *Journal of Propulsion and Power*, vol. 22, pp. 188–196, Jan-Feb 2006.

[137] Riggins, D. W., Moorhouse, D. J., and Camberos, J. A., "Characterization of Aerospace Vehicle Performance and Mission Analysis Using Thermodynamic Availability," *Journal of Aircraft*, vol. 47, pp. 904–916, May-Jun 2010.

[138] Riggins, D. W., Taylor, T., and Moorhouse, D. J., "Methodology for Performance Analysis of Aerospace Vehicles Using the Laws of Thermodynamics," *Journal of Aircraft*, vol. 43, pp. 953–963, Jul-Aug 2006.

[139] Roberts, R. A., Eastbourn, S. M., and Maser, A. C., "Generic Aircraft Thermal Tip-to-Tail Modeling and Simulation," in *Joint Propulsion Conference*, (San Diego, CA), AIAA, 2011.

[140] Roberts, R. A., *A Dynamic Fuel Cell-Gas Turbine Hybrid Simulation Methodology to Establish Control Strategies and an Improved Balance of Plant*. PhD thesis, University of California, Irving, 2005.

[141] Rolls-Royce, *The Jet Engine*. Key Publishing, 2007.

[142] Roskam, J., *Airplane Design Part I: Preliminary Sizing of Airplanes*. DAR-corporation, 2005.

[143] Roth, B., "Work Potential Perspective of Engine Component Performance," *Journal of Propulsion and Power*, vol. 18, pp. 1183–1190, Nov-Dec 2002. Georgia Institute of Technology.

[144] Roth, B. and Mavris, D., "Method for Propulsion Technology Impact Evaluation via Thermodynamic Work Potential," *Journal of Aircraft*, vol. 40, pp. 56–61, Jan-Feb 2003.

[145] Roth, B. A. and Mavris, D. N., "Comparison of Thermodynamic Loss Models Suitable for Gas Turbine Propulsion," *Journal of Propulsion and Power*, vol. 17, pp. 324–332, Mar-Apr 2001. Georgia Institute of Technology.

[146] Roth, B. A. and Mavris, D. N., "Generalized Model for Vehicle Thermodynamic Loss Management," *Journal of Aircraft*, vol. 40, pp. 62–69, Jan-Feb 2003.

[147] Roth, B. A., *A Theoretical Treatment of Technical Risk in Modern Propulsion System Design*. PhD thesis, Georgia Institute of Technology, Mar 2000.

[148] SAE Aerospace Applied Thermodynamics Manual, "Aircraft Fuel Weight Penalty Due to Air Conditioning," 1989.

[149] Samad, A., Kim, K.-Y., Goel, T., Haftka, R. T., and Shyy, W., "Multiple Surrogate Modeling for Axial Compressor Blade Shape Optimization," *Journal of Propulsion and Power*, vol. 24, pp. 302–310, Mar-Apr 2008.

[150] Schilders, W. H., van der Vorst, H. A., and Rommes, J., *Model Order Reduction: Theory, Research Aspects, and Applications*. Springer, 2008.

[151] Schutte, J. S., *Simultaneous Multi-design Point Approach to Gas Turbine On-design Cycle Analysis for Aircraft Engines*. PhD thesis, Georgia Institute of Technology, 2009.

[152] Senzig, D. A., Fleming, G. G., and Iovinelli, R. J., "Modeling of Terminal-Area Airplane Fuel Consumption," *Journal of Aircraft*, vol. 46, pp. 1089–1093, Jul-Aug 2009.

[153] Setlur, P., Wagner, J., Dawson, D., and Chen, J., "Nonlinear Controller for Automotive Thermal Management Systems," in *Proceedings of the 2003 American Controls Conference*, 2003.

[154] Setlur, P., Wagner, J. R., Dawson, D. M., and Marotta, E., "An Advanced Engine Thermal Management System: Nonlinear Control and Test," *IEEE/ASME Transactions on Mechatronics*, vol. 10, pp. 210–220, Apr 2005.

[155] Shanmugasundaram, V., Ramalingam, M. L., and Donovan, B., "Continuous Cooling Loop Thermal Management for an Airborne Pulsed Power System," in *6th International Energy Conversion Engineering Conference (IECEC)*, (Cleveland, Ohio), UES, Inc. and Air Force Research Laboratory, AIAA, 28 - 30 Jul 2008.

[156] Shen, Z., Andrews, J. G., , and Evans, B. L., "Adaptive Resource Allocation in Multiuser OFDM Systems With Proportional Rate Constraints," *IEEE Transactions on Wireless Communications*, vol. 4, pp. 2726–2737, Nov 2005.

[157] Simmons, R. J., *Design and Control of a Variable Geometry Turbofan with an Independently Modulated Third Stream*. PhD thesis, The Ohio State University, 2009.

[158] Singer, J. and Jones, R. E., "Economic Theory for Memory Management Optimization," in *ICOOOLPS 2011*, Jul 26 2011.

[159] Smith, K. W., "Morphing Wing Fighter Aircraft Synthesis/Design Optimization," Master's thesis, Virginia Polytechnic Institute and State University, Jan 2009.

[160] Sobieszczanski-Sobieski, J., Agte, J. S., and Robert R. Sandusky, J., "Bi-Level Integrated System Synthesis (BLISS)," NASA NASA/TM-1998-208715, Langley Research Center, The George Washington University, Aug 1998.

[161] Spinney, C., "F-35: Out of Altitude, Airspeed, and Ideas But Never Money." http://battleland.blogs.time.com/2012/01/30/f-35-out-of-altitude-airspeed-and-ideas-but-never-money/, 30 Jan 2012.

[162] Stull, D. and Prophet, H., "JANAF Thermochemical Tables," tech. rep., National Bureau of Standards, 1971.

[163] Sulistio, A. and Buyya, R., "A Time Optimization Algorithm for Scheduling Bag-of-Task Applications in Auction-based Proportional Share Systems," tech. rep., The University of Melbourne, Australia, 2005.

[164] Szargut, J., Morris, D. R., and Steward, F. R., *Exergy Analysis of Thermal, Chemical, and Metallurgical Processes*. Hemisphere Publishing Corporation, 1988.

[165] Tipton, R., Figliola, R. S., and Ochterbeck, J. M., "Thermal Optimization of the ECS on an Advanced Aircraft with an Emphasis on System Efficiency and Design Methodology," in *SAE*, 1997.

[166] Tong, M. T. and Naylor, B. A., "An Object-Oriented Computer Code for Aircraft Engine Weight Estimation," NASA TM 2009-215656, NASA, Dec 2009.

[167] Trzebinski, D. and Szczygiel, I., "Thermal Analysis of Car Air Conditioning," *Archives of Thermodynamics*, vol. 31, no. 4, p. 7180, 2010.

[168] United States Department of Labor, "CPI Inflation Calculator." http://www.bls.gov/data/inflation_calculator.htm, 24 Aug 2012.

[169] United States Government Accountability Office, "Aviation and Climate Change: Aircraft Emissions Expected To Grow, but Technological and Operational Improvements and Government Policies Can Help Control Emissions," report to congressional committees, United States Government Accountability Office, Jun 2009.

[170] Vanderplaats, G. N., *Numerical Optimization Techniques for Engineering Design*. Vanderplaats Research & Development, Inc., 2005.

[171] Vargas, J. V. C., Bejan, A., and Siems, D. L., "Integrative Thermodynamic Optimization of the Crossflow Heat Exchanger for an Aircraft Environmental Control System," *Journal of Heat Transfer*, vol. 123, pp. 760–769, Aug 2001. Duke University and The Boeing Company.

[172] Vavalle, A. and Qin, N., "Iterative Response Surface Based Optimization Scheme for Transonic Airfoil Design," *Journal of Aircraft*, vol. 44, pp. 365–376, Mar-Apr 2007.

[173] Veres, J. R., "Overview of High-Fidelity Modeling in the Numerical Propulsion System Simulations (NPSS) Project Activities," NASA Technical Memorandum NASA/TM–2002-211351, Glenn Research Center,, Cleveland, Ohio, Jun 2002.

[174] Vincenti, W. G. and Kruger, C. H., *Introduction to Physical Gas Dynamics*. Krieger Publishing Company, 2002.

[175] von Spakovsky, M. R., Riggins, D., and Marley, C., "Non-equilibrium Thermodynamic Issues Related to On-demand Systems," in *48th AIAA Aerospace Sciences Meeting Including the New Horizons Forum and Aerospace Exposition*, (Orlando, Florida), Virginia Polytechnic Institute and State University and Missouri University of Science and Technology, AIAA, 4 - 7 Jan 2010.

[176] von Spakovsky, M. R., *A Practical Generalized Analysis Approach to the Optimal Thermoeconomic Design and Improvement of Real-World Thermal Systems*. PhD thesis, Georgia Institute of Technology, Dec 1986.

[177] Vrable, D. L. and Donovan, B. D., "Thermal Management for High Power Microwave Sources," in *1st International Energy Conversion Engineering Conference*, (Portsmouth, Virginia), TMMT, Inc. and Air Force Research Laboratory, AIAA, 17 - 21 Aug 2003.

[178] Vrable, D. L. and Yerkes, K. L., "A Thermal Management Concept for More Electric Aircraft Power System Applications," in *Aerospace Power Systems Conference*, (Williamsburg, Virginia), SPARTA, Inc. and Air Force Research Laboratory, 21-23 Apr 1998.

[179] Walters, E. A., Iden, S., McCarthy, K., Amrhein, M., OConnell, T., Raczkowski, B., Wells, J., Lamm, P., Wolff, M., Yerkes, K., and Wampler, B., "INVENT Modeling, Simulation, Analysis and Optimization," in *48th AIAA Aerospace Sciences Meeting Including the New Horizons Forum and Aerospace Exposition*, (Orlando, Florida), PC Krause and Associates, Inc. and Air Force Research Laboratory and Wampler Defense Analysis, AIAA, 4 - 7 Jan 2010.

[180] Warwick, G., "New AFRL Program Focuses On Aircraft Energy." http://www.aviationweek.com/aw/generic/story_channel.jsp?channel=defense&id=news/asd/2010/07/12/10.xml, 12 Jul 2010.

[181] Weimer, J. A., "Electrial Power Technology for the More Electric Aircraft," in *12th AIAA/IEEE Digital Avionics Systems Conference*, (Fort Worth, TX), pp. 445 – 450, Wright Laboratory, 25-28 Oct 1993.

[182] Weston, N. R., Balchanos, M. G., Koepp, M. R., and N.Mavris, D., "Strategies for Integrating Models of Interdependent Subsystems of Complex System-of-Systems Products," in *38th Southeastern Symposium on System Theory*, IEEE, 5-7 Mar 2006.

[183] Wolski, R., Plank, J. S., Brevik, J., and Bryan, T., "Analyzing Market-Based Resource Allocation Strategies for the Computational Grid," *International Journal of High Performance Computing Applications*, vol. 15, no. 3, pp. 258–281, 2001.

[184] Woodburn, D. A., Wu, T., Chow, L., Leland, Q., Brokaw, W., Bindl, J., Rolinski, N., Zhou, L., Lin, Y.-R., and Jordan, B., "Dynamic Heat Generation Modeling of High Performance Electromechanical Actuator," in *48th AIAA Aerospace Sciences Meeting Including the New Horizons Forum and Aerospace Exposition*, (Orlando, Florida), AIAA, 4 - 7 Jan 2010.

[185] Wu, C. F. J. and Hamada, M., *Experiments: Planning, Analysis, and Parameter Design Optimization*. Wiley, 2000.

[186] Younossi, O., Arena, M. V., Moore, R. M., Lorell, M., Mason, J., and Graser, J. C., "Military Jet Engine Acquisition Technology Basics and Cost-Estimating Methodology," project air force, RAND, 2002.

[187] Zaki, A. N. and Fapojuwo, A. O., "Optimal and Efficient Graph-Based Resource Allocation Algorithms for Multiservice Frame-Based OFDMA Networks," *IEEE Transactions on Mobile Computing*, vol. 10, pp. 1175–1186, Aug 2011.

[188] Zumberge, J., Wolff, J., McCarthy, K., O'Connell, T., Walters, E., Russell, G., and Lucas, C., "Integrated Aircraft Electrical Power System Modeling and Simulation Analysis," in *SAE Power Systems Conference*, 2 Nov 2010.

VITA

Adam Maser was born in Norfolk, Virginia, on May 3, 1985. He grew up in Chesapeake, Virginia, where he graduated from Hickory High in 2003.

After high school, he traveled to Atlanta to attend Georgia Tech. He graduated with a Bachelor's degree in Aerospace Engineering with Highest Honor in May 2007. He also had the opportunity to study abroad in the summer of 2005 at Georgia Tech Lorraine in Metz, France. As an undergraduate, he conducted research on aircraft engine design at the Aerospace Systems Design Laboratory (ASDL) and electric propulsion at the High-Power Electric Propulsion Laboratory. His senior design team was awarded first place in the 2007 AIAA Undergraduate Team Space Design Competition.

After graduation, he joined the ASDL and earned his Master's degree in Aerospace Engineering in May 2009 under the direction of Prof. Dimitri Mavris. During his first year of graduate school, Adam was the program manager of the 2008 AIAA Graduate Missile Design Competition team, which was awarded first place.

During his academic career, Adam interned or co-oped at the Air Force Research Laboratory, Rolls-Royce, NASA Langley Research Center, and Honeywell. He also completed a graduate certificate in engineering entrepreneurship through the Business School at Georgia Tech. In 2012, his team, Cerevis, was a finalist in the Georgia Tech Business Plan Competition and winner of the Elevator Pitch Competition.